University of Cape Town

Department of Geology

Chamber of Mines Precambrian Research Unit

BULLETIN 23

# STRUCTURAL-METAMORPHIC IMPRINT ON PART OF THE NAMAQUA MOBILE BELT IN SOUTH WEST AFRICA

by

H J BLIGNAULT

The text of this publication is from a thesis submitted in fulfilment of the requirements for the degree of Doctor of Philosophy

1977

University of Cape Town

The University of Cape Town has been given the right to reproduce this thesis in whole or in part. Copyright is held by the author.

The copyright of this thesis vests in the author. No quotation from it or information derived from it is to be published without full acknowledgement of the source. The thesis is to be used for private study or non-commercial research purposes only.

Published by the University of Cape Town (UCT) in terms of the non-exclusive license granted to UCT by the author.

University of Cape Town

STRUCTURAL-METAMORPHIC IMPRINT ON PART OF THE NAMAQUA MOBILE BELT IN SOUTH WEST AFRICA

ABSTRACT

The cross-section of the part of the Namaqua Mobile Belt investigated, comprises tectonic domains differing in structural and metamorphic character. The upper-crustal Richtersveld Province is separated from the lower-crustal central zone by a marginal zone across which there is a sharp increase in P and T. A continuous prograde metamorphic zonation is established which is bounded on the low-grade side by the 'hornblende in' reaction and includes with increasing grade 'muscovite + chlorite out', andalusite/sillimanite inversion, minimum melt line, 'epidote out', 'K-felspar + sillimanite in' and a brown hornblende zone. The PT conditions inferred for the K-felspar + sillimanite zone is in the order of 6 kb and 740°C. This metamorphic zonation is defined by the metamorphic peak at any one point and is associated with the early structures. Subsequent deformations indicate a continuous retrogression. The early kinematic event includes at least two phases of coaxial and coplanar folding giving rise to the main planar fabric which is interpreted as a shear surface. It is concluded that the first kinematic event constitutes a thrust regime. The late kinematic event is represented in the central zone by two phases of macroscopic folding which yielded basin and dome structures. To accommodate the resultant lateral shortening in the central zone, the Kanabeam shear zone developed between the central zone and the more upper-crustal domains where the late phase folding is not developed. Two discrete magmatic events, yielding differentiated intrusives are closely related in time to the early kinematic event. These intrusives underlie at least 50 per cent of the area. The Vioolsdrif Suite (1900 Ma) is genetically related to the Orange River volcanics. The intersheeted volcanics (2000 Ma) and intrusives form the Vioolsdrif igneous complex which is correlated with the grey gneiss of the lower-crustal domains. In the high-grade central zone aluminous paragneisses structurally overlie the grey gneisses and are interpreted as a mudstone/wacke sequence.

The early kinematic event, associated with thrusting, the main metamorphism and extensive intrusion, constitutes the main phase of the Namaqua tectogenesis which commenced at least at about 1900 Ma. The late kinematic event is associated with lateral movement and shortening during the waning stages of the Namaqua tectogenesis at about 1000 Ma.

TABLE OF CONTENTS

# 1 INTRODUCTION

The present investigation was initiated by the late Prof John de Villiers who realized that markedly different types of basement rocks underlie the area of study (Fig. 1.1). 4 800 $km^2$ of gneissic terrain was mapped and compiled on a scale of 1:100,000 (Annex. 1, 2 & 3). Reconnaissance mapping towards the north-east was subsequently undertaken. Published maps differentiating basement were not available.

The research grant by Rio Tinto Exploration (Pty.) Limited is gratefully acknowledged. The investigation was initially conducted under the supervision of the late Prof John de Villiers and concluded under Prof P Joubert whose contribution is much appreciated.

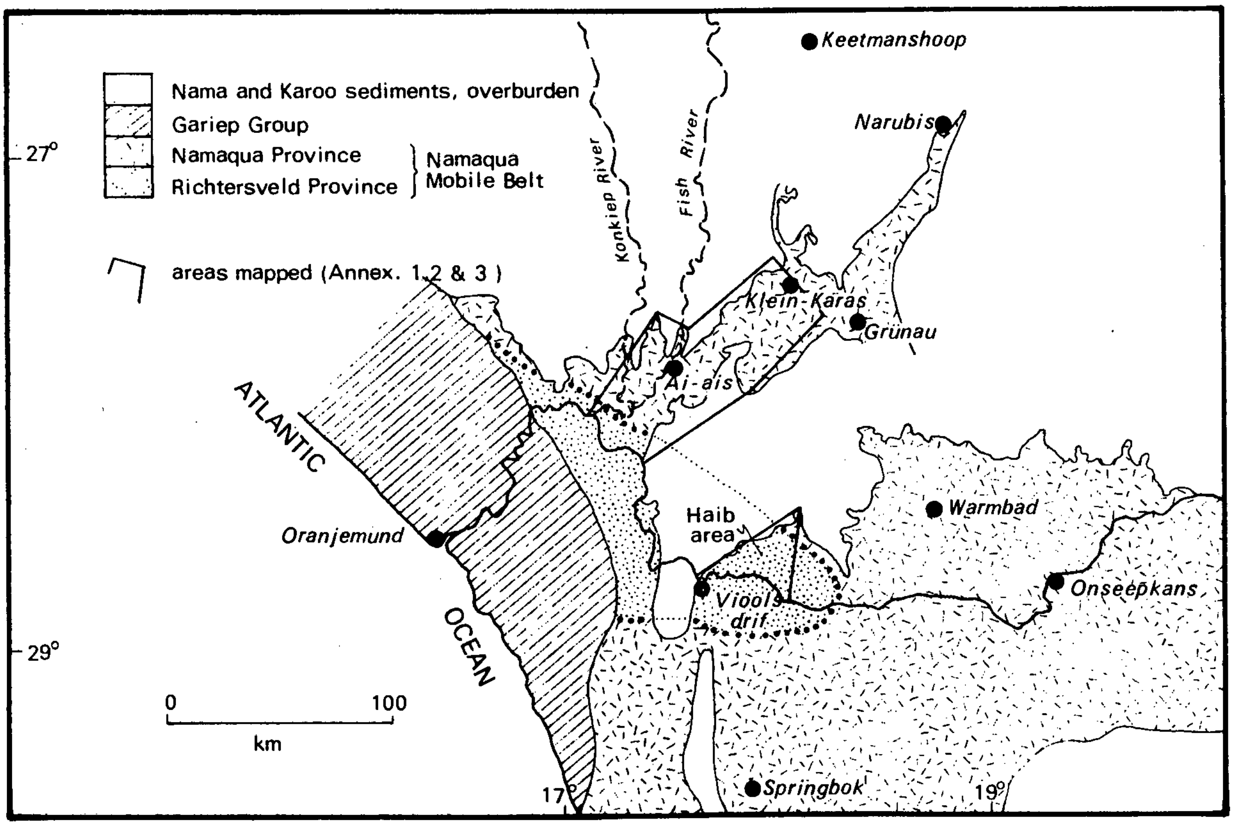


*Fig. 1.1. Locality map.*

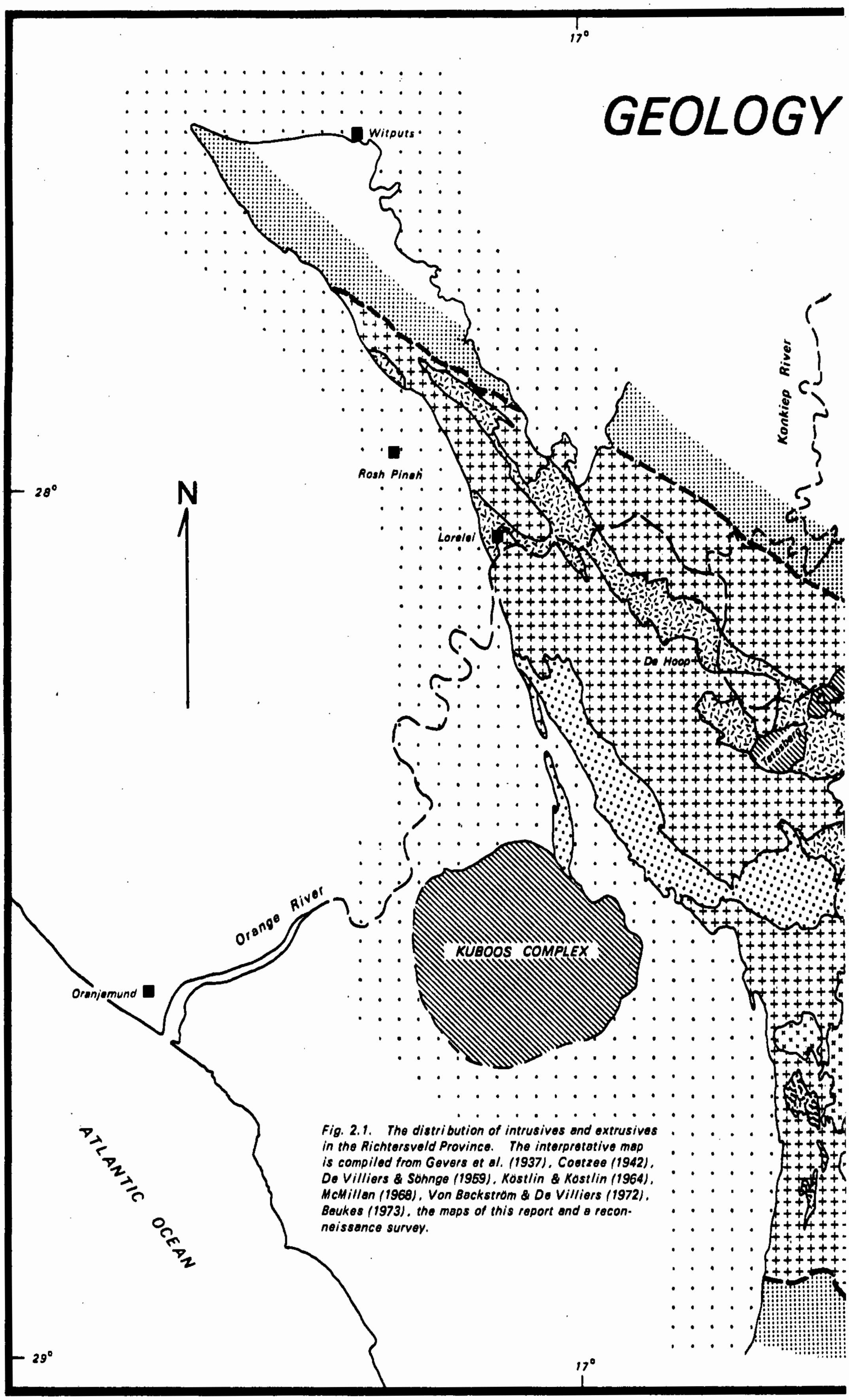


*Fig. 2.1. The distribution of intrusives and extrusives in the Richtersveld Province. The interpretative map is compiled from Gevers et al. (1937), Coetzee (1942), De Villiers & Söhnge (1959), Köstlin & Köstlin (1964), McMillan (1968), Von Backström & De Villiers (1972), Beukes (1973), the maps of this report and a reconneissance survey.*

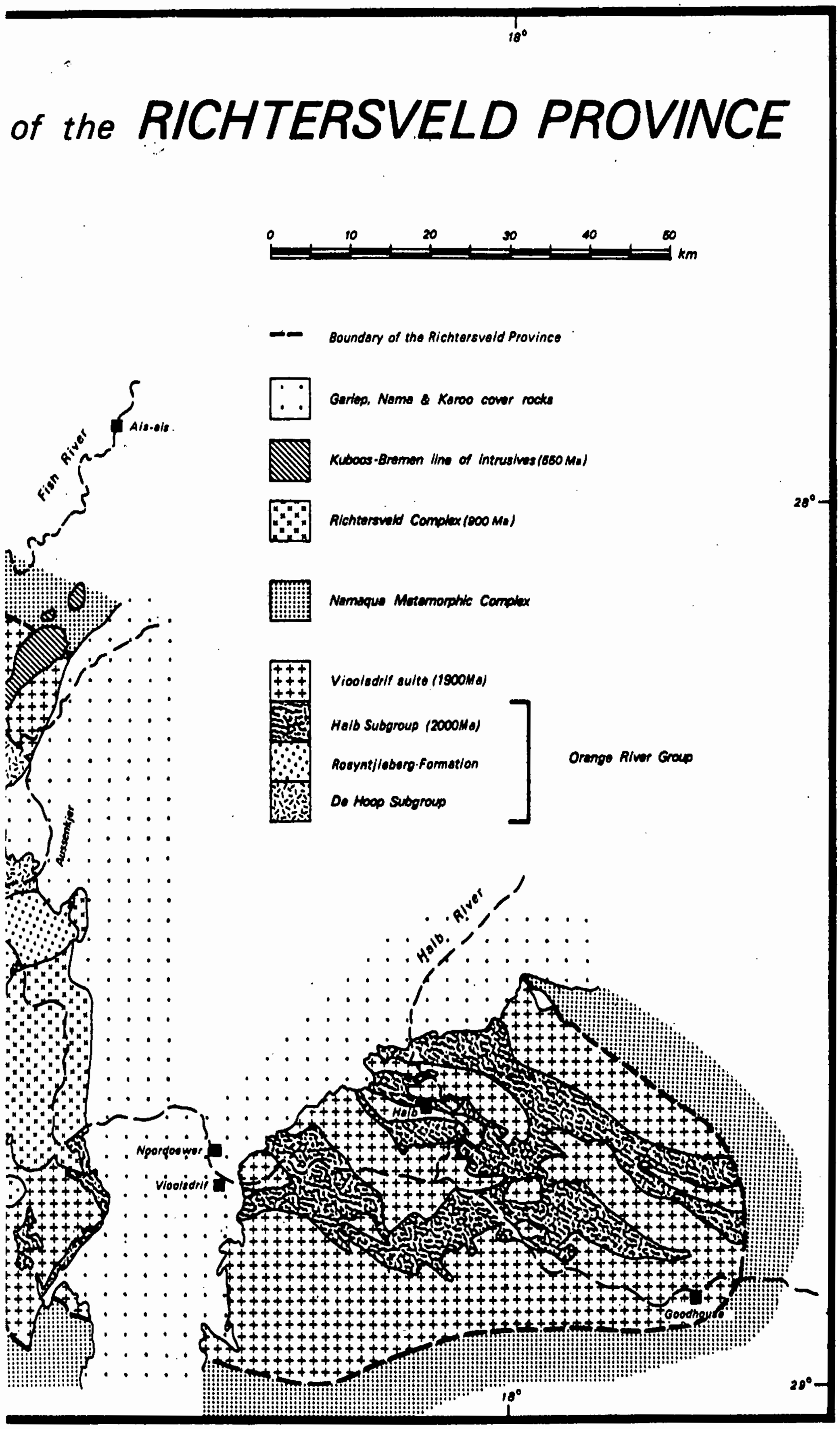

18°
of the RICHTERSVELD PROVINCE
0
10
20
30
40
50
km
Boundary of the Richtersveld Province
Gariep, Nama & Karoo cover rocks
Kuboos-Bremen line of intrusives (550 Ma)
Richtersveld Complex (900 Ma)
Namaqua Metamorphic Complex
Vioolsdrif suite (1900Ma)
Haib Subgroup (2000Ma)
Rosyntjieberg Formation
De Hoop Subgroup
Orange River Group
Ais-ais
Fish River
28°
Haib River
Haib
Noordoewer
Vioolsdrif
Goodhouse
29°
18°

# 2 LITHOLOGY

Because a strong tectonic imprint alters the lithologic aspect of a rock, description of the various rock units are presented for each of three structural domains (Section 3.1, Fig. 3.1).

## 2.1 Richtersveld Province

### 2.1.1 Introduction

The Richtersveld Province is underlain by the volcano-sedimentary sequence of the Orange River Group and the younger (1900 Ma) intrusive Vioolsdrif Suite with an approximate 2:1 areal distribution of intrusives to extrusives (Fig. 2.1). As such, the Vioolsdrif Suite constitutes an igneous massif of batholithic proportions intruded into discontinuously dispersed volcanic units. The Vioolsdrif batholith extends beyond the limits of the Richtersveld Province where the reconstituted intrusives form part of the gneissic terrain of the Namaqua Province.

Lithologically the Richtersveld Province is distinct from the infrastructural Namaqua Province in deformation and metamorphic aspect and an attempt is made here to describe mainly the primary lithological characteristics. The relatively low grade of metamorphism and deformation, especially in the central portion of the Richtersveld Province, allows for the recognition of primary textures and structures in the intrusive-extrusive complex.

Aspects of these lithological units from various parts of the Richtersveld Province are described by Gevers et al. (1937), De Villiers & Söhnge (1959), Middlemost (1963, 1964, 1965), McMillan (1968), Von Backström & De Villiers (1972), Blignault (1974b), Ward (1972, 1973, 1974), Beukes (1973) and Reid (1974, 1975).

The lithological account below is largely based on field mapping in the Haib and lower Fish River areas (Annex. 1 & 3) and reconnaissance work elsewhere in the Richtersveld Province.

## 2.1.2 Orange River Group

The volcano-sedimentary Orange River Group forms the oldest rocks encountered in the Richtersveld Province. For these rocks De Villiers & Söhnge (1959) used a stratigraphic scheme that is upheld for the present with only a change in nomenclature (Kröner & Blignault, 1976) necessary so as to avoid the traditional correlation with the type Kheis :

| | | |
|---|---|---|
| Orange River Group (Kheis System) | Haib Subgroup | (Wilgenhoutdrift Series) |
| | Rosyntjieberg Formation | (Kaaien Series) |
| | De Hoop Subgroup | (Marydale Series) |

(The nomenclature of De Villiers & Söhnge (1959) in brackets)

### 2.1.2.1 Rosyntjieberg Formation

The stratigraphic subdivision of De Villiers & Söhnge above is based on the Rosyntjieberg Formation (Fig. 2.1) which, in the Richtersveld, forms a distinct unit constituting virtually all the sediments of the Orange River Group in the form of a prominent quartz arenite (in the sense of Pettijohn et al. 1972). A ripple-marked iron-formation bed situated close to the base of the Rosyntjieberg Formation was observed on Aussenkjer and locally forms an important marker horizon. Similar strata of 'magnetite rocks', reported by De Villiers & Söhnge (1959), seem to occur towards the top of the Rosyntjieberg Formation representing the only recognised chemical sediments belonging to the Orange River Group.

### 2.1.2.2 De Hoop Subgroup

The De Hoop Subgroup (Fig. 2.1) underlies the Rosyntjieberg Formation (as indicated by cross-bedding, De Villiers & Söhnge, 1959, p. 34) conformably and forms the lowermost exposed portion of the Orange River Group. At Aussenkjer the upper portion of the De Hoop volcanics is distinctly mafic and includes layers of volcanic breccia. In the Richtersveld these volcanics consist 'for the most part of mafic lavas with bands of felsic lavas' (De Villiers & Söhnge, 1959, p. 29).

In the lower Fish River area the volcanics of the De Hoop Subgroup form a small but continuous body structurally underlain and overlain by granitoids of the Vioolsdrif Suite (Annex. 1, Fig. 2.1). The stratification and trend of the volcanic unit is conformable with the regional structural grain, while the conformable lithological contacts are usually foliated.

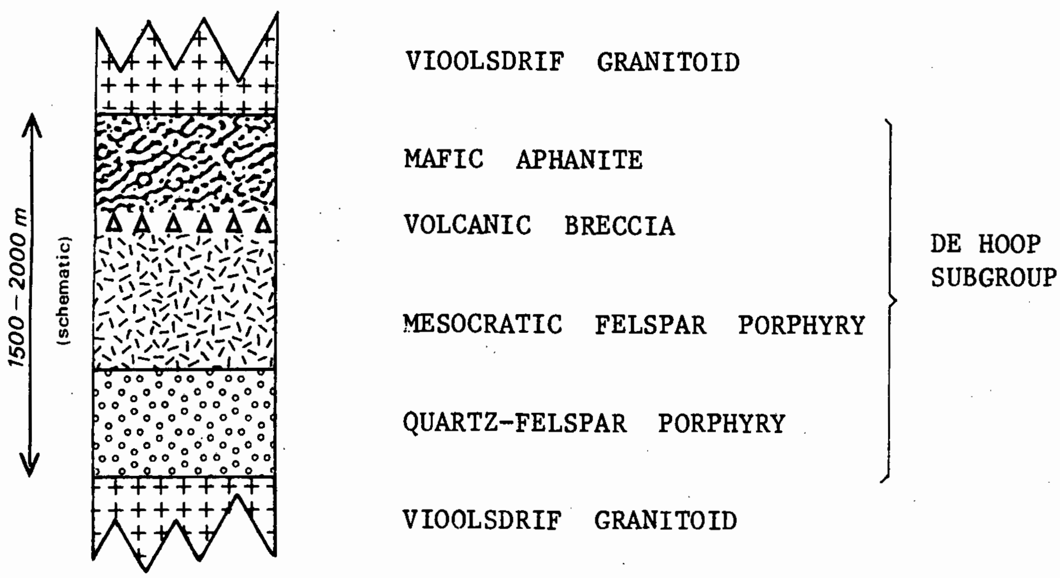


Fig. 2.2 Structural sequence of the De Hoop Subgroup as exposed in the lower Fish River area.

Three volcanic units were recognised (Fig. 2.2) : a leucocratic quartz-felspar porphyry structurally overlain by a darker felspar porphyry, in turn overlain by a mesocratic mafic aphanite. The quartz-felspar porphyry unit is lithologically homogeneous and no primary layering has been observed. An eutaxitic texture seen in places, is defined by lenticular dark coloured fragments and might indicate an ash-flow origin for this unit or for parts of it. The rounded quartz phenocrysts are commonly embayed while the euhedral felspar insets are invariably altered. The microcrystalline matrix is composed of regularly outlined and polygonal leucocratic minerals. The appearance of this rock suggests a composition more basic than that of a rhyolite.

The dark coloured felspar porphyry constitutes a uniform unit with a general lack of primary layering and lithological variation, but with occasional lithic fragments in evidence. The bulk composition of this unit is expected to be dacitic. Situated along, or in the vicinity of, the contact between this unit and the mafic aphanite, is a volcanic breccia horizon with some associated tuffs. The volcanic breccia contains predominantly felsic fragments which in the east are angular, but distinctly rounded towards the west. Clasts as large as 0,5m were observed. The matrix consists of well-recrystallised microcrystalline material. The breccia is unsorted and unstratified and contain no sediments or other evidence indicative of subaqueous deposition.

The mafic aphanite forms a more variable lithological unit in that it is interlayered with more acid lava types. Thin felsic layers, three to four metres thick, are prominently developed towards the west and characterise this unit in the Richtersveld. The dark aphanite locally contains felspar phenocrysts and pseudomorphic aggregates of chlorite ± biotite ± epidote ± amphibole, possibly after primary pyroxene or amphibole. Randomly oriented metamorphic hornblende needles are typically developed, while most of the aphanite is composed of a microcrystalline intergrowth of leucocratic minerals plus chlorite, biotite, epidote and ore. The bulk composition of this unit is expected to be andesitic.

### 2.1.2.3 Haib Subgroup

Rocks of the Haib Subgroup are not in contact with the main outcrop of the Rosyntjieberg Formation, and the stratigraphic position is therefore a matter of conjecture at present. The possibility of stratigraphic equivalence with the De Hoop Subgroup, however, cannot be precluded. In the Richtersveld (west of Vioolsdrif) most of this sequence appears to consist of 'dark lavas' with some felsic lavas and metasedimentary schists (De Villiers & Söhnge, 1959).

The type area of the Haib Subgroup is located east of Vioolsdrif (Fig. 2.1, Annex. 3). The subgroup consisting of a differentiated suite of lavas, volcaniclastics and minor sediments, are subdivided into two mappable formations (Fig. 2.3) :

Nous Formation

Tsams Formation (informally referred to as the Mafic and Felsic Volcanic Formations respectively; (Blignault, 1974b)).

Normal graded bedding, observed at one locality, suggests that the Nous Formation stratigraphically overlies the Tsams Formation. Further stratigraphic subdivision is, at this stage, tentative only and largely impeded by the lack of marker horizons and by the discontinuous exposures. Concordant lithological contacts, especially those with the Vioolsdrif granitoids, are commonly foliated over a limited width, whereas the discordant contacts are not foliated. The foliation is, as in the lower Fish River area, better developed in the volcanics than the granitoids. Furthermore, the primary nature of the more ductile horizons, preserved as phyllites, phyllonites and schist, is largely destroyed by the deformation and generally thought to have been tuffs.

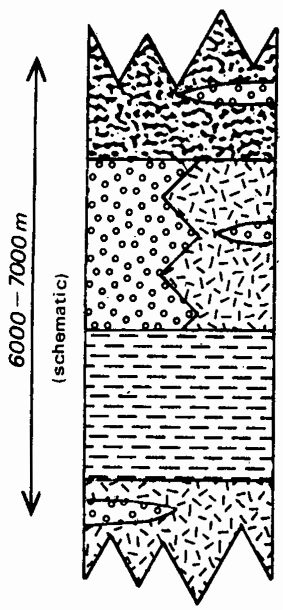


*(andesitic aphanite with felsite intercalations)* — NOUS FORMATION

UPPER FELSPAR PORPHYRY MEMBER
*(felspar porphyry with minor felsite intercalations; represented along strike by a quartz-felspar porphyry)*

VOLCANICLASTIC MEMBER

LOWER FELSPAR PORPHYRY MEMBER
*(felspar porphyry with minor felsite intercalations)*

} TSAMS FORMATION

Fig. 2.3 *Idealized* stratigraphic column for the Haib Subgroup as exposed in the type area. The lower and upper felspar porphyries might be a structural repetition of the same stratigraphic unit.

*Nous Formation*

The Nous Formation forms a distinct mappable unit easily recognised in the field and defines a macroscopic fold structure extending from the Neint Nababeep plateau in the west, to the vicinity of Goodhouse further to the east. Towards the east the Nous volcanics become increasingly deformed, to such an extent that primary features are completely obliterated by the more intensely and penetratively developed regional foliation. This formation is predominantly composed of dark coloured lavas and volcanic breccias interlayered with thin leucocratic acid flows.

The melanocratic lavas are andesitic[1] in composition (Table 2.1), locally contain spheroidal or pipe amygdales and are commonly interbedded with dark-coloured volcanic breccias and laminated tuffs. The lava units themselves are generally massive and appear structureless. The andesite is an aphanite

[1] The chemistry of these volcanics was obtained from D Reid; see also Reid (1974) for further information.

with local development of dark mineral phenocrysts, commonly containing plagioclase phenocrysts which are invariably altered, in part, to epidote and white micas. The albite twinning which can only rarely be recognised, indicates an anorthite content of ca. 45 per cent. The dark phenocrysts are usually twinned hornblende or else represented by biotite ± epidote ± amphibole aggregates interpreted as the product of retrogressive breakdown of primary hornblende or pyroxene grains. The matrix is usually a microcrystalline decussate-like intergrowth of predominantly dark and minor light-coloured mineral grains such as epidote, biotite ($\gamma = \beta$ = strong green; $\alpha$ = colourless), actinolite? ($\gamma$ = bluish; $\alpha = \beta$ = colourless) and chlorite.

Volcanic breccias and tuffs, as dark in colour as the andesitic lavas, constitute a considerable proportion of the Nous Formation and are persistently intercalated with the lavas. The composition of some of these volcaniclastics, as determined by Reid, is predominantly dacitic (Table 2.1). The volcanic breccias typically consist of widely spaced lithic fragments contained within a very fine-grained or microcrystalline matrix, with the latter predominating over fragments. Clasts as large as 0,3m have been observed, and finely laminated tuffs which are sometimes graded, are common, but no primary structures indicative or subaqueous deposition were observed.

Thin (several metres) leucocratic layers, representing more acid flows, form an integral part of the Nous Formation and are sparsely but persistently present throughout. Some are finely banded and cryptocrystalline with a 'glassy' appearance, while porphyritic varieties have been observed. These leucocratic flows are predominantly dacitic (Table 2.1) in composition.

*Tsams Formation*

The Tsams volcanics stratigraphically underlies the Nous Formation and are virtually only exposed north of the Orange River (Annex. 3). Farther north and east towards the tectonic boundary with the Namaqua Province, the primary characteristics are progressively obliterated by the deformation and metamorphic effects. A three-member subdivision is tentatively proposed (Fig. 2.3) with a felspar porphyry unit both overlying and underlying a volcaniclastic unit. It is possible, but considered unlikely, that the lower and upper felspar porphyry members represent the same stratigraphic unit, structurally duplicated.

The upper *Felspar Porphyry Member* forms an intercalatory contact with the Nous Formation. The mesocratic felspar porphyry is sporadically interlayered with thin (several centimetres) leucocratic bands, apparently more acid flows. Along strike to the west, the felspar porphyry becomes a mesocratic quartz-felspar porphyry of dacitic composition (Table 2.1). This unit is, apart from some sparsely developed volcanic breccia zones, lithologically homogeneous.

| STRATIGRAPHY | | LITHOLOGY | COMPOSITION (after Taylor 1969) | NUMBER of SAMPLES |
|---|---|---|---|---|
| Nous Formation | | dark lava | andesitic | 16 |
| | | | dacitic | 4 |
| | | minor leucocratic inter-calations | rhyolitic | 1 |
| | | volcanic breccia & tuffs (cliff section) | predominantly dacitic | 14 |
| Tsams Formation | upper Felspar Porphyry Member | quartz-felspar porphyry | dacitic | 3 |
| | Volcaniclastic Member | dark aphanite | andesitic | 3 |
| | | volcanic breccia | andesitic | 2 |
| | | minor leucocratic inter-calations & felspar porphyry unit | dacitic | 2 |
| | | major quartz porphyry units | rhyolitic | 2 |
| | | thin leucocratic flow | rhyolitic | 1 |
| | lower Felspar Porphyry Member | felspar porphyry – melanocratic | andesitic | 3 |
| | | felspar porphyry – mesocratic | dacitic | 1 |
| | | quartz-felspar porphyry | rhyolitic | 1 |

Table 2.1. Composition of the Haib Subgroup volcanics in the type area after Reid (1974).

Primary layering (on a centimetre scale) was infrequently observed whereas the bulk of the quartz-felspar porphyry appears massive. Spheroidal and pipe amygdales are present as local phenomena and the quartz and felspar phenocrysts are volumetrically subordinate to the microcrystalline[1] groundmass. The quartz insets are typically blue and commonly embayed, while the largely altered K-felspar and plagioclase (An 33) form euhedral to subhedral phenocrysts.

The *Volcaniclastic Member* is composed of a variety of volcanic rock types, typically interstratified on a small scale with volcanic breccias and tuffs forming characteristic components. The larger proportion of this stratigraphic unit is penetratively foliated, which is attributed to the general anistropy of the Volcaniclastic Member and relative ductility with respect to the surrounding granitoids and porphyries. The various interstratified rock types are described as follows :

(i) The original nature of a large proportion is obscure as it is now represented by porphyroclastic mylonites, mica phyllonites, quartz-white mica schist, chlorite schist, etc.

(ii) Volcanic breccias and laminated tuffs are characteristic, but proportionally subordinate. Andesitic volcanic breccias form distinctive units in the field and are commonly stratified. A characteristic white mica phyllonite and/or schist unit, locally containing flattened fragments, is commonly found intimately interlayered with lavas and are most probably deformed and recrystallised tuffs.

(iii) Minor andesitic lavas occur both as thin intercalations and larger mappable bodies (Annex. 3).

(iv) Thin intercalations as well as major units of quartz porphyry are prominent, with both the major quartz porphyry units and a thin flow-folded cryptocrystalline band being rhyolitic (Table 2.1) in composition; other minor leucocratic intercalations are dacitic. Felspar porphyry layers (several metres) were occasionally observed in association with quartz porphyries.

(v) A felspar porphyry unit is extensively developed on the south-western corner of the farm Kromrivier and is dacitic in composi-

---

[1] The matrix of the Haib Subgroup porphyries, in general, is coarser than would be expected for unaltered lavas and vitric features, glass shards, etc. have not been recognised. It is thought that the groundmass texture is largely the result of annealing and neomineralisation associated with low-grade metamorphism (Section 4).

tion (Table 2.1). Several features suggest that this unit constitutes an ignimbrite as lithic fragments were occasionally observed, an apparent eutaxitic texture, locally developed, is defined by dark lenticular shapes and as light-coloured lenticular fragments are common as an integral part of the felspar porphyry. The felspar porphyry is not a consistently uniform unit and bands of andesites, breccia-like horizons and felsitic layers break the otherwise lithological monotony.

The *lower Felspar Porphyry Member* is situated in the cores of two macroscopic structures. It is a monotonously uniform succession of felspar porphyries of which the bulk appears massive with no visible development of stratification. Subordinate lithological variation in the form of thin quartz-felspar porphyry bands, markedly discontinuous felsitic units and the odd volcanic breccia and tuff bed are present. The felspar porphyry itself has a colour variation from mesocratic to melanocratic; the very dark type is andesitic (Table 2.1), while the mesocratic felspar porphyry which predominates, is dacitic. The euhedral to subhedral felspar insets which consist both of K-felspar and plagioclase (An 30-42), are invariably altered in part to white mica and/or epidote. Quartz phenocrysts, commonly embayed and sometimes bluish in appearance, are locally developed.

A minor outcrop of ripple-marked fine-grained arenites along the lower Haib River (near farmhouse) appears to form part of the lower Felspar Porphyry Member. These arenites seem to represent the only recognised sediments of the Haib Subgroup in the type area.

#### 2.1.2.4 Concluding remarks

The De Hoop Subgroup is estimated here to consist mainly of 'dacites' while the full range from 'andesitic' to 'rhyolitic' lavas are present. It is overlain by a considerable thickness of 'clean' metaquartzites. In the type area of the Haib Subgroup there is a near equal distribution of andesitic and dacitic lavas. The Orange River Group, therefore, consists of a differentiated suite of lavas with a preponderance of dacite and andesite. This volcanic suite constitutes a rock series which is shown by Reid (1974) to be calc-alkaline. The volcanic breccias and tuffs of the Haib Subgroup lack primary structures indicative of subaqueous deposition. Pillow structures are absent and it is inferred that the volcanic sequence in the type area, was deposited predominantly in a subaerial environment.

### 2.1.3 Vioolsdrif Suite

The grey gneissic granite of De Villiers & Söhnge (1959, p. 64) which was later renamed the Vioolsdrif granite (De Villiers & Burger, 1967), constitutes the bulk of what is now defined as the Vioolsdrif Suite (Blignault, 1974b). The intrusive suite forms the Vioolsdrif batholith (Section 2.1.1), and is ubiquitously intrusive into the volcano-sedimentary sequence of the Orange River Group. The Vioolsdrif Suite is composed of spatially associated intrusives varying widely in composition, but with each phase or parts thereof bearing the imprint of the regional foliation ($s_1$) as its first structural label.

The various members of the intrusive suite are recognised in the field (Annex. 1 & 3), on textural and compositional criteria to form discrete mappable bodies, separated from each other along sharp boundaries. Further petrographic data confirm the consistent difference in composition (Figs. 2.4 & 2.5). Ultramafic rocks, dioritoids, granodiorites, adamellites and leucogranites are thought to constitute the main members of the Vioolsdrif Suite in the lower Fish River and Haib areas. It is noteworthy that in both these areas, two widely separated localities within the Richtersveld Province, a similar set of phases displays the same intrusion history. The sequence of intrusion, as established in the field, is schematically illustrated in Fig. 2.6 and suggests that emplacement took place in a general order from mafic to acid.

#### 2.1.3.1 Ultramafic, gabbroid and dioritoid phases

These more basic members of the Vioolsdrif Suite constitute the oldest intrusives that invade the volcano-sedimentary Orange River Group and therefore also form the earliest members of the Vioolsdrif Suite. Earlier reports from various parts of the Richtersveld Province (Gevers et al., 1937; De Villiers & Söhnge, 1959; Middlemost, 1965 and Beukes, 1973) mention serpentinites, hornblendites and gabbroids typically occurring as small bodies in, and are intruded by, the more widely distributed Vioolsdrif granitoids. Most previous workers agree that these mafic and ultramafic bodies intrude the volcanics of the Orange River Group. In the Vioolsdrif-Goodhouse area (Gevers et al., 1937, p. 30) mafic diorites are found gradational with hornblendites while more leucocratic diorites both grade into and are intruded by the granitoids.

In the lower Fish River and Haib areas the gabbroids are absent. The hornblendites and dioritoids, sparsely distributed as small bodies in a sea of granitoids, in some instances form clustered pips (Annex. 3). Two types of dioritic rocks are recognised :

MAIN MINERAL MODES

Vol (%)

| | LEUCOGRANITE PHASE | | | | | | Average | PORPHYRITIC GRANITE PHASE | | | | Average | ADAMELLITE PHASE | | | | | | Average |
|---|---|---|---|---|---|---|---|---|---|---|---|---|---|---|---|---|---|---|---|
| | B-322 | B-425 | B-517 | H-158 | H-163 | H-202 | | B-395 | H-111 | H-119 | H-123 | | B-99 | B-328 | B-354 | B-370 | B-601 | H-49 | |
| M | 0 | 0 | 0 | 1 | 0 | 1 | 0 | 6 | 3 | 1 | 6 | 4 | 8 | 10 | 8 | 3 | 4 | 11 | 7 |
| Q | 41 | 41 | 40 | 33 | 46 | 35 | 39 | 33 | 45 | 48 | 52 | 45 | 47 | 27 | 21 | 41 | 40 | 32 | 35 |
| A | 52 | 58 | 37 | 42 | 40 | 51 | 47 | 28 | 20 | 15 | 14 | 19 | 10 | 24 | 31 | 18 | 19 | 23 | 21 |
| P | 7 | 1 | 23 | 24 | 14 | 13 | 14 | 33 | 32 | 36 | 28 | 32 | 35 | 39 | 40 | 38 | 37 | 34 | 37 |

| | GRANODIORITE PHASE | | | | | | | | | | | Average | DIORITOID PHASE | | | | | Average |
|---|---|---|---|---|---|---|---|---|---|---|---|---|---|---|---|---|---|---|
| | B-315 | B-321 | B-351 | B-352 | B-452 | H-12 | H-24 | H-94 | H-106 | H-125 | H-295 | | B-107(a) | B-349 | B-418 | H-225 | H-298 | |
| M | 8 | 9 | 11 | 6 | 28 | 24 | 12 | 7 | 10 | 4 | 18 | 12 | 32 | 29 | 80 | 25 | 29 | 39 |
| Q | 42 | 32 | 41 | 27 | 22 | 11 | 26 | 39 | 26 | 23 | 15 | 28 | 5 | 4 | 0 | 4 | 10 | 5 |
| A | 14 | 17 | 14 | 28 | 9 | 0 | 6 | 6 | 17 | 2 | 33 | 13 | 0 | 0 | 0 | 0 | 0 | 0 |
| P | 36 | 42 | 34 | 39 | 41 | 65 | 56 | 48 | 47 | 71 | 34 | 47 | 63 | 67 | 20 | 71 | 61 | 56 |

Table 2.2. Main mineral modes (volume %; visually estimated with the aid of comparison charts) of the Vioolsdrif Suite. The samples are from both the Haib and lower Fish River areas. M mafic and related minerals, Q quartz, A alkali felspars, P plagioclase so that Q + A + P = 100; according to the IUGS Subcommission, 1973.

(i) A coarse meladiorite, generally quartz free, is found associated with hornblendite; leucocratic layering was observed in the meladiorite part of the small mafic/ultramafic complexes. These mafic and ultramafic bodies are intruded by the granodiorite phase.

(ii) Fine to medium, even-grained quartz diorites, commonly more leucocratic, form larger bodies with sharp contacts with the granodiorite. These diorites which have been observed to contain hornblendite inclusions, post-date the ultramafic phase.

The dioritic rocks (Table 2.2, Fig. 2.4) consist predominantly of blue-green ($\gamma$) hornblende (one sample is composed mainly of biotite ($\gamma \simeq \beta$ = green)) with subordinate biotite ($\gamma \simeq \beta$ = brown or green) and minor chlorite. The plagioclase is invariably altered. The hornblendite is typically composed of coarse equant hornblende grains ($\gamma$ = blue-green) and sometimes contains subordinate biotite ($\gamma \simeq \beta$ = brown).

The hornblendite and meladiorite appear undeformed, a foliation being normally only evident at the contacts with the granitoids where the marginal shearing can be ascribed to the marked ductility difference. The finer grained quartz diorites are penetratively foliated in areas where $s_1$ is developed in the surrounding rocks.

De Villiers & Söhnge (1959), Middlemost (1965) and Beukes (1973) suggest that the ultramfic and gabbroid bodies are preferentially situated along linear zones in their respective areas of investigation.

2.1.3.2 Granodiorite and adamellite phases

The granodiorites and adamellites constituting the bulk of the Vioolsdrif Suite (cf. Annex. 1 & 3) represent the biotite and hornblende granites of Gevers et al. (1937), the basement granodiorite of Coetzee (1942), the grey gneissic granite of De Villiers & Söhnge (1959) and Von Backström & De Villiers (1972), the Gn2 of Middlemost (1963), the Vioolsdrif granite of De Villiers & Burger (1967) and McMillan (1968) and the older mesocratic Vioolsdrif granite of Beukes (1973). Extensive masses of these granitoids intruding the whole stratigraphic sequence of the Orange River Group (De Villiers & Söhnge, 1959, p. 64), include the scattered pips of the older mafic phases and in turn are pervaded by small bodies of the younger and more acid members of the Vioolsdrif Suite. The De Hoop volcanics in the lower Fish River area are intruded by both these granitoids which intrude the entire sequence of the Haib Subgroup in the type area. Sharp contacts have been observed between granodiorites and adamellites, the time relation, however, could not be conclusively established. Within adamellite bodies multiple intrusive pulses are evident from the juxtaposition of two or more adamellites across sharp boundaries.

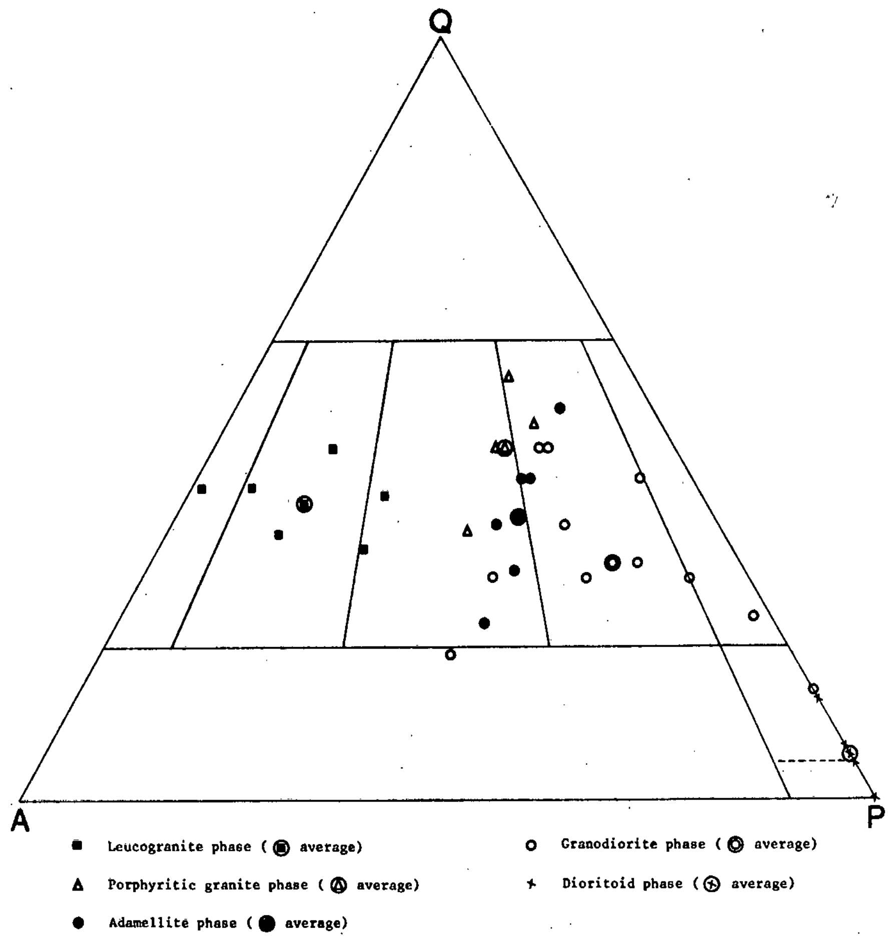


Fig. 2.4. QAP (modal quartz, alkali felspar and plagioclase) plot of the Vioolsdrif intrusives from the lower Fish River and Haib areas. See Table 2.2 for mineral modes.

The granodiorite and adamellite, both dark coloured (M <30), typically contain rounded mafic inclusions. It is usual to find local concentrations where the enclave density approaches several inclusions/m$^2$, the contacts of these hand-sized inclusions may be diffuse, and felspar blasts are developed in some. The adamellite though, is texturally distinct in that it contains coarse K-felspar phenocrysts (Plate 1) set in a medium-grained groundmass which resemble the granodiorite; the grey granodiorite is medium even grained

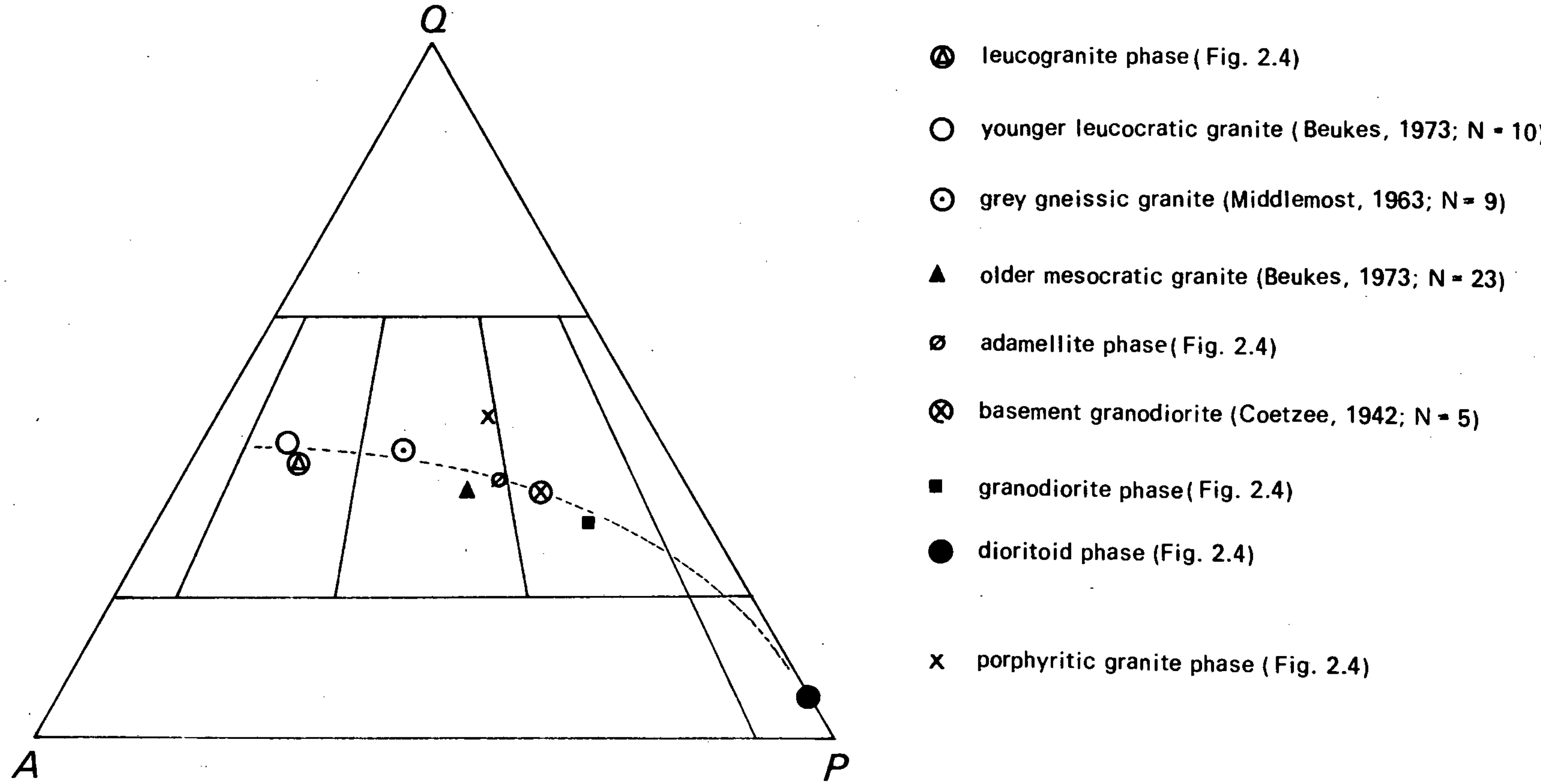


*Fig. 2.5. Regular variation pattern defined by average mineral modes of various intrusive phases of the Vioolsdrif Suite (cf. Section 2.1.3.6).*

and slightly darker coloured. These textural entities persist throughout the Richtersveld Province with remarkable consistency.

As an exception to the normal homogeneous appearance (on small and large scale) of the granitoids, the granodiorite phase is distinctly banded (schlieric) over several hundred metres in the vicinity of the Fish River/Orange River confluence. This structure (Plate 2) is thought to be a primary flow phenomenon with the heterogeneity resulting from the assimilation of mafic inclusions which abound in the vicinity. Although the schlieren are subparallel to the regional structural grain, a penetrative foliation is not developed there and the mafic inclusions around which the flow-banding curves, are not flattened. The leucocratic component of this mixed rock is a siliceous adamellite (Q:A:P = 48:22:30) which (on the basis of field observation), by contamination of mafic enclaves, appears to progress through a schlieric stage to produce a homogeneous rock forming part of the granodiorite phase. Further heterogeneities result from the local concentration of angular volcanic blocks varying in size from metres to up to 100 metres in length.

The two textural varieties, as recognised in the field to represent different intrusive phases, are also distinct in mineral composition (Fig. 2.4, Table 2.2). The average granodiorite and adamellite plot in fields 4 and 3b of the QAP triangle respectively and were named accordingly. Samples of the granodiorite phase are widely scattered and fall mainly in fields 3b, 4 and 5. The individual adamellite points are more closely grouped on the QA side of the field occupied by the granodiorite phase.

The granitoids have the following petrographic features :

(i) The plagioclase, which is conspicuously sub- to euhedral, appears greenish in hand specimen due to well advanced alteration to white mica and minerals of the epidote group.

(ii) The K-felspar is unaltered microcline-microperthite and microperthite.

(iii) The granodiorites in general appear darker in colour than the adamellites which also have a more variable mafic mineral content. Biotite ($\gamma \simeq \beta$ = green) is more commonly the main mafic mineral than hornblende ($\gamma$ = blue-green) which was noticed only in granodiorite; chlorite and epidote are present in minor amounts.

(iv) Interstitial granophyric intergrowths were observed in a couple of the samples and is certainly not a well-developed feature in the granodiorite or adamellite.

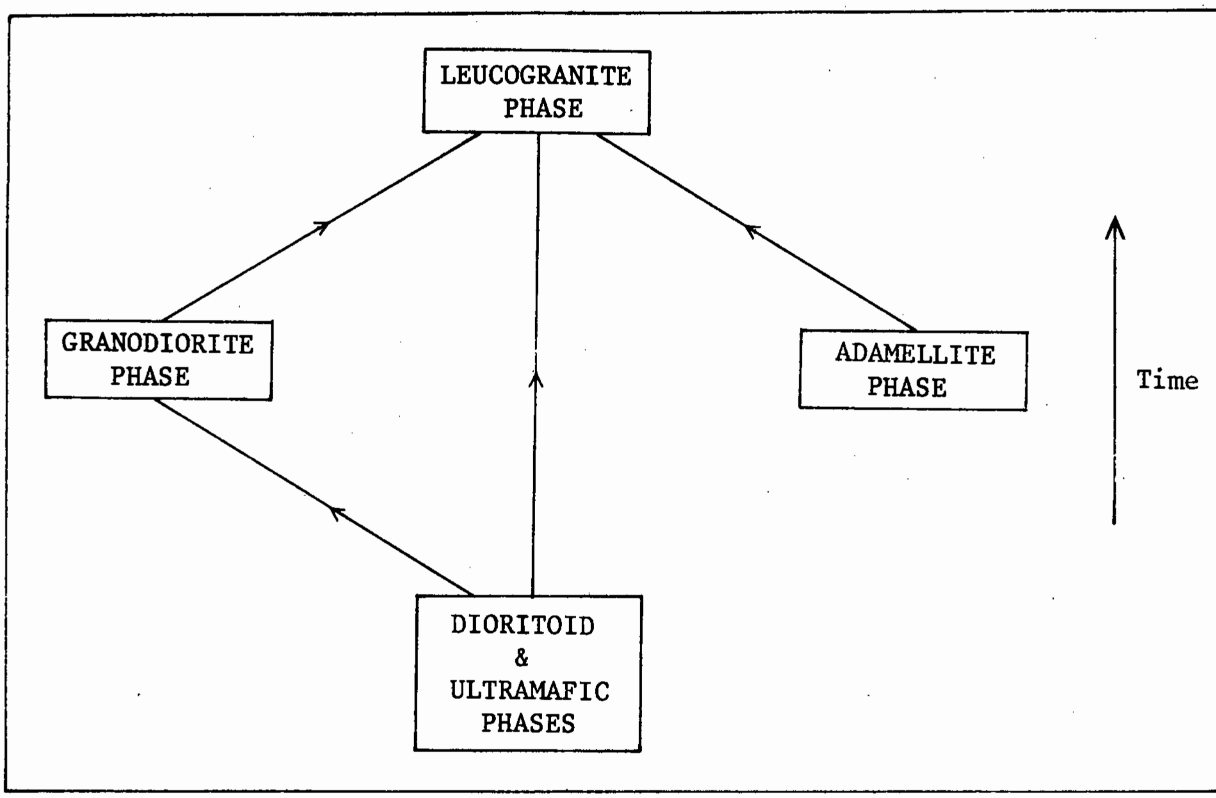


Fig. 2.6. The intrusion sequence of the various phases of the Vioolsdrif Suite. The tie lines represent established relationships with the arrows pointing to the younger phase.

2.1.3.3 Porphyritic granite phase

The porphyritic granite phase has a limited distribution, but is significant in that it is associated with copper mineralization. The type example is situated in the Haib area (Annex. 3) where porphyritic granite forms a large mappable sill-like unit, grossly conformable with respect to the structural grain. A similar rock was sampled in close proximity to the Tatasberg prospect in the Richtersveld. It would appear that although the porphyritic granite phase is volumetrically rather insignificant, it does occur over widely separated areas in the Richtersveld Province. As is evident from small dyke-like offshoots and volcanic inclusions which are locally situated close to the granite/lava contacts, the porphyritic granite is intrusive into the adjacent volcanics of the Haib Subgroup.

The later members of the Vioolsdrif Suite postdate the porphyritic granite while its relation with the granodiorite is more complex. Major boundaries with granodiorite bodies are both diffuse and sharp. Some large-scale contacts represent transitional zones in which both rock types are found as well as transitional types; in these zones no sharp contacts were observed. The porphyritic granite also abuts against granodiorite bodies of smaller dimensions with knife-sharp contacts, a complete transition over one metre or with a mesoscopic chill phase. These contact relationships are interpreted as suggesting that the porphyritic granite is a differentiate of the granodiorite phase re-intruding the parent body or protrusions thereof.

The porphyritic granite is more leucocratic than the granodiorite and contains some sparsely scattered inclusions which, like those typically found in the adamellites and granodiorites, are mafic and rounded with their boundaries not always well defined. These inclusions are quite different from those found close to the contacts with volcanics and are easily recognised as volcanic in origin.

The porphyritic granite phase is texturally distinct and quite different from any other phase of the Vioolsdrif Suite. The insets volumetrically constitute close to 50 per cent of the rock and consist predominantly of plagioclase with quartz, bluish in places, and some K-felspar. The phenocrysts vary in size from fine to medium-grained while the groundmass is formed of grains generally $\geq$ 0,1mm. Although the grain-size distribution defines two distinct modes (insets and matrix), there is a seriate-like tendency which inhibits the recognition of the porphyritic texture in the field to some extent. Granophyric intergrowths, although not common, are present in the groundmass.

The subhedral to euhedral plagioclase grains are invariably altered to white mica and minerals of the epidote group while the mafic minerals present are predominantly chlorite.

The modal mineralogy of the light-coloured minerals (Table 2.2 & Fig. 2.4) indicates an average composition along the border of fields 3b and 4. It is important to note that the individual samples all plot on the silicic side just outside the granodiorite field. Furthermore, the modal average of the porphyritic granite falls well above the curve (Fig. 2.5) defining the Vioolsdrif rock series, showing that it forms, with respect to the other members of the Vioolsdrif rock series (Section 2.1.3.6) an abnormally high siliceous phase. It is concluded that the position of the porphyritic granite on the QAP triangle substantiates the field evidence suggesting that it is a differentiate of the granodiorite phase and also suggests that the process of differentiation deviated from that which gave rise to the Vioolsdrif rock series.

Spatially associated with the sill-like porphyritic granite in the Haib area is a white alteration rock which occurs firstly, as small bodies within the porphyric granite and secondly, as major units generally disposed along its boundaries with the volcanic rocks of the Haib Subgroup. Gradational contacts between porphyritic granite/volcanics and the fine-grained white rock conclusively point towards an alteration process. Where developed on a mesoscopic scale, irregularly arranged tongues of alteration rock commonly have the following zonation from the core outwards :

(i) sugary-textured quartz rock

(ii) fine-grained white rock

(iii) a greenish transitional rock with conspicuous green mica grains.

The white rock which forms the most abundant alteration type, is fine-grained equigranular and composed of only quartz, white mica and some limonite, apparently after pyrite. It locally bears the imprint of the regional foliation, which in places is better developed than in the adjoining volcanic porphyries, indicating differences in competency and that the alteration predates the tectonic imprint.

2.1.3.4 Leucogranite phase

The leucogranite phase, the youngest member of the Vioolsdrif Suite, has been described by Gevers et al. (1937, p. 33; red aplitic granite and aplite), Von Backström & De Villiers (1972, p. 47; red granite and p. 53; part of the so-called Richtersveld igneous complex) and Beukes (1973, p. 71; younger leucocratic Vioolsdrif granite). The leucogranites are ubiquitously found throughout the Richtersveld Province as small mappable bodies (Annex. 3) and more commonly as mesoscopic bodies, irregular or dyke-like in shape, with hand-sized aplitic veins abounding in places.

These granites are commonly pinkish, typically fine to medium even-grained with sparsely developed granophyric intergrowths and do not contain inclusions. In the lower Fish River area a large mappable quartz porphyry body appears transitional in the field with leucogranite. A similar quartz porphyry in the Haib area (on Witputs) is here considered part of the leucogranite phase, but might be volcanic of origin (cf. Beukes, 1973, p. 45). The leucogranite phase is alaskitic (M=o) and comprises predominantly microcline-micropherthite, altered plagioclase and quartz. The average mineral modes (Figs. 2.4 & 2.5) indicate a granitic composition (field 3a).

2.1.3.5 Minor intrusives

Acid porphyry and mafic dykes of minor dimensions are rare. They intruded after the granodiorite phase, but their time relation with the leucogranite is not conclusively known. Quartz-felspar porphyries with a very distinct aphanitic matrix, form a few small cross-cutting bodies in the Haib area. Similar rocks are described by Gevers et al. (1937, p. 34) and Von Backström & De Villiers (1972, p. 53) from the Bergadderkop body. Pegmatites which can be related to the Vioolsdrif Suite are rare and small while several mafic dykes, in both the lower Fish River and Haib areas, were observed in granodiorite terrain. They form an acute angle with the regional foliation trend and are themselves moderately foliated.

### 2.1.3.6 Vioolsdrif rock series

The various phases of the Vioolsdrif Suite characteristically occur together in a district which also by metamorphic and structural parameters define a tectonic domain, the Richtersveld Province (Section 5). It is furthermore shown (Fig. 2.5) that the average mineral modes of the various members of the intrusive suite vary regularly from the one end member of the series (ultramafic rocks) to the other (leucogranite phase). In addition, the sequence of intrusion follows the same trend (Fig. 2.6) : ultramafic & dioritoid complexes and gabbroids ⟶ dioritoids ⟶ granodiorites — ? ⟶ adamellites ⟶ leucogranites. The intrusion is bracketed in time by the intruded Orange River volcanics and the regional foliation ($s_1$) which is imprinted on all the members of the Vioolsdrif Suite. These spatial, temporal and compositional relationships define the Vioolsdrif rock series as a differentiated suite of probable related parentage. An important aspect of the rock series is the preponderance of granodiorites and adamellites.

### 2.1.3.7 Mode and environment of emplacement

The geometry and fabric of the intrusive bodies, contact relationships and enclave characteristics are discussed here to clarify aspects of emplacement. Only the relationship of the intrusive suite with respect to its volcanic pile is discussed; the relation of the Vioolsdrif batholith, so to speak, and the adjoining infrastructural gneisses is discussed elsewhere (Section 5).

*The regional fabric and geometry*

The fabric of the Richtersveld Province is grossly conformable with the regional structure of the Namaqua Province. The fabric is defined by the distribution and shape of tilted and folded volcanic remnants and intrusives (Fig. 2.1). The intrusive/extrusive boundaries are mainly concordant with respect to stratification in the volcanic pile. Individual granitoid bodies are predominantly oblong, resulting in a roughly parallel arrangement of rock types and they also occur as sills within the major volcanic exposures. Although the conformable pattern dominates the fabric of the Richtersveld Province, discordant relations are by no means uncommon. Smaller subcircular bodies of granitoid are common and result in crosscutting contacts with respect to both bedding and the regional foliation. Major contacts which are concordant on a regional scale, may be extremely irregular on a smaller scale with some several kilometer of volcanic protrusions in the main granitoid mass.

*Contact relationships*

The concordant contacts between the intrusives and extrusives are invariably foliated, even between different granitoid bodies. The foliation is commonly developed over a wider zone in the volcanics than in the granitoids, a characteristic reflecting the more competent behaviour of the granitoids during deformation. Discordant boundaries are unfoliated and always sharp on a small scale. It is important to note that the boundaries of discrete intrusive bodies are not foliated all round, but vary in the manner described above.

The absence of obvious contact metamorphic phenomena in the volcanic rocks can be attributed to several factors, the most important perhaps being the high temperature mineralogy and low water content of the volcanic rocks. In addition, the superimposition of low-grade regional metamorphism might have obscured poorly developed thermal metamorphic effects. Chill phases were not recognised along major intrusive/extrusive boundaries and have not been recorded elsewhere in literature. Minor occurrences of such features were, however, observed at the granite porphyry in the Haib area where thin chill selvages developed both against lava and granodiorite, and at small offshoots of adamellite in both the Tatasberg and lower Fish River areas with chill phases against the volcanics.

Evidence of the intrusive nature of the Vioolsdrif Suite was ubiquitously found, mainly in the form firstly, of lenses and apophyses of granitoid invading the volcanic rocks and secondly of volcanic xenoliths within granitoids.

*Enclaves*

Along contacts the adamellite and granodiorite members locally include a multitude of angular volcanic fragments, some of which display rectangular fracture systems intruded by the granitoid. Elsewhere small, hand-sized mafic inclusions (clots), commonly rounded to subrounded and in various stages of digestion, are characteristic of the adamellite and granodiorite phases, the younger leucogranite phase being notably void of inclusions. In the Haib area, downstream from the Haib and Orange River confluence (Annex. 3), large terrains shown as granitoid on the map comprise volcanic rocks penetrated by granitoids on all scales and to such an extent that the fieldworker finds difficulty in deciding the main rock type for the map. The volcanic fragments (on various scales) in this type of terrain notably have angular outlines and probably constitute a roof zone in part. On the farms Witputs in the Haib area, and Sperlingsputs, east of the mapped area, the granitoids include large bodies of aluminous rock indicating that an alumina-rich sequence, not known in the Haib area, was intruded.

*Planar structures*

There is marked lack of readily recognisable primary flow structures in the granitoids. The alignment and associated flattening of xenoliths are associated with the more penetrative development of the regional foliation ($s_1$) which is interpreted as a later imprint because of the consistent cross-cutting relation of $s_1$ with respect to the various intrusive phases (see also Section 3.3.5). 'Schlieric' banding which was observed at two localities only (Plate 2), is the only flow structure recognised and typically has the banding curved around the xenoliths; the regional foliation, on the other hand, cuts straight across xenoliths.

*Mode and environment of emplacement*

Following the criteria listed by Hyndman (1972, p. 143) there is no direct evidence for forcible emplacement of the Vioolsdrif granitoids in the Richtersveld Province, but some to justify that emplacement took place by stoping and incorporation of the volcanic rocks in a more 'brittle' environment.

The pre-$D_1$ fabric in the volcanic remnants (Section 3.3.2) could be temporally related to the Vioolsdrif intrusive event. That the emplacement took place in a tectonic environment is indicated by the associated pre-$D_1$ and $D_1$ deformation phases.

*Level of emplacement*

The bulk of the Richtersveld Province is underlain by the Vioolsdrif granitoids which include discontinuously disposed volcanic remnants. This distribution pattern suggests that the present level of erosion is in the root zone of the Orange River volcanic pile. Following the criteria and scheme of Buddington, 1959 (see also Hyndman, 1972, p. 140) the Vioolsdrif Suite was emplaced in the transitional epizone-mesozone (6 - 10 km down). Aspects relating the Vioolsdrif intrusives to the epizone are as follows :

(i) Close association with volcanic rocks.

(ii) Minor occurrences of granophyric textures (Barker, 1970).

(iii) Absence of a planar flow fabric which in mesozonal plutons are often well developed towards the boundaries.

The mesozonal characteristics include :

(i) Partly discordant and partly concordant contact relationships.

(ii) Virtual absence of chilled borders.

Further evidence of upper-level emplacement is the development of the porphyritic granite phase, quartz porphyries associated with the leucogranite phase and the occasional occurrence of small bodies of quartz-felspar porphyry. The evidence of aphanitic textures in the younger phases might indicate that the younger members of the Vioolsdrif Suite were emplaced at a higher level and therefore relative upward movement of the present level of erosion at the time is inferred.

The porphyritic granite (Section 2.1.3.3) which is interpreted as a differentiate of the granodiorite, is locally the host to copper and molybdenum sulfides (Haib prospect) and is spatially associated with a quartz-sericite alteration zone. These features and the lithological environment correspond very well with the porphyry copper model of Sillitoe (1973), who estimates that the uneroded system could have a vertical extent of 8 km down to the level where the porphyritic host rock is transitional into the underlying phaneritic intrusive. The transitional boundary between the porphyritic granite and granodiorite phases is thus considered to be important evidence regarding the present level of erosion and 8 km corresponds well with Buddington's transitional epizone-mesozone.

2.1.3.8 Time of emplacement

The intrusion of the Vioolsdrif Suite is temporally related to the following discernable geological events (cf. Section 5) :

(i) Extrusion and sedimentation of the Orange River sequence : the entire sequence as exposed in the root zone of the volcanic pile, predating the granodiorite member of the Vioolsdrif Suite.

(ii) Establishment of the pre-$D_1$ structural fabric (Section 3.3.2) which could be concurrent with the Vioolsdrif intrusive event.

(iii) Emplacement of the Vioolsdrif Suite : the relation between the mafic and ultramafic phases and the two lower units of the Orange River Group is not known, but the Haib Subgroup predates all the phases of the Vioolsdrif Suite, while the granodiorite phase, at least, postdates the Rosyntjieberg Formation and De Hoop Subgroup.

(iv) Emplacement of mafic dykes (west-northwestern trend).

(v) Establishment of the $D_1$ planar fabric and concurrent development of low-grade regional metamorphism.

The 1850 Ma discordant U-Pb age from zircons (De Villiers & Burger, 1967) and the 1750 Ma whole rock Rb-Sr isochron (Corner, 1969) derived from the adamellite phase, are interpreted as indicating the age of crystallisation of the bulk of the Vioolsdrif Suite. The intrusives are relatively high-level emplacements which have not undergone subsequent higher grade metamorphism than low-grade. There is therefore no geological evidence for isotopic rejuvenation since the systems closed at the time of upper-level ($\pm$ 8 km) emplacement. The low initial $Sr^{87}/Sr^{86}$ ratio of 0,708 (Corner, 1969) is consistent with this interpretation. Further isotopic age dating was carried out by Reid (1975).

#### 2.1.4 Concluding remarks

##### 2.1.4.1 Intrusive/extrusive rock series

It is argued below on compositional, spatial and temporal grounds, that the Orange River volcanic sequence and Vioolsdrif intrusives constitute an igneous rock series lithostratigraphically referred to as the 'Vioolsdrif Igneous Complex'. Both the intrusives and extrusives are composed of a differentiated igneous suite with a preponderance in an overlapping compositional range - the extrusives are more basic with a significant development of andesites while diorites are volumetrically subordinate. The scatter diagrams of Reid (1974, p. 62), furthermore, show that the major element oxides of both the intrusive and extrusive rock series vary regularly in a similar fashion. There is no evidence for a marked time break between the extrusive and intrusive events, although available field evidence indicate that the intrusion of the Vioolsdrif Suite forms a discrete event postdating the formation of the Orange River Group; Rb-Sr isochron ages (Reid, 1975) for the Haib extrusives are 2010 Ma and Vioolsdrif intrusives 1960 Ma and 1810 Ma. The igneous rock series, thus defined, is likely to be genetically related.

##### 2.1.4.2 Plate tectonics

The igneous rock series, as defined above, forms a typical magmatic arc assemblage as found along present-day convergent plate margins. The calc-alkaline nature and predominance of dacitic-andesitic/granodioritic-adamellitic rocks in the Richtersveld Province favour a continental margin-type comparison (Miyashiro, 1974; Dickinson, 1972) such as the Coastal Batholith of Peru (Pitcher, 1972). Indications are that at least semi-rigid plate systems existed in mid-Proterozoic times (Burke & Dewey, 1973; Engel et al., 1974), a condition favourable for plate interaction giving rise to petrotectonic assemblages comparable in tectonic environment to the Mesosoic scene. The Vioolsdrif Igneous Complex can, therefore, be considered to represent a Proterozoic magmatic arc regime, situated along the margin of a continental-type plate.

## 2.2 Front zone

The tectonic front between the Richtersveld and Namaqua Provinces (defined in Section 3.1) is structurally defined as the position from where, towards the Namaqua Province, the regional foliation is homogeneously developed at a scale of penetration which renders the rock a general gneissic appearance. In the Namaqua Province the rocks are homogeneously and penetratively foliated everywhere, but this is not necessarily the case in the Richtersveld Province. This structural change is not everywhere abrupt and is sometimes transitional, but in either case, there is a transitional or front zone (Fig. 3.1), where the original character of the reconstituted rocks are readily recognisable.

The front and front zone vary in character from west to east in such a fashion that it is better defined, and more abrupt, where the front is parallel to the regional grain (e.g. in the Ai-ais area, Annex. 1). In the Haib area (Annex. 3) where the front is at an acute angle to the structural trend, this front has a more transitional character and the front zone itself is wider in extent. In the vicinity of Goodhouse where the transition can be observed along strike, the front is normal to the structural grain and the change is much more gradual taking place over several kilometres.

### 2.2.1 Ai-ais area

Along the lower reaches of the Fish River the onset of the more intensely and penetratively developed foliation is very abrupt and forms a conspicuous linear feature in the field, also easily recognisable on aerial photographs (Job 525; strip 1, 1741 & strip 2, 1664). The structural change across the front here is affected in the various intrusives of the Vioolsdrif Suite. In the front zone the various Vioolsdrif units are still recognisable, but occur as flattened bodies (bands) with a more rapid lithological variation across strike.

The hornblendite bodies acted competently and were not penetratively foliated; they form elongate and slightly fragmented units, while all the other lithological units of the Vioolsdrif Suite are indiscriminately foliated. The sparse, but pervasive concordant amphibolite bands (1 - 2 m) are correlated with the late mafic dykes of the Richtersveld Province (Section 2.1.3.5).

Other than the homogeneity of the Vioolsdrif igneous rocks in the Richtersveld Province, a small-scale banding is developed in the front zone. A distinct dynamic matamorphic banding is formed in granodiorites and adamellites on the front itself, whereas banding elsewhere in the front zone is defined by the distribution of hornblende or micas, and on a larger scale the different lithologies as a smaller scale 'mixing' of the same lithologies found in the Richtersveld Province or as a type of tectonic mélange. The north-eastern boundary of the front zone (Fig. 3.1) is taken at the mafic gneiss unit. Towards the south-east where this unit is absent the following characteristics mark the north-eastern boundary of the front zone :

(i) whereas the small augen and/or flaser structures of the rocks are pronounced within the front zone, it is less so towards the north-east

(ii) along the boundary of the front zone and further north-east, micas become prominantly developed rendering the rocks schistose

(iii) concordant leucocratic pegmatoidal and granitic arterites, up to a few centimetres in width, become pervasively developed, imparting a 'migmatitic' appearance to the gneisses

(iv) pegmatites, ubiquitous in the Namaqua Province, are first found along this boundary.

The reconstituted rocks of the front zone are finer grained than their equivalents in the Richtersveld Province. The deformed Vioolsdrif granodiorite and/or adamellite are typically small augen gneisses with readily recognisable flattened inclusions. The regional foliation is penetrative on thin section scale and wraps around small augen, giving the rock its characteristic spotted appearance. These lenticular white domains and medium-grained hornblende impart a medium-grained appearance to the rock; the lenticular white domains are, however, granular and in general the rock is fine grained with post-tectonic hornblende porphyroblasts. The random growth of large hornblende is characteristic of rocks in the front zone. Megascopically the front zone rocks have a cataclastic-like appearance, evident in the white domains of the augen or flaser; the foliation typically has an anastomosing pattern. The same texture is developed in deformed Vioolsdrif leucogranite. The fine-grained varieties have on cross-section a streaky megascopic appearance which is due to discontinuous linear arrays of ore, plagioclase and quartz and a very finely anastomising foliation. The coarser varieties commonly have medium-grained augen consisting of quartz and/or felspar.

On microscopic scale the 'cataclastic' nature is not so apparent as deformation features are rare. Some pretectonic felspar grains were recognised by their undulose extinction and fracturing with slight misorientation across the fractures. The white lenticular domains (augen or flaser) consist of aggregates of quartz and felspar, predominantly plagioclase, commonly with regular straight boundaries. The felspar augen or flaser may be wrapped around by quartz ribbons with the quartz generally in an unstrained state. As the helicitic hornblende is posttectonic and unstrained micas (biotite, chlorite and white mica) define the foliation, the bulk of the constituent mineral grains are therefore strain-free and considered to be recrystallised and/or neomineralised during the deformation. It is clear that the same rock units occupy both the Richtersveld Province and front zone.

### 2.2.2 Haib area

The front zones includes the whole area north-east of the front (Annex. 3). The pretectonic units here are subdivided into the mylonite gneiss and blastomylonite, streaky gneiss and porphyroblastic orthogneiss units. It will be argued that perhaps apart from the streaky gneiss, the other rock units are reconstituted equivalents of rocks of the Richtersveld Province.

The quality of outcrops are such that no complete gradation can be demonstrated across the front from the Vioolsdrif intrusives on the one side, to the deformed granitoids on the other side. A more abrupt onset of an intense cataclastic fabric in granitoid rocks is evident towards the south-eastern part of Witputs and marks the position of the front.

#### 2.2.2.1 Mylonite gneiss and blastomylonite unit

The mylonite unit is characterised by its megascopic cataclastic appearance and heterogeneity. Its contact towards the north-east with the streaky gneiss is concordant with the structural grain (Annex. 3), but towards the south-west the front forms a boundary with various units of the Vioolsdrif intrusive suite at an acute angle with the structural grain (Fig. 3.2). This arrangement substantiates the contention that the mylonite unit is the deformed equivalent of the Vioolsdrif Suite and associated volcanics and that the front is a structural boundary. Apart from a smaller scale heterogeneity the mylonites include mappable bodies of metasediments, metavolcanics and amphibolite, shown as a separate unit on the legend of Annex. 3. The bulk of the unit consists of deformed granitoid rock of predominantly more basic composition as judged by the amount of plagioclase and mafic minerals, with the deformed granitoids commonly containing mafic inclusions.

A typical aspect is a smaller scale or mesoscopic heterogeneity over a large part of the unit in the form or banding. The mesoscopic banding is due to the juxtaposition of several compositional types of granitoids in various states of deformation, a factor which considerably affects the appearance of a rock in the field. Interspersed are mesoscopic lenses and bands of (i) metavolcanics, so-called because of some associated 'volcaniclastics' and fine grain size; these have a completely recrystallised texture and show no signs of deformation on microscopic scale; at one locality intrusive relations can still be recognised between the granitoid and 'metavolcanics', and (ii) possible metasediments which include aluminous zones with a crystalloblastic fabric. A mesoscopic banding ($\leq$ 20 m) is particularly well developed in the north-eastern corner of Kromrivier where massive units of a fine-grained leucocratic rock (quartzo-felspathic), fine-grained pinkish rock (quartzo-felspathic), lenses of amphibolite (hornblendite) in texture resembling the basic phase of the Vioolsdrif suite, mylonite orthogneisses with inclusions and megascopic porphyroclasts commonly arranged in trains, schists and aluminous granoblastic rocks, alternate.

2.2.2.1.1 Cataclastic granitoids

*Less deformed granitoid*

Domains, or slabs, of less deformed granitoid were infrequently observed interbanded in the more intensely deformed cataclastic granitoids. The less deformed granitoid, nevertheless, displays an incipient mortar texture with the felspar megacrysts well deformed as evident from undulose extinction, fracturing and misoriented domains within a grain. In such a low-strain domain south-west of the Witputs/Kromrivier/Soekwater beacon, largish felspar porphyroclasts tend to abound locally, where they typically have their long dimensions parallel to the planar fabric, are irregular and rounded in shape, are fractured, and have a seriate size distribution (unlike syn- or postectonic blasts which tend to have a unimodal size distribution). The porphyroclastic rocks are thought to represent porphyritic granitoids while the more even-grained rocks were probably even grained granitoids; these two types compare with the adamellite and granodiorite of the Vioolsdrif Suite.

*More advanced deformed granitoid : mylonite gneisses*

The bulk of the deformed granitoids have a more advanced developed cataclastic microstructure and might be considered a further stage in the development. According to the nomenclature of Higgens (1971), some of these are termed mylonite gneisses and are megascopically characterised by a white spotted appearance. The white domains usually constitute more than 20 - 30 per cent by volume of the rock and comprise well-altered plagioclase grains, which are angular and considered pretectonic with respect to the foliation, because zoned grains are obviously broken, plagioclase grains have tapering twin lamellae due to mechanical twinning (see Smith, 1974, pp. 345 & 348), twin lamellae are bent, fracturing as seen in a slight optical misorientation across fractures and undulose extinction. An interesting feature here is that the white plagioclase grains in some samples are granular with regular contacts between the new grains and it is suggested that the formation of new grains is due to annealing of the plagioclase grains during their deformation. The grain size distribution is polimodal in most samples with the felspar porphyroclasts defining a distinct mode with average grain diameter in the order of 1,4 mm. The matrix consists of grains with an average diameter of 0,1 - 0,2 mm. The grain size distribution in some samples are such that it resembles a mortar texture, the quartz/quartz contacts in the matrix are regular which, together with the strain-free character of the quartz grains, points to recrystallisation while the felspar contacts are irregular and suggest a pretectonic origin for the felspar in the matrix. An intermediate stage in the development of the mylonite gneiss as described above is evident where remnants of felspar phenocrysts are still recognisable.

The use of the term mylonite gneiss instead of protomylonite is arbitrary, as it is difficult to judge the degree of recrystallisation against the degree of cataclasis (see Higgens 1971). Towards the north-west basement outcrops on Witputs, the mylonite gneisses complete with inclusions, carry coarse lath-like idioblastic felspars attributable to syntectonic felspar blastesis. The felspar idioblasts obviously escaped the cataclastic deformation and must therefore be of later origin. Unstrained poikiloblastic plagioclase with both quartz and felspar inclusions are present in some samples. The fabric is usually defined by the dimensional orientation of unstrained micas and hornblende; large hornblende needles are locally characteristic, while random or statistically oriented poikiloblastic or skeletal hornblende testify to their late growth. Quartz, where not affected by later deformation, is usually unstrained. Although felspar blastesis is present, the bulk of the felspar is pretectonic whereas the remaining mineralogy originated by recrystallisation or neomineralisation.

*More advanced deformed granitoid : blastomylonites*

Blastomylonites together with mylonite gneisses constitute most of the deformed granitoids. The blastomylonites are fine grained and difficult to identify as such in the field, especially where a granoblastic texture prevails. Trains of felspar porphyroclasts (Plate 3), together with augen and flaser forms, remained at places and allowed for field identification. Occasional idioblastic felspar, aligned parallel to the fabric, was also observed. The even-grained matrix of the rock shown in Plate 3 is fine with a mean grain size of ca. 0,2 mm. Most grain contacts are irregular, while undulose extinction is common for the leucocratic minerals. A perthitic K-felspar porphyroclast was seen to have a patchy cross-hatched development, incompletely developed along the margin of the grain from where it spreads irregularly inwards in a patchy vein-like manner. In accordance with Smith (1974, p. 386) the cross-hatched microcline twinning seem to be nucleated along the grain margin, possibly due to externally applied stresses. The blastomylonites are collectively called thus, although much of the material including the example above are better termed mylonites, according to the usage of Higgens, 1971. Megascopically the mylonites appear fine grained, but at least two grain size modes are developed : 1 - 0,5 mm and 0,1 mm. The distribution is not mortar-like, since the smaller fraction is irregularly distributed, while irregular contacts prevail and felspar, which predominates, shows deformation features like bending, mechanical twinning and uneven extinction. In the same rock a thin millimetre-wide banding is acquired by the arrangement of broken felspar fragments in stringers. The blastomylonites, *sensu stricto*, show an appreciable amount of felspar blastesis as is evident from poikiloblastic plagioclase and K-felspar. In such rocks large ($\leq$ 5 cm) K-felspar idioblasts may be megascopically scattered with their long axes preferentially in the fabric plane. The K-felspar idioblasts appear optically unstrained and contain inclusions of the surrounding matrix material. A seriate grain-size distribution and deformed felspar grains, indicate the partial cataclastic character of the blastomylonites.

*Planar fabric*

The planar fabric (fluxion structure of Higgens, 1971) in the cataclastic rocks is not always readily discernible, a fine millimetre-wide banding is commonly developed and can be perceived in cross-section on wheathered surfaces only, stringers of felspar also giving the same effect. In the coarser mylonite gneisses the foliation is defined by elongated felspar and felspar-fragment trains while in the fine, even-grained varieties a foliation seems absent, especially if mafic minerals are sparse. In rocks of suitable bulk composition a dark mineral fabric is well developed, while poorly developed dimensional fabric of the leucocratic minerals may be present in the coarser varieties where the foliation is also commonly anastomosing. Depending on bulk composition and grain size, therefore, some of the cataclasites do not seem to have a foliation penetrative on thin section scale.

2.2.2.1.2 Mappable bodies of metasediment and/or metavolcanics

Along the eastern boundary of Witputs, metasediments and/or metavolcanics (shown as yellow on Annex. 3) are interbanded in the mylonite gneisses and blastomylonites and are possibly correlates of the smaller scale interbands of metavolcanics and aluminous metasediments mentioned above. Schematic sections through two of these outcrops are shown in Fig. 2.7.

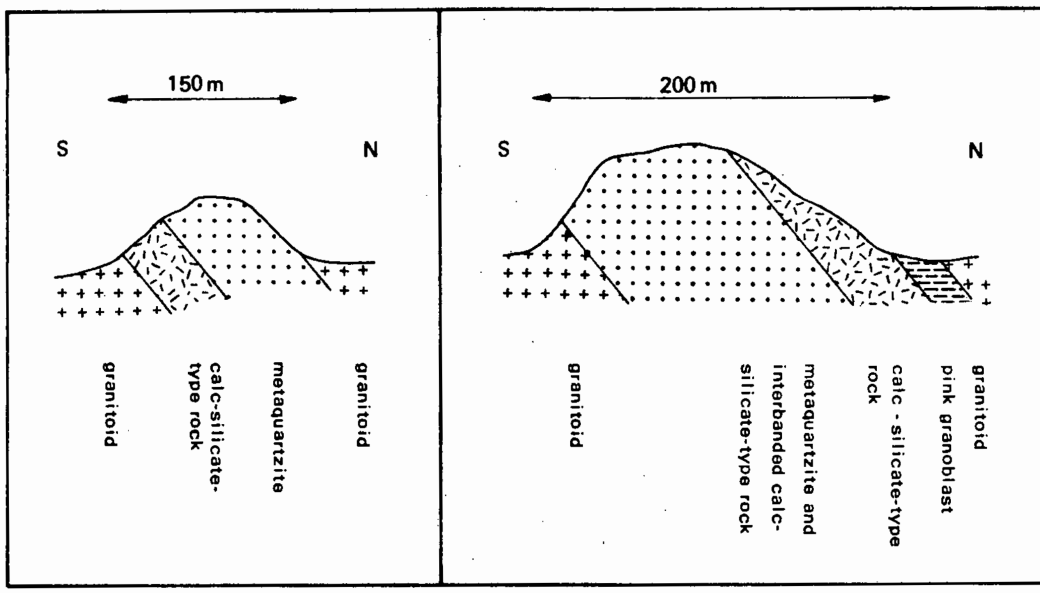


Fig. 2.7. Schematic field sketches of metasedimentary slabs in the cataclastic granitoids on Witputs. No intrusive relations were recognised.

2.2.2.1.3 Amphibolite

Sub-circular and mappable amphibolite bodies (Annex. 3) are situated within the mylonite gneiss and blastomylonite unit. The larger bodies are at most marginally foliated while the larger central portion lack a planar fabric. The smaller bodies of lenticular to banded form, constituting part of the smaller scale heterogeneity of the cataclastic granitoids, are more penetratively foliated with the regional foliation commonly wrapped around them. These relations indicate that the amphibolite bodies acted competently with respect to the deformation. The amphibolite bodies are not commonly homogeneous in make-up, but might comprise any number of the following rock types :

(i) a coarse hornblendite-type rock consisting of predominantly large ($\geq$ 1 cm) equidimensional hornblende grains

(ii) a finer grained quartz-plagioclase-hornblende phase which appears intrusive into the coarse variety, and

(iii) a breccia with angular fragments of the coarse variety embedded in a fine-grained quartzo-felspathic matrix.

A lenticular body situated in the north-eastern corner of Kromrivier (not shown on map) is atypical, due to its marked heterogeneity and garnet content. Apart from varieties (i) and (iii) mentioned above, plagioclase-biotite and garnet-biotite rock types occur; the garnet seems to be syn- or posttectonic with respect to the foliation which partially pervades the body. In the south-eastern corner of Witputs the breccia mentioned in (iii) occurs as bands parallel to the regional grain and are extensive along strike, although only several metres wide. The hornblendite-like angular fragments do not appear markedly flattened, although the regional foliation commonly pervades the breccia bands.

2.2.2.1.4 Discussion

The mylonite gneiss and blastomylonite unit with the associated amphibolite bodies and older metavolcanics differ from the Vioolsdrif intrusives and associated older volcanics only with respect to deformation imprint. The stronger deformational imprint commences along the front and remains such towards the north-east. The Vioolsdrif intrusives comprises a suite ranging from basic types to leucocratic granites. Deformed equivalents of a similar range of rock types were recognised amongst the cataclastic granitoids with granodiorite/adamellitic types predominating as is the case in the Richtersveld Province. The amphibolite bodies within the mylonite gneiss and blastomylonite unit resemble the basic phases of the Vioolsdrif Suite in composition, texture and mode of occurrence. In view of these features, together with the spatial arrangement (Section 2.2.2.1, first paragraph) it is concluded that the cataclastic granitoids represent more intensely deformed Vioolsdrif intrusives.

The occurrence of metasediments (metaquartzites, calc-silicate rocks and aluminous sediments) as minor bodies within the cataclastic granitoids is interesting, as sediments associated with the Haib Subgroup are virtually absent in the Haib area (Annex. 3).

From the description above, it is clear that largely the same spectrum of lithological units encountered in the Richtersveld Province is found within the mylonite gneiss and blastomylonite unit, with a markedly different structural imprint and scale of heterogeneity, however, attributable to more advanced flattening and transposition. A detailed account of the metamorphism associated with the regional foliation in the Haib area is not given in this report. The petrographic work done, however, does clearly show a prograde metamorphic zonation from the Orange River towards the north-east. Medium-grade conditions were attained several kilometres south-west of the front in the Richtersveld Province. Higher grade conditions towards the north-east is indicated by the presence of both fibrolite and andalusite in aluminous rocks of the mylonite gneiss and blastomylonite unit. This, together with the advanced stage of annealing in the same unit, as shown by the formation of new plagioclase grains in the deformed granitoid, testify to the relative high-grade associated with the increased deformation in the front zone as described above. A similar prograde metamorphic and deformational development is described in detail for the lower Fish River area (see e.g. Sections 4.1 & 4.2).

### 2.2.2.2 Porphyroblastic orthogneiss unit

The porphyroblastic orthogneiss unit is bounded on both sides by streaky gneiss, the contacts between these two rock units are obscured by cover. Apart from a few interspersed concordant amphibolite bands, the orthogneiss is homogeneous. The rock has a markedly dark-coloured groundmass, studded with large K-felspar porphyroblasts. Small, flat discoidal-shaped mafic inclusions are common and considered to indicate an intrusive origin. A foliation which is penetrative down to thin section scale, is megascopically well defined by the dark minerals. The K-felspar porphyroblasts are commonly wrapped around by the foliation, while some are idioblastic with their long axes (2 - 4 cm) preferentially, but poorly oriented parallel to the foliation so that the longer dimensions of some K-felspar laths lie at a large angle to the trace of the foliation. In keeping with the thesis developed in the following paragraph, these K-felspars are considered as the products of syntectonic metamorphic growth and not phenocrysts; the syntectonic growth is inferred as follows :

(i) a pretectonic origin is excluded by the common occurrence of felspar laths at large angles to the foliation, and the weak imprint of deformation features

(ii) the foliation which is wrapped around the felspars is evident of continuing progressive strain

(iii) idioblastic forms point to late blastesis (see Spry, 1969, p. 262).

Locally where the K-felspar porphyroblasts are more sparsely developed, the matrix together with the flattened inclusions, are strongly reminiscent of deformed Vioolsdrif granitoid as seen elsewhere in the front zone. If this is indeed the case, the matrix of the porphyroblastic orthogneiss should have an equally strong deformational imprint. A penetrative planar fabric and strong deformation of the inclusions is megascopically apparent. Microscopically, though, the texture is crystalloblastic, with regular and polygonal shapes testifying to a recrystallisation/crystallisation rate exceeding that of deformation; the foliation is defined only by the location and dimensional orientation of biotite and skeletal hornblende. The deformational textures typical of the cataclastic granitoids of the front zone (Section 2.2.2.1.1) are absent here, but the late growth of skeletal hornblende and poikiloblastic felspar (albite-twinned with a refractive index smaller than that of quartz) in the matrix suggests a metamorphic origin, and not syntectonic crystallisation from a melt.

It is concluded, therefore, that the porphyroblastic orthogneiss developed from a pretectonic rock, on megascopic appearance possibly the Vioolsdrif granitoids, under conditions more favourable for recrystallisation than further southwards towards the front. A discordant U/Pb zircon age of 1865 Ma (sample BB-3, Dr A J Burger, NPRL, CSIR) substantiates the contention that the porphyroblastic orthogneiss represents a reconstituted Vioolsdrif granitoid.

### 2.2.2.3 Streaky gneiss unit

Apart from some irregularly disposed heterogeneities, the streaky gneiss is a homogeneous rock on outcrop scale. Although no well-exposed contacts with the adjacent gneisses were found, the streaky gneiss outcrops along the contacts show no gradation from the mylonite gneisses, blastomylonites and porphyroblastic orthogneisses. It is a pretectonic unit in juxtaposition to reconstituted Vioolsdrif granitoids and in megascopic appearance unlike metavolcanics. Its pretectonic parentage remains a matter of conjecture. It is predominantly a fine-grained quartzo-felspathic gneiss with mafic minerals (biotite, epidote, muscovite and ore) preferentially located along millimetre-thin and discontinuous streaks; plagioclase is also concentrated along the mafic domains. The alternating leucocratic bands, also of millimetre width, consist of quartz, microcline and plagioclase with the plagioclase content being markedly less than in the mafic domains. In some samples the quartz/quartz contacts are regular and form polygonal grains, while the felspar boundaries are irregular. Deformation textures are subordinate and the texture is generally crystalloblastic. The partition of the mineralogy into basic and acid components here is suggestive of some metamorphic segregation process, but no conclusive arguments can be forwarded at the present qualitative state of the investigation.

The structural imprint of the streaky gneisses is different from that of the other gneisses in the front zone. The penetrative regional foliation is concordant with the general grain of the front zone, but defined by a penetrative microscopic banding (preferred location and orientation of the mafic minerals) of distinct crystalloblastic character. The banding/foliation is pervasively deformed by a set of small folds. The other rock units of the front zone are not penetrated by a small scale banding, their textures generally not crystalloblastic and the regional planar fabric is not pervasively deformed by subsequent minor folding.

Large mesoscopic lithological heterogeneities are irregularly disposed in the streaky gneiss unit and discontinuous along strike. These rock types include amphibolites, aluminous rocks, epidote-rich and calc-silicate rocks, some of which are reminiscent of the metasedimentary/volcanic heterogeneities in the mylonite gneiss and blastomylonite unit.

In conclusion, it is pointed out that the streaky gneisses have more in common with the higher grade terrain of the Namaqua Province towards the north-east and contrast with the rocks of the Richtersveld Province and their reconstituted equivalents in the front zone. A discordant U-Pb zircon age of 1790 Ma (Dr A J Burger, CSIR) can be considered a minimum for this unit.

## 2.3 Namaqua Province

### 2.3.1 Introduction

The areal distribution of the various rock units in the part investigated, of the Namaqua Province (defined in section 3.1), is shown in Annex. 1 & 2. It is customary to refer to these rock units, *in toto*, as the Namaqua Metamorphic Complex, according to lithostratigraphic principles. In a discussion on the subdivision of this stratigraphic unit (Blignault, 1974) the importance of classifying within tectonic domains prior to correlating between domains, is stressed.

### 2.3.2 Pretectonic gneisses

#### 2.3.2.1 Introduction

In the present investigation the first distinction within domains is according to tectonic category (after Wynne-Edwards, 1969). Pretectonic gneisses are considered to have been *in situ* prior to the first recognisable deformational imprint as defined for each domain (Section 3).

The deformational and metamorphic imprint on the pretectonic gneisses under consideration, is of such an intensity that stratigraphic facing directions were never recognised and the pretectonic nature of the rock units is not always clear from field observations.

### 2.3.2.2 Mafic gneiss unit

The mafic gneiss unit comprises mafic gneiss and a thin underlying metaquartzite band. The unit forms a macroscopic band (Annex. 1) which is concordant to the regional grain of the marginal zone and tapers off towards the east. The whole unit is situated within grey gneiss and might be similar to some of the mappable mafic bands in the grey gneiss of the central zone (Section 2.3.2.4.2). The underlying grey gneisses are recognisably reconstituted Vioolsdrif granitoids. No intrusive contacts were recognised, and on small scale the contacts are sharp, while on mesoscopic and macroscopic scale concordant interbanding[1] along the contact zone is common. The overlying grey gneisses form a relatively sharp and locally intercalated boundary with the mafic gneiss unit.

#### 2.3.2.2.1 Metaquartzite

The structurally underlying metaquartzite band pinches out westwards and bifurcates towards the east (Annex. 1); it is homogeneous in bulk with rare phyllitic bands. Some metaquartzite was locally found to overlie the mafic gneiss. Apart from the well-developed regional foliation, thin ($\leq$ 1 cm) black bands defined by a concentration of ore grains, and more leucocratic bands are locally present and probably represent primary stratification. Muscovite flakes, the dimensional orientation of quartz grains, as well as a fine 'tectonic' lamination, define the regional foliation. The metaquartzite is fine grained and granoblastic elongate, with no sign of any detectable primary grain outlines. The rock consists mainly of quartz (ca. 100 - 95 per cent) and muscovite (ca. 0 - 5 per cent) with subordinate amounts of felspar ($\leq$ 1 per cent).

#### 2.3.2.2.2 Mafic gneiss

The mafic gneiss/metaquartzite contact is consistently sharp and not interbanded as in the case of the 'lower' metaquartzite/grey gneiss boundary and the 'upper' mafic gneiss/grey gneiss boundary. The mafic gneiss includes at least two bands (5 - 30 m) of 'volcanic breccia' (in the broader sense of Parsons, 1969), situated at, or near, the contact with the metaquartzite and in the upper portion of the mafic gneiss sequence. The fragments are well flattened and composed of quartz porphyry, fine-grained leucocratic rock, pegmatoidal rock and other types. The bulk of the mafic gneiss is monotonously

---

[1] This type of contact, fairly common in the gneissic terrain, does not generally allow for conclusive interpretation and may be regarded as possibly primary, tectonic or both.

homogeneous on a mesoscopic scale, and weathers conspicuously dark with local occurrences of a more leucocratic variety. The planar fabric, very well developed and penetrative down to thin-section scale, is defined by the preferred dimensional orientation of the mineral grains; banding down to even this scale is noticeably absent. Porphyroblastic hornblende, set in a fine-grained matrix, gives the rock a decidedly spotted appearance on hand-sample scale. Hornblende and epidote are the main mafic minerals (Table 2.3) and generally constitute less than 50 per cent by volume of the rock. The leucocratic minerals quartz and felspar show very little strain features with regular grain boundaries.

2.3.2.2.3 Discussion

Most primary features are destroyed by the deformational imprint and grade of metamorphism. It is argued that the mafic gneiss unit represents a volcano-sedimentary sequence intruded by granitoids prior or early with respect to the deformation. The metaquartzite is considered to be of sedimentary origin[1] on the strength of its composition and nature of some compositional layering, but whether of clastic or of chemical origin, is unknown. The striking homogeneity of the mafic gneiss together with the horizons of volcanic breccia, so named on the basis of the porphyry-like nature of some of the

| Sample No. | Hornblende | Epidote | Chlorite | Biotite | Microcline | Plagioclase | Quartz |
|---|---|---|---|---|---|---|---|
| B-466 | X | X | | X | X | X | X |
| B-469 | X | X | | | | X | X |
| B-507 | X | X | | | | X | X |
| B-514 | X | X | X | | X | X | X |
| B-515 | X | X | | X | X | X | X |
| B-521 | | X | X | | | X | X |
| B-585 | X | X | | | | X | X |
| B-586 | X | X | | X | X | X | X |
| B-675 | X | X | | X | X | X | X |

Table 2.3. Main mineral assemblages of the mafic gneiss.

[1]Not all rocks in metamorphic belts, conveniently referred to as metaquartzites, need be of sedimentary origin as tectonically derived vein quartz on further deformation and metamorphism, should assume similar textural characteristics.

fragments, indicate a volcanic origin; the mafic gneiss is estimated to be andesitic in bulk composition. The interbanded contacts, as previously noted, especially that of the metaquartzite and underlying grey gneiss (reconstituted Vioolsdrif granitoids), can be of tectonic origin. If this was the case, similar contact relationships should exist between the metaquartzite and mafic gneiss; this contact is remarkably sharp and lacks interbanding. It is therefore inferred that the concordant bands and lenses of grey gneiss situated within the mafic gneiss unit along the contact zones are flattened offshoots of intrusive granitoid.

On the basis of the inferences above, it seems likely that the mafic gneiss unit represents tectonically reconstituted volcanics of the Orange River Group.

### 2.3.2.3 Banded amphibolite unit

The banded amphibolite unit (Annex. 1) is conformable to the other gneiss units in the marginal zone. It is bounded to the south by the syntectonic augen gneiss and structurally overlain by grey gneiss to the north. East of the Fish River it is tangentially disposed against a mylonite belt of regional extent, which also divides the marginal from the central zone. The banded nature ($\leq$ 10 cm) of the amphibolite is characteristic (Plate 4), but varies in regularity to such an extent that the amphibolite appears homogeneous in zones ($\geq$ 100 m) especially along the Konkiep River where grey gneiss was also found interbanded with the amphibolite.

#### 2.3.2.3.1 Banding in the amphibolite

A significant, but irregularly scattered ingredient of this amphibolite unit, is metaquartzite bands, (Plate 5) varying in width from centimetres to mappable bodies along the Konkiep River (Annex. 1). Their sedimentary nature (chert or sandstone) is inferred from the predominant quartz content ($\pm$ minor quantities of muscovite, microcline and plagioclase) of the rock. The metaquartzite is fine to medium grained and no clastic grain boundaries were detected. The commonest type of heterogeneity rendering the amphibolite its banded nature (Plate 4) is best described as fairly thin ($\leq$ 10 cm) quartzo-felspathic somes with varying amounts of hornblende and/or biotite (Table 2.4). These leucocratic bands which are fine grained and exhibit some of the earliest structures recognised (Plate 4) in this domain, are, on the strength of their internal banding, interpreted as a primary component of the rock and not as migmatitic leucosomes. Pegmatoidal neosomes (1 - 3 cm) of concordant and lenticular habit are pervasive, but not regularly distributed in the amphibolite unit.

| | Hornblende | Biotite | Epidote | Plagioclase | Microcline | Quartz | |
|---|---|---|---|---|---|---|---|
| B- 70 | X | X | X | X | | X | |
| B-411 | X | | X | X | X | X | Plagioclase is predominant mineral |
| B-412 | X | | X | X | | X | Plagioclase is predominant mineral |
| B-413 | X | | X | X | | X | |
| B-623 | | X | | X | X | X | Microcline-microperthite |
| B-626 | X | | | X | | X | |
| B-670 | | | X | X | | X | |
| B-671 | | | | X | | X | |

Table 2.4. Mineral assemblages of the leucocratic bands in the banded amphibolite unit. Epidote is present in minor quantities while secondary chlorite is associated with refoliation.

2.3.2.3.2 Amphibolite

Apart from the banding described above, the bulk of the unit consists of amphibolite of consistent appearance throughout the area, although locally, a thin banding (centimetre scale) can be recognised by a slight variation in hornblende content. The regional foliation is, apart from the banding, penetrative down to grain scale and defined by the dimensional orientation of the constituent mineral grains; hornblende prisms generally define the regional lineation in the plane of the foliation.

The amphibolite is fine to medium grained, granoblastic elongate with the mineral grains appearing unstrained, except where a later deformation affected the rock with the additional retrogressive development of chlorite. The hornblende locally displays a poikilobastic habit. Quartz, with peculiar rounded to cuspate contacts with other minerals, is present in varying amounts, but the hornblende generally predominates over the leucocratic minerals giving the rock its characteristic dark colour. The mineral assemblages are listed in Table 2.5.

| | Hornblende | Epidote | Plagioclase | Quartz | An content of plagioclase | |
|---|---|---|---|---|---|---|
| B- 18 | X | X | X | X | 36 | |
| B-406 | X | | X | X | - | some carbonate-mineral grains |
| B-414 | X | X | X | X | - | |
| B-554 | X | X | X | X | 35 | |
| B-573 | X | | X | | 41 | |
| B-672 | X | | X | X | 43 | |

Table 2.5. Mineral assemblages of the amphibolite in the banded amphibolite unit. Epidote is present as minor quantities.

2.3.2.3.3 Discussion

The stratigraphic position of the unit is not clear and apart from the underlying sheet of augen gneiss interpreted as an early syntectonic intrusive, is situated amid a vast terrain of grey gneiss. By virtue of its primary banding, this amphibolite is lithologically not comparable to the mafic gneiss unit or other amphibolites which form part of either the paragneiss or grey gneiss units. The lithological characteristics recognised in the field do not suffice for conclusive statements regarding a sedimentary or volcanic origin for the unit. The primary lithological variation of the unit - amphibolite, leucocratic bands and metaquartzite - might conceivably represent reconstituted basalts with intercalated acid volcanics and chert, especially when it is considered that the now thinnish leucocratic bands were considerably flattened. Through lack of more data, though, it is also possible to invoke a full sedimentary sequence of comparable composition.

2.3.2.4 Grey gneiss unit

The term grey gneiss is used here to designate a distinctly heterogeneous pretectonic gneiss and should not be confused with the terminology of Von Backström (1964) who used grey gneiss for a syntectonic granite in the Keimoes area.

The present usage of the term is preferred as it is well entrenched amongst local geologists, and similar looking rocks in mobile belts elsewhere are similarly described (Dearnley & Dunning, 1968; Wynne-Edwards & Hasan, 1972). The various corresponding rock units in neighbouring areas are grouped under the term mixed gneiss in Blignault et al. (1974). The grey gneiss unit as mapped in the Ai-ais area (Annex. 1) combines a fairly broad spectrum of rock types, but is more consistent in appearance when divided according to tectonic domain. The grey gneiss of the front zone, between the front and the mafic gneiss unit, is recognisably reconstituted Vioolsdrif granitoids and associated rocks as described in Section 2.2, while that of the remainder of the marginal zone and the central zone is described under separate headings below.

#### 2.3.2.4.1 Marginal zone

The reworked Vioolsdrif granitoids of the front zone (Section 2.2) passes imperceptibly into the more typically banded grey gneiss of the marginal zone, situated to the north-east of the mafic gneiss unit. This lithological change is accompanied by an increase in metamorphic grade and more complex and intense structural development (Sections 3 & 4). The main characteristic of this grey gneiss is the banding in a matrix of granitoid composition. The contacts of the grey gneiss with the other pretectonic units of the marginal zone are either sharp or interbanded over a limited distance. Primary features possibly relating the bulk of the grey gneiss conclusively to either an igneous or sedimentary origin are sparse, or non-existent, over large areas. Interbanded occurrences of indubitable metasediments are rare and cannot be considered a characteristic feature. A most striking mesoscopic feature of grey gneiss is the lithological variability, repeated in monotonous succession, to yield a rather overall homogeneous rock when viewed on a regional scale. The bulk, or matrix of grey gneiss accommodating the small scale banding, is predominantly a greyish quartzo-felspathic rock with biotite and/or hornblende as the mafic constituent. Texturally the rock is equigranular and fine grained ($\leq$ 1 mm); two varieties of the grey component are distinguished on the basis of mineral distribution

(i) on thin section scale the dark minerals are uniformly distributed

(ii) the dark minerals tend to group in streaks which might be anastomosing around leucocratic domains consisting predominantly of fine-grained quartzo-felspathic aggregates, or else felspar; this domainal fabric tends to give the rock a coarser appearance.

These two varieties of grey gneiss are interbanded on both mesoscopic and macroscopic scale. A smaller scale mesoscopic banding is generally in the order of centimetres and range in thickness to several metres, comprising predominantly mafic gneiss, amphibolite and leucosomes. Some local descriptions follow to illustrate variations from the general appearance given above. On the south-western part of the farm Kanabeam the deformed Vioolsdrif granitoids of the front zone grades (described in Section 2.2.1) into banded gneisses with a marked schistose character. This is also the approximate locus from where concordant leucosomes become more prominent towards the north-east. The prominent cataclastic texture of the front zone gneisses is hardly discernible here, while the new growth of micas and the compositional banding defines the regional foliation. Amphibolite bands (1 - 2 m), sparsely developed in the front zone, become more prominent here and alternate with quartzo-felspathic bands of several metres varying in mafic mineral content to produce a prominent variability across strike; bands of augen gneiss can be observed at irregular intervals. Discontinuous bands of aluminous gneiss and metres-thin metaquartzite bands were observed at four localities only. The pretectonic nature of these rocks is largely obscured by tectonic reworking, but the available evidence nevertheless suggests that, at least in this vicinity, the banded gneisses are reconstituted rocks of the Richtersveld Province and largely derived from granitoids and volcanics. The following arguments suggest this inference :

(i) The banded gneisses include some small hornblendite bodies resembling the earlier basic phase of the Vioolsdrif Suite (Section 2.1.3.1) and escaped much of the deformation due to their more competent nature.

(ii) The grey quartzo-felspathic gneiss in this region also includes some widely scattered mafic inclusions, mostly flattened and drawn out into lenses, but locally having a more equidimensional shape. Their tectonic derivation from the extension of a competent mafic band is a possibility, but their complete isolation favours a xenolithic origin.

(iii) There is no distinct tectonic or lithological discontinuity between the deformed Vioolsdrif granitoids of the front zone and the banded gneisses on Kanabeam.

Northwards from the mafic gneiss unit in the vicinity of the type Gannakouriep dyke (Annex. 1), a leucocratic quartzo-felspathic gneiss (ca. 10 m units) alternates with a more mafic variety also containing amphibolite bands. Augen gneiss bands are irregularly repeated in the banded sequence and commences, from south to north, more or less in the same position as the pegmatoidal leucosomes which remain part of the grey gneiss unit further to the north-east.

Along and east-wards of the Fish River and immediately north of the mafic gneiss unit the quartzo-felspathic gneiss is distinctly pinkish with a low mafic mineral content imparting a streaky appearance to the rock. Locally, felspar augen are preserved, suggesting an igneous origin, a notion further substantiated by the occurrence of flattened xenoliths in a more mafic quartzo-felspathic gneiss, alternating here with the pinkish variety on a macroscopic scale.

Both types display a smaller scale banding and are pervaded by amphibolite bands ($\leq$ 2 m). These characteristics persist upstream along the Fish River to the syntectonic augen gneiss. Attention should be drawn here to the juxtaposition of a leucocratic and more mafic 'orthogneiss' sequence which compares well with the deformed leucogranite and granodiorite phases of the Vioolsdrif Suite situated immediately south of the mafic gneiss unit.

North of the Konkiep/Fish River confluence, towards the syntectonic augen gneiss, a body of mafic gneiss is situated within the grey gneiss. This mafic gneiss is hornblende-rich and homogeneous in part, but a small-scale banding is typical and due to the variation in mafic mineral content. In the homogeneous portion some flattened amphibolitic inclusions were observed, while within the banded part, a discontinuous zone (0,3 m wide) with deformed amphibolite and more leucocratic clasts resembling a volcanic breccia or psephite, were found. These primary features are interpreted as suggesting that the gneisses represent a deformed intrusive/extrusive complex.

### 2.3.2.4.2 Central zone

There is no obvious lithological difference between the grey gneiss of the marginal and central zones when compared locally across the mylonite belt. Some important differences emerge though, when compared on a regional scale. Relict primary features by which its pretectonic nature can be judged, virtually are non-existent. Whatever its origin, the subsequent tectonic reconstitution was complete and produced a well-banded migmatitic gneiss with amphibolite bands and leucosomes embedded in a quartzo-felspathic rock of a greater consistent appearance than that of the marginal zone. Similar to the grey gneiss of the marginal zone, the two textural types of the grey component (domainal and non-domainal) persist here in the same fashion. Locally, the grey gneiss is reconstituted to advanced stages of migmatization, but is predominantly in a stage of metatexis. Characteristic for part of the central zone is the frequent occurrence of mappable amphibolitic and mafic gneisses with associated metaquartzites (Annex. 1).

For the purpose of convenience and a more detailed description of field aspects the area in the central zone, underlain by grey gneiss, is subdivided into subareas.

(i) The zone immediately north of the mylonite belt and in the vicinity of Dreikopf and Leikop.
A particularly well-banded variety is depicted in Plate 6; the quartzo-felspathic greyish paleosomes is also commonly homogeneous across larger dimensions (metres). Together with the concordant pegmatitic leucosomes (centimetres) and amphibolite bands (centimetres), augen gneiss bands contribute to the heterogeneity of the gneiss, with the

gneisses locally attaining a more schistose character. Around Dreikopf the grey gneiss unit is more leucocratic and apart from the migmatitic banding, rather homogeneous. This variety of the grey gneiss unit forming a macroscopic heterogeneous element, has not been regionally recognised as a distinct stratigraphic band within the unit. The mappable amphibolites are not ubiquitous and at the Konkiep River marble lentils were found to overlie the amphibolites. At two localities metaconglomerate/volcanic breccia, with limited local extent were found interbanded in the grey gneiss; at the one outcrop on Kanabeam aluminous knotty schist and marble are associated.

(ii) The zone of grey gneiss immediately (ca. 3 km south-west of the paragneiss unit contact) underlying the paragneiss unit.
The gneisses here are essentially similar to those elsewhere in the central zone. The mafic mineral content of the paleosome is predominantly biotite and the schistose character locally encountered southwards in the central zone, is here lacking. In the vicinity of Attie Se Kop the grey gneiss underlying pink gneiss, has a more homogeneous character, is coarser grained and even the ubiquitous leucosome banding is sparsely developed. The foliation in this granoblastic rock is conspicuous as dark mineral streaks. Several tens of metres below the pink gneiss contact, megascopically visible quartz ribbons were locally observed as a typical characteristic of the grey gneiss fabric. The frequency of amphibolite interbanding is variable, whereas the thickness of individual bands range from approximately 1 cm to several metres; boudinage structures are common.

(iii) The 'embayment' of grey gneiss within the Ai-ais Complex at Ai-ais deserves special comment due to its slight atypical appearance. The paleosomes here are distinctly medium to coarse granoblastic, whereas the gneiss is riddled with concordant leucosomes varying from millimetres to centimetres in thickness. In part, the rock appears to consist only of neosomes and melanosomes, these effects can be interpreted as being due to more advanced metatexis than found elsewhere.

(iv) The northernmost grey gneiss encountered on the farms Wegdraai and Kochas (Annex. 1) exhibits a regular stratigraphy. Repeated by late east-west antiforms and synforms are mappable amphibolite and mafic gneiss[1] zones associated with thin metaquartzite bands. Some of these zones have a symmetrical internal arrangement thus :

---

[1] The term mafic gneiss is used here to denote a dark weathering gneiss with a prominent mafic mineral content, yet more leucocratic and variable in mineralogy than the typical plagioclase-hornblende amphibolite.

| | | |
|---|---|---|
| grey gneiss | or | grey gneiss |
| metaquartzite | | amphibolite |
| amphibolite | | metaquartzite |
| metaquartzite | | amphibolite (thick) |
| grey gneiss | | metaquartzite |
| | | amphibolite |
| | | grey gneiss |

The repetition suggests stratigraphic duplication by earlier isoclinal folding in view of mesoscopic structural evidence presented elsewhere.

2.3.2.4.3 Discussion

The pretectonic parentage of the grey gneisses of the central zone presents a problem not conclusively solved by the scale of mapping employed. Similar gneisses elsewhere (e.g.Wynne-Edwards, 1972, p. 282) are regarded as constituting the pretectonic basement complex, but apart from the fact that the paragneiss sequence structurally overlies the grey gneisses, no evidence in this regard was recognised. A volcano-sedimentary origin for at least part of the sequence is suggested by the amphibolite-metaquartzite interbands and by the few odd metasedimentary beds which cannot be attributed to infolding of the paragneiss unit. Large portions are homogeneous on a large scale, and an intrusive origin cannot be disregarded. The mineralogy of the paleosomes suggests a bulk granitic to granodioritic composition, which means that the grey gneiss might either represent tectonically reworked greywackes, granitoids and/or dacites. The ubiquitous presence of the small-scale amphibolite bands, in centimetres to metres, suggests an original layered sequence, or may represent a mafic dyke suite rotated in the main fabric plane. It is thought that the grey gneiss with distinct domainal fabric represents sheets of early intrusives while the finer and uniformly textured grey gneiss, amphibolite and metaquartzite are the remains of a volcano-sedimentary pile.

The grey gneisses of the marginal zone contain relict features pointing to an intrusive/extrusive origin. In view of the progressive transition from the rocks of the Richtersveld Province to the marginal zone gneisses, it is reasonable to assume that they represent reconstituted Vioolsdrif granitoids and Orange River volcanics. It is perhaps important to note that the lithological variations within the marginal zone and the compositional variation of the grey gneiss as described above, taken together with the mafic gneiss unit (Section 2.3.2.2) and the banded gneiss unit (Section 2.3.2.3), reflect the lithology of the Richtersveld Province. Mafic dykes 'predating' the regional fabric are present in the Richtersveld Province, but were infrequently observed towards the front zone; the frequency of occurrence of amphibolite bands in the marginal zone may be accounted for by structural duplication.

### 2.3.2.5 Paragneiss unit

The paragneiss unit which occurs only in the central zone, with respect to the late folding, structurally overlies the grey gneiss unit and in places are infolded by early folding in the grey gneiss. Towards the north it is intruded by the early megacrystic granite gneiss. The paragneiss sequence, where fully developed, consists of a pink gneiss structurally overlain by an amphibolite band (Plate 7) and aluminous gneisses constituting the bulk of the paragneiss unit. It is important to note that the distribution of indubitably infolded relicts in grey gneiss is limited to close proximity to the regional grey gneiss/paragneiss contact. The few paragneiss outcrops interbanded in grey gneiss elsewhere, seem stratigraphically unrelated to the paragneiss unit.

#### 2.3.2.5.1 Pink gneiss

The term pink gneiss conveniently describes the field-appearance of this rock and was first used by Lamont (1947) to describe similar looking rocks. The distribution of the pink gneiss is limited and only locally, in the Attie Se Kop area, forms the structural base of the paragneiss unit. Elsewhere, at Kwaggasnek, it is absent from the stratigraphic sequence. Its lower contact with grey gneiss is generally sharp, but interbanding has been observed. The grey gneiss underlying the pink gneiss in the Attie Se Kop area (Section 2.3.4.2 (ii)) is slightly atypical in being more homogeneous, and typically contains quartz ribbons. This can be interpreted as a lithological likeness to pink gneiss, but may also represent a macroscopic variation of the grey gneiss unit fortuitously located with no genetic bearing on a stratigraphic sequence. The pink gneiss is, on both small and large scale, lithologically, mineralogically and texturally homogeneous. The bulk of the rock is poorly foliated, granoblastic fine grained and consists predominantly of quartz, K-felspar and plagioclase, with biotite not uncommonly rendering the gneiss a streaky character. Leucosomes are sparsely developed, while amphibolite bands were infrequently observed.

#### 2.3.2.5.2 Amphibolite

The amphibolite which forms the middle unit of the paragneiss sequence is hardly mappable on the scale of the map (Annex. 1), but has a more widespread distribution than the pink gneiss. Where the pink gneiss is absent, the amphibolite forms the boundary between the aluminous gneisses and underlying grey gneisses; this amphibolite is similar in appearance to the numerous amphibolites of the grey gneiss unit, but is characterised by an underlying aluminous marker zone of minor dimensions. Near Klipbokkop this aluminous zone, containing hand-size discoids of sillimanite, immediately underlies the amphibolite, while along the Ai-ais main road it is interbanded in the grey gneiss underlying the amphibolite. There is locally a greyish homogeneous quartzo-felspathic gneiss developed between the pink gneiss and amphibolite; the contact, however, is generally sharp or there might be a thin (1 m) transitionary zone developed consisting of thin calc-silicate and aluminous bands. The amphibolite itself is a fine-grained granoblastic rock and homogeneous over its entire width. The mineral assemblage of the amphibolite is as follows :

hornblende + labradorite $\pm$ diopside $\pm$ quartz.

At one locality, close to the northern boundary of Kwaggasnek, part of the amphibolite has a mottled (serpentine) appearance with the following mineralogy :

cummingtonite + orthopyroxene (pink pleochroic and optically positive) + serpentine + green spinel.

Its ultramafic character suggests an igneous origin.

2.3.2.5.3 Aluminous gneisses

The aluminous gneisses form the bulk of the paragneiss unit and structurally overlie a large mass of grey gneiss to the south-west with a thin veneer of pink gneiss and amphibolite in between. To the north-west, the aluminous gneisses are intimately associated with large massifs of syntectonic granitoid (Annex. 1). The aluminous gneisses crop out over a large area and is thought to be the dominant pretectonic gneiss from Kwaggasnek towards Lord Hill in the north-east, beyond Grünau, a distance of 140 km across strike extending outside the map boundaries. Within this wide expanse of aluminous rock obvious marker horizons are absent, lithological variation is limited and the gneisses repeat themselves monotonously. Structural evidence indicates stratigraphic duplication, but the lateral persistence of the aluminous sequence, without the reappearance of other pretectonic gneiss types, suggests a considerable stratigraphic thickness.

On Kwaggasnek and adjoining areas the lower boundary with the amphibolite is sharp; thin calc-cilicate and amphibolite intercalations sometimes occur along the contact. Calc-silicate and metaquartzite bands (centimetres) are also prominently developed where the aluminous gneisses directly overlie the pink gneiss. The aluminous sequence is conspicuous for its brown weathered surface.

A variety of interbanded lithological types constituting the sequence of which garnet-sillimanite-cordierite gneisses and biotite gneisses form the main components[1] alternating in units varying in thickness from one to several metres to yield a mesoscopic banding. Also characteristic are sparsely developed thin (centimetres) metaquartzite and calc-silicate bands; the latter are disrupted locally and deformed into cylindroidal boudins. Amphibolite or mafic varieties are sparse while concordant leucosomes are present, but generally do not form a significant proportion of the rock. This interbanding of lithological types gives rise to a heterogeneous gneiss as seen on large mesoscopic scale, but repeats itself on a regional scale to yield a macroscopically homogeneous gneiss.

Apart from the coarse blastic growth of garnet and sillimanite the aluminous gneisses in general are fine grained ($\leq$ 2 mm). The southernmost outcrops on the farms Kwaggasnek and Gaibes are distinctly schistose, but become markedly less so north-wards towards the higher grade metamorphic terrain. A foliation is well developed and generally parallel to the lithological interbanding described above. Peculiar, but significant perhaps, is the rhythmic banding (Plate 8) in an aluminous rock on Gaibes which strongly suggests sedimentary layering. A typical characteristic of the garnet-sillimanite-cordierite gneisses, the highly aluminous type component of the sequence, is a persistent small scale (millimetres) banding defined by the distribution of the aluminous minerals. Apart from the layering no other primary structures or textures were observed.

The biotite gneisses are typically fine grained ($\leq$ 1 mm) and locally contain sufficient biotite to render the rock schistose. Towards the north-east (beyond Grünau) biotite schists constitute a much larger proportion of the aluminous gneisses than in the Ai-ais area where the garnet-sillimanite-cordierite gneisses predominate.

2.3.2.5.4 Discussion

The prominent aluminous character and presence of biotite gneiss, metaquartzite and calc-silicate layers suggest a pelitic and semi-pelitic origin. The paragneisses are, across the tectonic grain, distinctly separated from the grey gneiss unit and underlie a vast terrain further towards the north-east. The paragneiss unit clearly constitutes an important pretectonic stratigraphic horizon, the equivalent of which do not crop out outside the boundaries of the Namaqua Province.

---

[1]At Gifberga homogeneous leucogneiss component with a granitoid appearance has been mapped as part of the sequence (Annex. 1). Little is known of this gneiss component and the possibility should be considered that it may form part of the syntectonic plutonic suite.

The nature of the contact with the grey gneiss unit which is interbanded gradational in places, suggests that the sequence from grey gneiss to paragneiss belongs to a single volcano-sedimentary pile. The alternating pelites (garnet-sillimanite-cordierite gneiss) and semi-pelites (biotite gneiss) compare well with a mudstone/wacke sequence; possibly a distal turbidite facies.

### 2.3.3 Syntectonic gneisses

#### 2.3.3.1 Introduction

A syntectonic gneiss is an intrusive (magmatic or anatectic) which came into place during the tectogenetic development of the Namaqua Mobile Belt. The time of emplacement with respect to the structural development is discussed in Section 3.

#### 2.3.3.2 Granodioritic augen gneiss

The augen gneiss is an early syntectonic unit in the marginal zone and is erroneously shown on the map (augen gneiss, Annex. 1) as a pretectonic unit. It is limited to the marginal zone (Fig. 2.8) where it occurs as a stratiform body structurally underlying the banded amphibolite unit and infolded as a dome within the banded amphibolite. The contact with the banded amphibolite unit is interbanded. As the banded amphibolite is approached from the south, the amphibolite banding of the augen gneiss becomes more frequent, more closely spaced and develops eventually into the banded amphibolite unit. The contact with the grey gneiss unit is interbanded over a limited width, while the contacts between such bands on a mesoscopic scale are always abrupt. Along the contact zone at one locality some small crosscutting augen-gneiss bodies were observed in grey gneiss and are indicative of an intrusive behaviour. The stratiform body is a two-component rock unit comprising irregularly spaced amphibolite bands in the grey augen gneiss, forming the bulk of the unit.

##### 2.3.3.2.1 Augen granodiorite

The granodiorite is a homogeneous rock with a similar field appearance throughout the stratiform body, whereas the domal exposure is more leucocratic. Hand-sized inclusions, some amphibolite, are sparsely present and form the most important evidence for an intrusive origin. The augen gneiss is generally not banded, but towards the northern boundary contains concordant pegmatoidal leucosomes.

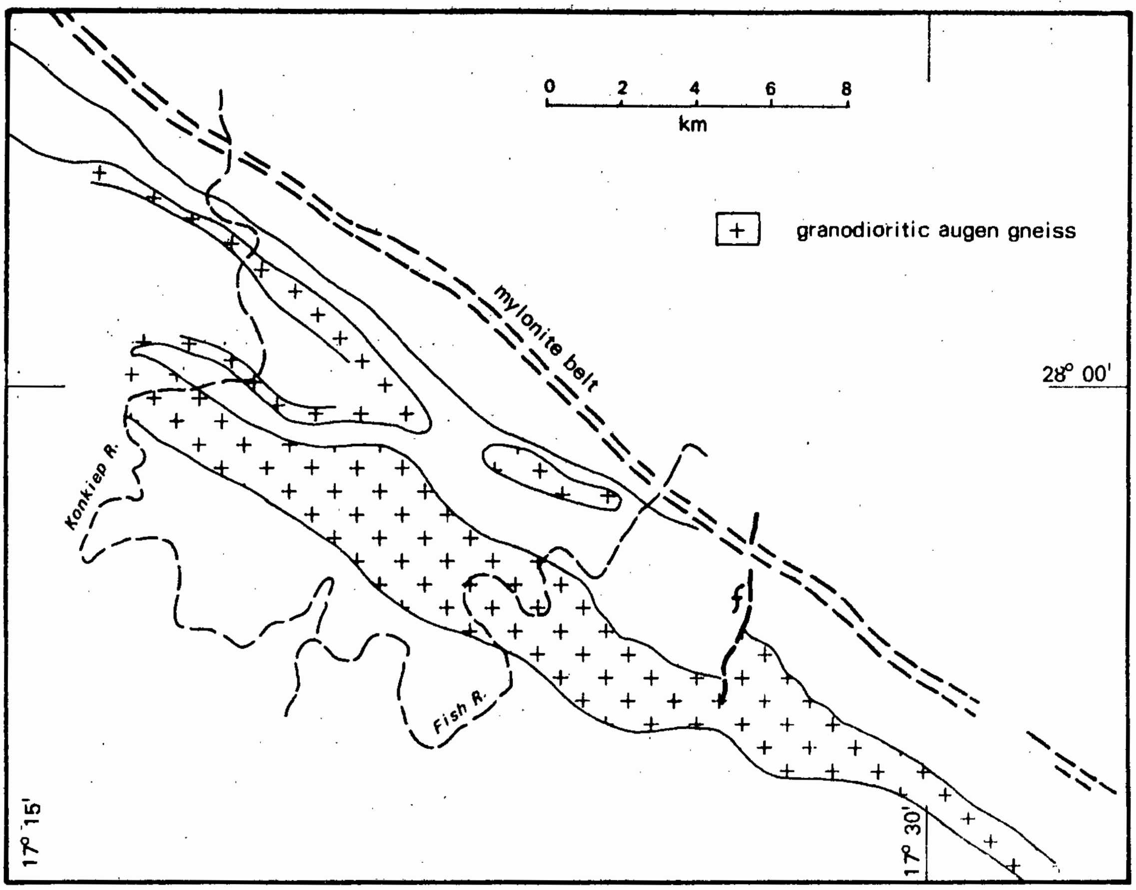


*Fig. 2.8. Distribution of the granodioritic augen gneiss in the marginal zone.*

Closely spaced augen give the gneiss its characteristic appearance. The augen predominantly comprises felspar megacrysts which are deformed and lenticular in the plane of the regional fabric with the foliation curving around them. Locally these felspar megacrysts are idioblastic laths with a poorly defined preferred orientation. There is, in fact, a correlation between the shape of the augen and intensity of foliation development; in zones of increased foliation development, the augen are more lenticular and thin discontinuous pegmatoidal bands also develop. The augen, in intermediate and more extreme stages of lenticular development are commonly elongated on the foliation surface, defining the regional lineation. The augen consist of both K-felspar and plagioclase megacrysts or of granular felspar aggregates ($\pm$ quartz). Myrmekitic intergrowths were observed along the edges of megacrystic augen. The granular felspar are interpreted as the result of new grain formation within original K-felspar and plagioclase megacrysts, which also show deformation structures like uneven extinction, bent twin lamellae and thin cross-cutting fracture zones.

The darker coloured matrix is schistose owing to the prominent presence of biotite together with epidote and hornblende as the other dark mineral constituents; some secondary chlorite, after biotite, is rarely present. The modal mineralogy (Table 2.8b) indicates a granodioritic composition (Fig. 2.9).

#### 2.3.3.2.2 Amphibolite bands

Amphibolite bands, normally thinner than 2 m, are pervasively present in the augen gneiss, but only locally form a regular interbanding; it renders the augen gneiss unit heterogeneous on large outcrop scale. The bands are perfectly concordant with the foliation developed in both the amphibolite and augen gneiss, and appear to be similar to the ubiquitously present amphibolite bands of the grey gneiss unit.

The amphibolite itself is homogeneous with no migmatitic or any other mesoscopic banding present. The penetrative foliation is defined by the dimensional habit of the hornblende and plagioclase grains; plagioclase locally forms a thin lenticular banding (millimetres) while the hornblende is invariably aligned parallel to the regional lineation. The amphibolite is typically fine grained, granoblastic-elongate, and the hornblende, commonly idiomorphic in habit, normally predominates over plagioclase (Table 2.6).

| | Hornblende | Plagioclase | Quartz | Plagioclase composition (% An) | |
|---|---|---|---|---|---|
| B- 25 | X | X | | 44 | |
| B- 26 | X | X | | 40 | Plagioclase altered to white mica |
| B-530 | X | X | X | - | ditto |
| B-553 | X | X | | 43 | |
| B-844 | X | X | | 38 | ditto |

Table 2.6. The mineral content of the amphibolite bands in the augen gneiss; epidote is also present in minor quantities. The plagioclase composition was determined by the Michel-Lévy method on a fixed stage microscope.

#### 2.3.3.2.3 Discussion

The structural dating of the augen granodiorite is discussed in Section 3.4.6.2 and a late-$D_1$ to syn-$D_2$ time of emplacement is inferred. The survival of deformation textures on grain scale relates to a relatively low rate of recrystallisation and suggests that the deformation was affected, or continued, after the culmination of $M_1$. This is consistent with the conclusion (Section 3.4.7) that $D_2$ postdates $M_1$ if the deformation giving rise to the foliation progressed during $D_2$.

The amphibolites are considered as inclusions akin to the country rock which was invaded in a *lit-par-lit* fashion.

### 2.3.3.3 Megacrystic granite

This syntectonic granite occupies a vast area (Annex. 1 & 2) and is limited to the highest grade terrain. On a regional scale (Fig. 4.14), it can be seen that together with other syntectonic plutonites, these rocks predominate in the highest grade central zone flanked by lower grade margins.

The megacrystic granite is conspicuous for its homogeneity and broadly retains a similar field appearance as mapped on the farms Altdorn, Kanebis, Frankfurt, Karios, Kuduberg, Haruchas, Nakais, Tsawisis, Grabwasser and others (Annex. 1 & 2). This entire area south-west of Klein-Karas is underlain by a single phase of the granite, although minor textural differences exist from place to place, no contacts separating different possible phases were observed. On Rosyntjiebos and along the Fish River upstream from Kochas Drif, however, a granodiorite phase (Section 2.3.3.4) was encountered which forms discrete contacts with the megacrystic granite.

The intrusive nature of the megacrystic granite is evident from the many inclusions and contact relationships. In the area covered by the map (Annex. 2) inclusions were only observed near the contact with the paragneiss unit while the large granite massif south-west of Klein-Karas is generally void of inclusions; these inclusions are invariably paragneissic, with the foliation of the granite penetrating across the granite/inclusion contact to correspond geometrically with that of the paragneiss inclusion. This feature indicates that the foliation was superimposed on the inclusion and surrounding granite at the stage when both acted rheologically in a similar fashion. Calc-silicate boudin, typical of the paragneiss unit, were also found as inclusions and illustrate that a strong deformation of the paragneisses predated the emplacement of the megacrystic granite. Stretching of the calc-silicate bands could not have taken place after intrusion as most paragneiss inclusions are irregularly shaped and not flattened in the plane of the foliation. Two large mesoscopic inclusions with a long dimension of at least several metres were observed on Altdorn and several more north of Grünau; these aluminous and biotite-rich xenoliths are atypical with respect to their size and dark colour. In the Klein-Karas Mountains on the farm Goedemoed, a swarm of inclusions were found which differ markedly from those described above and any other known gneiss in the area. They are very fine grained (< 0,5 mm) and sometimes contain a few scattered felspar megacrysts. In handspeciman a fabric is hardly visible, but the biotite grains have a preferred orientation as seen microscopically. The mineral composition, quartz-plagioclase-orthopyroxene-biotite, is rare in that it includes appreciable amounts of orthopyroxene and defines the only granulites recognised in the area.

The foliation of the megacrystic granite which is wrapped around the granulite inclusions are defined by the preferred orientation of felspar laths; which are locally not deformed into augen shapes, while the xenoliths have rounded discoidal shapes with a marked long direction. It is clear that these granulite inclusions were significantly more rigid than the flowing magma which here contributed largely to the preferred orientation of the felspar megacrysts in the granite. All these inclusions described above make sharp distinct contacts with the granitoid. No inclusions of grey gneiss were observed in the granite.

The three major types of inclusions described above can be compared with the classification of Didier (1973) in the following manner :

(i) the paragneiss enclaves are clearly derived from the neighbouring paragneiss unit and are termed xenolithic enclaves,

(ii) the surmicaceous enclaves of Didier (1973) are represented by the aluminous and biotite-rich enclaves of large dimensions while

(iii) the granulite inclusions of Goedemoed compare with the microgranular types of Didier but for the fact that they are not shown to be igneous of nature.

The surmicaceous and granulite types are very sparsely distributed while the xenolithic enclaves are the most abundant, but virtually absent in the central part of the massif south-west of Klein-Karas. Although most abundant, the xenolithic enclaves are few (<< 1%) in number and this aspect, together with the marginal distribution of these enclaves, argue for an intrusive origin (criteria of Didier, 1973, p. 323). As substantiating evidence against *in situ* migmatitic origin, it must be stressed that the xenolithic enclaves are predominantly not nebulous or schlieric and ghost inclusions of unknown origin, were only observed at one or two localities.

The megacrystic granite is found in contact with both the grey gneiss and paragneiss units. On the farm Kochas the contact with grey gneiss is fairly abrupt and interbanded over a narrow, few metres-wide, zone. The grey gneiss in contact with the granitoid has an atypical appearance and forms a zone of approximately 100 - 300 m thick around the antiformal structure on Kochas.

The grey gneiss in this zone resembles that outcrop within the Ai-ais Complex at Ai-ais (Section 2.3.2.4.2 (iii)).

Small mesoscopic pips of the granite occur in the paragneiss unit, some considerable distance away from large bodies of the megacrystic granite. On Kanebis an offshoot from one of these pips was observed to crosscut the foliation/banding in the paragneiss, while all other observed contacts are concordant and commonly interbanded. One such contact, which is very well exposed at a waterfall downstream from the farmstead on Altdorn, displays the *lit-par-lit* nature of the contact zone. At several localities situated close to or at the paragneiss contact, the granite was observed to be markedly contaminated by alumina and contains appreciable amounts of biotite, cordierite, garnet and sillimanite. The contaminated granite, which also includes a larger than normal proportion of paragneiss inclusions, bands, and ghost relicts, forms intercalated contacts with the paragneisses. Such outcrops are interpreted to convey an intrusive origin for the megacrystic granite.

Apart from its homogeneity the most conspicuous character of the granite is the closely spaced K-felspar phenocrysts, attaining a long dimension of up to 15 cm, but more commonly the laths are shorter than 5 cm. In the smaller and/or sheet-like bodies of the granite the porphyritic texture may not be so well developed, and locally on Kanebis, the texture is predominantly medium even-grained, and large regularly spaced (10 - 20 cm) garnets, with circular cross sections, are sometimes present. The deformation of the felspar phenocrysts are closely related to the intensity of the development of the foliation. Completely undeformed laths are preferentially oriented to define a planar structure while, when they are augen-shaped, a higher degree of preferred orientation parallel to a more penetrative foliation in the matrix, is displayed. The foliation is pervasively developed throughout the body as mapped. The augen character of the granite (Plate 9) on Kochas, is more distincly developed, in places to such an extent that the augen are stretched out into linear forms lying within the foliation and flattened into lenticular bands. Pegmatitic pockets and concordant leucocratic veins, without mafic rims, and up to 1 m in width, were observed locally. The formation of the concordant leucosomes are thought to be penecontemporaneous with that of the granite, because some of them are clearly affected by the same foliation which pervades the granite regionally.

The foliation which pervades the megacrystic granite varies in intensity, but there is no systematic decrease away from its boundaries and broadly the foliation is penetrative throughout. As described above, it is generally defined by the preferred orientation of the felspar phenocrysts/augen, but dark streaks of mafic minerals depict the foliation locally. The foliation might be defined by the dimensional orientation of both quartz and felspar in the matrix, or only by the preferred orientation of the biotite flakes. It is important that the felspar phenocrysts are aligned in places where no other deformational features or habit orientation are apparent in the rock. Thus it is inferred that the granite possesses a primary flow fabric along which a tectonic foliation developed (augen structure), during the protracted effects of tectonic movement during and after the time of the crystallisation of the magma. The granite lacks isoclinal folds and linear structures on the foliation are very sparse, with the only folding affecting the foliation being that of the late phases which are prominent as large open macroscopic structures. The scarcity of minor folds of late generation reflects the homogeneity of the granite which precluded the development of higher order buckles. In Section 3.5.6.1 it is shown that the foliation which pervades the granite can be correlated with $s_2$.

The phenocrysts of the granite are orthoclase-microperthite, although microcline and microcline-microperthite were also observed; antiperthite is sparse. The anorthite content of the plagioclase varies from 27 - 33 per cent. The biotite is characteristically red-brown ($\beta = \gamma$) and commonly altered to chlorite. Although in small amounts, the aluminous minerals garnet, cordierite and sillimanite are ubiquitous, with the cordierite usually altered to pinite. The felspars are partly altered to white mica, and according to the mineralogical composition (Table 2.7) the granite falls in field 3a of the QAP triangle (Fig. 2.9). The mineralogy of the granite situated in the Kochas antiformal structure is somewhat different in that microcline is the dominant K-felspar and epidote and brown biotite (instead of $\beta = \gamma$ = red-brown, as elsewhere) is present (cf. sample B-860 in Table 2.7).

#### 2.3.3.4 Granodiorite

On Rosyntjiebos (Annex. 1) the granodiorite phase has sharp interbanded contacts with the megacrystic granite, but the time relation could not be established. In the Fish River Canyons, though, a similar looking granitoid was observed as xenoliths in the megacrystic granite and the granodiorite also has sharp contacts with a nebulitic plutonite (migmatite nomenclature of Mehnert, 1968). The granodiorite is mesocratic, predominantly medium even grained, with scattered felspar phenocrysts. Its mineralogical composition is given in Table 2.7; the K-felspar occurs both as microcline and orthoclase, while biotite, the dominant mafic mineral, defines a poor to moderate fabric. The foliation is pervasive and small structures deforming the foliation were not observed, but it is deformed by the late macroscopic folds. No lithological heterogeneities were observed, apart from the inclusions apparently derived from the paragneiss unit. The granodiorite is very similar in appearance and structure to the granite and is thought to represent, together with the granite, different phases of a possible suite of early syntectonic intrusives.

#### 2.3.3.5 Charnockite

A large massif of charnockitic composition was found north-east of Klein-Karas and extends at least 35 km in one dimension (Fig. 3.42). Centrally situated

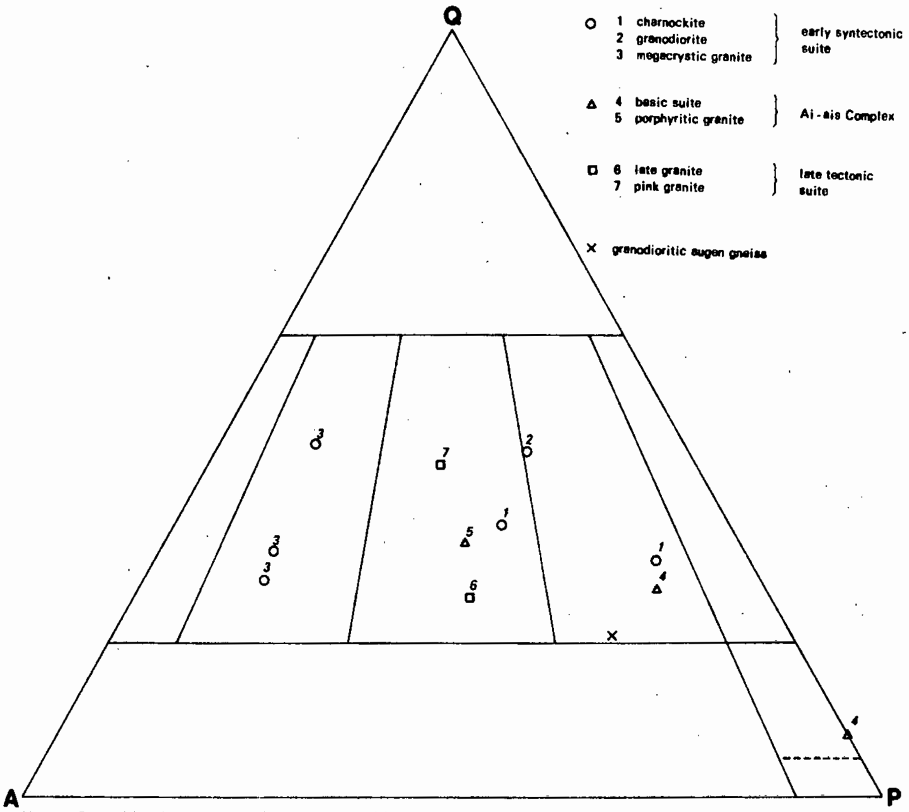


*Fig. 2.9. Composition of syntectonic gneisses based on modal mineralogy.*

planar fabric is pervasively developed and defined in hand speciman by the preferred orientation of the dark minerals, or microscopically more conspicuous by the alignment of biotite. Deformation features of individual grains are not distinct and are limited to the slight bending of some plagioclase twin lamellae.

a.

| | Charnockite | | | |
|---|---|---|---|---|
| | N-31 | N-40 | N-29 | N-42 |
| K-felspar | 9 | 21 | X | X |
| Plagioclase | 45 | 30 | X | X |
| Quartz | 24 | 27 | X | X |
| Biotite | 5 | 7 | X | X |
| | $\beta=\gamma$=red-brown | | | |
| Hypersthene | 17 | 14 | X | X |
| Opague minerals | tr | 1 | | |
| Number of points counted | 900 | 1000 | | |

b.

| | B-531 & B-550 |
|---|---|
| K-felspar | 17 |
| Plagioclase | 46 |
| Quartz | 17 |
| Biotite | 14 |
| Epidote | 2 |
| Hornblende | 1 |
| Sphene, ore & apatite | 3 |
| Number of points counted | 988 |

Table 2.8. Mineralogical compositions (volume %) of (a) the charnockite and (b) the augen granodiorite.

The mineralogical composition of two samples (Table 2.8a) plots within fields 3b and 4 (Fig. 2.9); according to the nomenclature of Tobi (1971), the composition varies from charnockitic to enderbitic. The K-felspars are orthoclase and orthoclase-microperthite, while mesoperthites were not observed; plagioclase is commonly zoned and hypersthene is abundantly present in all samples.

### 2.3.3.6 Ai-ais Complex

The Ai-ais intrusive complex constitutes one large body, at least 32 km in length , with several sattelite bodies (Fig. 2.10, Annex. 1); it is situated in the central zone and is tangentially disposed to the Kanabeam mylonite belt. The complex comprises a spatially associated suite of intrusives, consisting of an older gabbroid, and younger porphyritic and pink granite phases. In Section 3.5.6.2 it is argued that the complex was emplaced in the interval between $D_2$ and $D_4$.

#### 2.3.3.6.1 Gabbroid and associated granitoids

These mafic intrusives form the oldest component of the Ai-ais Complex and are largely retrogressed. The map (Annex. 1, Fig. 2.10) does not differentiate between gabbroid and granodiorite/tonalite; the gabbroids and metagabbroids do, however, areally predominate. The mafic suite is marginally well foliated against the grey gneiss unit and no intrusive relations were observed. The central portion of the body is generally massive and not continuously pervaded by a planar fabric. The bulk of the intrusives appear melanocratic, are commonly porphyritic with a variable felspar content and are fine to medium grained. A large portion comprises metagabbroid, amphibolite and mafic gneisses. The gabbroids comprise quartz gabbro, gabbro-norite and hornblende gabbros with labradorite as the felspar (see Tables 2.9 & 2.13 for the mineralogy); quartz is a common but minor constituent with ore minerals present in accessory amounts. Some of the granodiorite/tonalite contains clinopyroxene as an additional mafic mineral (Table 2.9).

*Retrogressive effects*

To investigate the areal distribution of the retrogressive effects, the rocks of the mafic suite are subdivided into three types (A, B & C) according to intensity of fabric development and the presence or absence of pyroxene :

A. The pyroxene-bearing gabbroids and granitoids (Table 2.9) generally lack any fabric imprint, or at the most show a very poor foliation. The granitoids

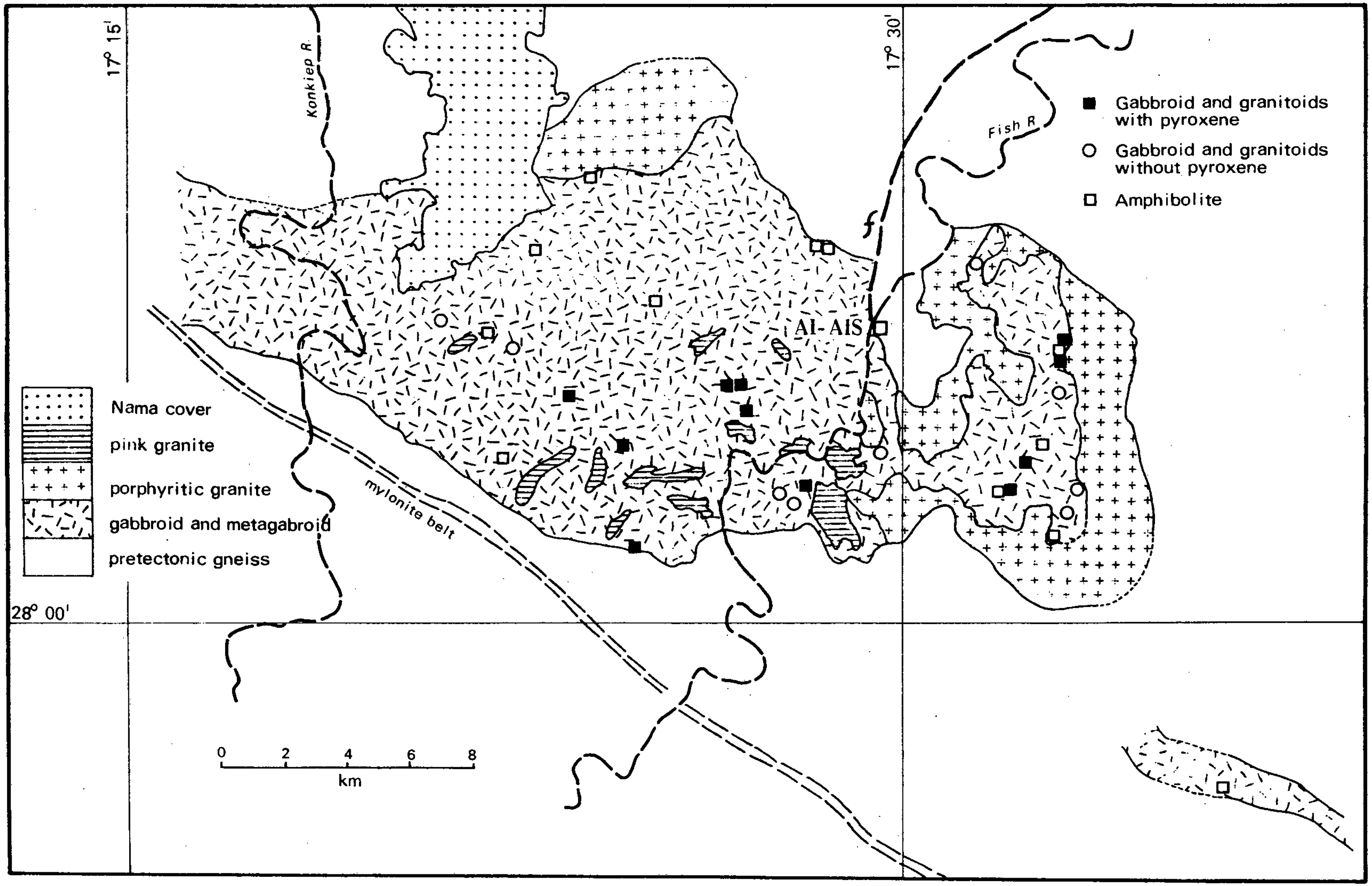


*Fig. 2.10. Ai-ais Complex.*

have a quartz content of approximately 20 per cent while the K-felspar, content in the form of microcline, approximates 10 per cent. The biotite is more typically red-brown ($\gamma = \beta$) and the hornblende green ($\gamma$). The clinopyroxene is commonly rimmed by hornblende and hornblende grains include cores of clinopyroxene, pointing to the breakdown of pyroxene in favour of hornblende. The spatial association of magnetite and hornblende (sample B-690) and quartz inclusions in hornblende with a core of clinopyroxene, suggest that the breakdown reaction of clinopyroxene involved the formation of magnetite and quartz together with the hornblende as end products.

B. Gabbroids and granitoids without pyroxene (Table 2.10) and without any marked planar fabric. The colour of the biotite ($\gamma = \beta$) is both brown and red-brown, while more hornblende is blue-green than green ($\gamma$). The granitoids have a similar composition to those described in (A) above.

| | Gabbroid | | | | | | | | Granitoid | | |
|---|---|---|---|---|---|---|---|---|---|---|---|
| | B-138 | B-146 | B-398 | B-533 | B-543 | B-544 | B-665 | B-666 | B-133 | B-161 | B-690 |
| K-felspar | X | | | | | | | | | X | 8 |
| Plagioclase | X | X | X | X | 45 | X | X | X | X | X | 37 |
| An per cent | | | 54 | 60 | 63 | | 50 | 52 | | | |
| Quartz | X | X | | X | 4 | X | X | X | X | X | 17 |
| Clinopyroxene | X | X | X | X | 38 | X | X | X | X | X | 2 |
| Orthopyroxene | | | X | X | | | | X | | | |
| Hornblende | X | | X | | 7 | X | X | X | | X | 25 |
| Biotite | X | | X | X | 6 | X | X | X | X | X | 7 |
| Epidote | | | | | | X | | | | | |
| Chlorite | | X | | | | | | | | | |
| Ore | | | | | | | | | | | 4 |

Table 2.9. Mineral assemblages and modal compositions (volume per cent) of the pyroxene-bearing gabbroids and granitoids (type A).

C. The well-foliated and gneissic rocks generally conforming to the definition of amphibolite (Table 2.11), although some are mesocratic and contain less mafic minerals. Three of the samples contain clinopyroxene, distinctly distributed along thin ($\leq$ 1 mm) bands parallel to the planar fabric. The clinopyroxene shows no sign of alteration and probably remained in equilibrium due to the effect of bulk composition (Fig. 2.11). Microcline and quartz are sometimes present as minor constituents; the hornblende is predominantly blue-green ($\gamma$) and the biotite is brown ($\gamma = \beta$).

| | Gabbroid | | | | | | | Granitoid | |
|---|---|---|---|---|---|---|---|---|---|
| | B-142 | B-144 | B-153 | B-164 | B-540 | B-545 | B-685 | B-126 | B-160 |
| K-felspar | | | | | | X | X | X | X |
| Plagioclase | X | X | X | X | X | X | X | X | X |
| An per cent | 50 | | 50 | 56 | | | | | |
| Quartz | X | X | X | | X | X | X | X | X |
| Hornblende | X | X | X | X | X | X | X | X | X |
| Biotite | X | X | X | X | X | X | X | X | X |
| Epidote | | | | | X | X | | | X |
| Chlorite | | | | | | | | | X |

Table 2.10. Mineral assemblages of the gabbroids and granitoids without pyroxene (type B).

| | B-832 | B-127 | B-134 | B-139 | B-534 | B-535 | B-536 | B-538 | B-539 | B-541 | B-657 | B-693 |
|---|---|---|---|---|---|---|---|---|---|---|---|---|
| K-felspar | X | | X | X | | | | | X | | | X |
| Plagioclase | X | X | X | X | X | X | X | X | X | X | X | X |
| An per cent | | | | | | | 59 | | | 54 | 49 | |
| Quartz | X | X | X | X | X | X | | X | X | | X | X |
| Clinopyroxene | | | | | X | | | X | | X | | |
| Orthopyroxene | | | | | | | | | | | | |
| Hornblende | X | X | X | X | X | | X | X | X | X | X | X |
| Biotite | | | | X | | X | | | X | | X | X |
| Epidote | X | X | X | | | | | | X | | | X |
| Chlorite | | X | X | | | | | | X | | | |
| Garnet | | | | | | X | | | | | | |

Table 2.11. Mineral assemblages of the amphibolites and mafic gneissis (meta-gabbroid and metagranitoid, type C).

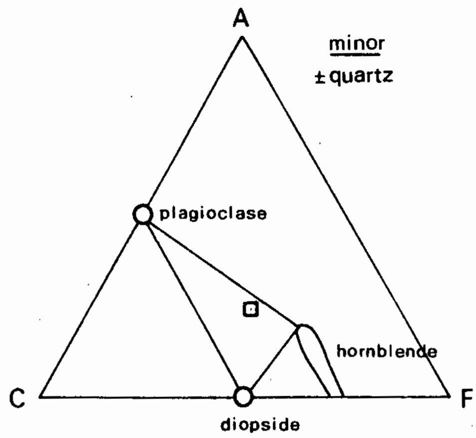


Fig. 2.11. The probable bulk composition of a labradorite-amphibolite (cf. samples B-534, 538 and 541 of Table 2.11) which allow for the presence of diopside at sufficiently high temperatures (ACF diagram after Winkler, 1974, p. 164).

By comparing the distribution (Fig. 2.10) and the mineralogy and deformation (Table 2.12) of the three types of rock (A, B & C above) the following aspects are noted :

| | Rock type | | |
|---|---|---|---|
| | A | B | C |
| Pyroxene | present | absent | absent[1] |
| Hornblende ($\gamma$) | green | green & blue-green | blue-green |
| Biotite ($\gamma = \beta$) | red-brown | red-brown & brown | brown |
| Plagioclase | Labradorite An 50 - 63% | Labradorite An 50 - 56% | Labradorite An 49 - 59% |
| Planar fabric | absent/poor | absent/poor | gneissic |

Table 2.12. Retrogression of gabbroids and granitoids from A to C (cf. areal distribution, Fig. 2.10).

[1]The clinopyroxene present in three samples, is considered to be controlled by the bulk composition (see text and Fig. 2.11).

(i) The pyroxene in A breaks down (hornblende rims) to yield types B and C. This can be demonstrated on a small scale where the core of a body is undeformed and consists of a pyroxene-bearing rock (B-690), while the well-foliated contact zone (B-693), several metres away, is deformed by contact shearing and lacks pyroxene.

(ii) According to Miyashiro (1968, p. 818 and 1973, p. 259) the blue-green and brown colours of the hornblende and biotite respectively in C, indicate a lower grade than the green and red-brown colours in A, the colours of type B being intermediary.

(iii) Contrary to expectation (Winkler, 1974, p. 163) the anorthite content of plagioclase is similar in A, B and C and essentially labradorite. This is possibly a reflection of both the PT conditions of equilibration and bulk composition which precluded the formation of a more Na-rich plagioclase.

(iv) The more advanced retrogression as manifested in type C, also coincides with the more advanced deformation fabric. The crystalloblastic character of the deformation fabric and general lack of deformation features on a grain scale (only the occasional fractured and bent plagioclase and blastomylonite were observed) point to a high rate of recrystallisation and neomineralisation. The resultant planar fabric is most noticeable by its granoblastic elongate nature, preferred orientation of mica and thin mineralogical banding.

(v) The areal distribution of types A, B & C (Fig. 2.10) shows that the pyroxene-bearing rocks are preferentially located in the southern part of the body facing the lower grade part of the main metamorphic zonation (Section 3.5.6.2).

#### 2.3.3.6.2 Porphyritic granite

The porphyritic granite (gneissic granite on the legend of Annex. 1) is intrusive into the metagabbroid and apart from the two main bodies to the north and south-east of the mafic rocks (Fig. 2.10) numerous small bodies and veins cross-cut the main body. Chill selvages are developed in the granite where it intruded as small veins into a large mass of gabbroid. East of the Fish River the concordant contact with the grey gneiss is obscured by the very intense marginal foliation of the granite. North of Ai-ais the granite was also found as intercalated sheets of augen gneiss in the grey gneiss. The granite is leucocratic to mesocratic, typically porphyritic and develops into an augen gneiss where it is well foliated. Scattered mafic xenoliths with discoidal shapes are common.

The modal mineralogy (Table 2.13) defines a granite in field 3b (Fig. 2.9) of

Streckeisen's triangle, its mesocratic nature being due to appreciable amounts of biotite ($\gamma = \beta$ = brown) which, together with minor amounts of hornblende ($\gamma$ = blue-green) and epidote form the mafic mineral component. The K-felspar is microcline. In hand speciman the felspar phenocrysts are obviously deformed to augen and even smaller porphyroclastic fragments. Microscopically, though, no deformation textures were recognised as all minerals appear strain free.

### 2.3.3.6.3 Pink granite

The pink weathering leucogranite has cross-cutting relations with respect to the porphyritic granite and is markedly less deformed than the older gabbroid and porphyritic granite. It is typically fine to medium even grained, and occurs as irregular smaller bodies within the complex and at the Leikop satellite body (Annex. 1). In contrast to the older components of the complex, the bodies of pink granite are not marginally foliated and rarely possess a poor planar fabric defined by the dimensional orientation of the constituent leucocratic minerals.

| | quartz gabbronorite (B-543) | granodiorite (B-690) | porphyritic granite (B-137) | pink granite (B-532) |
|---|---|---|---|---|
| K-felspar | | 8 | 28 | 29 |
| Plagioclase | 45 | 37 | 30 | 26 |
| Quartz | 4 | 17 | 29 | 42 |
| Hornblende | 7 | 25 | 1 | |
| Pyroxene | 38 | 2 | | |
| Biotite | 6 | 7 | 10 | |
| Epidote | | | 2 | |
| Chlorite | | | | 3 |
| Ore | | 4 | tr | |
| Number of points counted | 1000 | 1000 | 1076 | 1139 |

Table 2.13. Modal mineralogy (volume per cent) of the various phases of the Ai-ais Complex.

According to the mineral composition (Table 2.13) the pink granite falls into field 3b (Fig. 2.9) of the Streckeisen triangle. The K-felspar is predominantly microcline-microperthite, with subordinate orthoclase-microperthite, while the plagioclase is altered. Mafic minerals are generally absent, or may be present only in minor amounts, and inclusions are virtually absent being observed on only one occasion.

The absence of contact shearing, a feature common along contacts of the two older phases, indicates the development of deformation phase(s) after the emplacement of the porphyritic granite and prior to the intrusion of the pink granite. The pink granite may, possibly, not be genetically related to the Ai-ais Complex, but belong to the suite of late granites (Section 2.3.3.7).

### 2.3.3.7 Late granites

The late granites are very distinctly zonally distributed and limited to the more upper-crustal tectonic domains i.e. (i) the marginal zone in the south and the southernmost portion of the central zone immediately north of the mylonite belt, and (ii) a zone north of the Lord Hill mylonite belt (Fig. 4.14).

The granite bodies generally occur as small pips, or narrow ($\leq$ 3 m) subconcordant sheets concentrated in small areas; the northernmost occurrence (Annex. 1) of such an area is the southernmost outcrop of the paragneiss unit (Klipbokkop) which is densely intruded. Mappable bodies were found at Ou Ai-ais, Dreikopf and in the mafic gneiss unit, with these larger bodies commonly containing pegmatitic pockets. The late granites are generally cross-cutting and discordant with respect to the regional fabric. The granite bodies might be feebly foliated, but are usually unfoliated, while some smaller bodies are boudinaged. Where a planar fabric is developed, it has a cataclastic character with the development of mylonite gneiss in places. Bodies situated close to the mylonite belt are affected and they therefore predate the Kanabeam shearing (Section 3.6).

Table 2.14. Modal mineralogy (volume %).

| Late Granite : | B-513 |
|---|---|
| K-felspar | 33 |
| Plagioclase | 37 |
| Quartz | 25 |
| Chlorite | 5 |
| Epidote | tr |
| Number of points counted | 1000 |

The granite is leucocratic, even and fine to medium grained. Muscovite and garnet were commonly observed to form part of the mineralogy and other mafic minerals such as chlorite, epidote, biotite and ore, are present in minor amounts. The K-felspar is microcline-microperthite. The modal mineralogy of sample B-513 (Table 2.14), considered to be typical, defines a granite in field 3b (Fig. 2.9) of the Streckeisen triangle.

Granophyric intergrowths were observed in sample B-513, collected from the southernmost mappable body (Annex. 1) which is intrusive into the mafic gneiss unit.

The syntectonic character of these late granites are evident from their deformation, while the discordant contact relations, lack of a penetrative fabric, cataclastic nature of the fabric (where present) and granophyric intergrowths point to emplacement at a late stage and in a more upper-crustal environment.

#### 2.3.3.8 Pegmatites

Pegmatites are distinctly more numerous in the central zone than in the marginal zone and absent from the part of the Richtersveld Province investigated (Annex. 1). Viewing northwards the first pegmatites are observed in the transition zone between the Richtersveld and Namaqua Provinces while greater densities of pegmatite intrusion are spatially associated with the front zone, Ai-ais Complex and the paragneiss unit between Grünau and Lord Hill.

All the pegmatites are late and lack a fabric except where affected by the Kanabeam shearing. Some pegmatites were emplaced prior to $D_4$ and $D_5$. The front zone pegmatites predate the Gannakouriep dyke suite, while the pegmatites in the central zone were not observed to intrude the dykes.

#### 2.3.3.9 Haib area

##### 2.3.3.9.1 Syntectonic granite

Small bodies of a leucocratic granite are exposed on Witputs and Belda (Annex. 3) in the front zone. These have a poorly developed foliation and include some amphibolite enclaves with a well-developed fabric similar to the surrounding gneisses; the time of emplacement therefore, being after the main fabric-forming deformation. On Belda the granite is characterised by small euhedral felspar phenocrysts preferentially oriented along the foliation, while the larger part of the outcrop on Witputs consists of a fine-grained equigranular muscovite-bearing rock with a pinkish weathering surface; it is locally gradational into the porphyritic type such as that found on Belda.

##### 2.3.3.9.2 Late tectonic granite

This granite (Annex. 3) straddling the boundary between the Richtersveld and

Namaqua Province, occurs as a small sub-circular body on the farm Witputs. Superficially it resembles some of the Vioolsdrif granitoids, but is clearly intrusive and post-dates the planar fabric imprinted on the surrounding rocks. Apart from a few scattered gneissic inclusions along the margin, the granite is further devoid of enclaves. The granite is intruded by a suite of pegmatites (Section 2.3.3.9.3) and both the granite and the pegmatites are affected by a set of north-northwestern shears (Annex. 3).

The field appearance is constant throughout, the granite (field 3a of the Streckeisen triangle) is predominantly medium grained with a slightly porphyritic tendency in containing small euhedral K-felspar insets. The mafic minerals are mainly biotite ($\leq$ 5 per cent), while the K-felspar consists of both microperthite and microcline-microperthite.

2.3.3.9.3 Pegmatites

A suite of vertical and discordant pegmatites is spatially associated with the front and disposed in *en echelon* fashion. These are correlated with the concentration of pegmatites in the vicinity of Goodhouse and the Orange River pegmatite belt (Gevers et al., 1937) south of the river closely following the structural boundary between the Richtersveld and Namaqua Province. The arrangement and orientation of the pegmatite suite is schematically illustrated in Fig. 3.21.

2.3.3.10 Time relations and concluding remarks

All the syntectonic plutonites are considered to have been derived from elsewhere as field evidence substantiating *in situ* anatectic development is lacking.

Relative time relations of intrusive rocks, with respect to the deformation phases, are schematically shown below for each of the structural domains.

Marginal zone

| | 1900 Ma | $D_1$ | $D_2$ | | $D_6$ | 880 Ma |
|---|---|---|---|---|---|---|
| Vioolsdrif Suite | ———— - - | - - - | | | | |
| $M_1$ | | ———— | - | | | |
| Augen granodiorite | | - | ——— | | | |
| Late granites | | | | ———— | | |
| Front zone pegmatites | | | | - - | - - - | |
| Gannakouriep dykes | | | | | | ———— |

Central zone

| | $D_1$ | $D_2$ | | $D_4$ & $D_5$ | $D_6$ | 880 Ma |
|---|---|---|---|---|---|---|
| $M_1$[1] | — | — | | | | |
| Charnockite | | | | | | |
| Granodiorite | | — | | | | |
| Megacrystic granite | | | | | | |
| Ai-ais Complex | | | — | | | |
| Pegmatites | | | — | — | — | |
| Gannakouriep dykes | | | | | | — |

It is clear from the diagram (Fig. 2.9) that the intrusive phases of a particular syntectonic suite vary in composition from basic to acid and also young in the same sequence. The same pattern is repeated in the early syntectonic suite, the later Ai-ais Complex and also the Vioolsdrif Suite (Vioolsdrif rock series; Section 2.1.3.6). It is thought likely that the processes giving rise to these phenomena, are also similar, so that the same process producing differentiated intrusive suites, repeated itself during the tectogenetic development of the area under consideration.

### 2.3.4 Post-tectonic intrusives

#### 2.3.4.1 Bremen Complex

The older part of the Bremen Complex (Kröner and Blignault, 1976) gives a reliable Rb-Sr isochron age of 920 Ma (Welke et. al., in press). This is a minimum age for the tectonic activity of the Namaqua Province, as the older phase lacks a tectonic imprint and cross-cuts the surrounding megacrystic granite. The younger part of the Bremen Complex is associated with the Kuboos-Bremen line of intrusives (see legend, Annex. 1).

---

[1] The relation $M_1$/deformation is that for the domain of $s_2$ refoliation only.

### 2.3.4.2 Gannakouriep dyke suite

A swarm of vertical diorite dykes regionally pervades the Ai-ais area and continues southwards into the Richtersveld (De Villiers & Söhnge, 1959) and Namaqualand. Along the Orange River the dykes are pervasively present eastwards as far as Goodhouse (Annex. 3, Beukes, 1973). North of the Orange River the dyke trend is north-northeast and becomes more north-south in the Richtersveld. The dykes are commonly associated with faulting and shearing, with apparent horizontal displacement of as much as 300 m as evident on the maps.

This dyke suite is named (Prof John de Villiers, pers. comm.) after one member of major proportions along which, in the Richtersveld, the Gannakouriep river bed was subsequently carved. The Gannakouriep dyke itself was followed northwards up to the farmstead Mara for a distance of 90 km. Along the Fish River the type dyke forms a layered complex whereas the other members usually consist of a single diorite phase.

In the Ai-ais and Haib areas the dykes are melanocratic and more commonly medium than fine grained. The main mineral constituents are plagioclase + clinopyroxene + ore + chlorite ± hornblende ± epidote. Pyrite was often observed in the field as an accessory mineral and chlorite was formed by the breakdown of the clinopyroxene. The plagioclase usually is andesine and exceptionally labradorite.

The Gannakouriep dykes are unaffected by the deformation phases related to the Namaqua Mobile Belt and postdate the mylonite belt ($D_6$). West of Tatasberg, in the Richtersveld, a set of north-westerly shear zones become prominent and deflect the dykes in a left-lateral sense. These shears, which are preferentially located in the west, are related to the late Precambrian deformation along the coast. The dykes where pervasively developed, act as a useful upper bracket for the Namaqua structures. A whole rock K-Ar age of 878 Ma is reported by De Villiers (1968).

# 3 DEFORMATIONAL AND METAMORPHIC DEVELOPMENT

## 3.1 Structural domains

During the initial stages of the investigation it soon became apparent that the area can be subdivided on the basis of easily recognisable field aspects relating to structural imprint only. The subdivision is independent of genetic consideration and a useful analytical approach. During the course of the investigation, the subdivision became more meaningful as additional data were acquired. The full character of the various domains is synthesised in Section 5. The domains were initially distinguished as follows :

(i) The Richtersveld Province (Fig. 1.1) extends beyond the areas investigated. In the Haib and lower Fish River areas (Fig. 3.1) the main planar fabric imprint is not penetratively developed throughout.

(ii) In the marginal zone (Fig. 3.1) the main planar fabric is penetrative on all scales down to thin section scale. The boundary between the Richtersveld Province and marginal zone is not a discrete structure; it is referred to as a front (Section 2.2) and need not have any special tectonic connotation. The attitude of the main planar fabric throughout the marginal zone remains virtually constant.

(iii) The central zone (Fig. 3.1) is characterised by macroscopic crossfolds, giving rise to a relatively low direction stability of the penetrative main planar fabric. The marginal and central zones are conveniently separated by a regionally prominent mylonite belt.

The marginal and central zones which are similar with respect to the main planar fabric, together form part of the Namaqua Province as opposed to the Richtersveld Province. Both provinces constitute different parts of the Namaqua Mobile Belt.

## 3.2 Structural analysis

A structural analysis of the sequence of deformation is presented for each domain. Correlation between domains is attempted in Section 5. That this approach is necessary, is clearly demonstrated by Robinson & Fyson (1976) who

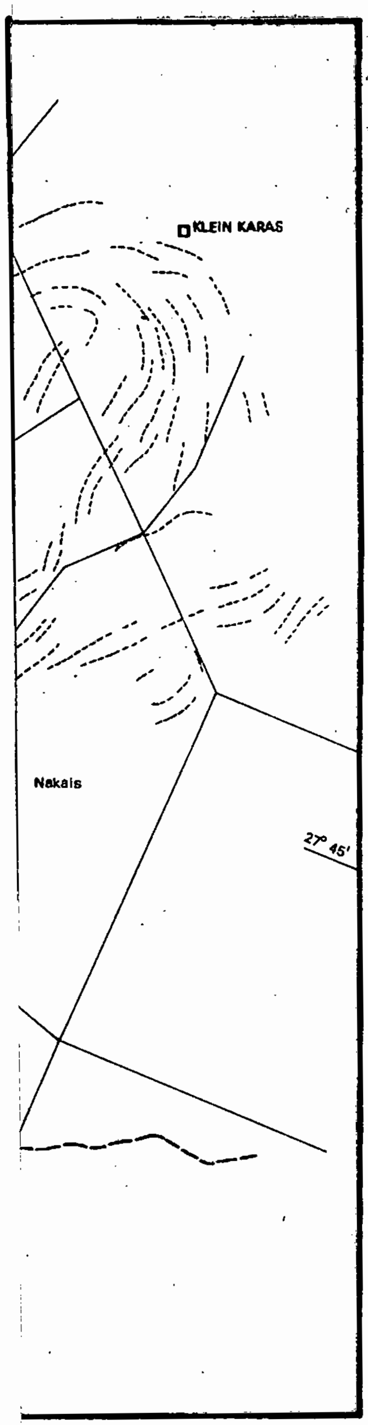

KLEIN KARAS
Nakais
27° 45'

point out the inherent danger in correlating $F_2$-type structures over long distances.

Correlation within domains were carried out according to standard procedures (Hobbs et al., 1976, p. 364), and the criticism of Park (1969) on using style only as a correlating criterium is underlined. Strong emphasis is placed on overprinting criteria (cf. Williams, 1970) and correlation by means of orientation, especially of the early structures, was found to be unsound, even within outcrops. The present analyses within domains are based on the establishment of the structural sequence around macroscopic structures and the subsequent correlation between and outwards from major structures.

In this investigation emphasis is placed on the development of microstructures and the associated metamorphism. These phenomena are related where possible to the deformational sequence, thus providing more meaningful structural correlations.

Orientation data are compiled on equal-area stereographic nets (lower hemisphere). Trend and plunge notations for linear structures are such that the last two numbers indicate the amount of plunge while the strike and dip notation (e.g. 09030) for s-structures are such that the last two numbers indicate the amount of dip towards the right-hand when facing the strike direction.

## 3.3 Richtersveld Province

### 3.3.1 First post-Vioolsdrif deformation phase - $D_1$

$D_1$ is defined as the first deformation affecting the Vioolsdrif Suite pervasively on a regional scale and is also the only component of the Namaqua tectogenesis that developed structures pervasively in the area studied. It can be shown that the Orange River lavas were deformed prior to $D_1$, though no such small structures were recognised. The widely developed, roughly north-south foliation present in the rocks from Vioolsdrif westwards towards the Stinkfontein quartzites (Late Precambrian Gariep Sequence), is considered as part of the late Precambrian tectogenesis. In the Richtersveld, south of the Fish River, this late Precambrian grain has a north-western trend and could easily be misread for $s_1$; the late Precambrian structures affected the Gannakouriep dyke suite postdating the Namaqua foliation ($s_1$) and provides a means of differentiation. In the lower Fish River area this younger imprint is not widely developed.

### 3.3.1.1 Regional Foliation, $s_1$

*Character*

The foliation, $s_1$, defined as the first structural imprint on the Vioolsdrif granitoids, is the most pervasive structural element present and forms the axial-plane foliation to $F_1$ folds in the volcanics. The scale of penetration and character of $s_1$ vary in such a manner that a progressive increase in deformation intensity is evident from south to north, i.e. from the Orange River towards the front (Figs. 3.2 & 3.3). Southwards, away from the margin of the Namaqua Province, the regional foliation is either non-penetrative or absent. The mesoscopic and microscopic characteristics of $s_1$ are summarized in Table 3.1 and discussed below (see also Section 4.1 for more detail on the microstructures) :

(i) On the basis of the scale of penetration of the regional foliation, the areas studied can be subdivided into low and high-strain subdomains; in both the lower Fish River and Haib areas the two subdomains are separated by major intensely foliated zones (Figs. 3.2 & 3.3) with the high-strain zone bordering the front. In the low-strain subdomain $s_1$ is virtually absent or locally poorly developed and more penetrative in the high-strain subdomain.

(ii) The microstructures (Table 3.1) defining $s_1$, suggest a cataclastic nature (after Higgens, 1971) of the foliation in both the granitoids and lavas.

(iii) The coarser rock types of the Vioolsdrif granitoids are markedly less affected by $s_1$ than the finer grained Orange River lavas; the basic phases of the Vioolsdrif Suite reacted the most competently and is generally only marginally affected by $s_1$.

(iv) Deformation and recrystallisation textures in the low-strain subdomain are best developed in the lavas where the foliation locally appears as a fracture cleavage, while the granites mostly seem undeformed. Typical microstructures in the lavas are the flattening of phenocrysts, fracturing and pull-apart features of insets; quartz exhibits undulose extinction and new strain-free grains developed. The microcrystalline matrix of the porphyries is probably due to neomineralisation and recrystallisation producing the characteristic porphyroidal (after Spry, 1969, p. 237) texture (see Section 4.1.1.1).

(v) In the high-strain subdomain, recrystallisation and deformation textures are typically developed in the granitoids. On a mesoscopic scale $s_1$ generally remains poorly defined, but is evident to a more or lesser extent from (a) a parallel to subparallel arrangement of the ubiquitously present mafic xenoliths; $s_1$ cuts through the inclusions and is not

Table 3.1. Character of the regional foliation in the Richtersveld Province (lower Fish River and Haib areas).

| | Low-strain subdomain (towards the Orange River) | | High-strain subdomain (towards the front) | |
|---|---|---|---|---|
| | Vioolsdrif Granite Suite | Orange River Lavas | Vioolsdrif Granite Suite | Orange River Lavas |
| Mesoscopic | foliation generally absent; xenoliths locally subparallel to foliation | foliation locally prominently developed as a refracting fracture cleavage; absent over large areas | commonly defined by alignment of flattened xenoliths and arrangement of dark minerals; incipient augen development locally; infrequently gneissic and locally poorly defined | well-defined mylonitic with phyllonitic zones; also developed as fracture cleavage |
| Neomineralisation | | common as a very fine-grained mica foliation in matrix of porphyries | common mica foliation | distinctly developed - especially in phyllonitic schistose zones |
| Cataclastic nature | deformation textures generally absent on scale of thin section | phenocrysts and porphyroclasts exhibit microstuctures e.g. flattening, fractures, deformation, etc. | mortar texture commonly developed in the medium to coarse-grained granitoids; felspar phenocrysts become porphyroclastic | porpheroidal and blastomylonitic |
| Annealing | | matrix recrystallised; porpheroidal textures common | matrix of cataclasites largely recrystallised | recrystallisation of microcrystalline matrix far advanced; equilibrium textures developed in some zones |
| Penetration | non-penetrative | only locally pervasive; the foliation generally, is not penetrative on scale of a thin section | macroscopically pervasive, but not always on microscopic scale | microscopically penetrative on regional scale |

wrapped around, (b) a poorly defined preferred orientation of felspar porphyroclasts; augen structures are infrequently developed and (c) a dark mineral fabric. The foliation $s_1$ in the lavas is microscopically penetrative, neomineralisation and recrystallisation features are well advanced with the development of blastomylonites and equilibrium textures in some suitable lithological horizons (probably water-containing volcaniclastics).

(vi) A characteristic feature of the $D_1$ strain distribution is the presence of zones of intense foliation which (a) are commonly located along lithological boundaries and elsewhere irregularly disposed throughout the Richtersveld Province; in the Haib area the major zones of intense foliation seem to form an anastomosing pattern (Fig. 3.2) largely controlled by lithological distribution and preferentially developed in rocks of the Haib Subgroup, (b) vary in width from 1 - 100 m and more rarely may be several kilometres wide, (c) have the same attitude as the regional foliation and have similar, down-dip plunging lineations and, (d) consist of augen gneiss, blastomylonites and phyllonites. These deformed rocks are generally well recrystallised and exhibit the same grade of metamorphism that is regionally developed (Section 4.1). That these zones of intense foliation are zones of high $D_1$ strain, is evident from the increased flattening of xenoliths towards the cores and the gradual increase in the intensity of $s_1$ (mylonitic banding) development. Recrystallisation and neomineralisation in these high-strain zones are far more advanced than that of the region in both the low and high-strain subdomains and equilibrium textures are developed. It is evident that a strong correlation exists between the amount of strain and the state of recrystallisation-neomineralisation, an observation that substantiates the notion of dynamic recrystallisation (White, 1973) and/or syntectonic recrystallisation-neomineralisation (Higgens, 1971).

*Geometry*

The $s_1$ strike lines in the lower Fish River area (see Fig. 3.3), are arranged parallel to the front and regional grain of the adjacent marginal zone of the Namaqua Province. The $s_1$ strike lines in the Haib area make an acute angle with the front and the grain (Fig. 3.2) is less consistent. The anastomosing pattern is largely controlled by the lithological distribution. The foliation is better developed in the lavas while the Vioolsdrif granitoids reacted more competently with the foliation wrapped around granitoid bodies.

In general, the regional grain of $s_1$ in the Richtersveld Province is uniform and suggests the absence of large-scale post-$D_1$ folding; no macroscopic folds defined by $s_1$, were recognised. The strike-consistency of $s_1$ is borne out by the stereographic plots (Fig. 3.4) representing data from the two areas investigated.

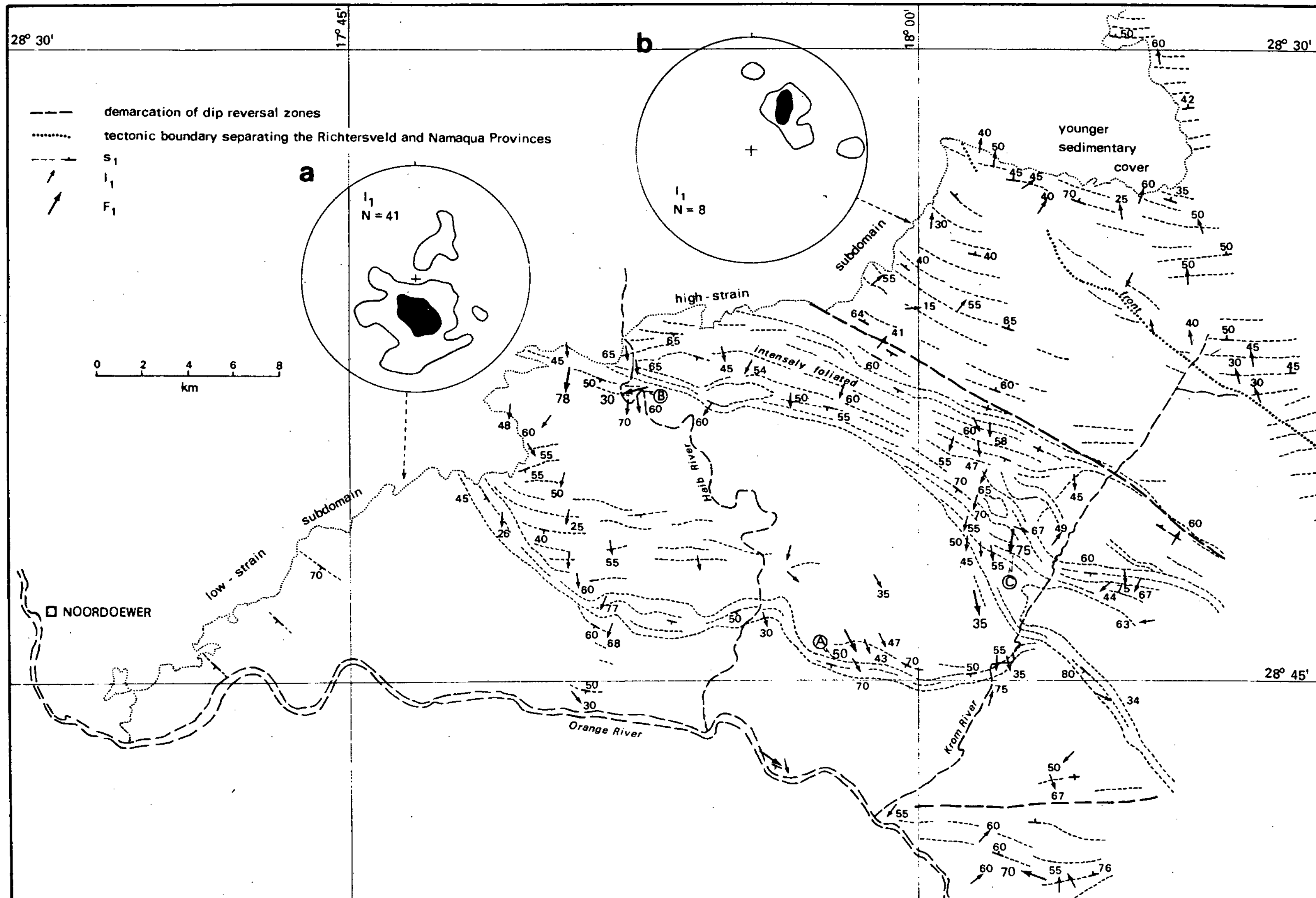


*Fig. 3.2. Structural domains in the Haib area. An intensely foliated zone subdivides the area into low and high-strain subdomains. The stereograms represent equal-area plots of $l_1$ for the two subdomains. Contours: a. > 0%, 20% per 1% area and b. > 0%, 25% per 1% area.*

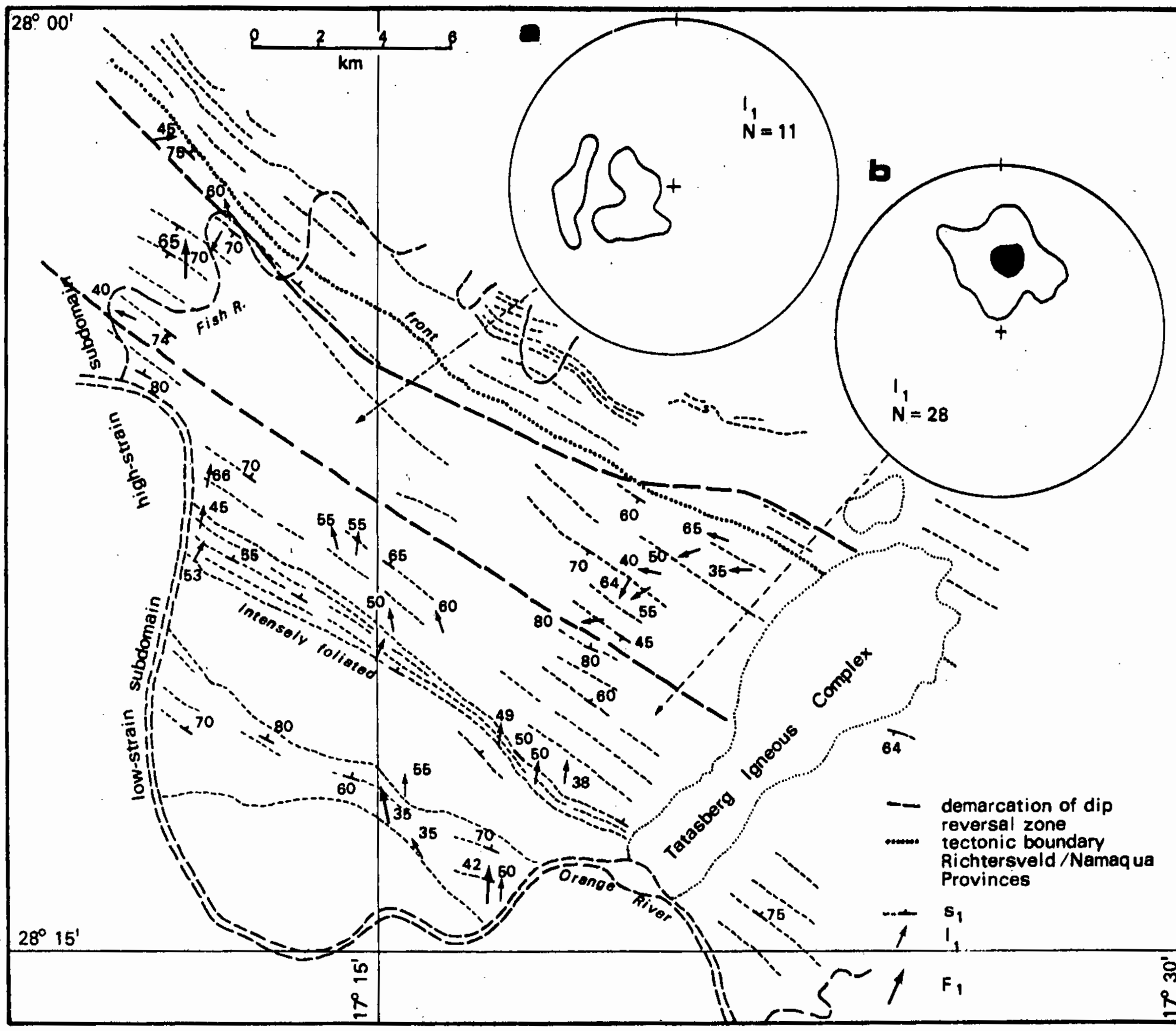


*Fig. 3.3. Structural domains in the lower Fish River area. In contrast to the Haib area (Fig. 3.2), the front is here parallel to the regional grain on both sides. The part of the Richtersveld Province shown here, is subdivided into high and low-strain subdomains by an intensely foliated zone. The stereograms represent equal-area plots for $l_1$ in domains of consistent $s_1$ attitude. Contours: a.> 0% and b.> 0%, 25% per 1% area.*

The stereograms (Fig. 3.4) also illustrate the dip reversal of $s_1$. It is significant that a zone of dip reversal of the regional foliation is present in both the lower Fish River and Haib areas : these zones are areas in which the foliation has a southern dip instead of the general northerly dip direction. The area of dip reversal in the lower Fish Rver area constitutes a discrete zone bordering the front (Fig. 3.3). In the Haib area the zone of dip reversal forms the core of the Richtersveld Province (Figs. 3.2 & 3.6). This zonal change of dip direction is not due to rotation through the horizontal (buckling), but due to rotation through the vertical (see the absence of subhorizontal attitudes in Fig. 3.4).

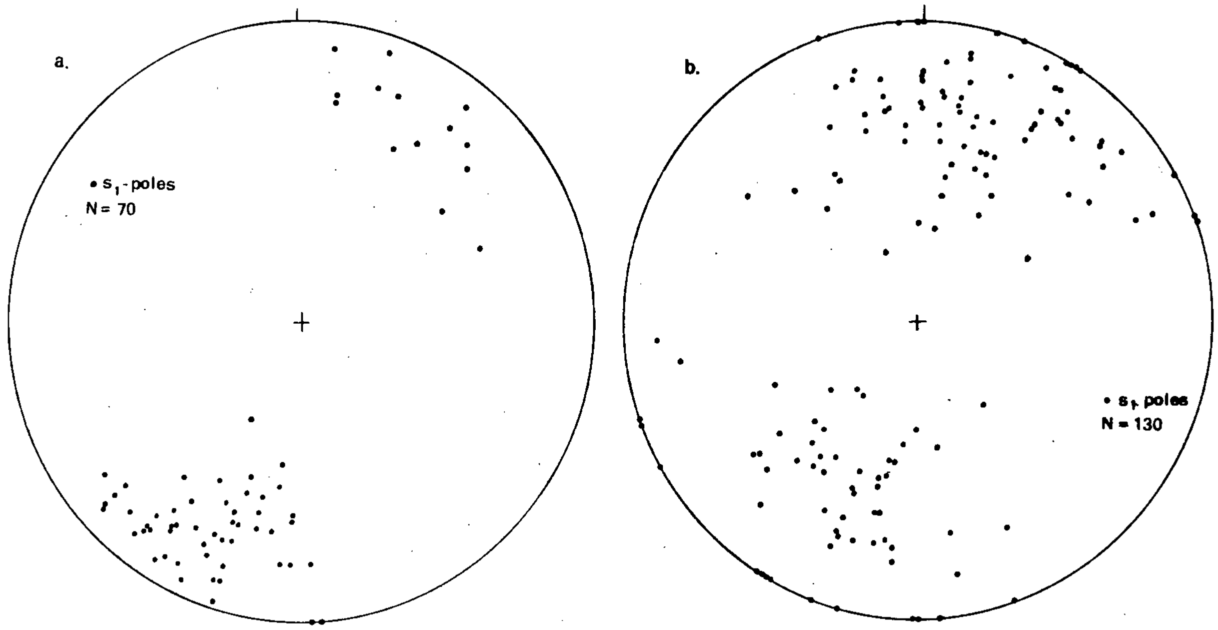


*Fig 3 4 Equal-area stereographic plots of $s_1$-poles for the parts of the Richtersveld Province a. in the lower Fish River area, and b. the Haib area.*

### 3.3.1.2 Regional Lineation, $l_1$

*Character*

The regional lineation $l_1$, situated in $s_1$, forms an integral part of the foliation and is ubiquitously present where $s_1$ is developed. Structures such as small fold hinges, wrinkles, boudin, mullions, intersections of s-surfaces, etc. are not here considered as $l_1$. The lineation $l_1$ forms small linear features, usually smaller than a few cm in length, and is identified as follows :

(i) The most common type of lineation in this low-grade terrain is a colour striping or mineral streaking. The colour striping is more typical where $s_1$ has a mylonite character while the streaking is defined by the mineral distribution in the form of linear mineral aggregates which may consist of either (a) leucocratic minerals e.g. small white streaks identified as lenticles of quartz grains, or, (b) micas; micaceous aggregates were identified to consist of randomly oriented chlorite or biotite, or, (c) a mixture of dark minerals with a decussate texture and consisting of chlorite, biotite, hornblende and epidote, or, (d) dark mineral trains.

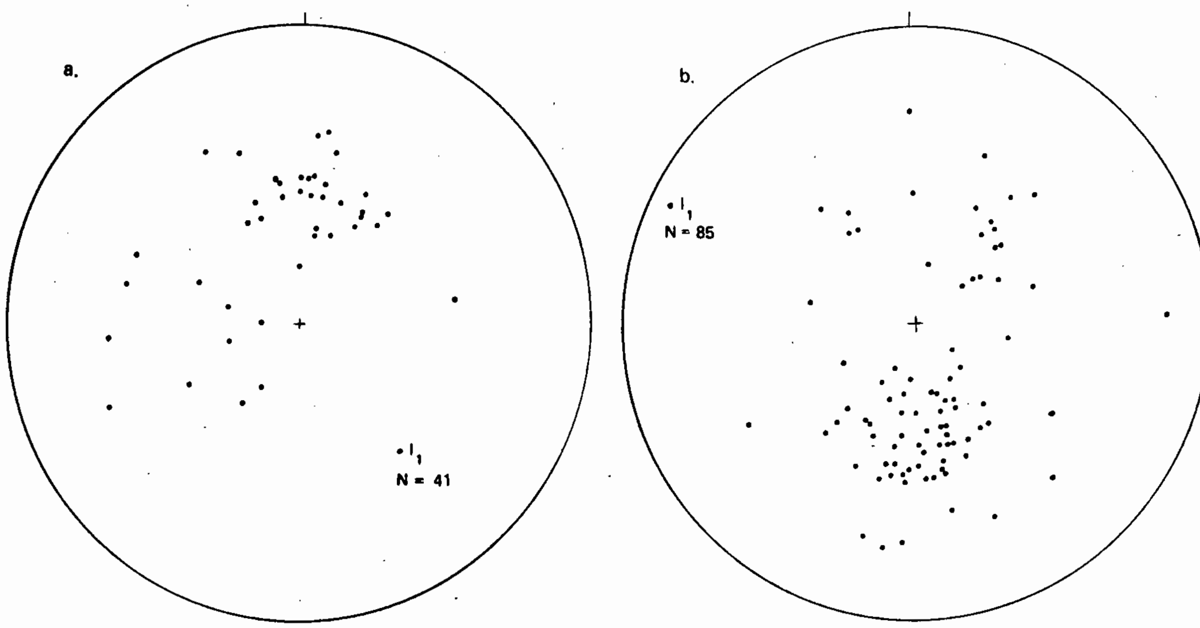


*Fig 3.5 Equal-area stereographic plots of $l_1$ for the parts of the Richtersveld Province a. in the lower Fish River area, and b. the Haib area.*

The mineral aggregates are either rod-like or blade-shaped with the long axes and flat surfaces of the blades lying within $s_1$.

(ii) Hornblende prisms partly define $s_1$ and are arranged within $s_1$ in a random fashion or with a preferred linear orientation. Microscopic evidence such as the idioblastic shapes, skeletal forms and poikiloblastic nature of the hornblende suggest growth late during the process of $s_1$ development.

(iii) Prisms of tourmaline are sparse, but usually have a preferred linear orientation within $s_1$; the grains tend to be idioblastic and helicitic indicating late-stage growth with reference to $s_1$.

(iv) Linearly deformed fragments are disposed with their long axes and flat surfaces within the regional foliation; elongate shapes of deformed amygdales, felspar phenocrysts and fragmental material define $l_1$.

*Geometry*

The various linear structures, described above, geometrically constitute a single population; i.e. within an outcrop homogeneous with respect to $s_1$ the

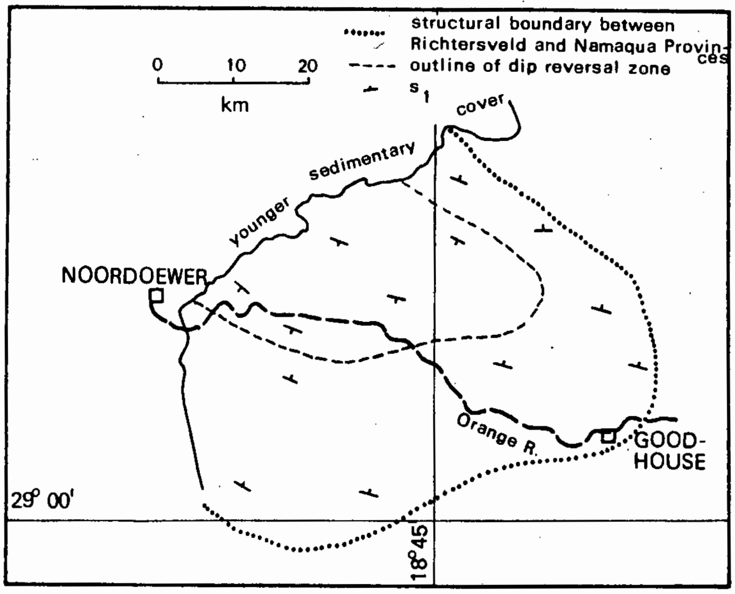


*Fig. 3.6. The area of dip reversal closely simulates the outline of the Richtersveld Province.*

striping, mineral streaks, prismatic mineral grains and linear deformed objects would all be sub-parallel to each other (Figs. 3.15 & 3.18). Because of this relation $l_1$ is considered to be a stretching lineation indicating the attitude of X, the maximum elongation direction. The XY planes of the deformed objects are always situated within $s_1$.

Typically $l_1$ has a near down-dip trend; the average pitch of $l_1$ on $s_1$, in part of the lower Fish River area for example, is 76° (Fig. 3.7), indicating a constant relationship between $l_1$ and $s_1$. The regional pattern of $l_1$ (Figs. 3.2 & 3.3) shows a consistent trend in domains homogeneous with respect to $s_1$. The spread of $l_1$, compiled over the whole of the Haib and lower Fish River areas (Fig. 3.5) is due to the dip reversal of $s_1$ (Fig. 3.4).

In summary, $l_1$ is a stretching lineation which forms a transverse set of structures with respect to the regional grain.

### 3.3.1.3 $F_1$

*Structures deformed by $F_1$*

The only pre-$s_1$ surfaces recognised defining the $F_1$ folds, are the primary layering in the volcanic rocks. Because of the paucity of primary

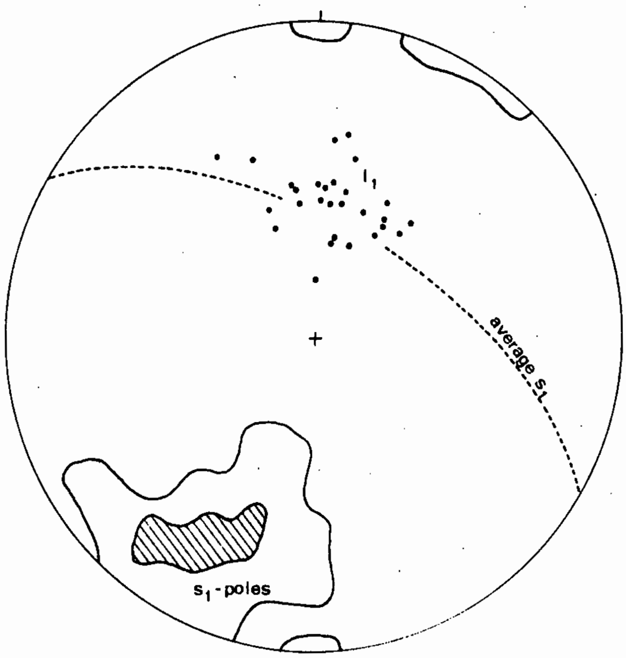


*Fig. 3.7. A domain within the Richtersveld Province (lower Fish River area) homogeneous with respect to $s_1$, showing the constant relationship between $s_1$ end $l_1$ (N = 28). Contours, 1%, 13%, per 1% area (N = 52).*

layering and perhaps the lack of ductility contrast between layers, small folds are sparse. The Vioolsdrif granitoids possess no pre-$s_1$ surfaces with the result that $F_1$ folds were only observed in contacts between the various intrusive phases.

*Correlation and definition of $F_1$*

Considered as $F_1$ are fold structures with the regional foliation $s_1$, as the axial-plane foliation; the correlation of $F_1$ folds throughout the areas investigated, is therefore dependant on the correlation of the foliation (see Section 3.3.4). The possibility of a pre-$F_1$ fold phase is considered (Section 3.3.2). If so, it is likely that pre-$F_1$ and $F_1$ folds in the high-strain subdomain approach coplanar attitudes and that some of the folds considered here belong to a pre-$F_1$ phase. No superposed folding were, however, observed.

3.3.1.3.1 Haib area

*Major $F_1$ fold*

The macroscopic structure is defined by the distribution of the Nous Formation

(Fig. 3.8). It is an open (interlimb angle approximately $110^{o}$) upright syncline in the west (i.e. in the low-strain subdomain) and an overfolded isocline at the closure towards the east (high-strain subdomain). The trace of the regional foliation, $s_1$ (Fig. 3.8) is geometrically consistent with the axial-plane trace. In the west along the main road, for example, the volcanic rocks are not penetratively cleaved; from the position where the structure crosses the Orange River eastwards, the lavas are penetratively foliated on hand-sized scale. Sympathetically with this variation in intensity of $s_1$, the large structure tightens eastward. The geometry of the open syncline in the west is depicted in Fig. 3.9. The $\pi$-pole represents the macroscopic fold axis plunging $20^{o}$ in a direction $272^{o}$. Shear zones, in the vicinity of domain A (Fig. 3.8), roughly parallel to the grain of the regional foliation, have variably oriented small fold structures which are at variance with the geometry of the macrostructure. These shear zones can be interpreted as part of the $D_1$ phase representing local high-strain zones in which the minor structures are differently oriented or as belonging to a different deformational phase.

The geometry of minor $F_1$-folds at domains B, C & D (Fig. 3.8) is different to that of the large structure at A (cf. Figs. 3.9, 3.10, 3.11 & 3.12). At B the mesoscopic folds are close (*sensu* Fleuty, 1964) and similar-like, with a penetrative axial-plane foliation, $s_1$. The variation in orientation of the different types of lineations (Fig. 3.10) is due to a variation in the orientation of $s_1$. Allowing for this the regional lineation, the maximum finite elongation direction and fold axes roughly group together within an angular distance of $30^{o}$ on $s_1$. At domain C (Fig. 3.8) macroscopic fold closures in stratification ~~is~~ are clearly recognisable on macroscopic scale. On outcrop scale, however, the intensity of $s_1$ is such that stratification surfaces are largely obscured and ~~the~~ at macroscopic fold hinges, $s_1$ cuts across the layering in the volcanics at large angles. A compilation of the minor $D_1$ structures (Fig. 3.11) demonstrates the orientation of $F_1$ and geometric relationship between $F_1$ and the various associated lineations. Minor post-$D_1$ folding is developed at C and might have contributed to the spread of the linear elements; in measuring $D_1$ elements, care was taken, however, to avoid outcrops where post-$D_1$ folds are present. Allowing for the variation in orientation of $s_1$, it seems that the principal finite elongation direction are close to that of the fold axes (Fig. 3.11). In the vicinity of the macroscopic closure at D (Fig. 3.8), the relationship between $s_1$ and $s_o$, the stratification, is similar to that described for domain C; the stratification describes a fold axis ($\pi$-pole) which groups within a small spread, together with $F_1$ and $l_1$ (Fig. 3.12).

There is a marked variation in attitude of $F_1$ folds from west to east across the macroscopic structure. The fold attitutes (Fig. 3.13), as measured on small hinge zones, $s_1/s_o$ intersections and $\pi$-poles, approximately describe a small circle girdle. This phenomenon can be interpreted in two ways :

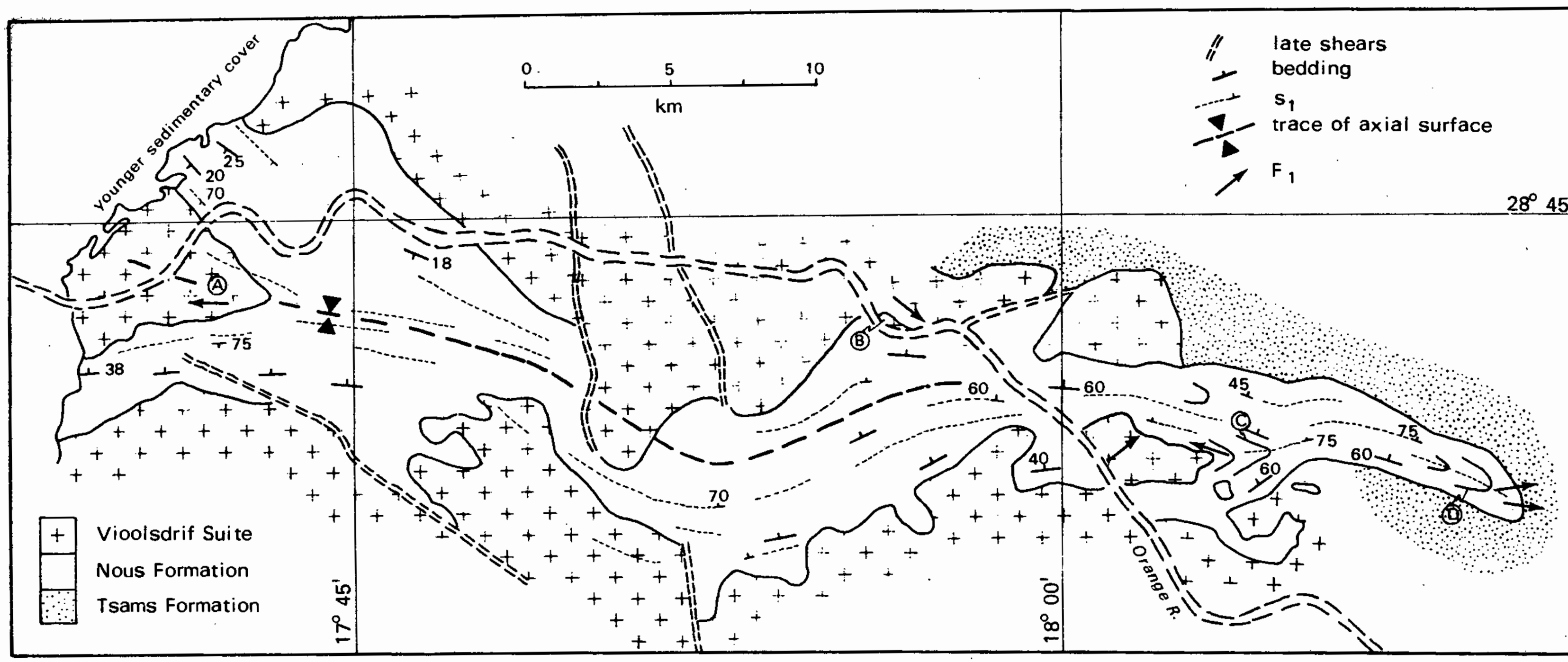


*Fig. 3.8. Macroscopic fold outlined by the distribution of the Nous Formation. Details of associated minor structures at A, B, C and D are discussed in text.*

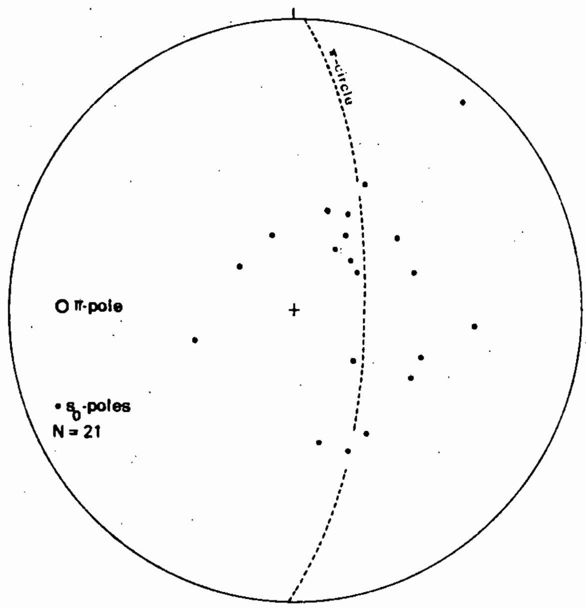


*Fig. 3.9. The geometry of the macroscopic syncline at A (Fig. 3.8) as defined by stratification in the Haib volcanics. An upright, open and shallow (20°) westerly-plunging (272°) fold is depicted.*

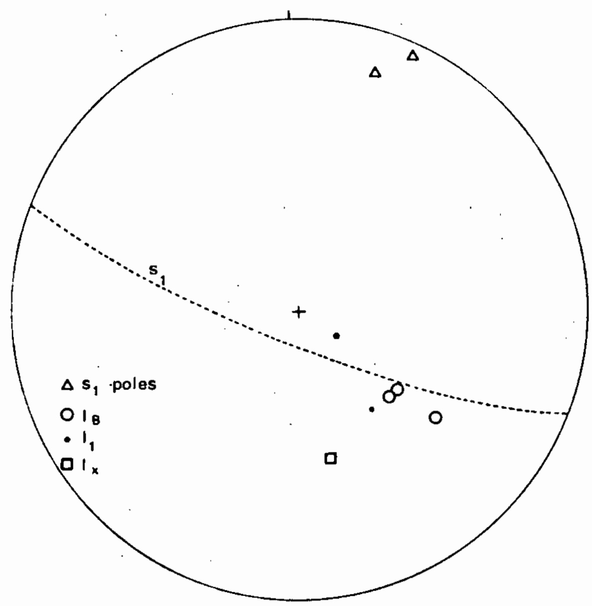


*Fig. 3.10. $D_1$ fold elements at domain B (Fig. 3.8); $l_B$ is an intersection lineation $s_1/s_0$ and represents fold axes; $l_x$ is the principal finite elongation direction of a strained clast.*

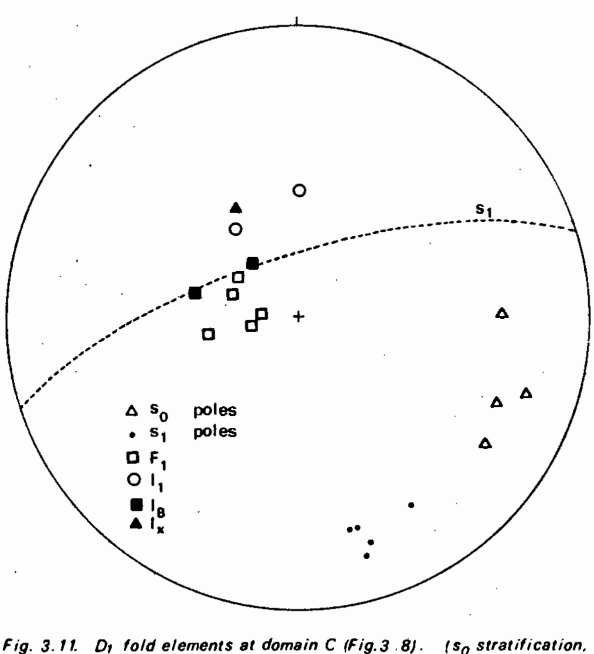


*Fig. 3.11. $D_1$ fold elements at domain C (Fig. 3.8). ($s_0$ stratification, $s_1$ regional foliation, $F_1$ fold axes, $l_1$ regional lineation, $l_B$ intersection $s_1/s_0$, $l_x$ principal finite elongation direction)*

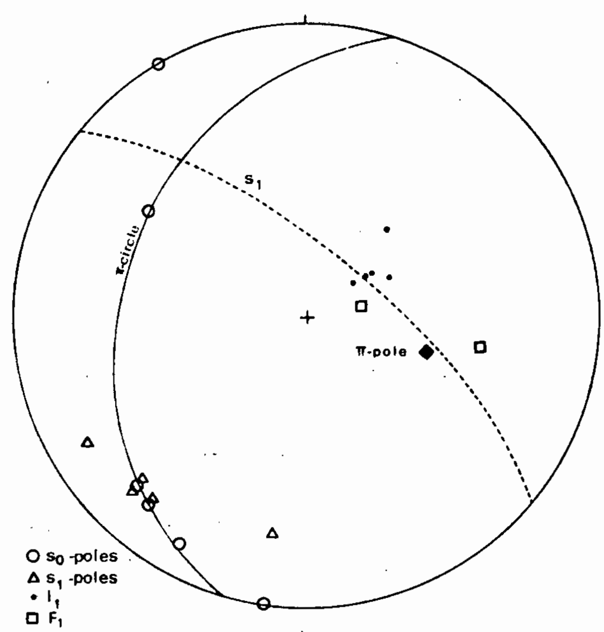


*Fig. 3.12. The π-pole of the fold closure at D (Fig. 3.8) in relation to the associated small structures $F_1$, $l_1$ and $s_1$*

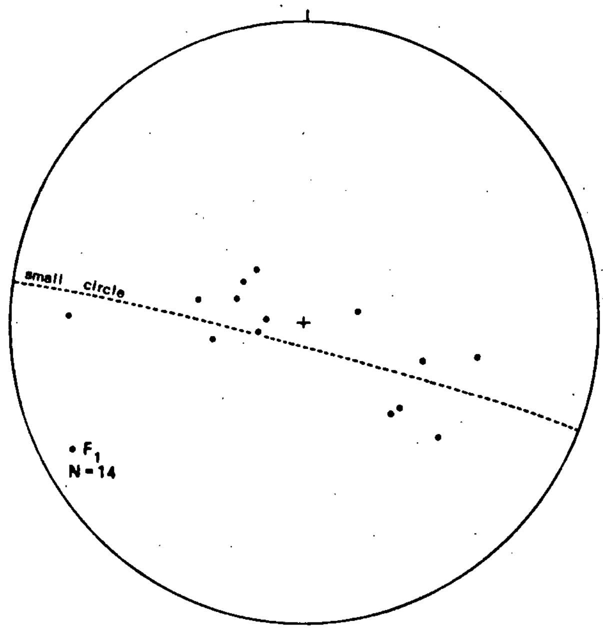


*Fig.3.13 A synoptic diagram of $F_1$ fold elements which define the axial attitude and are representative of domains A, B, C and D (Fig.3.8). The variation in attitude of $F_1$ throughout the major structure approximately describes a small circle girdle.*

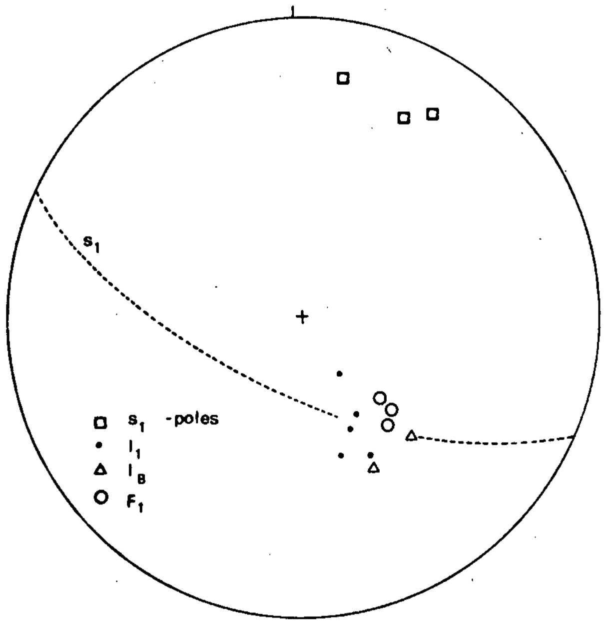


*Fig.3.14. $F_1$ fold elements at A (Fig 3.2). ($l_B$ $s_1/s_0$ intersection)*

(i) Sympathetically with the tightening of folds and increase of $D_1$ strain eastwards, the fold closures rotate during the progressive $D_1$ deformation. Theoretically (cf. rotation of lines and planes as a result of strain, Ramsay, 1967, p. 162) lines rotate, under the influence of flattening strain, to the XY-surface of the bulk strain ellipsoid and the $F_1$ fold axes should therefore be preferentially oriented along a great circle.

(ii) Bearing in mind the possibility that the $F_1$ folds considered here represent fold closures of both $D_1$ and pre-$D_1$ fold phases, the small circle girdle reminds of the geometric path of older lineations deformed by buckling (Ramsay, 1967); in the case of coplanar refolding by buckling, however, both the older and younger fold axes should fall on the same great circle.

With the poor definition of the small circle girdle (Fig. 3.13) both options, are possible and this is further discussed below.

*Mesoscopic and minor $F_1$ folds*

At A (Fig. 3.2) numerous minor $F_1$ folds are developed in an exceptionally well-layered part of the volcaniclastic member. The locality is situated in the low-strain subdomain, but within a broad zone of intense foliation which is either a reflection of high strain or the ductility and layering of the lithological unit or both. The folds are parallel with interlimb angles varying from open to close. In the hinge zones, $s_1$ forms a refracting pattern. The fold axes and mineral lineations ($l_1$) group together (Fig. 3.14).

A large mesoscopic $F_1$ fold closure at B (Fig. 3.2) along the Haib River, is situated in the high-strain subdomain. It is an overfolded antiform with a rounded hinge zone. The foliation $s_1$ forms a refracting pattern in the well-layered volcanics and is penetrative on the scale of the outcrop. Minor folds are not developed, but the axial direction was determined by measuring $s_1/s_0$ intersections ($l_B$); the principal finite elongation direction ($l_x$) was determined from flattened fragments in schistose volcaniclastic layers. The axial direction and regional lineation are separated by an angle of $60^o$ on $s_1$ (Fig. 3.15); this large angular difference between $F_1$ and $l_1$ is atypical for the Haib area. Elsewhere in the high-strain subdomain, for example at C, (Fig. 3.2) $l_1$ (hornblende needles) are parallel to the fold hinges. In the vicinity of locality C, the shape of the folded layers are more parallel-like than similar; both isoclinal and tight folds were observed.

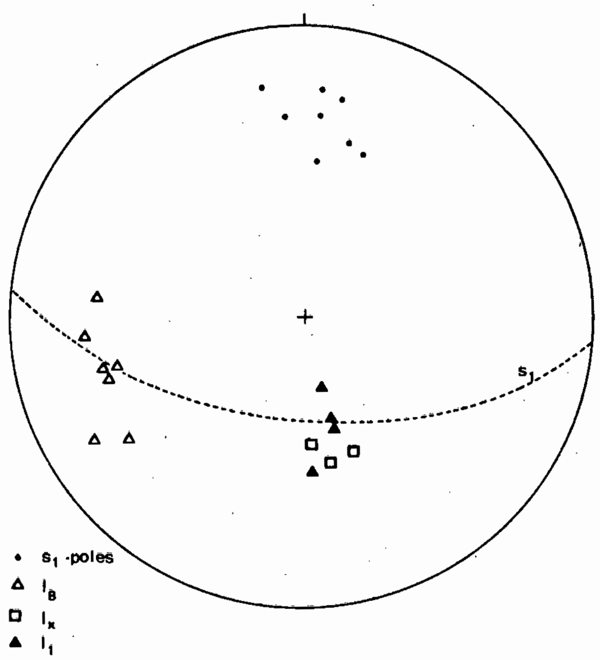


*Fig. 3.15. $F_1$ fold elements of a large mesoscopic structure at B (Fig. 3.2). ($l_B$ $s_1/s_0$ intersection, $l_x$ principal finite elongation direction).*

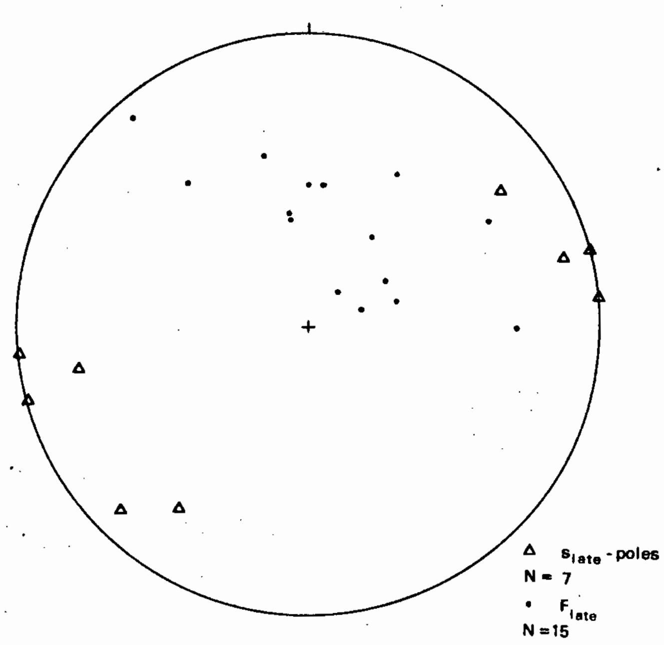


*Fig. 3.16. Post-D1 crenulations and associated foliations in the lower Fish River area*

*Synoptic view*

The variation in attitude of all the fold axes (Fig. 3.17) in the Haib area describes a small circle girdle-like pattern and strengthens the argument that at least some of the folds considered here as $F_1$, are refolded pre-$F_1$ folds. Whereas the fold axes are variably oriented, the stretching lineation has a more constant attitude. Stretching lineations associated with the folds depicted in Fig. 3.17 are compiled in Fig. 3.18; apart from the spread which is due to the dip reversal of $s_1$ (see also Section 3.3.1.2), $l_1$ plunges constantly in an approximately down-dip direction on $s_1$. With respect to $s_1$, $l_1$ is therefore geometrically a constant factor which is not the case for $F_1$.

3.3.1.3.2 Lower Fish River area

A macroscopic and tight $F_1$ closure is developed in the De Hoop volcanics (see Annex. 1) with its fold axis parallel to $l_1$ (Fig. 3.3). Only two other minor folds were observed and are both close and northerly plunging. A minor fold in the contact surface between two phases of the Vioolsdrif Suite is depicted in Plate 1.

3.3.1.3.3 Mechanism of folding

A buckling mode of folding (see Ramsay, 1967) is inferred from the parallel-like geometry of folded layers and the ubiquitous contact shearing between lithological units/layers suggesting a component of flexural-slip. Refracting cleavage patterns in the low-strain subdomains indicate a relative 'low' component of flattening strain.

3.3.1.4 Finite strain

The finite strain as recognised in the flattening of phenocrysts and xenoliths is mainly effected by $D_1$. Strained bodies have elongate oblate shapes with $X>Y>Z$; the XY-plane lies in the regional foliation, while the principal finite elongation direction X, is parallel to mineral lineations and define $l_1$, the regional lineation (Section 3.3.1.2). The regional compilations of $s_1$ and $l_1$ (Figs. 3.2, 3.3, 3.4 & 3.5) therefore depict the attitude of the bulk strain ellipsoid. In the Haib area close to the front (Fig. 3.2), deformed mafic inclusions in Vioolsdrif granitoids have an oblate shape with $X \simeq Y$. Twelve measurements at four localities give an average value of 5,8:1 for X:Z and assuming that the inclusions were originally spherical, the amount of flattening normal to the foliation is 69 per cent. As the strain distribution is markedly heterogeneous (Section 3.3.1.1), the figure 69 per cent pertains to the maximum strain for the area it represents.

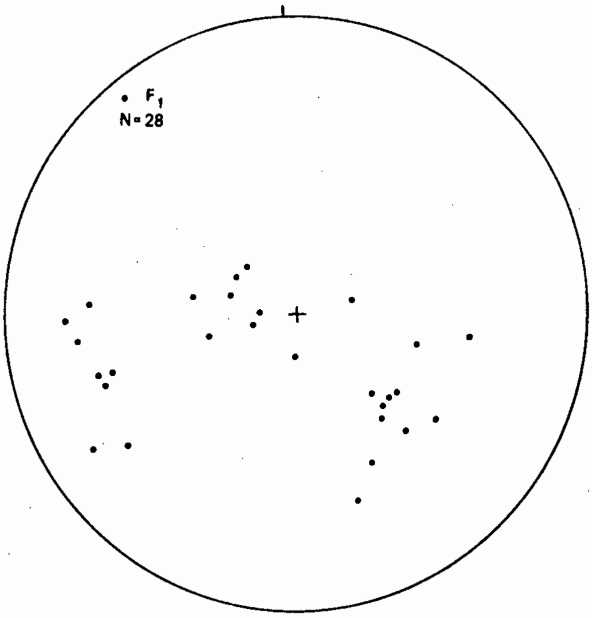


Fig.3 .17. Compilation of $F_1$ axial attitudes in the Haib area ; a small circle girdle distribution pattern is suggested.

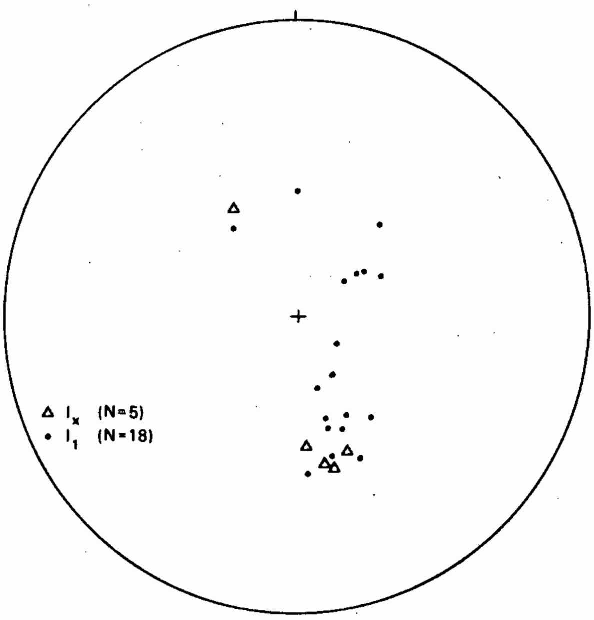


Fig. 3.18. The distribution pattern of the stretching lineations ($l_1$) associated with the folds compiled in Fig. 3.17. The long axes of strained fragments ($l_x$) are parallel to $l_1$.

### 3.3.2 Pre-$D_1$ folding in the Orange River volcanics

A pre-$D_1$ fold phase affecting the Orange River volcanic sequence prior to the emplacement (or penecontemporaneous) of the Vioolsdrif intrusives, is postulated here. In the areas investigated, $D_1$ small structures were never observed to be overprinted on older structures. In areas where the volcanics are tightly folded, however, a strain imprint on the Vioolsdrif intrusives are lacking or surprisingly poor. The tight to isoclinal macroscopic folding in the De Hoop volcanics (Annex. 1) and in the Haib volcanics east of the Orange River (Fig. 3.8) must be considered. If all the flattening giving rise to the folding was affected after the emplacement of the Vioolsdrif intrusives, a considerable fabric imprint should be developed in the intrusives, although they are more competent than the volcanic rocks. This, however, is not the case and the granitoids surrounding the De Hoop volcanics have virtually no imprint of $s_1$. Judging by the shape of phenocrysts and inclusions, the finite strain is negligible or not apparent and the same is true for the granitoid bodies in the vicinity of B and C (Fig. 3.8) in the Haib area.

The $D_1$ folds discussed in Section 3.3.1.3 can therefore be considered a mixed bag of $F_1$ and pre-$F_1$ folds. The small circle distribution pattern of these folds (Fig. 3.17) substantiates the impression that some of the folds predate $D_1$. All the so-called $F_1$ closures have $s_1$ as a common element and it is necessary therefore for $F_1$ and pre-$F_1$ phases to have been initially close to being coplanar or to have been rotated into such an attitude.

### 3.3.3 Post-$D_1$ deformation

Post-$D_1$ deformation is extremely sparsely developed, even in localities where $s_1$ is well developed. The structural division across the front between the Richtersveld and Namaqua Provinces also separates domains with respect to the frequency of post-$D_1$ folds and north of the front such folds become conspicuously more common. Macroscopic post-$D_1$ folds are not developed in the parts of the Richtersveld Province investigated.

#### 3.3.3.1 $D_2$

Spatially associated with the structural boundary separating the Richtersveld and Namaqua Provinces is an *en echelon* arrangement of pegmatites, most abundantly developed in the south (the Orange River pegmatite area of Gevers et al., 1937) and in the vicinity of Goodhouse (Beukes, 1973). Between Goodhouse and Witputs and in the lower Fish River area, the pegmatites are less abundant, but persist in an *en echelon* fashion along the front. The pegmatites are subvertical and discordant with respect to $s_1$ and their contact surfaces with the country rock are sharp with generally no sign of movement. Their arrangement and orientation is schematically shown in Fig. 3.21. These features are interpreted as pegmatite-filled tension fractures. Their arrangement suggest an approximately east-west lateral stress condition (Fig. 3.21) in the crust at that time which caused some relative movement between the 'isotropic' and anisotropic domains of the Richtersveld and Namaqua Provinces respectively.

U-Pb and Rb-Sr dating of two of these pegmatites yielded ages of 960 and 950 - 956 Ma respectively (Burger & Coertze, 1973, nos. 40 & 49 for the Republic of South Africa).

#### 3.3.3.2 $D_3$

The correlation of the $D_3$ structures between the Haib and lower Fish River areas is tenuous, although similar time intervals and tectonic environments are apparent.

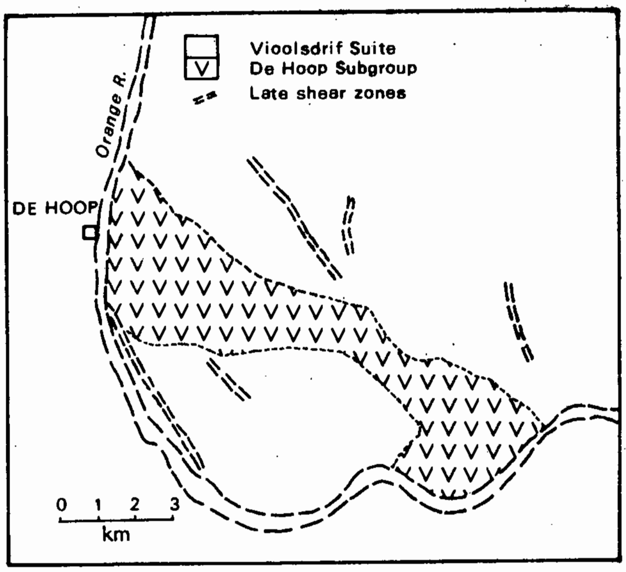


*Fig. 3.19. A set of subvertical shear zones in the lower Fish River area which are correlated with late Precambrian deformation along the west coast.*

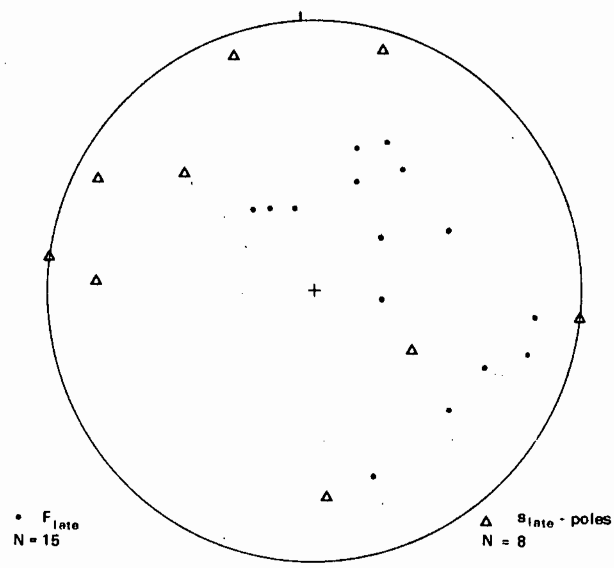


*Fig. 3.20. Post-$D_1$ structures in the Haib area; the majority are kink bands.*

3.3.3.2.1 Lower Fish River area

*Shear Zones*

Late subvertical shear zones are developed in the south-western portion of the area (Fig. 3.19) and they become more common and of larger magnitude towards the south and west in the Richtersveld. They differ from the $D_1$ shear zones in that they have a more northerly trend (320° - 340°) and left-laterally displace the Gannakouriep dykes which post-date $D_1$. The age and optimum development of the shears along the coast associate them with the late Precambrian deformation of the Gariep sequence (Joubert, 1971; Joubert & Kröner, 1972; Kröner, 1974).

*Small structures*

Small crenulations and associated crenulation foliations deform $s_1$ in a non-pervasive manner and are recognisable in zones of intensely developed $s_1$.

The geometry of these structures for the part of the Richtersveld Province in the lower Fish River area are shown in Fig. 3.16. The foliation is subvertical with a mean trend of 330° and the hinges of the crenulations are more variable in attitude, possibly because of the initial variation of $s_1$. These structures are tentatively correlated with each other on the basis of style and post-$D_1$ nature and their correlation is substantiated by the reasonable constant attitude of the crenulation foliation. The similar geometry of the foliations and the late Precambrian shear zones (above) suggests that these structures belong to the same deformation phase.

#### 3.3.3.2.2 Haib area

*Shear zones*

A number of subvertical shear zones with significant strike lengths are present in the Haib area trending approximately north-northwest (± 345°) (see Annex. 3 & Fig. 3.8). Judging by the configuration of the foliation along their margins and offset of lithological contacts (Fig. 3.8), the displacement has a horizontal component in a right-lateral sense. Their age with respect to the Gannakouriep dykes is not known, but they post-date the pegmatites and the late tectonic granite (Section 2.3.3.9.2). Their trend is similar to the post-$D_1$ shear zones found in the lower Fish River area, but the sense of displacement differs.

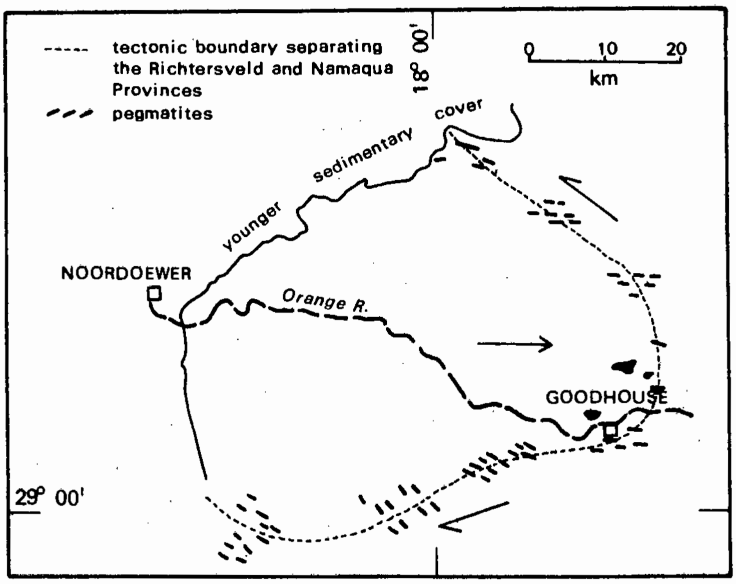


*Fig. 3.21. Schematic illustration of spatial association between the front and an en echelon array of pegmatites. The arrows indicate the relative movement required for the formation of pegmatite-filled tension fractures.*

*Small structures*

All the post-$D_1$ small structures are considered here. Although kinking deformation is prevalent, all these structures do not necessarily belong to the same phase of deformation; the paucity of the structures renders proper correlation and statistical treatment during a regional survey impossible. The geometry of the structures are shown in Fig. 3.20, with both structural elements showing a large variation in orientation. The fold hinges comprise some parallel folds (open to close), kinks and small wrinkles. The associated late foliation is defined by kink bands, crenulation foliations and axial planes.

The correlation of these structures with each other and with the shear zones described above, is questionable. It is possible that at least some of the structures are pre-$D_2$ and are perhaps the equivalent in the Richtersveld Province of the later deformations of the Namaqua Province.

### 3.3.4 Correlation of $s_1$ and relationship to $M_1$

That the regional foliation in the parts of the Richtersveld Province investigated is the same structure throughout, are substantiated by the following :

(i) In Section 4, it is shown that there is a sympathetic relation between $M_1$ recrystallisation and intensity of $D_1$; this relationship holds for both the De Hoop volcanics and Vioolsdrif intrusives throughout the lower Fish River area and also in the front zone. The metamorphic aspect associated with $s_1$ is a strong characterisation.

(ii) The foliation $s_1$ was not observed to cross-cut older foliations.

(iii) In the areas investigated the Vioolsdrif intrusives do not truncate an older planar fabric in the volcanics.

(iv) The geometry of $s_1$ is consistent with characteristic down-dip plunging stretching lineations. The zones of dip reversal do not represent a different phase of foliation as there is no cross-cutting phenomena and $s_1$ gradually rotate through the vertical to dip in the opposite direction.

### 3.3.5 Relation between $D_1$ and the Vioolsdrif intrusive event

In view of the difficulties in distinguishing between primary and secondary structures in granite (Berger & Pitcher, 1970), it is necessary to be more specific about the time relation between $D_1$ and the emplacement of the Vioolsdrif Suite. The imprint of $s_1$ is regarded to have taken place after or late with respect to the emplacement of all the intrusive phases since (i) a flow banding (described in Section 2.1.3.7) was recognised at two localities only, where it is parallel to $s_1$. (ii) The $s_1$ planar fabric has a deformation character (Section 3.3.1.1). (iii) The $s_1$ fabric cuts across the contact surfaces between the different intrusive phases and do not follow the boundaries of individual bodies. (iv) The foliation $s_1$ is imprinted on all the intrusive phases, while younger phases do not cross-cut planar fabrics in older phases.

It is shown by Berger & Pitcher (1970) that a granite below the liquidus transmits stress and therefore rheologically behaves similar to a solid. To distinguish, therefore, between structures imprinted on granitoids in the solid and in a crystal mesh state, is difficult. That the Vioolsdrif granitoids reacted competently during $D_1$ is demonstrated as follows :

(i) In the Haib area (Annex. 3) the regional anastomosing grain of $s_1$ in the volcanics is controlled by the disposition of granitoid bodies so that, on the farm Kromrivier, an augen-shaped granitoid body is situated within the Volcaniclastic Member with $s_1$ draped around it.

(ii) Flattened mafic inclusions have $s_1$ cutting through and not draped around, a relationship indicating a competency comparable to that of a basic rock.

It is also argued that $D_1$ was active after complete crystallisation and at temperatures below the solidus. The temporal association of $D_1$ with $M_1$ (Section 4.1) which affected a dark mineral fabric ($s_1$), are of retrogressive character, and show that the temperatures at the time of $D_1$ were well below the solidus temperatures for granitic melts. The process protoclasis (Waters & Krauskopf, 1941) accounts for much of the structures and textures developed in the marginal zone of the Vioolsdrif batholith (i.e. more or less the marginal tectonic domain as defined here). Protoclasis requires increased temperatures of recrystallisation towards the core of a batholith, while the opposite is true for the Vioolsdrif batholith (see Sections 4.1 & 4.2).

The possibility that $D_1$ was active during the emplacement of the Vioolsdrif intrusives cannot be totally excluded. It can be argued though, that if this was the case (i) a flow foliation should have developed (granitoid bodies along the Orange River are isotropic), and (ii) synkinematic recrystallisation at temperatures above the solidus would possibly have resulted in more advanced annealing textures and would not have been strictly dependant on strain energy as shown by the good correlation $D_1$-intensity/$M_1$-recrystallisation (Section 4.1.2.1). Finally, the evidence do not conclusively point to a pre-$D_1$ emplacement of the Vioolsdrif Suite, but do indicate that the deformation progressed after the emplacement.

### 3.3.6 Summary

Only the earlier part of the Namaqua tectogenesis (pre-$D_1$ and $D_1$) is represented in the Richtersveld Province. The $D_2$ pegmatite-filled tension fractures are located along the front and therefore cannot be considered as a structural imprint of the Richtersveld Province *in toto*.

| | | |
|---|---|---|
| Namaqua tectogenesis | Pre-$D_1$ | folding of volcanics |
| | $D_1$ | late syn- to post-Vioolsdrif pervasive foliation and folding |
| | $D_2$ | pegmatite-filled tension fractures |
| Late Precambrian tectogenesis | $D_3$ | post-Gannakouriep shear zones and kink structures |

## 3.4 Marginal zone

### 3.4.1 $D_1$, the first phase of deformation

### 3.4.1.1 Regional foliation

*Character*

The regional foliation ($s_1$) forms part of the oldest suite of structures recognised in the marginal zone and its character, as defined my microstructures, differs from that of the regional foliation of the Richtersveld Province. The transition is recognisable in the front zone (Section 4.2). Except in the hinges of $F_1$ minor folds, the regional foliation is invariably parallel to a lithological banding and is predominantly gneissic and defined by the dimensional orientation of constituent mineral grains. Strain-free grains and equilibrium-type grain boundaries indicate a crystalloblastic origin during the main metamorphism (Section 4). The general absence of deformation features suggests that the rate of recrystallisation and neomineralisation ($M_1$) exceeded that of deformation during $D_1$ or that $M_1$ outlasted $D_1$. The degree of penetration of $s_1$ is uniform throughout the marginal zone which, unlike the Richtersveld Province, is homogeneous in this respect.

*Geometry*

The most significant aspect of the marginal zone is the orientation stability of $s_1$ (Fig. 3.22). The homogenous grain indicates the absence of cross folding on a macroscopic scale.

### 3.4.1.2 Regional lineation

The lineation $l_1$ lies within the $s_1$ surface and is most commonly defined by a mineral grouping (streaking) and hornblende needles. At two localities a close angular relationship was observed between the principal finite elongation direction and the mineral lineation (Figs. 3.23 & 3.24). The mineral lineation is therefore essentially a stretching direction. The invariably down-dip plunge of $l_1$ on $s_1$ is a characteristic feature of the marginal zone and the average angle of pitch of $l_1$ on $s_1$ (Fig. 3.22) is $80^o$. The direction stability of $l_1$ can be evaluated on Fig. 3.22.

### 3.4.1.3 $F_1$ folds

$F_1$ folds are sparse and not everywhere distinguishable from $F_2$ folds. Dubious cases are not discussed and not included in the geometric compilations. In $F_1$ generation hinges a primary lithological layering only is folded with $s_1$ as the

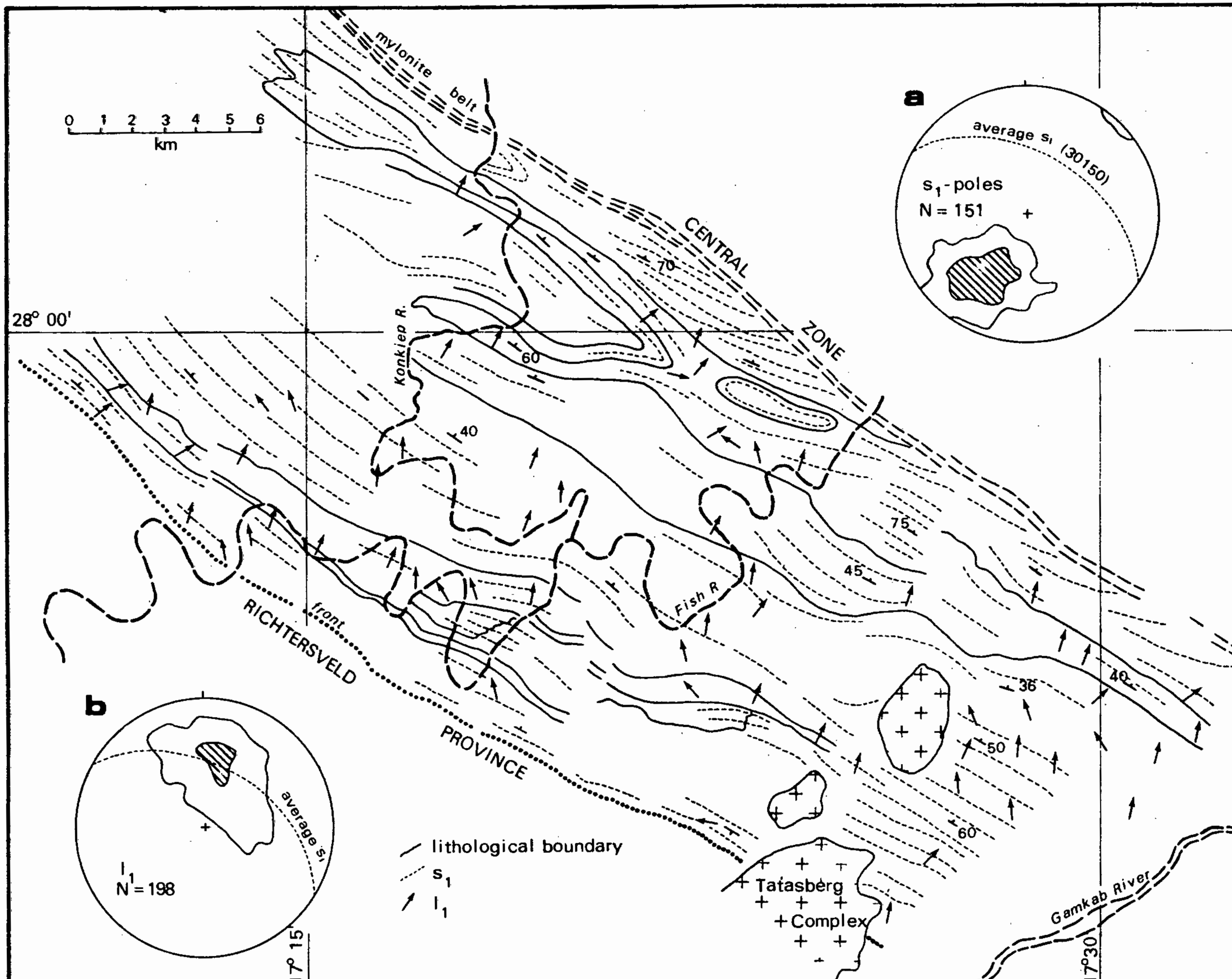


*Fig. 3.22. Areal and stereographic compilations of $s_1$ and $l_1$ in the marginal zone. Contours: a. 1,3% , 7% and b. 1% , 10% per 1% area.*

axial-plane foliation. Apart from the association with the regional foliation, considered to be the main discrimination factor, some aspects of style are characteristic. $F_1$ folds were observed to be coaxially refolded by both $F_2$ and $F_3$ at several localities (Plate 10). The style of the folds are depicted in Plates 4, 5 & 10 and judging by their appearance, the shape of $F_1$ folded layers closely approximates class 2 (similar) (Ramsay, 1967), markedly more so than the other fold phases. The hinges tend to be angular and the limbs are attenuated with a tendency to become disrupted. The folds are always isoclinal.

The relationship between $F_1$ and $l_1$ is variable. At some outcrops mineral lineations ($l_1$) are parallel to $F_1$ fold hinges (Fig. 3.24), while at others there is a distinct angular discrepancy (Fig. 3.26). A synoptic diagram (Fig. 3.25) of $F_1$ for the marginal zone shows a spread of the fold axes along the average $s_1$ for the marginal zone (from Fig. 3.22). The preferred orientation of $F_1$ (maximum density of $F_1$ on stereogram Fig. 3.25) though, is approximately similar to that of $l_1$ for the marginal zone (Fig. 3.22).

The $F_1$ data considered in this section are representative of the grey gneiss unit, mafic gneiss unit and banded amphibolite unit. All $D_1$ structural elements are imprinted on these gneissic units; the term pretectonic for these units therefore refers to pre-$D_1$.

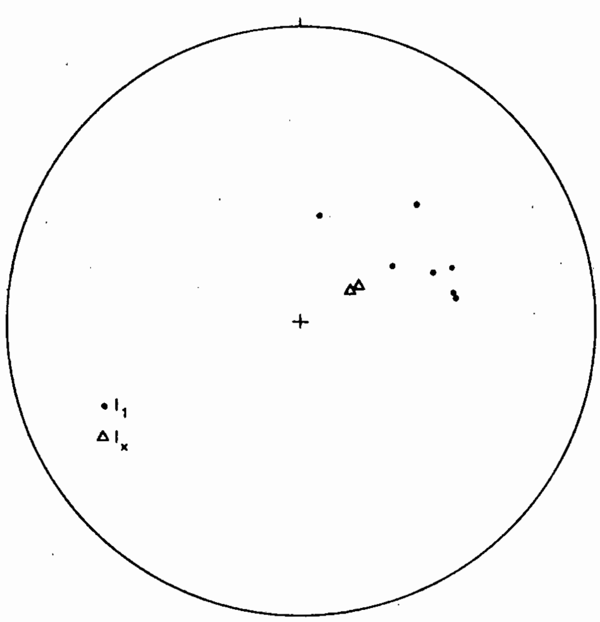


*Fig. 3. 23. The long direction of flattened clasts ($l_x$) in the mafic gneiss unit and its relation to the mineral lineations ($l_1$) in the vicinity.*

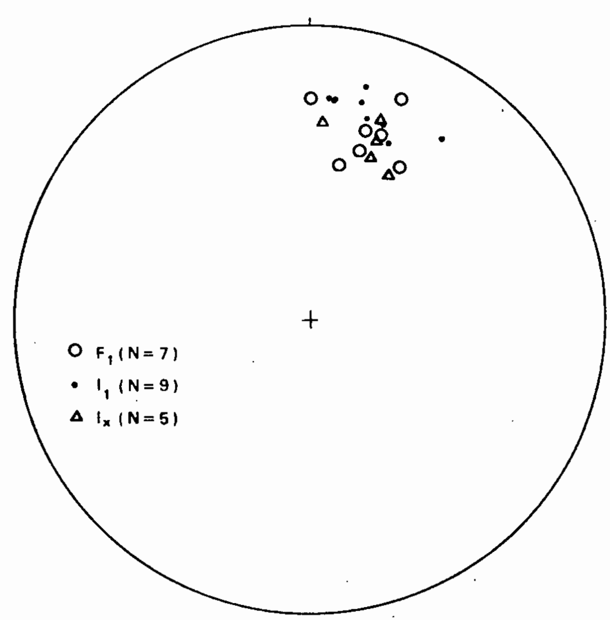


*Fig. 3. 24. Orientation data from an outcrop near the confluence of the Konkiep and Fish Rivers showing a coaxial relation between $D_1$ fold hinges ($F_1$), the mineral lineation ($l_1$) and the principal finite elongation direction ($l_x$).*

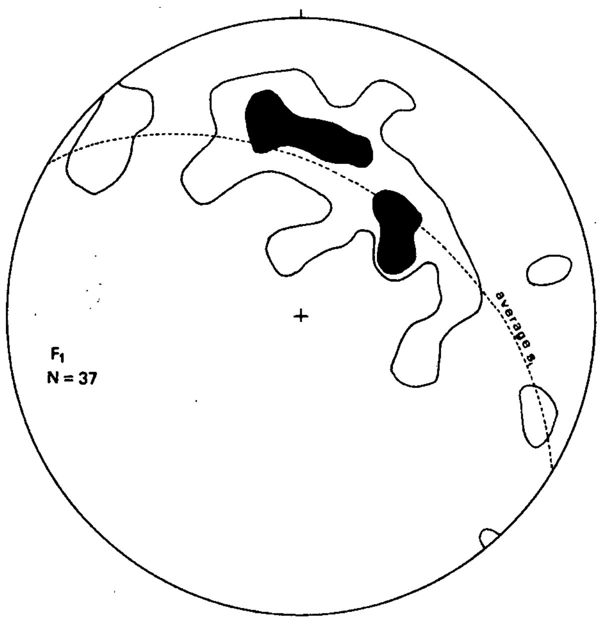


*Fig. 3.25. A compilation of all $F_1$ data from the marginal zone. Contours, > 0%, 7% per 1% area.*

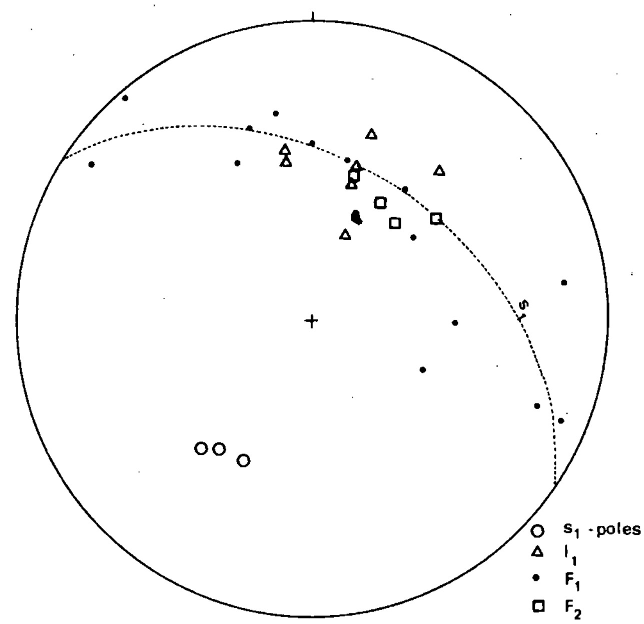


*Fig. 3.26. Angular relations between $F_1$, $F_2$, and $l_1$ from a single outcrop in the banded amphibolite unit. $F_1$ is variable in a domain of constant $l_1$, $F_2$ and $s_1$. The linear data are distributed along $s_1$.*

### 3.4.2 $D_2$

The second phase of deformation is mainly evident in the form of a penetrative suite of minor folds. These folds are typically isoclinal and fold $s_1$ in such a way that the axial planes are parallel, to the more regional attitude of $s_1$. Folds $F_1$ and $F_2$ are therefore coplanar. In Figs. 3.27 and 3.28, a regional and more local compilation, it can be seen that $F_2$ is preferentially oriented along $s_1$. $F_2$ also coaxially refolds $F_1$ (Plate 10).

Apart from the overprinting and geometric aspects, the $F_2$ isoclines differ from the $F_1$ isoclines in aspects of style when the group characteristics are compared. These features overlap for individual folds and cannot be used as the only discriminating factor. The shape of folded layers is both parallel and similar-like, most commonly approximating class 1c (Ramsay, 1967), the flattened parallel fold. The limbs lack a marked attenuation and disruption is virtually absent. In contrast to $F_1$, the hinges are rounded and a kink or chevron style is not uncommonly developed in the cores of folds. A slight or poor refoliation ($s_2$) was often observed and is developed in hinge zones only; the axial-plane foliation is not always developed and is never penetrative between outcrops. In a significant number of folds the refolia-

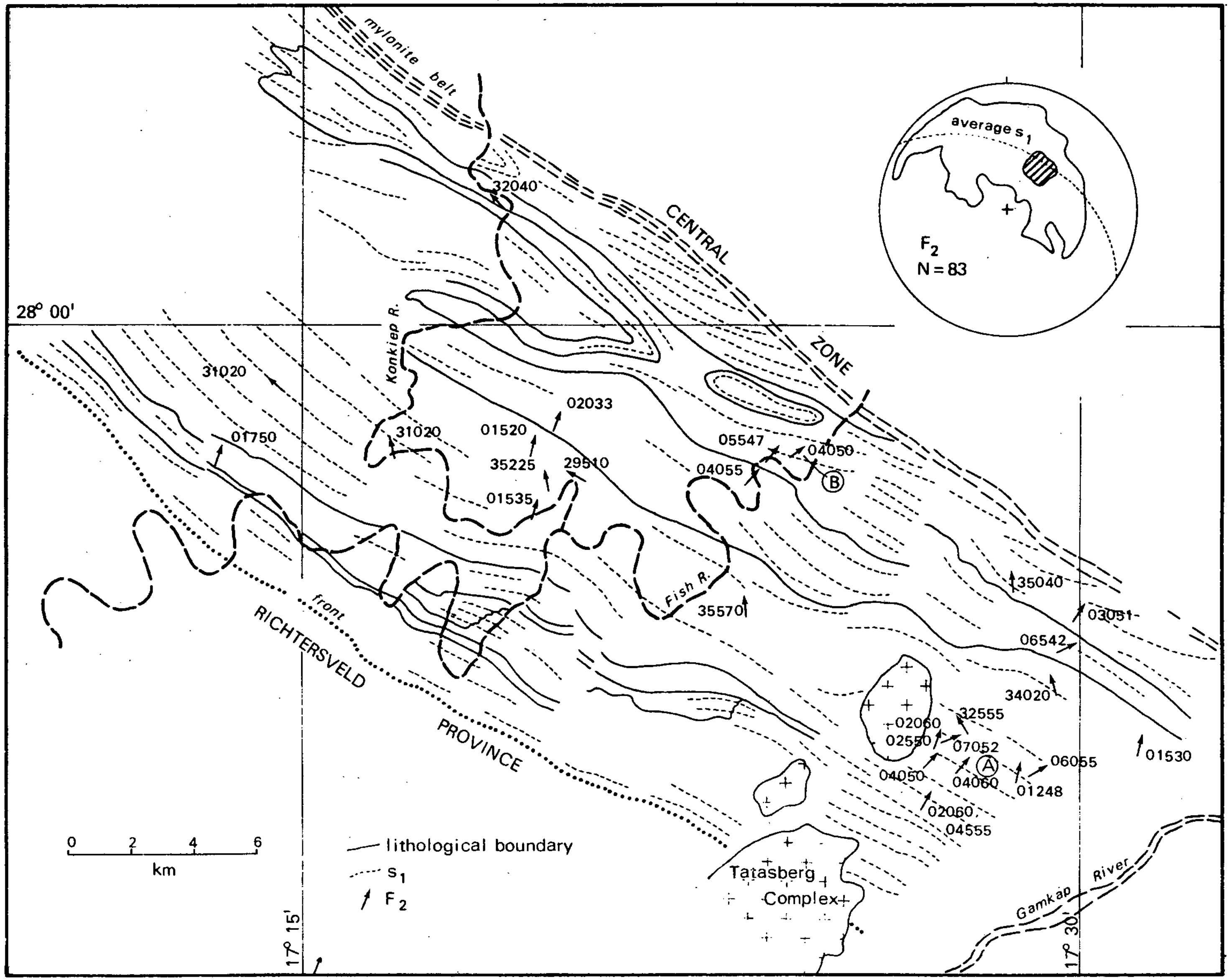


Fig.3. 27. Areal and stereographic compilations of $F_2$ in the marginal zone. Contours, > 0%, 12% per 1% area.

100

tion in incompetent bands is strong (Fig. 3.52a), so that the older foliation is visible only in the competent bands. In a sequence consisting only of ductile material a strong $D_2$ refoliation might result in folds resembling $F_1$.

A synoptic reduction of $F_2$ orientation data (Fig. 3.27) gives a distribution pattern between a point and girdle maximum. $F_2$ has a greater direction stability in a smaller domain (A, Fig. 3.27) where it is more homogeneous with respect to $s_1$ and $l_1$ (Fig. 3.28) and where no $F_3$ folding was observed. Within a second limited area (domain B; Fig. 3.27) the same feature apply (Fig. 3.29), although $F_3$ folds there are pervasive. Although $l_1$ is subparallel to $F_2$ axes in places, it was commonly observed that $F_2$ deforms $l_1$ so that $l_1$ curves around $F_2$ hinges and is curved on $s_1$ where the $F_2$ axial plane is parallel to $s_1$; this last phenomenon would be possible for $a_2$ (kinematic a) lying in the plane of $s_1$ and at an angle to $l_1$ (see Ramsay, 1967) and implies shearing movements. Comparing the synoptic orientation data of $l_1$ and $F_2$ for the marginal zone (Figs. 3.22 & 3.27), it is evident that the two linear elements are largely subparallel. Compilations from two local areas (Figs. 3.28 & 3.29) show that $l_1$ and $F_2$ occupy discrete but overlapping fields on the stereograms and the relation between $l_1$ and $F_2$ is thus largely coaxial.

$F_2$ is imprinted on all the pretectonic units as well as the syntectonic augen granodiorite gneiss (see Section 3.4.6.2). The common development of $F_2$ folds in the marginal zone is characteristic of the particular domain which, *inter alia*, differentiates it structurally from the Richtersveld Province.

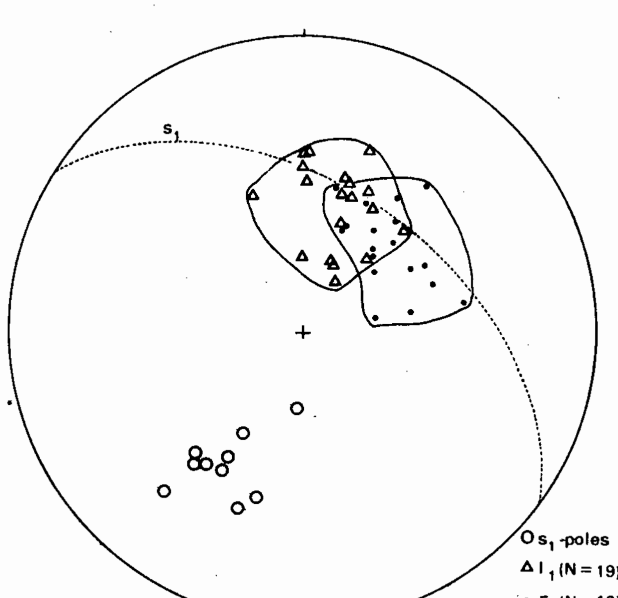


*Fig. 3.28. In domain A (Kanabeam; Fig. 3.27) which is homogeneous w.r.t. $s_1$, both $F_2$ and $l_1$ show a large direction stability with overlapping point maxima.*

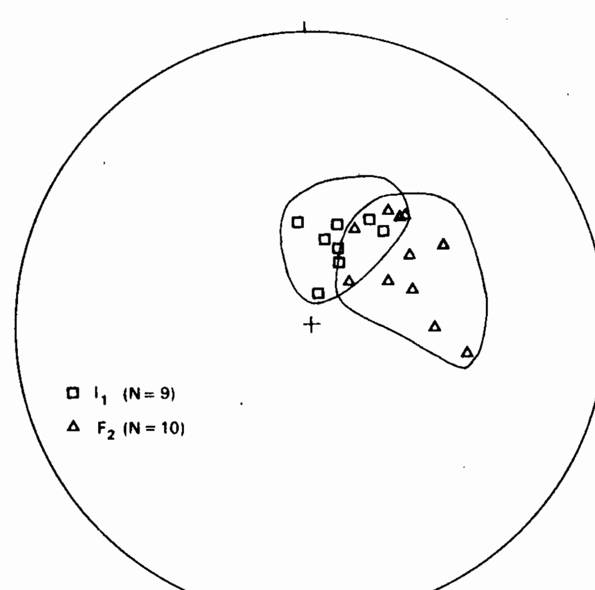


*Fig. 3.29. Domain B (Fig. 3.27).*

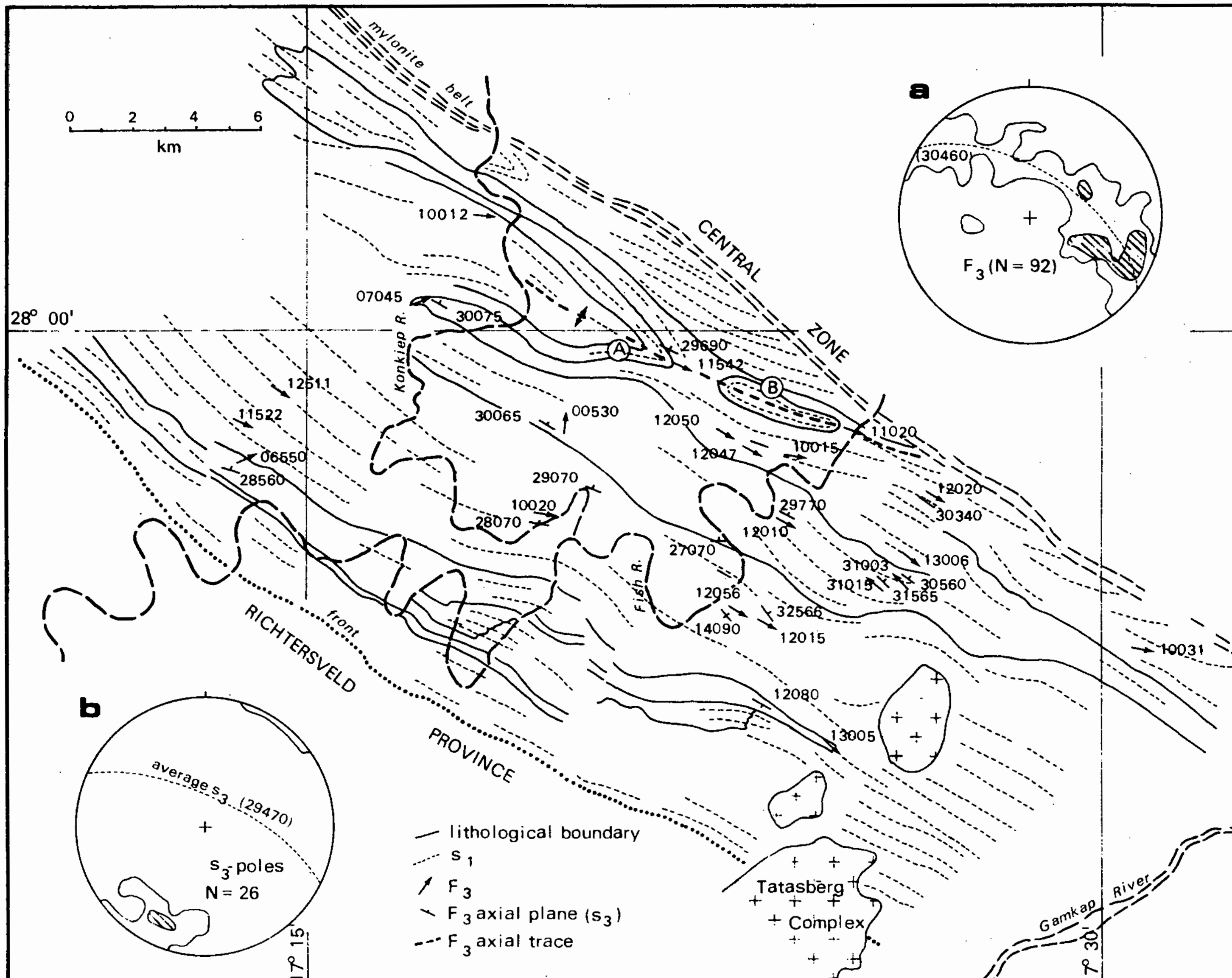


*Fig. 3.30. Areal and stereographic compilations of $F_3$ and $s_3$ in the marginal zone. Contours: a. >0%, 5%, and b. 6%, 14% per 1% area.*

### 3.4.3 $D_3$

Mesoscopic $D_3$ folds are penetratively developed in the marginal zone (see areal compilation, Fig. 3.30). $F_3$ coaxially refolds both $F_1$ and $F_2$ (Plate 11). By comparing Figs. 3.30b & 3.22a it is clear that $F_1$, $F_2$ and $F_3$ are coplanar, although in outcrop, the axial plane of $F_3$ characteristically makes a small angle with $s_1$. The style characteristics largely overlap with those of $F_2$. Compared to $F_2$, $F_3$ folded layers deviate the least from parallel forms. The hinges are rounded and disruption of limbs was not observed. In some fold cores a chevron style is developed. The interlimb angle varies from $30^{\circ}$ - $100^{\circ}$. Refoliation is generally not developed, but associated incipient crenulation foliation indicates right-lateral shear. Sporadically, leucosomes lie along these foliation surfaces.

A macroscopic $F_3$ antiform (Fig. 3.30) is outlined by the banded amphibolite unit. Minor Z folds are developed along the northern limb and S folds along the southern limb. Both limbs dip at the same angle in a north-eastern direction. The macroscopic fold is therefore isoclinal differing in this respect from the minor folds. A crenulation foliation ($s_3$) with right-lateral shear and leucosomes, is strongly developed in the hinge zone. The geometry of the minor fold elements is consistent with that of the macroscopic antiform (Fig. 3.31), but the axial surface has a steeper dip than the modal value for the marginal zone (Fig. 3.30b). This is thought to be the effect of the Kanabeam shearing giving rise to the mylonite belt and towards which all surfaces steepen ($D_6$, Section 3.6).

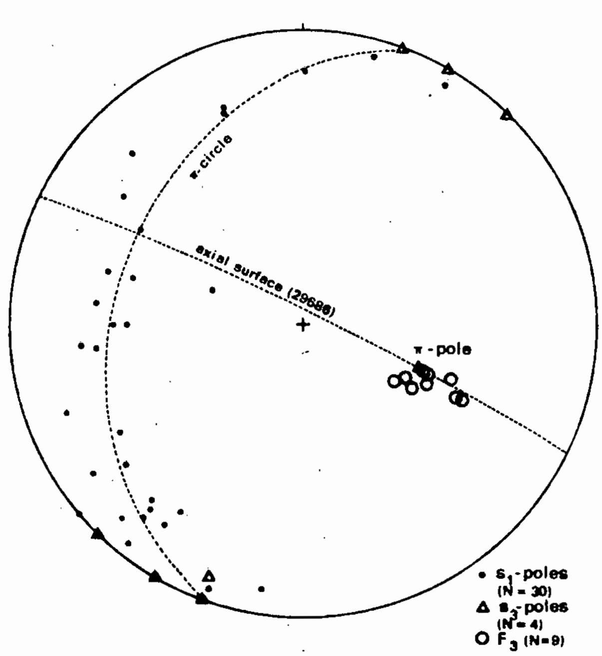


*Fig. 3.31. The fold elements of the macroscopic $F_3$ antiform at A (Fig. 3.30).*

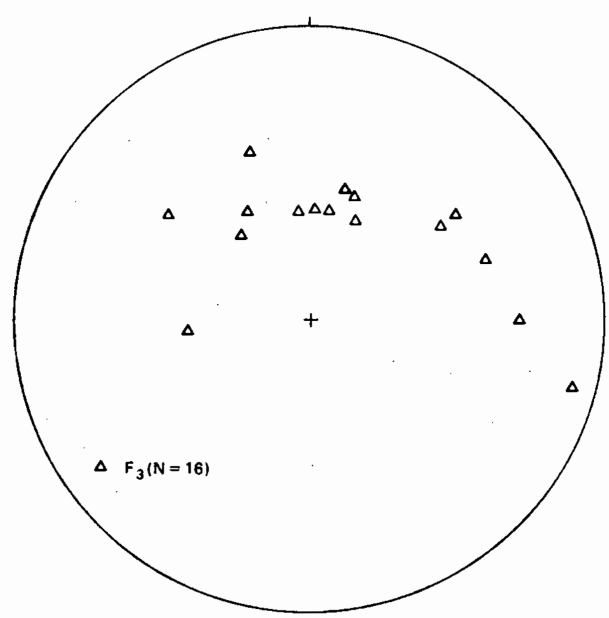


*Fig. 3.32. The low direction stability of $F_3$ within an outcrop at the confluence of the Fish and Konkiep Rivers.*

A compilation of all $F_3$ data in the marginal zone (Fig. 3.30a) yields a great circle girdle with a maximum in the southeast. The great circle girdle closely coincides with the modal $s_3$ (Fig. 3.30b). The fold axes are therefore spread along the axial surface and other than $F_1$ and $F_2$, has a distinctly preferred southeasterly trend. The orientation spread of $F_3$ is not limited to between sample stations; the same variability in orientation of the fold axes was recognised within an outcrop (Fig. 3.32), showing that the low direction stability is also due to the initial variation in $s_1$ and not entirely to differential rotation towards the principal finite elongation direction. The constant attitude of the axial surfaces at the sample station rules out refolding of $F_3$.

### 3.4.4 Late deformation phases ($D_4$)

The suite of structures grouped together here postdates $D_1$ and $D_2$ but their time relation with $D_3$ is not known. The various structures are considered together for convenience and do not necessarily belong to the same phase of deformation. The structures constitute the following :

(i) Kink bands and crenulation foliations with a large direction stability ($s_4$, Fig. 3.33). Leucosomes are located along some of the surfaces.

(ii) Small mesoscopic folds which typically have subvertical axial surfaces and very large interlimb angles. These structures characteristically have a wavy appearance with low amplitude and relative large wavelength. Some of them are related in outcrop to $s_4$. Their fold axes are variably oriented (Fig. 3.33).

(iii) The gentle waviness of the regional grain (cf. Annex. 1) might be the macroscopic expression of some of the small structures described above. The axial traces have a north-easterly trend and the interference of one of these with the macroscopic $F_3$ antiform is though to have resulted in the domal structure at B (Fig. 3.30).

Whereas $F_1$, $F_2$ & $F_3$ are coplanar, the $F_4$ axial-plane trace is predominantly at large angles to the older grain. $D_4$, therefore, represents a group of cross structures and it is for this reason that $D_4$ is thought to postdate $D_3$, which is geometrically more akin to $D_1$ and $D_2$.

### 3.4.5 Finite strain

An indication of the amount of finite strain is given below, but the measurements are too few in number to be representative. Deformed clasts have their XY-surfaces parallel to $s_1$ and X subparallel to $l_1$ (Section 3.4.1.2). The deformed clasts generally have the shape of flattened ellipsoids. The average ratios from two sample localities are 1,8: 1 : 0,3 for X:Y:Z. Assuming originally spherical clasts and no ductility contrast between clasts and matrix, the amount of flattening across the foliation is in the order of 63 per cent while the amount of stretching in the direction of the mineral lineation is 121 per cent. Judging by the smearing of xenoliths along the front zone, the amount of strain there greatly exceeds the bulk strain in the rest of the marginal zone.

The finite strain is considered largely the cumulative effects of $D_1$, $D_2$ and $D_3$. The coplanar nature of these deformations indicate that the XY-plane of the bulk strain ellipsoid remained more or less constant in attitude from $D_1$ through to $D_3$. The orientation of the XY-plane from $D_1$ to $D_3$ is approximated by the configuration of $s_1$ (Fig. 3.22). Because $F_2$ has a large spread with a distinct preferred orientation parallel to the $D_1$ linear elements, it is inferred that the stretching direction remained approximately constant in orientation during $D_1$ and $D_2$.

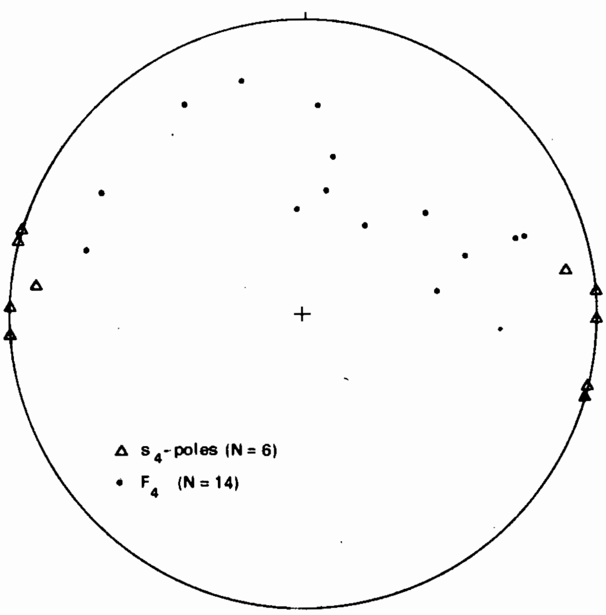


*Fig. 3.33. Late phase kink bands, crenulation foliations ($S_4$) and gentle subvertical folds ($F_4$) of the marginal zone.*

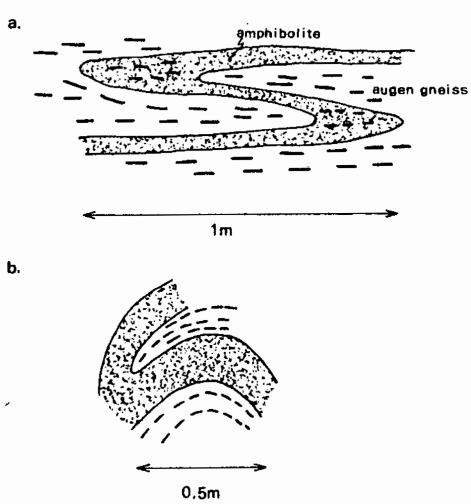


*Fig. 3 34. a. The earliest type of fold recognised in the augen gneiss unit. b. $F_3$ coaxially refolds the early folds.*

### 3.4.6 Structural dating of syntectonic intrusives

#### 3.4.6.1 Arterites

Arterites are prominently developed in the marginal zone (Section 2.2.1). The leucosomes are both concordant and cross-cutting with respect to $s_1$ and lack dark mineral selvages. Some of the concordant arterites are foliated while the crosscutting veins are ptygmatically folded, without $s_1$ being folded, with an axial-plane foliation geometrically similar to $s_1$; the arterites are sometimes disrupted along the fold limbs. In comparison to the country rock, the arterites are poorly foliated. Their injection therefore postdates the peak of $s_1$ development and because $D_2$ folded the arterites together with $s_1$, their intrusion is from late-$D_1$ to early-$D_2$.

#### 3.4.6.2 Granodioritic augen gneiss

The augen gneiss is penetratively foliated with the resulting deformation of the felspar megacrysts (Section 2.3.3.2). The long direction of the augen on the foliation defines a down-dip stretching lineation, geometrically consistent with $l_1$ of the country rock and of the included amphibolite bands (Fig. 3.22). The foliation of the augen gneiss is everywhere concordant with $s_1$ of the marginal domain (Fig. 3.22). Both hand-sized xenoliths and the amphibolite bands have a crystalloblastic planar fabric, presumably $s_1$.

The $F_3$ macroscopic antiform (at A, Fig. 3.30) folds the augen gneiss body, and small $D_3$ structures are common (Fig. 3.34b). In the *lit-par-lit* transition zone between the banded amphibolite unit and the augen gneiss, $F_2$ folds are developed in the interbanded augen gneiss and amphibolite. The oldest fold structures recognised in the augen gneiss unit are defined by the amphibolite banding (Fig. 3.34a). These similar-like tight to isoclinal folds have the foliation of the augen gneiss as their axial-plane foliation.

To conclude, the kinematic conditions for $D_1$ and $D_2$ prevailed during the emplacement of the augen granodiorite (cf. foliations and stretching lineations). The emplacement is prior to $D_3$ and postdate the $D_1$ fabric of the inclusions, and a late-$D_1$ to syn-$D_2$ time of intrusion is therefore suggested. (See also discussion in Section 2.3.3.2.3).

### 3.4.7 Deformation and metamorphism

The relation between $M_1$ (Section 4) and $D_1$, $D_2$ and $D_3$ was investigated in twelve fold hinges. The main metamorphism ($M_1$) produced crystalloblastic mineral assemblages which also define the planar fabric $s_1$, with this relationship holding for $F_1$ hinges as well. $M_1$ therefore is penecontemporaneous with respect to $D_1$.

In both the 'muscovite + chlorite out' and sillimanite zones, $D_2$ deforms the $s_1/M_1$ fabric. In micro-$F_2$ hinges, the following observations were made . The $s_1/M_1$ planar fabric is folded with individual mineral grains such as hornblende, biotite and fibrolite bent and showing strain extinction. Deformation features such as bent twin lamellae, deformation bands and strain extinction are developed in quartz and felspar in the hinge zones only. In one sample retrogressive chlorite was observed in the $F_2$ hinge. Retrogressive neomineralisation is not a conspicuous and conclusive feature, but deformation of the $s_1/M_1$ fabric is distinctly so. The development of deformation or crystalloblastic textures is a function of the interplay between rate of recrystallisation and rate of strain, i.e. largely temperature vs. strain rate. As there are no independent parameters available to conclusively evaluate the two controlling factors the following interpretation remains conjectural. It is reasonable to assume that during a single kinematic event (e.g. $D_1$ & $D_2$), there should be a positive correlation between the rate and amount of strain. Judging the amount of strain by the scale of penetration of axial-plane foliations, the $D_1$ strain greatly exceeds $D_2$ strain and therefore the $D_2$ strain rate should be less than that of $D_1$. Bearing in mind the assumption above, it is concluded that $D_2$ was active at depressed temperatures postdating the $M_1$ peak.

Chlorite is retrogressively developed after hornblende and biotite, along spaced $s_3$ surfaces and this retrogressive neomineralisation indicates a lower grade (with respect to $M_1$) metamorphic environment for $D_3$.

### 3.4.8 Summary

$D_1$, $D_2$ and $D_3$ are essentially coplanar while only the linear elements of $D_1$ and $D_2$ are coaxial. $D_1$ produced the planar fabric associated with $M_1$ and $D_2$ is inferred to postdate $M_1$. The orientation of $s_1$ and $l_1$ is consistent and gives the attitude of the bulk strain ellipsoid for $D_1$ and $D_2$. The similarities between $D_1$ and $D_2$ suggest progressive deformation during the same kinematic event (the formation of $F_2$-type folds is duscussed in Section 5) during which the augen granodiorite intruded and the main metamorphism reached its peak. Large scale transposition during $D_1$ is evident from the ubiquitous parallelism of the foliation and lithological banding, and paucity of $F_1$ hinges. The resulting fabric is homogeneously distributed. This aspect is the main criterion for the distinction between the Richtersveld and Namaqua Provinces.

$D_4$ structural elements are not penetrative in the marginal zone with macroscopic structures not significantly developed. The time relation between $D_3$ and $D_6$, which could be genetically related, is not conclusively known.

## 3.5 Central zone

### 3.5.1 $D_1$

Apart from domains in which a later refoliation is evident, the planar fabric in the pretectonic gneisses is labled $s_1$ and is defined by a foliation which is everywhere parallel to the lithological banding. On a microscopic scale $s_1$ is evident by the preferred orientation of sheet silicates and a granoblastic elongate microstructure. The mineral lineation $l_1$ is located within $s_1$ and is defined by either the habit orientation of individual minerals or the arrangements of mineral aggregates.

The ubiquitous parallelism of the foliation and lithological banding is attributed to large-scale transposition during $D_1$. Thin competent calc-silicate layers in aluminous gneiss are everywhere boudinaged in a chocolate-slab fashion, along two approximately perpendicular directions. The large-scale extension giving rise to these structures, is at the latest syn-$D_2$ because firstly, calc-silicate boudins are folded by $F_2$ and secondly, xenoliths in the megacrystic granite gneiss which is syn-$D_2$, include calc-silicate boudins. The chocolate-slab boudins also indicate that the bulk strain ellipsoid during $D_1$ and $D_2$ was of the oblate type with extention along both X and Y.

Very few $F_1$ fold closures were recognised. One example is a rootless similar fold illustrated in Fig. 3.37c. The macroscopic Gifberg antiform on Altdorn (Annex. 1) which is considered $F_1$, is described in detail. The lithological layering of the aluminous gneisses (paragneiss unit) is folded with the regional foliation as the axial-plane foliation. Along the axial trace of the fold $s_1$ crosses $s_o$, the lithological layering at large angles. The layering $s_o$ is, however, too poorly defined to measure the orientation. The foliation $s_1$ is reasonably constant in attitude and contain $F_1$ and $l_1$ (Fig. 3.35d).

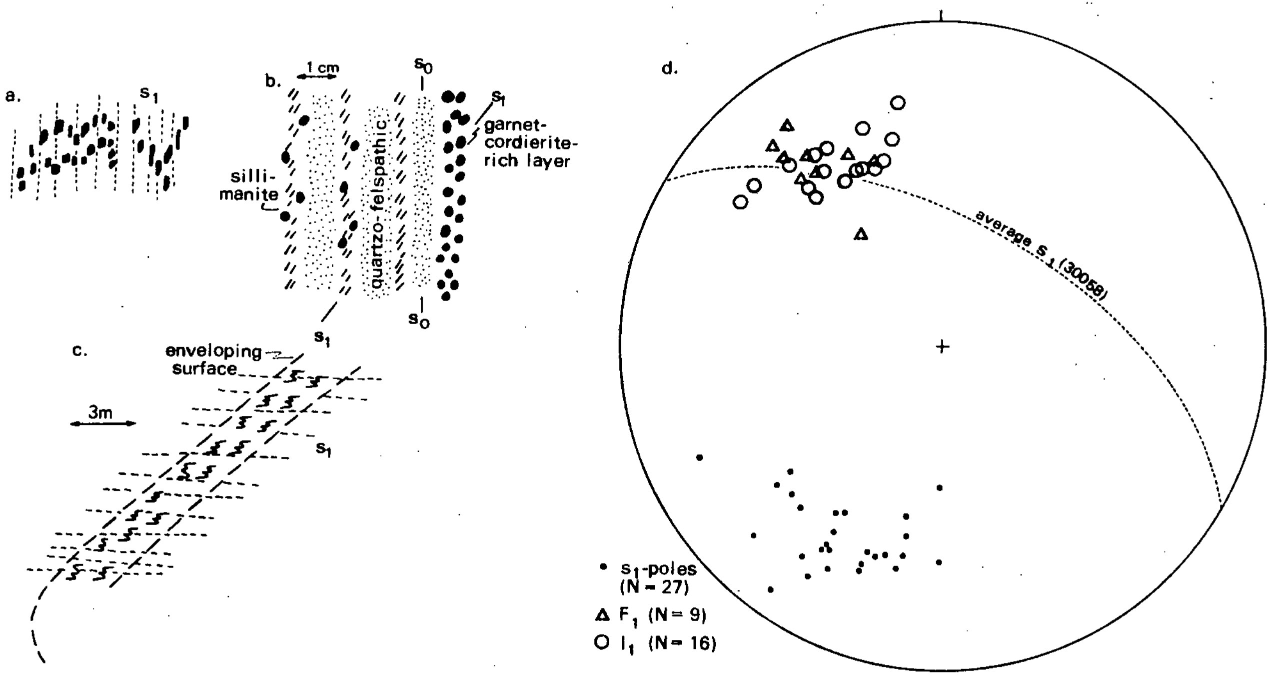


*Fig. 3.35. $D_1$ fabric elements of the macroscopic structure at Gifberg.*

The lineation $l_1$ which is predominantly defined by sillimanite, is parallel to $F_1$, both statistically (Fig. 3.35d) and as directly observed in the field. Minor folds vary from close to isoclinal and typically have similar-like shapes. Transposition was observed in some hinge zones (Fig. 3.35a) with a relatively small ductility contrast between layers. The older banding, which can best be observed where $s_1$ crosses $s_o$ at large angles (Fig. 3.35 b & c), constitutes a compositional layering on a millimetre to metre scale. No evidence of an older deformation/metamorphic fabric could be detected. On microscopic scale a crystalloblastic fabric defines $s_1$ and leucosomes, which elsewhere commonly are concordant with the foliation/banding, here developed parallel to the axial planes of minor folds. If the fine banding as depicted in Fig. 3.35b can be attributed to metamorphic segregation, it would constitute evidence for a pre-$D_1$ phase of deformation.

The regional foliation and mineral lineation outside domains of refoliation constitute penetrative fabric elements of $D_1$. These elements are deformed by all subsequent deformations (e.g. Fig. 3.46f) to the extent that in domains, which are by all appearances homogeneous with respect to $s_1$, $l_1$ is variable (e.g. Fig. 3.39a). It is shown in Section 3.5.2 that $D_1$ and $D_2$ linear elements have a coaxial tendency and $F_1$ and $F_2$ are by definition coplanar. An interesting aspect regarding the direction stability of $l_1$ in domains homoge-

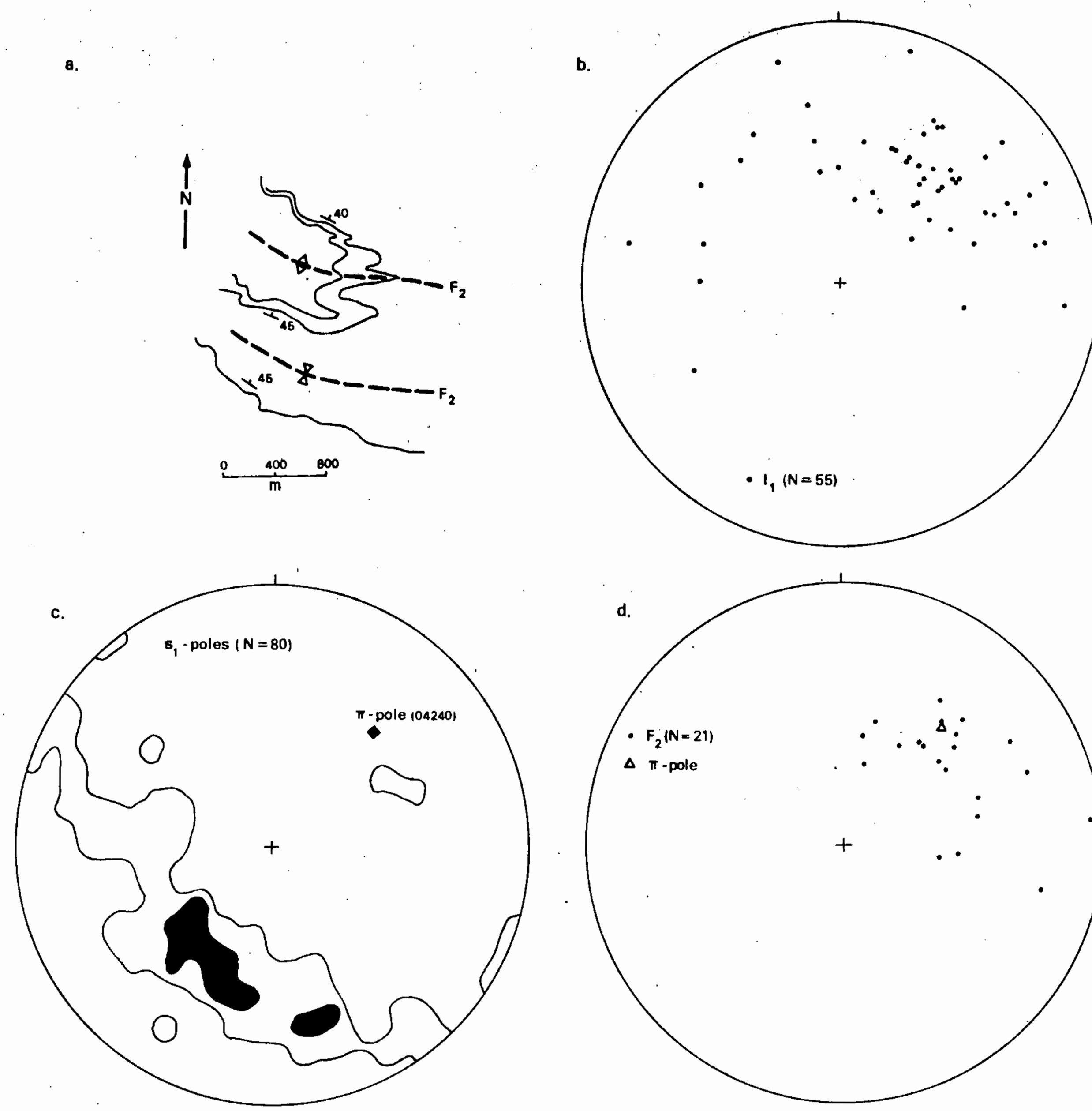


*Fig. 3.36. Fabric elements of a macroscopic antiform on Altdorn (A, Fig. 3.38) and the geometric relation to $l_1$.*

neous with respect to $s_1$, is that the $l_1$ direction stability seems to be a function of stratigraphic unit. In two such domains (the southern limb of the Wegdraai antiform (locality C, Fig. 3.43) and the northern limb of the Kochas antiform (Fig. 3.39a)) in the grey gneiss unit it was established that $l_1$ is variable in orientation. In similar domains in the paragneiss unit, outside the domain of $s_2$ refoliation, $l_1$ has a constant orientation e.g. at Gifberg (Fig. 3.35d), at Attie Se Kop in pink gneiss and immediately underlying grey gneiss (Fig. 3.37a), and on Altdorn, $l_1$ shows a preferred orientation (Fig. 3.36b) even though $s_1$ is folded in the hinge zone of a macroscopic $F_2$ fold. The sampling stations are too few for a proper comparison, but the available data do indicate a difference which can be due to the differential effect of superimposed strain or indicate a more complex pre-$D_2$ structural history for the grey gneiss unit.

The main metamorphism, $M_1$ as defined in the opening paragraphs of section 4, is determined by the crystalloblastic mineral assemblages of the pretectonic gneisses, which also define $s_1$, where not refoliated. As there are no deformation textures associated with $s_1$, $M_1$ is coeval or outlasted $D_1$.

### 3.5.2 $D_2$

Similar to $F_2$ in the marginal zone, the second phase folds in the central zone are those which fold the main planar fabric, $s_1$, with their axial planes strictly parallel to the more regional attitude of $s_1$, thus $D_1$ and $D_2$ are cop-

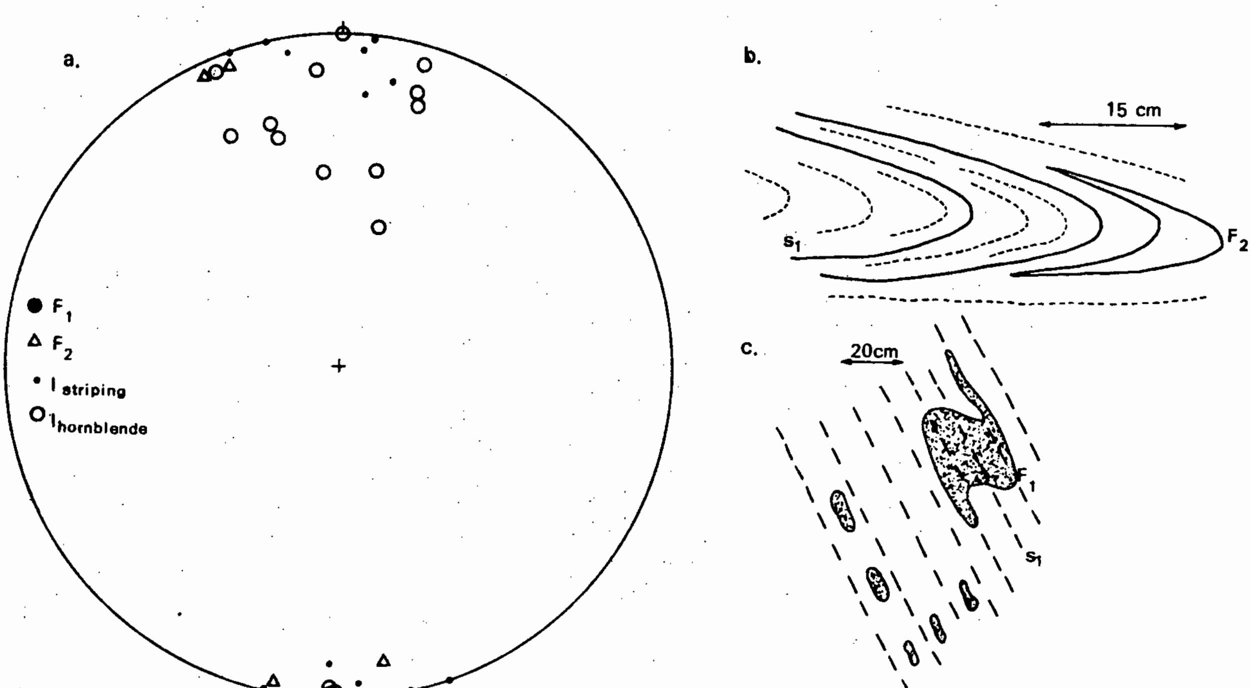


*Fig.3.37. a. Early fabric elements in a domain on Kwaggasnek (B, Fig. 3.38) homogeneous with respect to $s_1$.*

*b. and c. The difference between $F_1$ and $F_2$ within a small area at the same locality.*

lanar. The $F_2$ isoclines are the most common folds and are penetratively developed in the pretectonic gneisses of the central zone. $D_2$ is ubiquitously overprinted by $D_4$ and $D_5$, but at one locality only, observed to be older than $D_3$.

In the grey gneiss unit, $F_2$ is always isoclinal (Plate 12), but in the paragneiss unit may be tight or even close at places. A macroscopic synform on Altdorn (Fig. 3.36a) with a core of aluminous gneiss becomes extremely attenuated to the northwest (see map); the hinges of minor folds are usually rounded. All variations from parallel-like to flattened parallel and similar-like shapes of folded layers were observed. Competent layers along the limbs may be disrupted (Fig. 3.37b) e.g. the amphibolite at the base of the paragneiss unit becomes markedly disrupted towards the north-west along the limbs of the macroscopic structure on Altdorn (Fig. 3.36 & map). It is clear that the group characteristics of value for correlation are (i) deformation of $s_1$, (ii) predominant isoclinal shape and (iii) the parallel attitude of the axial surfaces to $s_1$. These features together with other overprinting criteria where available, were used for the correlation of $F_2$.

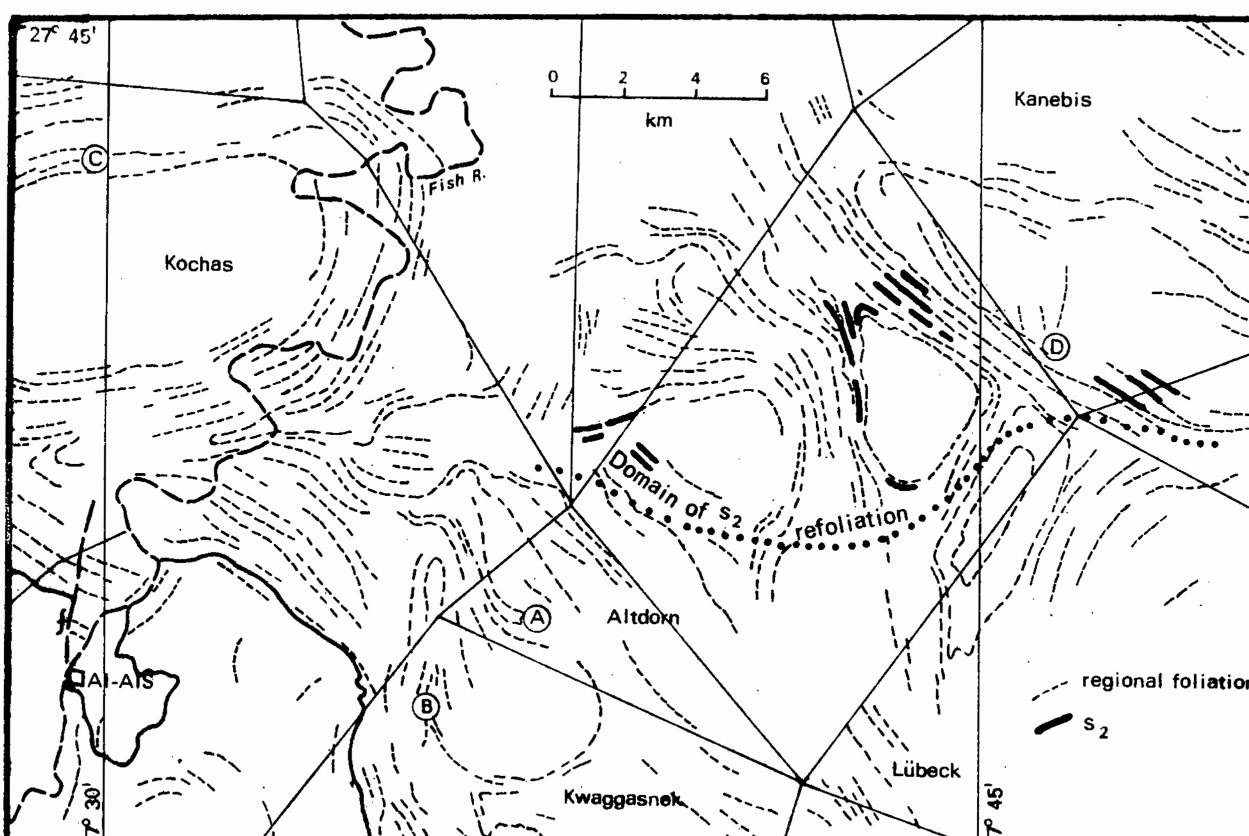


Fig. 3.38. Domain of $s_2$ refoliation. $s_2$ is denoted where recognisably developed in a penetrative fashion and is probably more pervasive in the domain of $s_2$ refoliation than shown.

*Refoliation*

The refoliation associated with $D_2$ is a variable characteristic, so much so that the central zone is subdivided into two domains with respect to $D_2$ refoliation (Fig. 3.38).

(i) Domain of no $s_2$ refoliation. A poor refoliation parallel to the axial plane of $F_2$ isoclines is developed in the hinges of some folds only and usually restricted to the ductile layers, but is not developed in the macroscopic folds of Altdorn (Fig. 3.36).

(ii) Domain of $s_2$ refoliation. A well-developed axial-plane foliation is common in the paragneiss unit so that it cross-cuts the older planar fabric (Plates 13 & 14) in hinge zones and is penetratively developed in the outcrop. The preferred orientation of biotite commonly defines $s_2$ and refoliates the thin (millimetres) leucosomes which are ubiquitously developed parallel to the older planar fabric and which are not foliated in the domain of no $s_2$ refoliation. The $s_2$ surfaces are generally spaced in the more competent layers, but become so penetrative in ductile horizons (cf. Plate 14) that the distinction between $s_1$ and $s_2$ can only be made in fold hinges. In Fig. 3.38 the outcrops where $s_2$ was recognised to be penetratively developed are shown and an arbitrary line is drawn partly delimiting the domain of $s_2$ refoliation. When compared with the maps (Annex. 1 & 2) it is clear that the grey gneiss unit is not refoliated and that the domain of $s_2$ refoliation is restricted to an area where large bodies of megacrystic granite gneiss are interspersed with the relatively ductile paragneiss unit; as described later, the foliation in the megacrystic gneiss is $s_2$. The outcrops of aluminous gneiss on the farms Wetterkopf and Kirchberg (Annex. 1) are well refoliated, but due to the paucity of minor folds it could not be established whether the new foliation is $s_2$ or $s_4$. There judging by the finely spaced nature of the new foliation as compared with the coarser $s_4$ on Gaibes (Section 3.5.4) in the same rock type, it is thought more likely to be $s_2$.

*Geometry*

Being deformed by several subsequent deformations, $F_2$ fold axes in the central zone are variable (cf. Fig. 3.41) in orientation. In domains homogenous with respect to the regional foliation, $F_2$ axes are reasonably constant in attitude (Figs. 3.37 & 3.39). The relation between $F_2$ and the regional lineation in such homogeneous domains, and aspects of a macroscopic $F_2$, are given below.

(i) A large antiform and complementary synform in the paragneiss unit is situated on Altdorn (Figs. 3.41(A) & 3.36) in the domain of no $s_2$ refoliation. The foliation/banding ($s_1$) is isoclinally folded

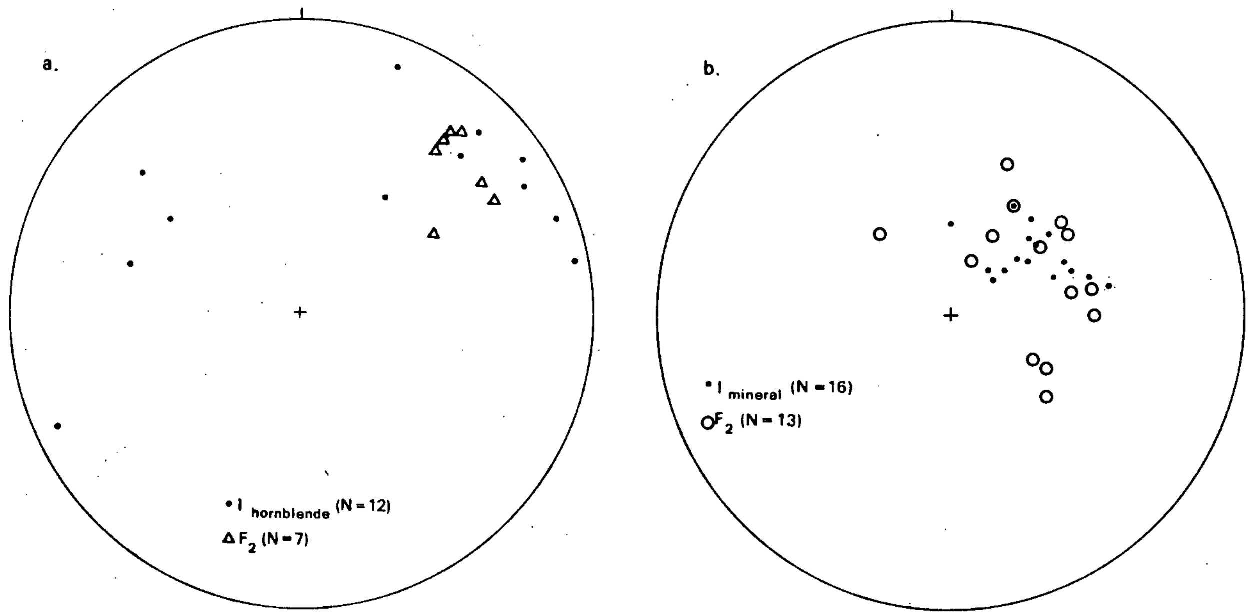


*Fig. 3.39.a. The relation between $l_1$ and $F_2$ in grey gneiss along the northern limb of the Kochas antiform (C, Fig 3.38)*
*b. The relation between $F_2$ and possibly $l_2$ in aluminous gneiss along the southern limb of the Kanebis synform (D, Fig. 3.38)*

with no refoliation in the hinge. The π-pole (Fig. 3.36c) coincides with the associated minor structures (Fig. 3.36d), while $l_1$ which is mostly defined by sillimanite and hornblende needles lying in $s_1$, have a preferred orientation parallel to $F_2$ (Fig. 3.36b), but is markedly less consistent in attitude than the minor fold axes.

(ii) In a domain south of Attie Se Kop (B, Fig. 3.38) where $s_1$ is constantly oriented, early fabric elements are compared (Fig. 3.37). The orientation data are from both pink gneiss, the structurally lower unit of the paragneiss unit and the underlying grey gneiss. The paucity of fold axes inhibits the significance of the conclusion somewhat, but it appears (Fig. 3.37a) as if the linear elements of the early fold phases are essentially colinear. The striping lineation (Fig. 3.37a) might be the effect of intersection between $s_1$ and the earlier lithological banding and orientation-wise equivalent to $F_1$. Along the contact between the grey gneiss and paragneiss units there is no difference between the two units with respect to the early fabric elements.

(iii) Along the northern limb of the Kochas antiform (C. Fig. 3.38) and the southern limb of the Kanebis synform (D, Fig. 3.38), both homogeneous with respect to the regional foliation, $F_2$ is fairly constantly oriented (Fig. 3.39 a & b). It is interesting to note, though, that the mineral lineation of the aluminous gneisses along the Kanebis limb (Fig. 3.39b) have a significantly larger direction stability than the hornblende lineations of the grey gneiss at Kochas (Fig. 3.39a). The lineations at both localities lie within the regional foliation, but the Kanebis structure is situated within the domain of $s_2$ refoliation. If the mineral lineation is $l_2$, a greater direction stability can be expected than for $l_1$. In the zone of $s_2$ refoliation, it is generally difficult to distinguish in the field between $l_1$ and $l_2$, but the argument above suggest that these mineral lineations are $l_2$. The argument is further strengthened by similar patterns at other sampling stations e.g. along the northern limb of the Kanebis synform (aluminous gneiss in $s_2$ domain) the mineral lineations have a strong preferred orientation, while in grey gneiss along the southern limb of the Wegdraai antiform (Fig. 3.43), hornblende lineations have a large orientation spread.

*Summary*

(i) It is indicated that the mineral lineation in the domain of $s_2$ refoliation, is $l_2$.

(ii) In domains homogeneous with respect to $s_1$, $l_1$ has a variable orientation, especially in the grey gneiss unit, but commonly with a modal attitude parallel to $F_2$. In some minor folds, $l_1$ was observed to be parallel and in others at an angle to the fold axes.

(iii) $F_1$ and $F_2$ are coplanar. The earlier ($D_1$ and $D_2$) linear elements have a colinear tendency. This can be the result of either coaxial refolding or rotation of the linear elements to the principal direction of finite elongation.

(iv) The domains homogeneous with respect to the regional foliation, above, are late-phase fold limbs. As $D_2$ linear elements in these domains have a large direction stability, the absence of $D_3$ effects are an enigma. $D_3$ is either not penetratively developed in the areas considered or coaxial with respect to $D_2$.

*Associated metamorphic conditions*

Constituent grains from $F_2$ hinge zones show no deformation effects whatsoever in the six samples of aluminous gneiss from the domain of $s_2$ refoliation investigated. On microscopic scale, $s_2$ is penetrative and defined by the preferred orientation of biotite flakes and the granoblastic elongate nature of the other mineral grains, including, *inter alia*, quartz, felspar, cordierite and garnet. The only evidence of an older fabric are small folds in the internal foliation of helicitic cordierite where the $s_i$ (internal) of cordierite is mainly defined by sillimanite needles preferentially located within cordierite grains.

As the domain of $s_2$ refoliation is situated within the $M_1$ K-felspar + sillimanite zone and the crystalloblastic mineral assemblages of the $D_2$ micro-fabric are consistent with and define the K-felspar + sillimanite zone, it is concluded that prograde ($M_1$) conditions lasted during $D_2$ in the domain of $s_2$ refoliation. It is argued in Section 4.3.1.3 that the bivariant equilibrium (reaction 11) is proceeding to the left. The area in which the parameter g approaches zero (i.e. the development of cordierite at the expense of garnet) coincides with the domain of $s_2$ refoliation (cf. Figs. 3.38 & 4.8b). The helicitic cordierite mentioned above, substantiates the idea that cordierite formed during $D_2$ and that reaction 11 developed to the left during this later phase of $M_1$. According to the principles set forth by Currie (1971), Henson & Green (1973) and summarized by Winkler (1976), relative lower pressures are inferred.

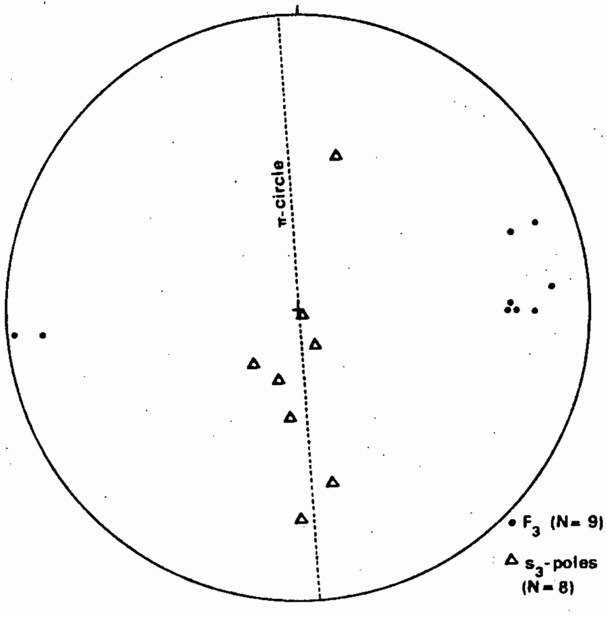


Fig.3.40. $D_3$ fabric elements in the vicinity of Ai- ais.

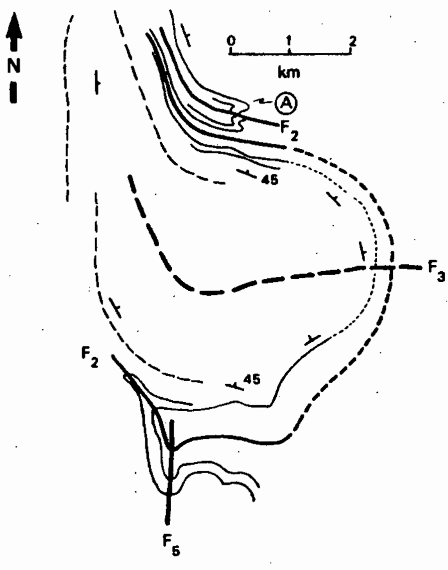


Fig. 3.41. An interpretation of the macroscopic structure on Kwaggasnek (cf. with Annex. 1 for lithology).

### 3.5.3 $D_3$

The third phase of deformation was not recognised until late in the investigation and details of minor structures are therefore presented from one locality only. Elsewhere, on Kwaggasnek a macroscopic $F_3$ (Fig. 3.41) refolds $F_2$ and is itself refolded by $F_5$; the $F_3$ fold is overfolded with an inclined axial surface, while its axial trace is markedly distorted by $F_5$. These characteristics distinguish $F_3$ from $F_4$ which is never overfolded and never distintly deformed by $F_5$.

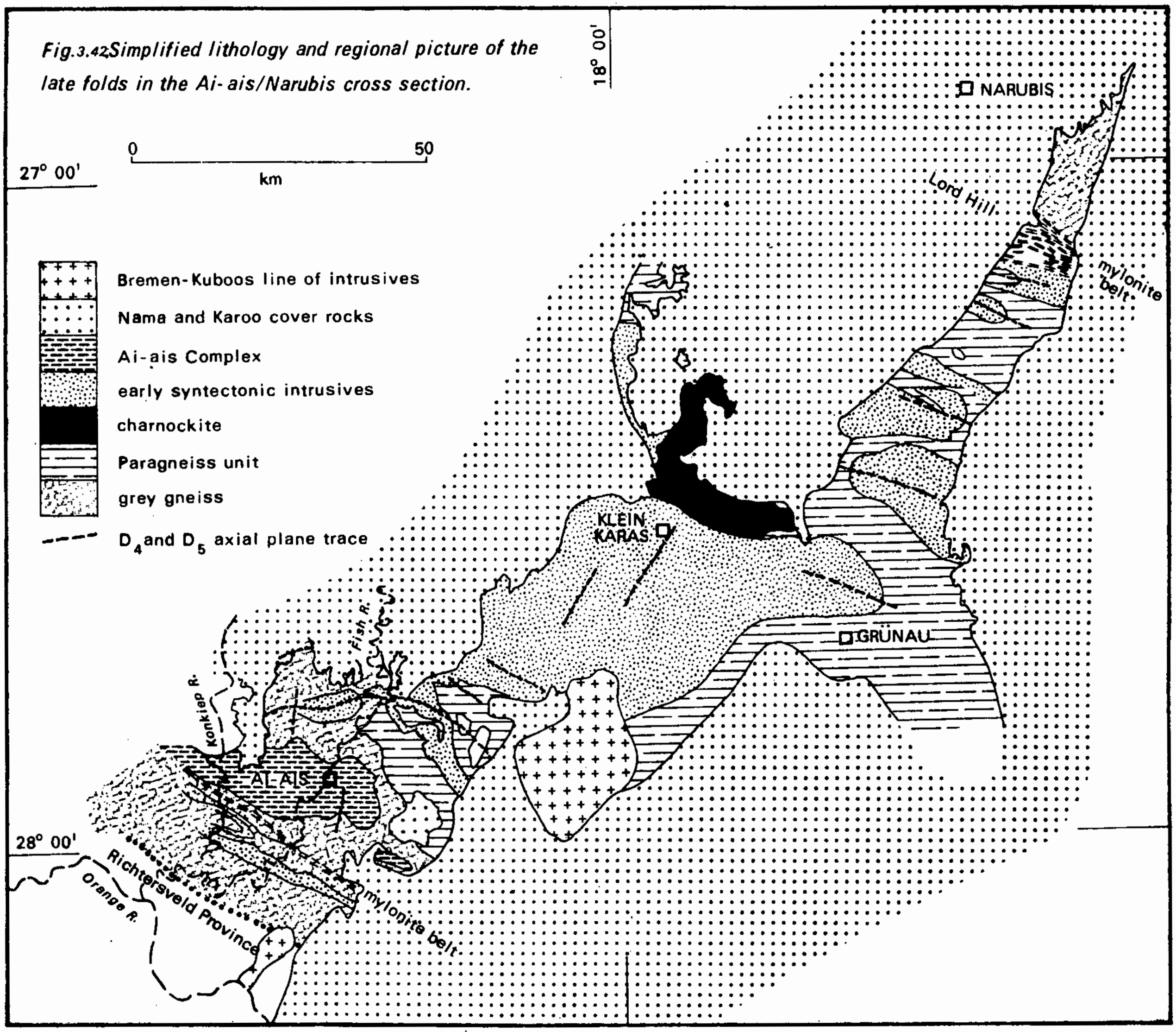


*Fig.3.42 Simplified lithology and regional picture of the late folds in the Ai-ais/Narubis cross section.*

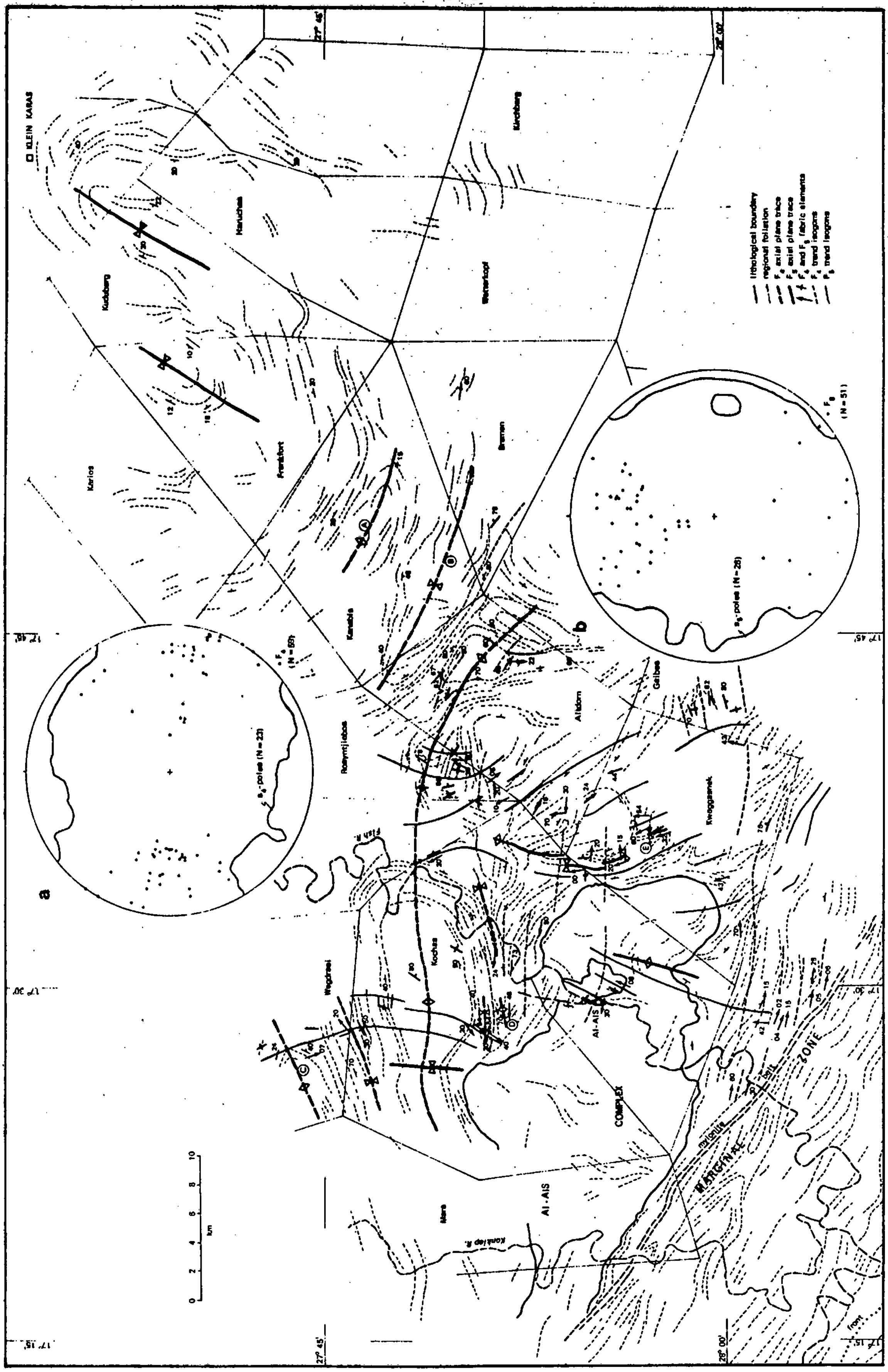
KLEIN KARAS
a
b
Karios
Kuduberg
Haruchas
Frankfort
Kanabis
Rosyntjiebos
Wegdraai
Kochas
Mara
Bremen
Wetterkopf
Kirchberg
Alidorn
Geibes
Kwaggasnek
Fish R.
Konkiep R.
AI-AIS
AI-AIS
COMPLEX
MARGINAL
mylonite
belt
ZONE
front
km
0 2 4 6 8 10
17° 15'
17° 30'
17° 45'
27° 45'
28° 00'
$s_4$-poles (N = 23)
$F_4$ (N = 59)
$s_5$-poles (N = 28)
$F_5$ (N = 51)
lithological boundary
regional foliation
$F_4$ axial plane trace
$F_5$ axial plane trace
$F_4$ and $F_5$ fabric elements
$F_4$ trend isogons
$F_5$ trend isogons

(v) association of minor folds with macroscopic folds by means of asymmetry and geometry.

The validity of the correlations is implied by the systematic areal pattern shown in Fig. 3.43.

The group style characteristics (Plates 6, 7, 15 & 16) of $F_4$ and $F_5$ largely overlap. Folded layers have a parallel shape, hinges are rounded, in some cases to such an extent that no limbs are developed, and interlimb angles vary from close to gentle with most folds open. Minor folds on outcrop scale, are virtually absent in the homogeneous megacrystic granite gneiss and are generally sparsely developed in the pretectonic gneisses. Refoliation (development of $S_4$ and $S_5$ surfaces) is not characteristic, but developed locally.

A new $s_4$ surface in the form of a spaced cleavage (cf. Plate 15 and Fig. 3.44) is pervasive in the paragneisses on the northwestern portion of the farm Gaibes, while the development of an axial-plane foliation elsewhere in the central zone was observed in only two fold structures. At three localities a $D_5$ refoliation along the short limbs of asymmetric $F_5$ folds were observed and leucosomes are formed along some. These folds resembling crenulations on a large scale with an incipient (Plate 16) or discrete crenulation foliation developed, are particularly common in the stream bed below the Altdorn farmstead; their fabric elements are depicted in Fig. 3.45. A spaced axial-plane foliation ($s_5$) was observed at one or two localities only. A crenula-

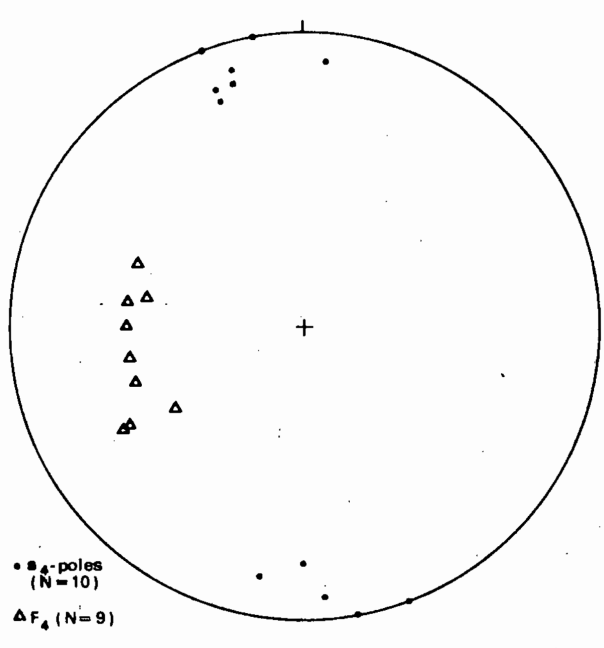


*Fig. 3.44 The geometry of a spaced cleavage ($s_4$) and associated folds (Plate 15) in the paragneiss unit, Gaibes.*

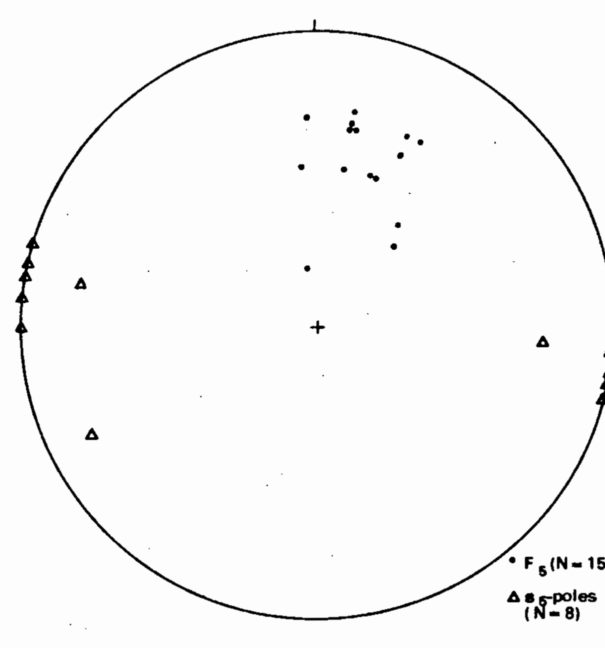


*Fig. 3.45 Fabric elements of large scale $D_4$ crenulations and associated crenulation foliation ($s_5$) in the stream bed below the Altdorn farmstead.*

tion foliation like that depicted in Plate 9 is pervasively developed in the central zone and particularly noticeable in the megacrystic granite gneiss, where leucosomes are commonly formed along the crenulation foliation. Two sets are developed which are geometrically consistent with $D_4$ and $D_5$ structures. It is interesting to note that both $D_4$ and $D_5$ include foliations which firstly, could be attributed to shear along the axial plane (crenulation foliation) and secondly, others like the spaced axial-plane foliations which are not necessarily shear planes, but may represent XY-planes of flattening (Ramsay, 1967). On a regional scale both genetic types are geometrically concordant.

*Geometry*

$\pi$-diagram analyses of some macroscopic folds are illustrated in Fig. 3.46. The $F_4$ antiforms (first order folds) tend to have their steeper limbs on the southern or southwestern sides and the fold axes of large $F_4$ & $F_5$ structures tend to be subhorizontal (Fig. 3.46 a & b) over several kilometres. The large $F_4$ folds are more common than $F_5$ (Fig. 3.42) with the result that the regional grain in the central zone is controlled by $F_4$ folds.

Synoptic diagrams of all the $F_4$ (Fig. 3.43a) and $F_5$ (Fig. 3.43b) fabric elements illustrate the subvertical attitude of $s_4$ and $s_5$ (axial surfaces, axial-plane foliations and crenulation foliations) and the spread in trend. The areal compilation (Fig. 3.43) shows that the variation in orientation forms a systematic pattern; from the normal or more regional orientation around Grünau (cf. Fig. 3.42) towards the mylonite belt in the south, there is a gradual change in the trends of both $F_4$ and $F_5$ as depicted in Fig. 3.43. This change in orientation of the late phase folds can be attributed either to the rotational strain of the Kanabeam shear zone (Section 3.6), the material inhomogeneity in the form of the Ai-ais Complex or both. The composition and largely isotropic character of the Ai-ais body suggest that it acted competently with respect to the surrounding gneisses. A competent body of such dimensions would deflect the strain pattern with the result that the original (pre-$D_6$) orientations of $F_4$ and $F_5$ in the vicinity of the Ai-ais Complex could have deviated from their normal regional trends towards the north-east.

*Associated metamorphism*

Insufficient petrographic data from fold hinges and axial-plane foliations are available to make a conclusive statement, but the indications are that the temperature at the time of $D_4$ and $D_5$ was at elevated levels because no deformation textures are developed in fold hinges and $s_5$ in the K-felspar + sillimanite zone ($M_1$) is not associated with obvious retrogression. The Altdorn and Leikop zones of refoliation, interpreted as $D_4$ and/or $D_5$ structures, yield more information regarding the physical environment (Section 3.5.5). Marked retrogression has been affected.

### 3.5.5 Zones of refoliation

Two major zones of late refoliation, recognised in the central zone (Fig. 3.47), are correlated with $D_4$ and $D_5$.

*Altdorn zone*

Most of the Altdorn zone of refoliation in the middle and towards the south is characterised by a new foliation. Towards the north the refoliation dissipates and is recognisable in that the pre-existing regional foliation has a different character. The nature of the new foliation is most obvious in the intercalated bands of megacrystic granite gneiss which megascopically develops a distinct cataclastic texture, becomes finer grained and especially in the north, retains felspar porphyroclasts. The development of a new foliation in the interbanded paragneisses is less obvious; but where the new foliation is developed a lineation on the foliation becomes distinct and more common. The lineation is defined by white streaks and dark mineral streaks and is predominantly a mineral lineation. In the megacrystic granite gneiss the lineation includes the long direction of garnet or granular trains. The appearance of these lineations are different from $l_1$ and $l_2$. Whereas the orientation of the Altdorn refoliation is variable, the lineation has a more constant attitude (Fig. 3.47).

In the northern part of the Altdorn zone it was observed that the older surfaces folded by $F_5$ show an incipient development of the new foliation along the older planar fabric. In the middle part of the zone a crenulation foliation, consistent with the geometry of $F_4$, is overprinted on the new foliation. The Altdorn zone of refoliation is interpreted to have developed penecontemporaneously with $D_4$ and $D_5$. The localised nature of the zone suggests that it constitutes a shear zone, the character of some of the lineations indicating that they represent slip directions on the shear surface. The incipient development of the new foliation along the older foliation/banding suggests that the shear movement, at least during the initial stages, was due to layer boundary slip during the late phase folding. This interpretation explains the position of the zone along the limbs or narrow synformal domain between macroscopic structures.

The Gannakouriep dykes were emplaced after the Altdorn refoliation, while some pegmatites are older.

---

Fig. 3.46. $\pi$-diagrams of the late macroscopic folds. The localities are indicated on Fig. 3.43. (a) Kanebis antiform at A. (b) Kanebis synform at B. (c) Wegdraai antiform at C. (d) Kochas south antiform at D. (e & f) Kwaggasnek synform at E. (f) The deformation of $l_1$ by $D_5$.

Fig.3.47.Major zones of refoliation in the central zone.

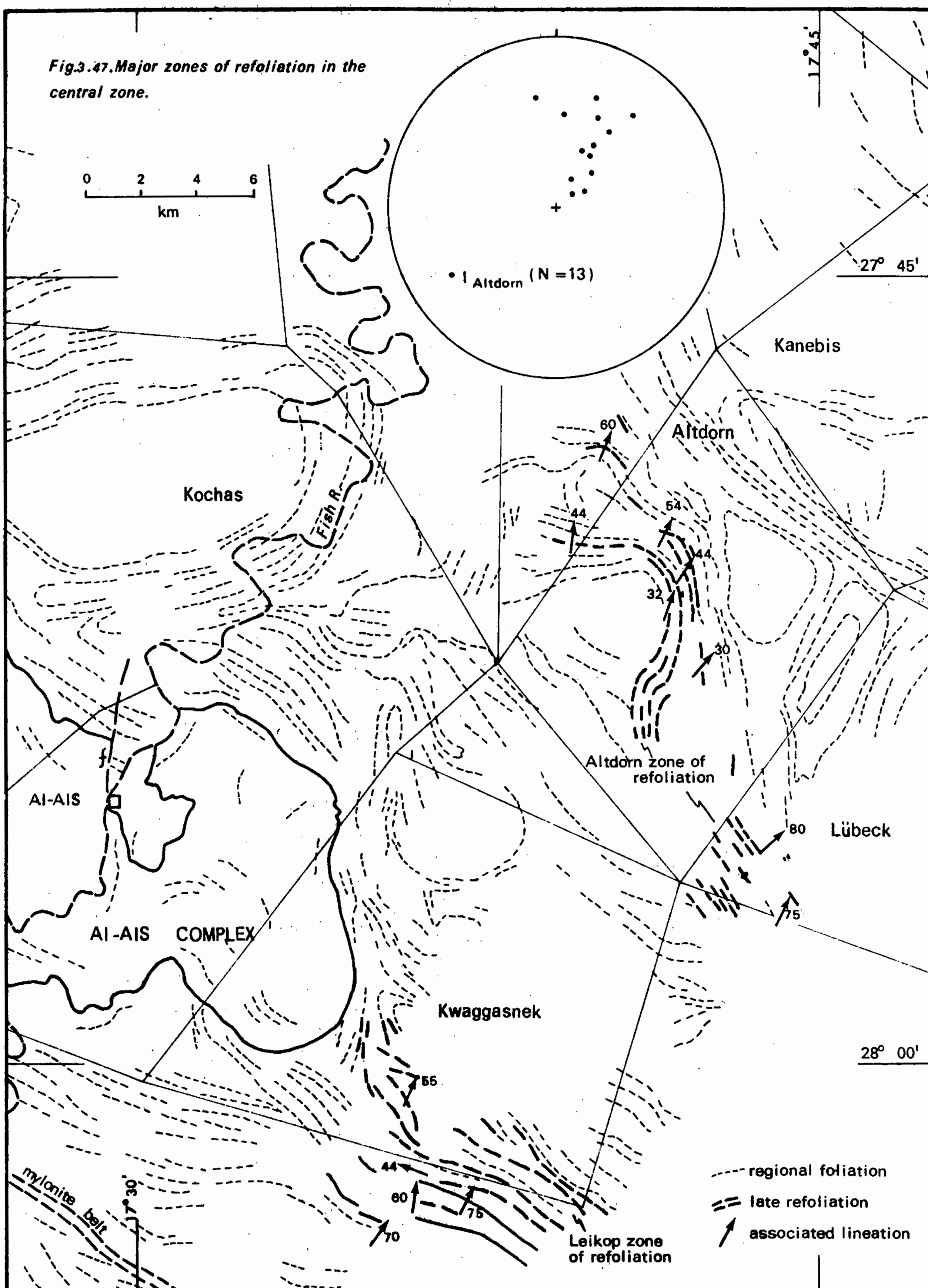

*Leikop zone*

The Leikop zone of refoliation (Fig. 3.47) is grossly similar in nature to the Altdorn zone, except that the older planar fabric remains the dominant foliation with the new foliation incipiently developed along $s_1$. The foliation in the Leikop zone is subvertical. Towards the south-east the refoliation in the grey gneiss unit extends at least up to the subvertical contact with the paragneiss unit, a refoliation in the schists of the paragneiss unit is not readily recognisable. The development of the new foliation along $s_1$ deforms the earlier concordant leucosomes which attains a cataclastic texture; porphyroclastic-like features in paleosomes of the grey gneiss are also characteristic. The heterogeneous nature of the deformation is locally evident from the development of the new foliation in discrete zones, where the gneisses have a distinctly finer grain size.

A geometrically consistent $D_4$-type crenulation foliation was observed with a cataclastic core defining the new foliation. The new Leikop foliation also defines $F_5$ folds. The localization and heterogeneous nature of the new foliation suggest a shear origin parallel to the pre-existing foliation/banding penecontemporaneously with $D_4$ and/or $D_5$. The Leikop refoliation predates the Gannakouriep dyke suite while pegmatites are both older and younger than the refoliation.

*Associated metamorphic conditions*

The Altdorn zone of refoliation is situated within the K-felspar + sillimanite zone of main metamorphism (Fig. 4.11) and 16 samples representing completely refoliated rock were investigated to determine the associated grade of metamorphism. Although distinct cataclastic features are megascopically visible, deformation textures are virtually absent on a microscopic scale. Some features like seriate grain-size distribution, bent twin lamellae and an incipient mortar texture relate to a relatively high strain rate or depressed temperatures. The textures are predominantly crystalloblastic and it is concluded that recrystallisation and neomineralisation during, and possibly after, the refoliation produced the new crystalloblastic planar fabric.

Touching grains of muscovite + quartz + plagioclase in six of the samples indicate retrogression with respect to the main metamorphism. The muscovite usually present in minor quantities, are commonly intergrown with biotite. Further effects of retrogression was observed in one sample of aluminous gneiss with an assemblage of biotite, cordierite, garnet, quartz and sillimanite. The sillimanite grains are zoned by a very fine aggregate of presumably white mica, while some regularly outlined pseudomorphs of the same material resemble cross sections of sillimanite. In the same thin section garnet is invariably zoned or partly zoned by cordierite, a texture which suggest that the garnet + cordierite assemblages of the main metamorphic K-felspar + sillimanite zone reacted towards a cordierite assemblage without garnet, indicating lower pressure conditions (Winkler, 1976).

## 3.5.6 Structural dating of the syntectonic intrusives

### 3.5.6.1 Megacrystic granite

Aspects relating to the time of emplacement of the megacrystic granite (Section 2.3.3.3) are as follows :

(i) The granite bodies are pervasively foliated; along the contacts the granite is interbanded with the pretectonic gneisses and a more intense marginal foliation is not developed.

(ii) The intensity of the foliation (scale of penetration) has a heterogenous character, pervasive throughout the bodies. The heterogeneity is distributed in zones where a stronger deformational imprint on the granites is megascopically visible; i.e. the foliation is penetrative on a smaller scale ('sheared' in more general terms) and the deformation of K-felspar and garnet megacrysts is evident by their augen, rod-like and lenticular shapes. On a microscopic scale, no deformation textures are visible. In the zones of least deformation the foliation is defined only by a statistically preferred orientation of the felspar megacrysts. In the absence of a lithological heterogeneity the only banding is locally concordant with the foliation are leucosomes ($\pm$ 0,5 m), sporadically affected by the foliation.

(iii) Paragneissic xenoliths on Altdorn have irregular shapes with no apparent flattening across the plane of the foliation. The foliation in the granite cuts across the xenolith/granite contacts and is concordant with the planar fabric of the inclusions. This is interpreted as a deformation effect under conditions which resulted in no significant ductility contrast between granite and paragneiss inclusion. On the farm Goedemoed in the Klein Karas district, another type of inclusion has a different relationship with the granite; 'foreign' granulite inclusions are disc-shaped with the foliation in the granite, defined by the arrangement of undeformed megacrysts, wrapped around. This relation indicates a ductility contrast or flow foliation, formed during the movement of magma. Calc-silicate boudins, characteristic of the paragneiss unit, were found as inclusions in the granite and show that the extention giving rise to the structure, predate the granite emplacement. In the Fish River Canyons well-foliated paragneiss xenoliths are included in very poorly foliated megacrystic granite. These relationships, between granite and inclusions show firstly, and older deformational imprint on some paragneiss inclusions and secondly, a foliation in the granite cutting across granite/xenolith contacts, implying that the granite foliation is also imprinted on the inclusion.

(iv) Macroscopic late phase folds deform the foliation of the granite (Section 3.5.4) but minor folds are extremely sparse and reflect the lithological homogeneity of the megacrystic granite.

(v) $D_3$ structural elements were not recognised.

(vi) The foliation in the granite described above to be a deformational effect, is related to $s_2$, with the older imprint as evident in some xenoliths, possibly $s_1$. The relationship between $D_2$ and the foliation in the granite is illustrated in Fig. 3.48. Macroscopic and mesoscopic $F_2$ folds with the axial-plane foliation traced, from paragneiss into granite and vice versa, (Fig. 3.48 a, b & d) prove that the foliation in the granite which is the first deformation imprint, is $s_2$. The intrusive vein in Fig. 3.48c is interpreted as having been emplaced during the progressive development of the $F_2$ fold and subsequently folded in a sympathetic fashion.

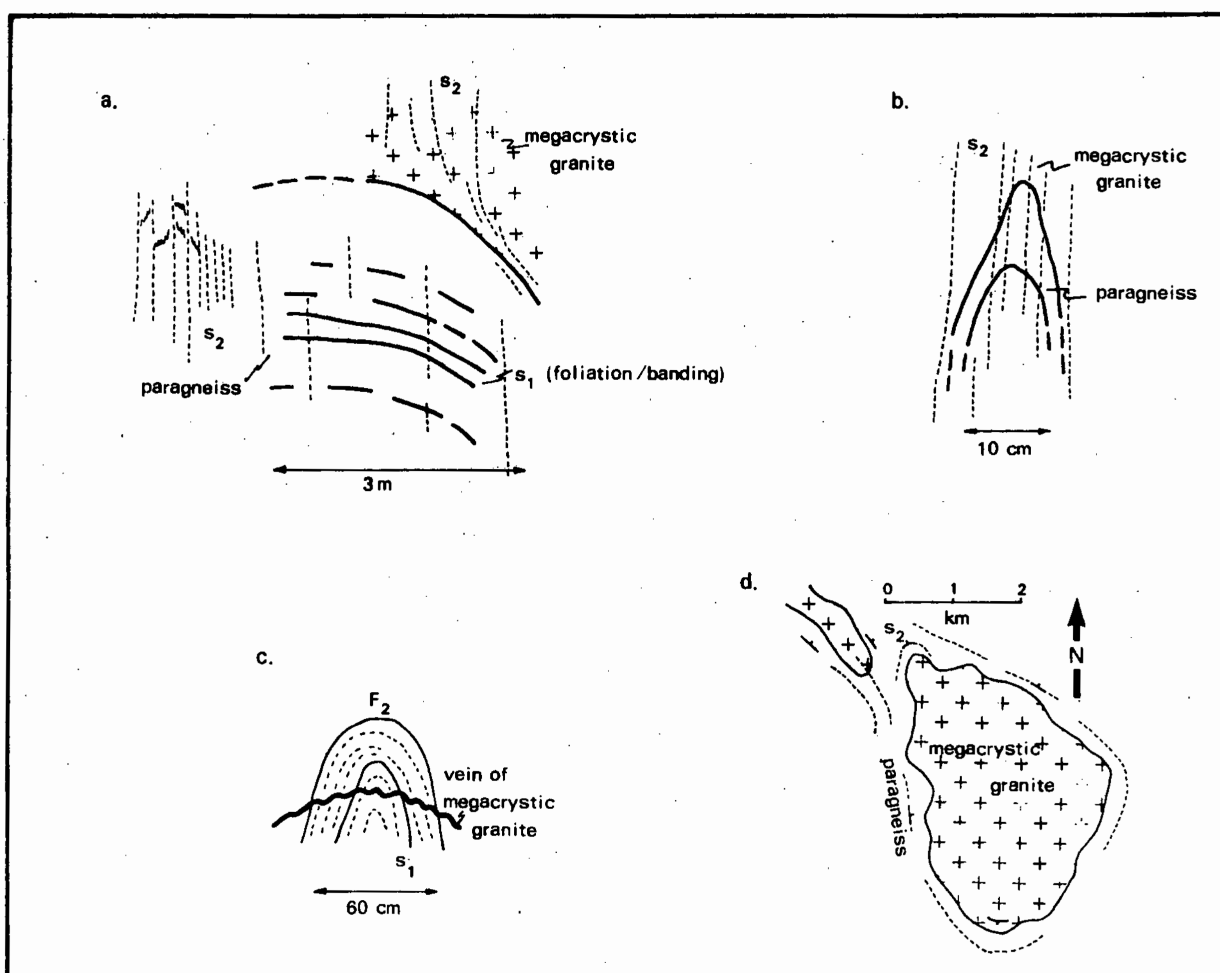


*Fig. 3.48 Field sketches illustrating the relationship between $D_2$, $D_1$ and the megacrystic granite.*

(vii) Cordierite and garnet, presumably almandine, very commonly form part of the mineral assemblage of the megacrystic granite, in both the deformed and undeformed zones. The coexistence of these two minerals indicates a depth of crystallisation emplacement which is roughly consistent with the pressure conditions of the $M_1$ K-felspar + sillimanite zone. $M_1$ and $D_2$ is considered penecontemporaneous (Section 3.5.2).

### 3.5.6.2 Ai-ais Complex

The Ai-ais Complex (Section 2.3.3.6) has the shape of a distorted ellipse with the regional foliation in the country rock draped around it (Annex. 1). The igneous body is marginally foliated with a core of predominantly unfoliated rock, but the development of the marginal foliation is uneven so that the zone is wider along the northern than along the southern boundary. The intensity of the marginal foliation is such that the metagabbroid cannot always be distinguished from amphibolite and the porphyritic granite resembles grey gneiss. On a microscopic scale the foliated rock of the marginal zone displays no deformation textures, although the felspar phenocrysts of the prophyritic granite phase are deformed into augen and flaser shapes.

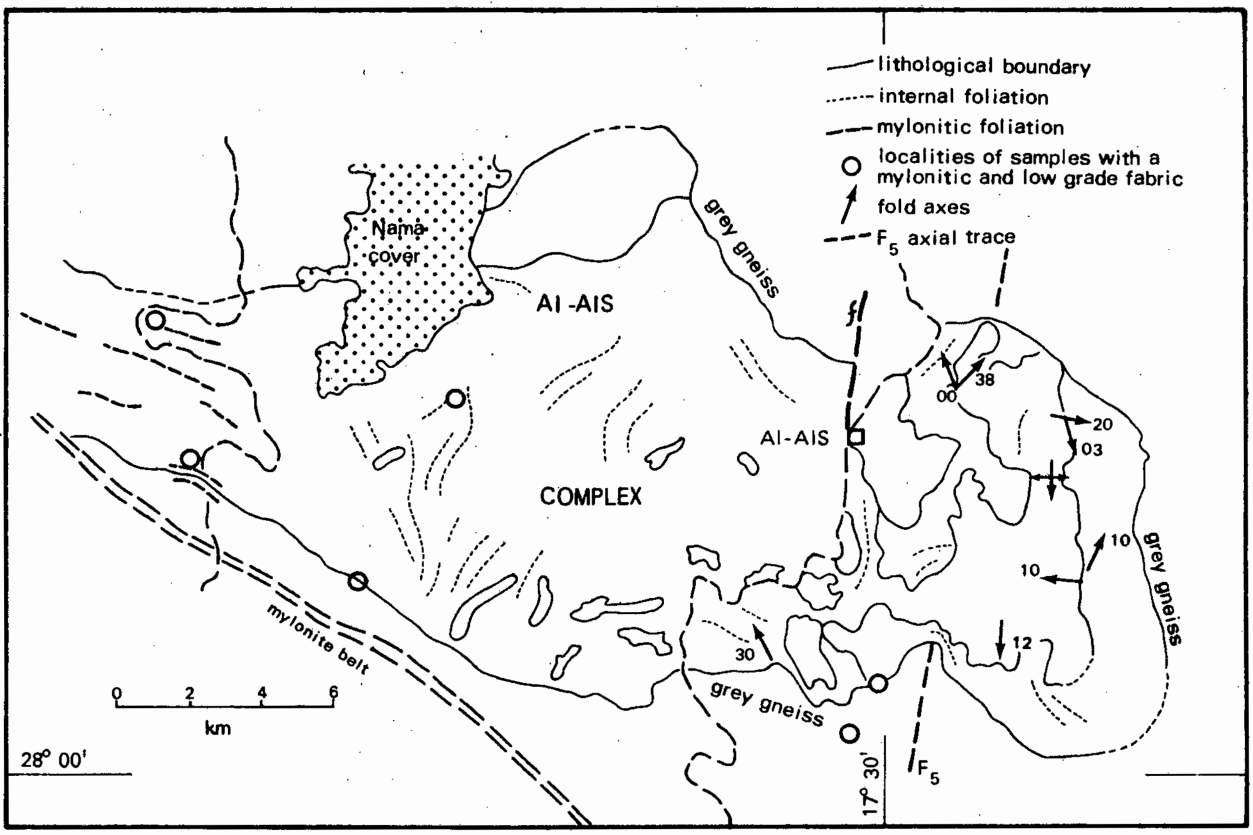


*Fig.3.49. Structural aspects of the Ai-ais Complex; the marginal foliation is not shown.*

The internal foliation (Fig. 3.49) is sparsely and sporadically developed and preferentially located along the contacts between the intrusives phases. The metagabbroid is characteristically veined by porphyritic granite, which is generally foliated parallel to the vein boundaries. The augen shape of the felspars shows that the internal foliation or layer boundary shear surface is a deformational effect. The contact shearing was frequently observed to be associated with folding (Fig. 3.52b); the fold axes as well as axial surfaces have a variable orientation (Fig. 3.49), but the lineation, mostly hornblende and long direction of felspar augen, are more constantly oriented (Fig. 3.52c) for the same area east of the Fish River. Some of the mesoscopic folds are consistent with the criteria for $F_4$ and $F_5$. The distortion of the Ai-ais body along a north-northeasterly axial trace (Fig. 3.49) is geometrically consistent with $F_5$ (cf. Fig. 3.43).

It was shown in Section 2.3.3.6 that the more intensely foliated metagabbroids retrogressed to a more advanced stage than the relatively undeformed gabbroids. An areal distribution of the various types of retrogressed rock (Fig. 2.10) indicates a more prominent or wider zone of retrogression along the northern boundary than along the southern boundary. If the metamorphic polarity i.e. the higher grade side to the north, was the same during and after the emplacement of the Ai-ais Complex than indicated by the $M_1$ zonation, the larger extent of retrogression on the northern side can be explained by a slower cooling on that side. The Ai-ais body is situated within the $M_1$ 'epidote out' zone (Fig. 4.11) and with respect to the pretectonic amphibolites, zone 2 (Section 4.3.2). The most advanced retrogressed metagabbroids are by all appearances amphibolites with the following mineral assemblages (B-536, B-541 & B-657 of Table 2.11, Section 2.3.3.6.1)
blue-green hornblende + An54 $\pm$ quartz $\pm$ clinopyroxene $\pm$ biotite
which is similar to that of the amphibolites of the $M_1$ zone 2 (Section 4.3.2, Table 4.4). This comparison suggests that the $M_1$ conditions prevailed during and/or after the emplacement of the gabbroids. Trace amounts of epidote is, however, present in the metagranitoids (Section 2.3.3.6.1, Table 2.11). As the $M_1$ 'epidote out' zone also refers to grey gneisses which have a bulk composition comparable to that of the metagranitoids, the evidence indicates that 'slightly' lower grade conditions than $M_1$ prevailed during and/or after the emplacement of the Ai-ais Complex.

Low-grade (chlorite) and mylonitic fabrics are developed along the southern boundary and are penetrative in the western portion of the body (Fig. 3.49). This structural and metamorphic imprint is, on the basis of the low grade, considered much later than the imprint of the marginal and internal foliations. The mylonitic and low-grade character is comparable to that of the mylonite beld (Fig. 3.49) which is an effect of $D_6$ (Section 3.6). The Ai-ais body is relatively isotropic and competent with respect to the surrounding anisotropic gneisses and it is proposed that due to this material inhomogeneity constituted by the Ai-ais body, the shear strain ($D_6$) caused relative movement along the southern contact where the shear strain, according to the progressive simple shear model of Ramsay & Graham (1970), is larger than towards the north or outside of the shear zone.

To sum up, the structural and metamorphic aspects discussed above indicate that firstly, the emplacement of the Ai-ais Complex is prior to $D_4$, $D_5$ and $D_6$ and secondly, the metamorphic conditions prevailing when the igneous mineralogy re-equilibrated retrogressively, were 'slightly' lower grade than $M_1$. Because of this and the lack of a penetrative fabric, the emplacement is considered to postdate $D_1$. It is further argued that if the emplacement was syn-$D_2$, a foliation should be penetratively developed (cf. with the foliated bodies of megacrystic granite outside the domain of $s_2$ refoliation). These arguments suggest that the intrusion took place in the interval between $D_2$ and $D_4$ and that the internal folding and layer boundary slip are effects of $D_4$ and $D_5$.

### 3.5.7 Summary

The early phases of deformation, $D_1$ and $D_2$, are colinear and coplanar. $D_1$ is associated with large-scale transposition. In the domain of $s_2$ refoliation, spatially coincident with large bodies of megacrystic granite, $M_1$ is associated with both $D_1$ and $D_2$. The emplacement of the megacrystic granite gneiss is synkinematic with respect to $D_2$. The imprint of the early phases of deformation is grossly similar in both the paragneiss and grey gneiss units; in view of the large-scale transposition and flattening character of $D_1$, it must be borne in mind that $D_1$ might include fabric elements of several older deformation phases.

The Ai-ais Complex was emplaced in the interval between $D_2$ and $D_4$, under the same or slightly lower grade metamorphic conditions that prevailed during $M_1$.

The absence of $D_3$ in the megacrystic granite gneiss may relate to the lithological homogeneity of the granite or show that $D_3$ is not penetratively developed throughout the central zone. Minor $D_3$ structures in the pretectonic units are not common, with the result that this phase of deformation was recognised late in the field investigation.

The late phase folding constitutes a perpendicular set of upright folds forming conspicuous macroscopic structures. The associated large-scale zones of refoliation are interpreted as being the effect of layer boundary slip during the formation of $F_4$ and $F_5$. The metamorphic conditions associated with the refoliation is retrogressive with respect to $M_1$.

The swing in the normal trend of the late phase folds, which spatially coincides with the Kanabeam shear zone ($D_6$; Section 3.6), is tentatively attributed to the combined effects of the relatively rigid and isotropic Ai-ais Complex of major dimensions and progressive simple shearing. The mylonite belt, situated in the core of the shear zone, is interpreted as the product of progressive simple shear, the associated metamorphic conditions were markedly retrogressive with respect to $M_1$ and also testify to the post-$D_4/D_5$ development of the Kanabeam shear zone. The shearing produced oblique displacement with a right-lateral horizontal and relative small vertical component, with down-movement of the northern block.

The sequence of six deformation phases constitutes the minimum number as the analytical technique involves a simplistic approach. On the basis of the same approach it is considered that the main metamorphism, $M_1$, was progressive and culminated penecontemporaneously with $D_2$ in the domain of $s_2$ refoliation. Retrogression was recognised only in domains of refoliation and proceeded to relative lower grade conditions from the time of emplacement of the Ai-ais Complex through $D_4/D_5$ to $D_6$.

$D_6$ deforms pegmatites, but predates the emplacement of the Gannakouriep dyke suite, which is then an upper-time marker for the sequence of deformations in the central zone.

## 3.6 Kanabeam shear zone ($D_6$)

The Kanabeam shear zone which is regionally extensive over hundreds of kilometres when correlating across younger sedimentary cover, is also known as the Tantalite Valley shear zone (Blignault et al., 1974).

### 3.6.1 Mylonite belt

The mylonite belt (Fig. 3.1) is a linear zone of refoliation trending 305$^{\circ}$ with a steep northerly or vertical dip. The mylonite belt, *sensu stricto*, is up to 500 m wide, whereas a subvertical foliation with cataclastic character defines a zone which could be a few orders wider. There is a complete textural transition from mylonite to the country rock gneisses. The planar fabric of the mylonites postdates pegmatites and predate the Gannakouriep dyke suite. Since the formation of the mylonite belt, movement along the belt displaced the Gannakouriep dykes and the Karoo sediments. Recent activity along the belt is evident from fault scarps and seismic activity in the area was reported by the inhabitants at the Kanabeam farmstead.

*Fabric elements*

The foliation is defined by microstructures typical of mylonites with little recrystallisation and neomineralisation. Within the mylonite belt the foliation is generally parallel to the attitude of the belt. Lineations on the foliation are of varied description and include felspar trains, long dimension of felspar porphyroclasts, mineral habit, arrangement of mineral grains and colour striping. The attitude of these lineations is variable to the extent that they define a great circle girdle, with a poorly defined mode (Fig. 3.50a), suggesting a preferred east-southeastern trend. The different types of lineations might have different origins as the felspar trains and long directions of porphyroclasts indicate stretching directions, while the striping might be due to the intersection of older surfaces with the mylonite foliation. The different processes of formation explain the variation in attitude. The preferred east -southeastern trend, however, agrees with the right-lateral movement inferred for the shear zone.

Folds of $F_2$-type deforming the mylonite foliation, with axial surfaces in the

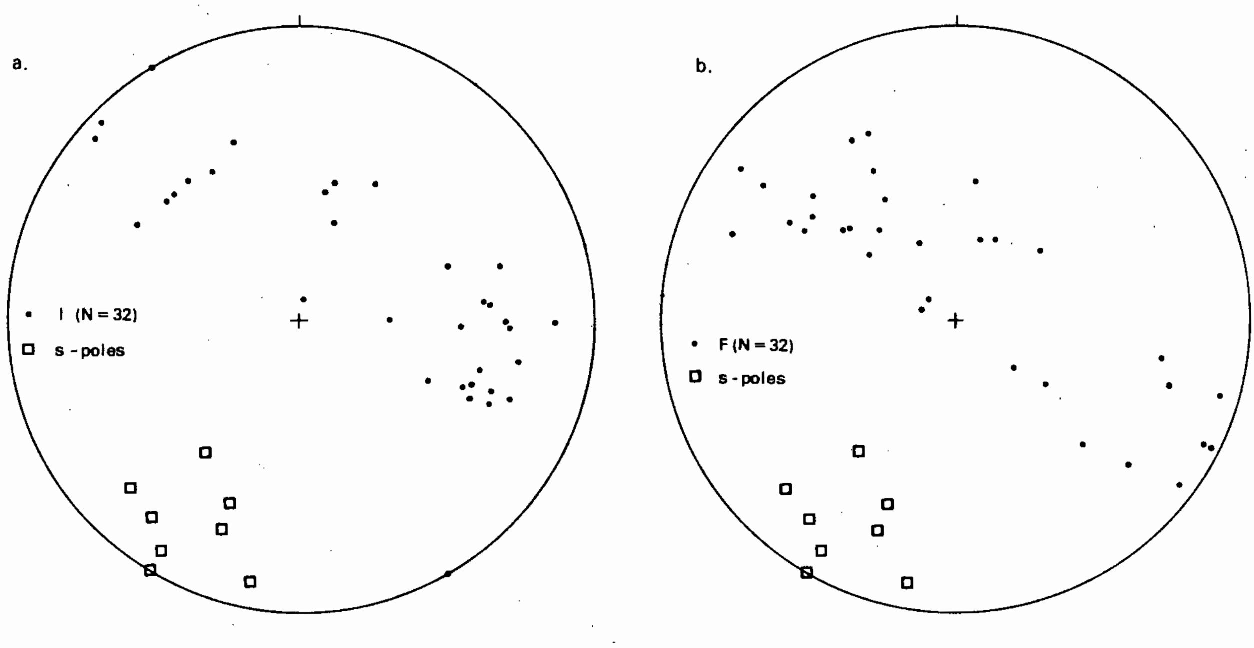


*Fig. 3.60a Fabric elements of the mylonite belt (s = mylonite foliation).*

plane of the mylonite belt, are ubiquitous. They vary in style from open to isoclinal and from parallel to similar. On micro-scale it was observed that a mylonitic axial-plane foliation is developed while the fold is defined by a similar type of foliation. These features suggest that folds developed progressively throughout the time of formation of the mylonite belt. The fold axes are distributed along a great circle girdle (Fig. 3.50b) with a poorly defined mode normal to that of the lineation on the mylonite foliation (cf. Figs. 3.50 a & b). The mylonite foliation is considered a shear surface (see Section 3.6.2) and therefore the fold-axes mode defines b and the lineation mode kinematic a, the direction of movement.

*Metamorphic grade*

Deformation microstructures predominate in the mylonites. Annealing effects are developed only in quartz and in the 24 samples investigated, only the primary recrystallisation stage is reached. The neomineralisation of micas along the foliation, although very subordinate, gives an indication of the prevailing temperature during the formation of the mylonite belt. Biotite, white mica and chlorite are the only products of neomineralisation recognised. The stable coexistence of touching chlorite and white mica (assumed to include a component of muscovite), indicates a low-grade metamorphic environment with an upper temperature limit of 500 - 550$^{\circ}$C. With respect to the main metamorphism, the mylonite belt is situated within the sillimanite zone (Fig. 4.11). The metamorphism associated with the formation of the mylonite belt is therefore retrogressive.

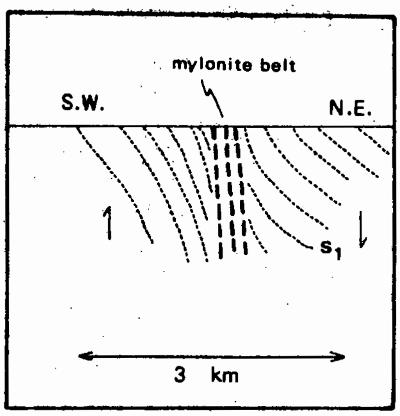


*Fig.3.51.Configuration of the older planar fabric in vertical cross section with inferred movement.*

### 3.6.2 Shear zone

The high-grade (sillimanite zone) planar fabric in the gneisses on both sides of the mylonite belt turns tangentially into parallelism with the belt (Fig. 3.1); this configuration being consistent with the model of a shear zone (Ramsay & Graham, 1970) in anisotropic material with a horizontal component of right-lateral movement. In cross section, the arrangement of the deformed foliation (Fig. 3.51) indicates downward movement of the northern block. This kinematic analysis is consistent with the preferred orientation of lineations on the mylonite foliation (Fig. 3.50a) which, if considered as *a* lineations, suggest oblique relative movement of the northern block in a direction 09633 along the plane of the mylonite belt. The order of displacement in the vertical was such that no metamorphic discontinuity (cf. Fig. 4.11) is apparent between the northern and southern blocks.

Together with the deformation of the regional planar fabric into parallelism with the mylonite belt, older folds also rotate towards a coplanar attitude with the mylonite belt. All earlier fabric elements are virtually obliterated in the mylonite belt. The trend of the shear zone, as defined by the configuration of the rotated foliation in the country rocks (Annex. 1), is grossly parallel to that of the mylonite belt situated in the core of the shear zone. A new penetrative cross-cutting foliation, overprinted on the planar fabric of the gneisses along the margin of the belt, was not observed. The planar fabric of the gneisses adjoining the mylonite belt, however, have a cataclastic character showing that the shear strain outside the mylonite belt affected the existing planar fabric. The angle between the new mylonite foliation and the trend of the shear zone is zero or indeterminably small; the geometry of the mylonite foliation is therefore consistent with that of a shear surface. If this interpretation is correct the mylonite belt is the culmination of progressive simple shear across which displacement is discontinuous.

### 3.6.3 Relation to $D_4$ and $D_5$

The change in orientation of $F_4$ and $F_5$ adjacent to the mylonite belt (cf. Figs. 3.42 & 3.43) is considered to be in part the effect of progressive rotational strain within the Kanabeam shear zone. On this basis the boundary of the shear zone is at least 31 km towards the northeast of the mylonite belt. The orientation pattern of the deflected structures (Fig. 3.43), however, does not conform to the expected pattern (according to the model; Ramsay & Graham, 1970) if the structures were originally oriented parallel and normal to the shear zone. It is argued that the Ai-ais Complex originally caused a deflection of $F_4$ and $F_5$ trends (Section 3.5.4) and for the same reasons increased the heterogeneous aspect of the progressive simple shear ~~during~~ $D_6$, to result in the deflected pattern illustrated in Fig. 3.43.

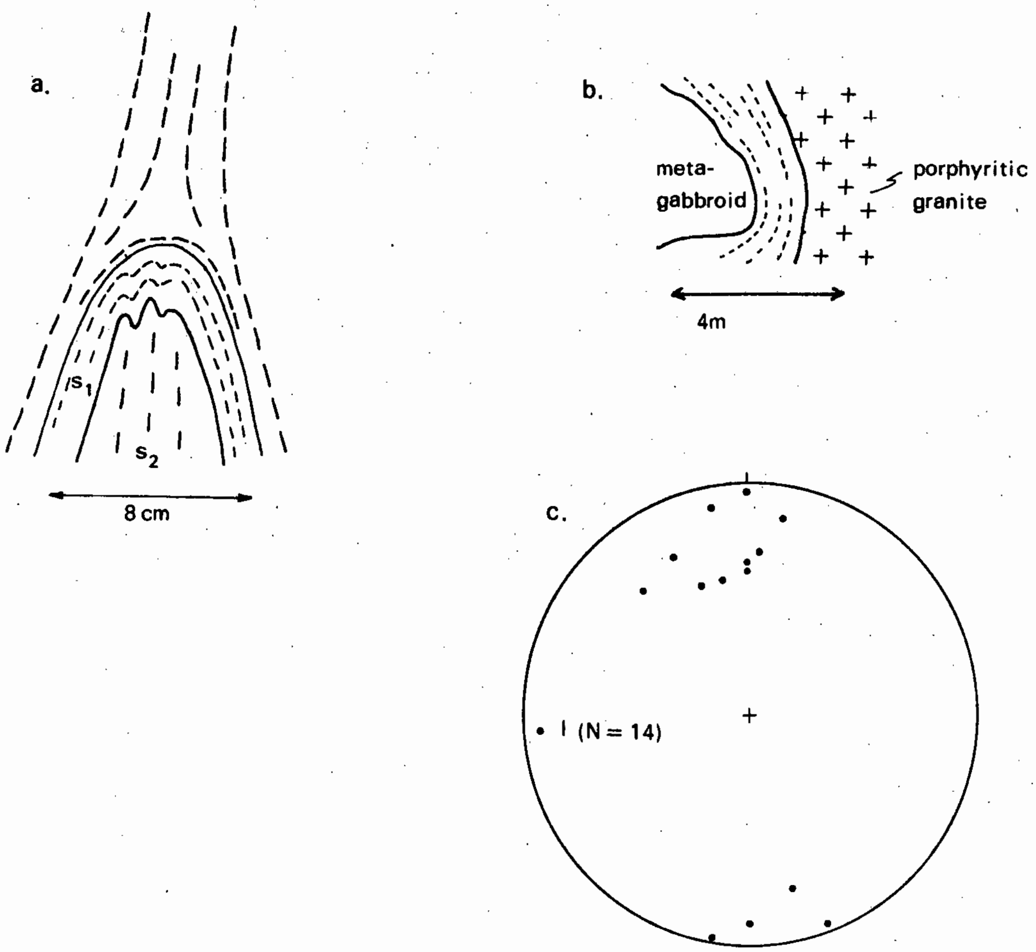


Fig. 3.52. a. Strong refoliation ($s_2$) in the ductile schistose material while $s_1$ remains recognisable in the competent band. b. Contact shearing due to the deformation of the Ai-ais Complex. c. Direction stability of lineations associated with the marginal and internal foliation of the Ai-ais Complex east of the Fish River.

# 4 MAIN METAMORPHISM

## *Main metamorphism*

### 1 Richtersveld Province

The main metamorphism, $M_1$, in the Richtersveld Province, is defined by the metamorphic mineral parageneses texturally associated with a pervasive planar fabric, $s_1$. The foliation $s_1$ is imprinted on intrusives and extrusives which are not completely reconstituted.

### 2 Namaqua Province

In the Namaqua Province the main metamorphism, $M_1$, is defined by prograde crystalloblastic mineral assemblages of completely reconstituted pretectonic gneisses.

## *Metamorphic mineral parageneses*

According to Winkler (1976) only minerals in contact are regarded to constitute a paragenesis because the bulk composition on thin section scale might be heterogeneous. The process of metamorphic reactions, as discussed by Carmichael (1969), allows for reactions taking place by means of metasomatic subsystems without the reactants and products being in contact. In this regard Winkler's approach is considered too rigid, but allowance must be made for heterogeneity on thin-section scale.

In this text the term paragenesis is used according to the definition of Winkler and the term mineral assemblages, when the component minerals are not mutually in contact or not established to be so. The term mineral assemblage, however, is restricted to homogenous domains with regard to bulk composition on thin section scale.

*Microstructure*

The relation between the main planar fabric of the different structural domains is demonstrated by giving special attention to aspects of microstructure. The relation between the main planar fabric and the main metamorphism is therefore separately treated for the different domains (Sections 4.1, 4.2 & 4.3).

## 4.1 Main metamorphic imprint ($M_1$) on the igneous rocks of the Richtersveld Province, Ai-ais

### 4.1.1 De Hoop volcanics

The petrographic data considered below were obtained from 69 thin sections.

#### 4.1.1.1 Textural aspects

The lavas are commonly blastoporphyritic and no other microtextural aspects like glass shards, etc. which indicate an extrusive origin, were observed. This is so because the matrix is recrystallised to a very fine-grained (0,014-0,028 mm) granoblastic state. The grain boundaries are regular (straight or slightly curved) and commonly polygonal. In the more acid volcanics, quartz and quartz-felspar porphyries, the matrix consists predominantly of leucocratic grains, presumably both quartz and felspar, although no twinning was recognised. In the more mafic volcanics epidote, white mica, biotite and/or chlorite might be present in the groundmass.

The only apparent deformation is developed in the quartz and felspar phenocrysts, and then only poorly in the form of pull-apart features and fracturing. The K-felspar insets are predominantly microcline while the plagioclase phenocrysts are partly altered to white mica and epidote with the latter mineral commonly distributed along the outer portion of the grain indicating reverse zoning of the primary plagioclase. Some quartz insets are resorbed, generally show poorly developed undulose extinction and new grain formation. Where developed, the quartz insets are subdivided into a few grains only. Theoretically the unstrained state of the quartz phenocrysts could be due to either coeval recrystallisation or it could reflect a low state of finite strain in the particular sampled outcrops. The first alternative is preferred, because, where the foliation is well developed, the state of finite strain can be assumed to be significant, yet the same unstrained state prevails in the quartz insets to the extent that a quartz phenocryst optically constitutes one grain. Mafic mineral aggregates are common in both the acid and more basic volcanic rocks. The regular outlines preserved in some aggregates suggest that the aggregates represent the retrogressive breakdown products of pyriboles.

In summary, it can be stated that the bulk of the volcanic material has recrystallised. K-felspar represents the only primary mineral. The paucity of deformation features, only apparent in some phenocrysts, indicates that the rate of recrystallisation exceeded that of deformation.

#### 4.1.1.2 Relation to the regional foliation

The regional foliation, $s_1$ (see Section 3.3.1.1), is developed discontinuously across strike in the volcanics with the result that high-strain zones of minor dimensions are situated at irregular intervals in a domain of relatively low strain. Of interest here is that the typical polygonal texture of the groundmass is equally well developed in the intensely foliated zones as it is in the areas with no apparent foliation; the most prominent differences being a well developed preferred orientation of micas in the groundmass and a lenticular habit of the mafic aggregates. Important to note, is the absence of deformation textures in the intensely foliated zones.

From these relations it is inferred that :

(i) the physical conditions giving rise to the blastesis of the polygonal leucocratic and mafic minerals acted during the development of the regional foliation in both the high and low-strain domains to such an extent that strain-free mineral grains resulted,

(ii) the physical conditions outlasted the deformation phase to allow for the late crystallisation of poikiloblastic hornblende and biotite, and

(iii) because the intensely foliated zones developed under the same metamorphic conditions as the foliation elsewhere in the volcanics and their geometry and lineations are similar (Section 3.3.1.1), it is reasonable to conclude that the foliation throughout developed during the same deformation phase.

The crystalloblastic parageneses defined by the matrix minerals and mafic aggregates therefore formed during and after $D_1$.

4.1.1.3 Metamorphic mineral parageneses

The metamorphic mineral parageneses are defined by minerals in contact and considered to reflect the physical conditions of neomineralisation and recrystallisation as described above. The following mineral parageneses were observed :

(i) In the mafic aggregates constituting isolated domains on a microscopic scale :

decussate biotite + epidote
tourmaline + biotite + epidote
chlorite + epidote + ore
white mica + biotite + epidote + leucominerals

Sphene and apatite were also identified in some of the mafic aggregates.

(ii) In the recrystallised matrix of the more basic lavas (felspar porphyry and mafic aphanite) :

white mica + chlorite + quartz
chlorite + epidote + quartz
hornblende + biotite + epidote + ore + quartz ± chlorite

(iii) In the recrystallised matrix of the more acid lavas (quartz-felspar porphyry) :

white mica + biotite + leucominerals
white mica + biotite + epidote + quartz

Plagioclase sometimes form part of the parageneses of (ii) and (iii) above, but could not be identified in the fine-grained polygonal groundmass of leucominerals; the altered plagioclase insets need not necessarily be in equilibrium with the metamorphic parageneses.

The hornblende and biotite occurring in the parageneses above have the following pleochroic characteristics, typical of biotite and hornblende in low-grade terrains (Miyashiro, 1968) :

hornblende : $\gamma$ = blue-green
biotite : $\gamma = \beta$ = green

4.1.1.4 Low-grade retrogressive metamorphism

The equilibrium textures indicate that virtually all the material re-equilibrated at lower grade conditions; the only exceptions possibly, being altered plagioclase insets, andesine in the mafic lavas and the occasional K-felspar which did not invert to microcline. The following evidence suggests retrogressive metamorphism from high-temperature stable igneous mineralogy :

(i) Various stages of plagioclase alteration are present e.g. (a) a plagioclase phenocryst with optical continuity, but clouded with white mica and epidote and (b) a regularly outlined and zoned aggregate of epidote along the outside, white mica and a polygonal leucomineral, presumably untwinned plagioclase in the core suggesting the following reaction :

igneous plagioclase + $H_2O$ = epidote + white mica + plagioclase (less calcic)

(ii) The predominance of microcline as K-felspar phenocrysts indicates that the high-temperature K-felspars of the lavas were inverted.

(iii) The regular outlines of some mafic aggregates suggest that they are pseudomorphs of possibly pyriboles e.g.

pyribole + $H_2O$ = epidote + apatite + ore
= biotite + epidote + ore + sphene
= chlorite + epidote + ore

The scale on which the retrogressive metamorphism took place in igneous rocks with a poor planar fabric suggests that either the volcanics contained sufficient water to allow for hydration reactions or water from outside was able to permeate the system.

The physical conditions at which these volcanic rocks re-equilibrated may be judged from the metamorphic mineral assemblages.

(i) The absence of actinolite and the presence of hornblende show that the metamorphic conditions lie on the high temperature side of the hornblende-generating reaction which is widely accepted to occur at the expense of actinolite.

(ii) According to Winkler (1974, p. 75 - 80), touching chlorite + muscovite is not stable in medium-grade and can be used as an indicator of low-grade. The assemblage chlorite + white mica was observed, not only in the matrix of the more mafic lavas (Section 4.1.1.3), but also in a thinly (mm) banded volcaniclastic rock; the alternating light and dark-coloured bands are respectively white mica and chlorite-rich. It is reasonable to assume that some of the white mica in the bands of acid composition is muscovite.

The metamorphic grade of the De Hoop volcanics is therefore defined by the two limiting reactions

actinolite → hornblende
chlorite + muscovite out.

Both reactions are shown by Winkler (1974) to have steep gradients in PT-space; a temperature interval of 500 - 550° C can be approximated and falls within the high temperature part of Winkler's low-grade metamorphism (Fig. 4.1).

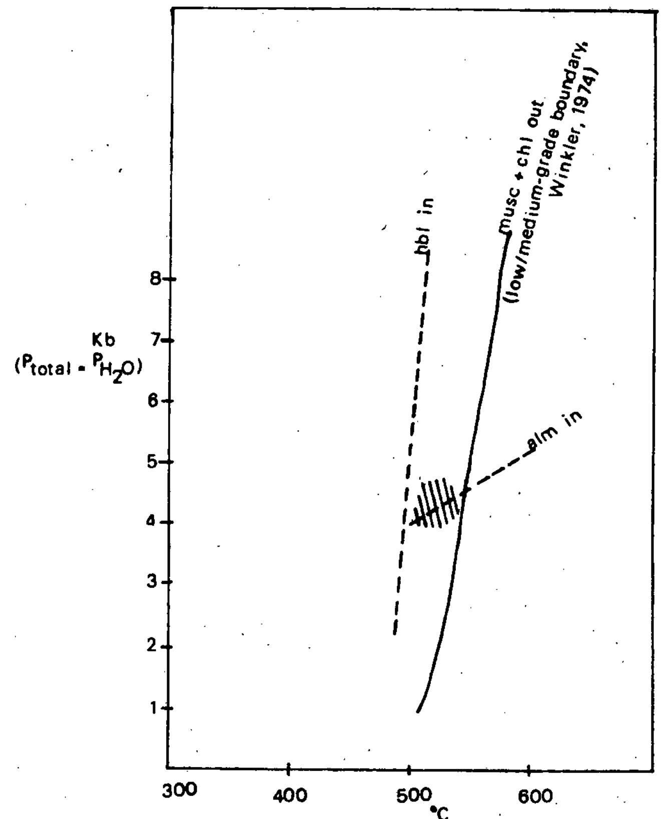


Fig. 4.1. The shaded area depicts the estimated P-T conditions for $M_1$ in part of the Richtersveld Province at Ai-ais. The reaction curve 'hbl in' is an estimation (Winkler, 1974); the 'alm in' curve is an extrapolation from experimental data (Hirschberg & Winkler, 1968).

### 4.1.2 Vioolsdrif intrusives

The petrographic data discussed below are based on observations from 73 thin sections.

#### 4.1.2.1 Textural character and relation to regional foliation

The microstructural character of a rock is dependent on the rate of deformation as opposed to the rate of crystallisation/recrystallisation, which in its turn is a function of temperature, pressure, water content, bulk chemical and mineral composition. (Tullis et al., 1973; Stauffer, 1970; Vernon, 1976). The degree of crystallisation/recrystallisation which accompanies the deformation of the granitoids is evaluated below.

The strain distribution in the Vioolsdrif intrusives is heterogeneous (Section 3.3.1.1), but sympathetic with respect to the regional metamorphic ($M_1$) polarity. The low-strain subdomain is situated towards the south-west and away from the higher grade gneisses. The regional foliation ($s_1$) over the larger part of the subdomain is not megascopically visible. In virtually all the samples an undeformed granitic texture is preserved, in some, however, polygonal new grains are developed in quartz. The mafic minerals, mostly biotite, epidote and sphene, are distributed in aggregates.

The high-strain subdomain is situated towards the north-east and the higher grade gneisses of the Namaqua Province. It is traversed by zones of intense foliation; one such major zone (Fig. 3.3) separates the low-strain from the high-strain subdomain. The bulk of the granitoid between the zones of intense foliation, is foliated to various intensities. The granitoids of this subdomain can be subdivided into the following types, according to the intensity of deformation as seen in the field :

A. Granitoids appearing unfoliated and with either no microstructural evidence of deformation, or sparsely developed distortion of twin lamellae and strain extinction of felspars; these rocks constitute a minor proportion of the high-strain domain.

B. Foliation is just visible.

C. The foliation is well defined by dark minerals, but the rock is still medium to coarse grained as in A and B.

D. Augen and flaser gneiss with the augen and flaser situated within a fine grained groundmass.

E. Phyllonite. The term as used here includes rocks which are very fine grained, granoblastic, very well foliated and/or finely banded i.e. not necessarily rich in phyllosilicates.

Microstructurally the deformed types B, C, D and E comprise various proportions of the following domains :

a. Pretectonic felspar porphyroclasts distinguished by the wrapped-around foliation and internal distortions such as fractures, bent twin lamellae, undulose extinction and pull-apart features.

b. Discontinuous bands (ribbons), as seen in two dimensions, or more irregularly shaped domains of coarse-grained quartz which are strain-free with straight, regular boundaries (less commonly sutured) and commonly polygonal or elongated in the same direction as the band.

c. Discontinuous bands, or lenticular domains (streaks) composed of dark minerals with the inequidimensional micas (biotite and/or chlorite) arranged both parallel or across, with respect to the long direction of the streaks (foliation); in some samples the micas are irregularly disseminated, but preferentially oriented parallel to the foliation.

d. Irregularly shaped domains or bands consisting of very fine-grained leucocratic minerals. This mortar-type domain also cuts through pretectonic felspars and constitute fracture-fillings in the felspars. The individual mineral grains are generally too fine grained for optical determination, nevertheless, the grain boundaries tend towards polygonal shapes and strain-free quartz, plagioclase and pretectonic felspar appear to be present.

Types A and E are considered the end-members of a deformation/recrystallisation-neomineralisation series. A gradation from A through B, C and D to E was commonly observed in the field where E constitute the core of a zone of intense foliation. As the intensity of the foliation/deformation increases from A to E the following trends are recognised :

(i) In types B, C and D the foliation is typically anastomosing on a microscale and tends to be perfectly parallel in the phyllonites (type E).

(ii) The proportion of domain a, the porphyroclastic felspars, decreases from B to E, which contains less than 10 per cent and normally only a trace.

(iii) The proportion of domains b and d increases from A to E and the domains become less irregularly shaped to define the foliation where more intensely developed.

(iv) In C, D and E hornblende commonly defines a lineation in the foliation.

(v) The largest proportion of recrystallised/neomineralised material is found in E.

From the relations above it is clear that there is a sympathetic relation between the intensity of deformation and microstructural development in the sense of recrystallisation/neomineralisation. The metamorphic development, therefore, is associated with $D_1$. Posttectonic (with respect to $s_1$) development of chlorite, biotite and hornblende (long dimensions of minerals are oriented across the foliation) is common, though not predominant, and indicates that the physical conditions of metamorphism outlasted $D_1$.

4.1.2.2 Metamorphic mineral parageneses

1. The phyllonites, augen/flaser gneisses and foliated granitoids (types B, C, D and E) of the high-strain subdomain.
The crystalloblastic parageneses listed below are developed in the granodioritic phase of the Vioolsdrif Suite; the bulk composition varies from adamellitic to tonalitic. Felspar, especially plagioclase, possibly forms part of the parageneses listed below. Due to the fine-grained size, it is difficult to conclusively identify crystalloblastic felspars. Pretectonic felspars are not considered and although the pretectonic plagioclase is generally altered, it is not known if it is in equilibrium with the other phases.

quartz + white mica + chlorite + biotite ± epidote
quartz + white mica + chlorite + almandine-rich garnet + ore; (garnet observed in one specimen only and identified (X-ray diffraction) by W. van der Westhuizen, U.O.F.S.)

quartz + white mica + biotite ± epidote
quartz + chlorite + epidote ± biotite

quartz + hornblende + epidote + chlorite
quartz + hornblende + epidote + biotite ± chlorite
quartz + hornblende + biotite ± epidote ± sphene ± ore

quartz + biotite + epidote ± sphene ± ore

The pleochroic formulas for the hornblende and biotite are

hornblende : $\gamma$ = blue-green
biotite : $\gamma$ = $\beta$ = green and brown

2. The undeformed granodiorites and adamellites (type A) of the high and the low-strain subdomain.

There is no textural evidence for considering the parageneses below of metamorphic origin, however, they are listed for comparison with those above. All the felspars are clearly not crystalloblastic and the altered plagioclase might form an additional phase.

| | |
|---|---|
| quartz + biotite + epidote ± sphene ± ore<br>quartz + hornblende + biotite + epidote ± sphene ± ore | low-strain subdomain |
| quartz + biotite + epidote ± sphene<br>quartz + hornblende + chlorite + epidote ± sphene | high-strain subdomain |

hornblende : $\gamma$ = blue-green
biotite : $\gamma$ = $\beta$ = green

3. The basic phases of the Vioolsdrif Suite do not possess a preferred planar or linear fabric and the amphiboles are interlocked in a decussate fashion.

hornblende + cummingtonite + chlorite + ore
hornblende + chlorite + epidote + biotite + quartz + plagioclase
hornblende + 'actinolite' + biotite + ore + quartz + plagioclase
hornblende + 'actinolite' + chlorite + epidote + albite

hornblende : $\gamma$ = blue-green
biotite : $\gamma$ = $\beta$ = green

The plagioclase is generally altered to epidote while some clear grains have an anorthite content of ca. 5 per cent.

4. Foliated amphibolite dykes.

On micro-scale, the foliation is defined only by the dimensional orientation of the hornblende ($\gamma$ = blue-green). The plagioclase is altered to epidote and white mica; a few clear grains, or portions thereof, indicate an anorthite content of approximately 40 per cent.

hornblende + epidote + quartz + plagioclase $\pm$ chlorite
hornblende + epidote + sphene + plagioclase

### 4.1.2.3 Evaluation of the metamorphism

The metamorphic grade is best evaluated by considering the parageneses in the phyllonites which have the largest component of crystalloblastic minerals. White mica and chlorite commonly coexist in the phyllonites. According to Deer, Howie and Zussman (1966, p. 204) the white micas resulting from the metamorphism of acid and intermediate rocks are muscovite and paragonite and it is therefore reasonable to assume that the white micas observed in the phyllonites include muscovite. The coexistence of muscovite + chlorite is diagnostic of low-grade metamorphism (Winkler, 1974); a maximum temperature limit for the metamorphic development of the phyllonite is the low-grade/medium-grade boundary in PT space.

In one particular specimen, an intensely foliated granitoid, the following elucidating paragenesis was observed :

quartz + muscovite + chlorite + almandine-rich garnet + ore

At sufficiently high pressures, garnet first develops in the higher temperature part of low-grade metamorphism (Winkler, 1976). From an extrapolated reaction curve, experimentally determined by Hirschberg & Winkler (1968, p. 30), it is estimated that in the high temperature part of low-grade (500 - 550°C), the pressure ($P_{total} = P_{H_2O}$) must have exceeded 4 kb to form almandine (Fig. 4.1). The assumption $P_{total} = P_{H_2O}$ is speculative, especially in the case of retrogressive metamorphism of dry granitoids where $P_{total}$ is likely to exceed $P_{H_2O}$. The garnet, however, is found in an intensely foliated zone facilitating the addition of water, a condition necessary for the abundant formation of micas in the phyllonites. The possibility for the local attainment of the condition $P_{total} \approx P_{H_2O}$ therefore cannot be excluded.

The ubiquitous presence of hornblende indicates conditions on the high-temperature side of the hornblende-generating reaction. This reaction is thought to take place over a range of PT conditions which are not known (Winkler, 1974, p. 233). The presence of chlorite in mafic rocks is diagnostic of low-grade metamorphism (Winkler, 1974, p. 165). The amphibolite dykes and basic phases of the Vioolsdrif Suite contain chlorite in parageneses (Section 4.1.2.2; Fig. 4.2) which, according to Winkler (1974), belong to the high-temperature part of low-grade metamorphism if hornblende is present and to the low-temperature part if actinolite is present. The presence of both hornblende and 'actinolite' in some samples indicates conditions close to the estimated reaction curve (Fig. 4.1). The basic phases of the Vioolsdrif Suite, although unfoliated, therefore retrogressed under low-grade conditions.

The hornblende and biotite are blue-green and green-brown, respectively, throughout and in metabasites designate greenschist, epidote-amphibolite or lower amphibolite facies grade (Miyashiro, 1973).

It is of interest to consider whether the mineral assemblages, or part thereof, of undeformed granitoids re-equilibrated at the imposed physical conditions as inferred from the crystalloblastic parageneses of the phyllonites. The predominance of perthitic K-felspar, microcline and orthoclase, in the undeformed granitoids and as porphyroclasts in the deformed granitoids, show that the whole rock did not re-equilibrate during metamorphism. The plagioclase in both the deformed and undeformed rocks retrogressed to form
epidote + white mica + plagioclase (presumably more albite rich)
The formation of new quartz grains in the undeformed granitoids and a strong tendency towards equilibrium textures of quartz in the deformed rocks, indicate that quartz recrystallised throughout. The following evidence suggests that the mafic minerals had undergone retrogressive changes :

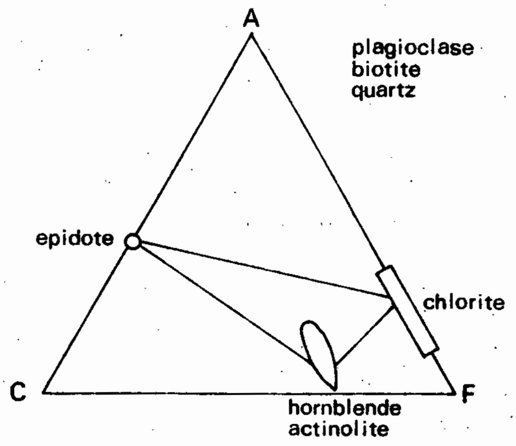


Fig. 4.2. ACF diagram (after Winkler 1974, p. 165 - 166) illustrating the low-grade parageneses of the basic phases of the Vioolsdrif Suite.

(i) The pleochroic characteristics of hornblende and biotite in the mafic rocks are typical of greenschist or low-amphibolite facies (cf. Miyashiro, 1973) i.e. temperatures well below the solidus of intermediate or basic igneous rocks. The colour of the hornblende and biotite is the same throughout the area under consideration, irrespective of bulk composition and intensity of deformation.

(ii) Chlorite and epidote, outside the grain boundaries of the altered plagioclase, are present in the undeformed rocks and are not known to form part of primary mineral assemblages of granitoids.

(iii) As the textural aspects of the mafic minerals in the foliated granitoids do not indicate pretectonic growth, but rather syn or late-tectonic (preferred and cross-cutting orientations) crystallisation, it is reasonable to assume that the mafic mineral suite in the undeformed granitoids, which is consistent with that in the foliated granitoids (types B and C), crystallised or recrystallised at the same time.

The considerations above suggest that retrogressive phase changes occurred throughout the intrusive complex. The microstructural evidence show that in the bulk of the intrusive complex equilibrium conditions were not attained, but approached in the phyllonites. It is considered that the degree of crystallisation/recrystallisation is largely controlled by the intensity of penecontemporaneous deformation (Section 4.1.2.1). The greater amount of crystallisation/recrystallisation in the high-strain subdomain therefore cannot be linked directly to a higher grade of metamorphism.

It is shown that the crystallisation/recrystallisation processes acted syn to late-kinematically with respect to $D_1$. As the retrogressive metamorphism was obviously affected after crystallisation of the intrusives, it follows that $D_1$ is also post-igneous crystallisation; a syn-crystallisation relationship, however, cannot be excluded.

### 4.1.3 Summary and conclusions

1. Evidence for polymetamorphism was not recognised.

2. A single main retrogressive metamorphic event, designated $M_1$, is imprinted on both the De Hoop volcanics and rocks of the Vioolsdrif Suite (see 12).

3. Metamorphism $M_1$ is related to $D_1$ by means of sympathetic regional variations of annealing and deformation; $M_1$ is synkinematic with respect to $D_1$ and outlasted $D_1$.

4. The relation above (3) implies that $D_1$ is also post-crystallisation of the Vioolsdrif intrusives.

5. The similar character of $M_1$ throughout the area substantiates the correlation of the planar structures, $s_1$, within the area under consideration.

6. The relation between $M_1$ and $D_1$ is similar in both the Vioolsdrif intrusives and De Hoop volcanics.

7. The low-grade temperature conditions are defined by two limiting reactions (Fig. 4.1) and is the same for both the Vioolsdrif intrusives and De Hoop volcanics.

8. The pressure conditions are based on the presence of almandine-rich garnet in a single specimen of deformed granitoid.

9. The estimated PT conditions are speculative in view of the assumption $P_{total} = P_{H_2O}$ and probably represent minimum conditions. The metamorphism of dry igneous rocks involve hydration reactions during the initial stages and a condition where $P_{H_2O} < P_{total}$ will favour the reverse dehydration, with the result that higher temperatures are necessary to drive the reaction in the hydration direction.

10. Hornblende and muscovite + chlorite are present in the larger part of the area (see Fig. 4.11 for distribution) which means that the estimated temperature interval is valid for the larger part of the Richtersveld Province in the Ai-ais area.

11. Equilibrium conditions were not attained over most of the intrusive complex, but were approached in relative narrow zones of intense deformation; similar, but partial retrogressive changes, are pervasive throughout the intrusive complex.

12. The definition of $M_1$ as a single main metamorphic pulse is substantiated by

    (i) the similar character of $M_1$ throughout the area
    (ii) the similar mutual relations between $M_1$ and $D_1$
    (iii) the absence of overprinting features.

## 4.2 Main metamorphic imprint ($M_1$) on the front zone, Ai-ais

### 4.2.1 Microstructure and relation to $s_1$

The bulk of the Vioolsdrif intrusives in the front zone are medium-grained augen/flaser gneisses (Section 2.2.1). The deformation as judged from the penetration of the regional foliation, $s_1$, is more homogeneous than in the Richtersveld Province. The intensity of deformation is, on appearance, comparable with that of type D (Section 4.1.2.1) in the Richtersveld Province and the microstructures of the augen/flaser gneisses are compared with those of type D there. The augen and flaser of type D gneisses consist of deformed pretectonic felspar, wrapped around by quartz ribbons and a very fine-grained mortar-type aggregate of leucominerals (domain d). The microstructure of the augen/flaser gneisses of the front zone is distinctly different :

(i) The augen and flaser are aggregates of quartz and felspar (both K-felspar and plagioclase) with regular straight grain contacts suggesting equilibrium (minimum energy) boundary conditions; deformation features are absent in both the felspar and quartz grains. The foliation is wrapped around the augen and flaser domains.

(ii) The size distribution tend to be unimodal and although the gneisses megascopically appear medium grained, they are fine grained granoblastic.

It is clear that recrystallisation in the augen/flaser gneisses of the front zone are much further advanced than in similar rocks of the Richtersveld Province to such an extent that new felspar grains were formed and normal grain growth advanced to an almost equigranular state. That this increase in the degree of recrystallisation is not abrupt across the front is evident from (i) the occurrence of advanced recrystallised augen gneisses close to the front on the Richtersveld Province side, and (ii) the presence of augen gneisses in the front zone with deformed pretectonic felspars, some of which are perthitic.

The increased recrystallisation in the front zone is not related to an increase in the intensity of deformation, because the rocks compared above, in the first place, show the same amount of strain as judged from the fabric and secondly, some of the specimens from the front zone show an almost intact primary igneous texture with some of the euhedral plagioclase grains recrystallised to an aggregate of new grains. As it is reasonable to assume that the rate of deformation across the front is comparable, a significant increase in temperature is necessary to explain the advanced recrystallisation.

The recrystallisation and neomineralisation is syn to late-tectonic with respect to $s_1$ because (i) the recrystallized quartz grains are commonly inequant (see Tullis et al., 1973) and preferentially oriented (ii) the micas define $s_1$ (iii) helicitic hornblende is both randomly oriented and disposed in the plane of the foliation.

### 4.2.2 Metamorphic grade

The metamorphic parageneses considered below do not include pretectonic felspars.

(i) In amphibolites

hornblende + plagioclase (An44-47) ± quartz
hornblende + plagioclase (An41) + epidote + quartz

(ii) In mafic gneisses

plagioclase + quartz + hornblende + epidote
plagioclase + quartz + hornblende + biotite
plagioclase + quartz + hornblende + biotite + chlorite + epidote

(iii) In granitoids

K-felspar + plagioclase + quartz + muscovite ± biotite
K-felspar + plagioclase + quartz + biotite + epidote ± chlorite
K-felspar + plagioclase + quartz + hornblende + epidote + biotite
K-felspar + plagioclase + quartz + hornblende + epidote + chlorite

plagioclase + quartz + epidote + biotite ± hornblende
plagioclase + quartz + epidote + chlorite

quartz + muscovite + biotite + epidote

The pleochroic characteristics of hornblende and biotite in the assemblages above are :

hornblende : $\gamma$ = blue-green, with some distinctly darker in colour than those from the Richtersveld Province,
biotite : $\gamma = \beta$ = brown.

The mineral parageneses above are not particularly diagnostic of metamorphic grade. The stable coexistence of chlorite + quartz and presence of epidote indicate maximum conditions, while the presence of hornblende indicates minimum temperature conditions.

Higher temperatures of metamorphism as compared with the Richtersveld Province (Section 4.1) are suggested by (i) the formation of new felspar grains (Section 4.2.1), and (ii) the pleochroic colours of biotite (Miyashiro, 1973), which are predominantly brown, as compared to the green biotites of the Richtersveld Province.

## 4.3 Metamorphism $M_1$ in the pretectonic gneisses of the Namaqua Province, Ai-Ais

The microstructures of the samples investigated generally show equilibrium-type grain boundaries and individual grains appear strain free. Prograde crystalloblastic mineral assemblages define the main planar fabric by preferred dimensional orientation. A poorly defined preferred orientation and/or random orientation of mineral grains are common and interpreted as continued growth late and after the fabric-forming deformation.

### 4.3.1 Aluminous and semi-aluminous rocks

Apart from the predominant aluminous paragneiss unit, a few scattered occurrences of aluminous gneisses southwards within the grey gneiss unit supply areal control for the investigation of metamorphic gradation. Semi-aluminous rocks, such as quartzo-felspathic gneisses rich in micas and some metaquartzites with aluminous microscopic subdomains, are an uncommon component in units other than the paragneiss unit.

#### 4.3.1.1 Andalusite/sillimanite isograd

The andalusite/sillimanite isograd (Fig. 4.3) is drawn through points where both minerals were found in the same thin section and is further constrained by lower grade parageneses (andalusite, muscovite + chlorite) to the south-west and sillimanite occurrences towards the north-east.

In the vicinity of the isograd sillimanite is produced by various reactions.

1. Andalusite-sillimanite inversion

In sample B-842, andalusite and sillimanite are always enclosed by cordierite, with the result that two parageneses are separated.

andalusite + sillimanite + cordierite
cordierite + garnet + biotite + quartz + plagioclase + ore

In the aluminous domains, cordierite distinctly embayes the enclosed andalusite (Fig. 4.4 a & c) and a reaction producing cordierite from andalusite is infer-

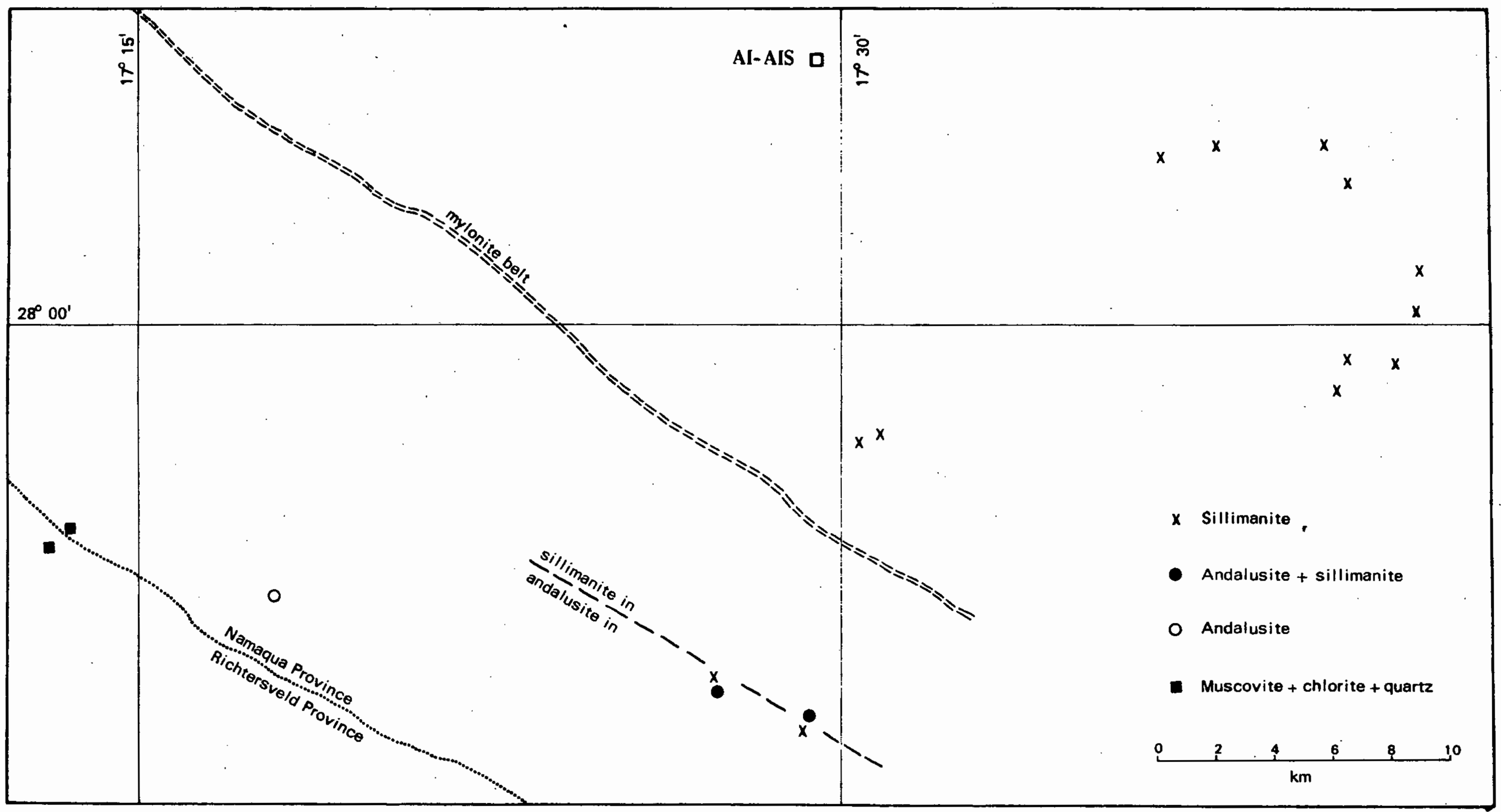


*Fig. 4.3. The andalusite / sillimanite isograd.*

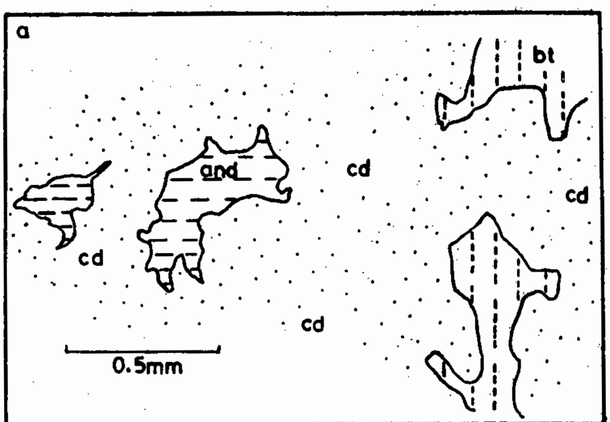


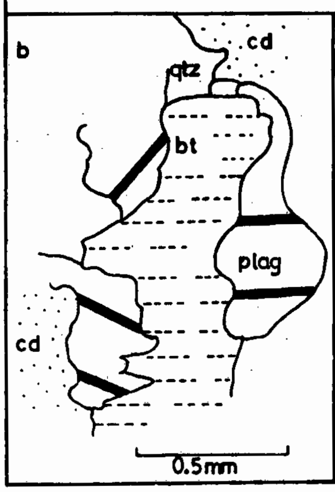


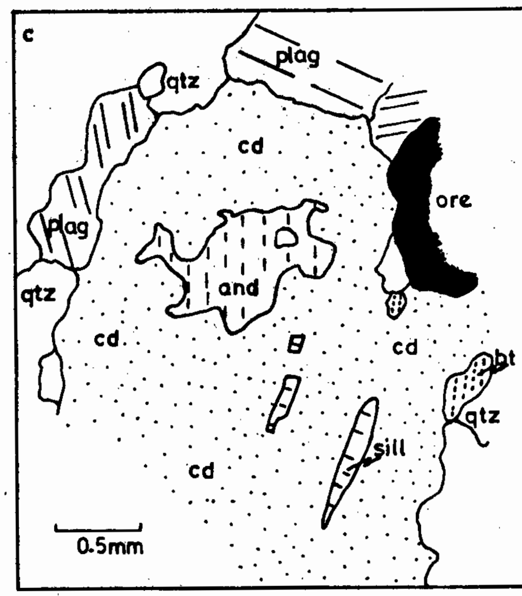


Fig.4.4. Microstructural evidence for the cordierite producing reaction(2). (a) Corrosion of andalusite and biotite by cordierite; the separated portions of the andalusite and biotite grains are in optical continuity (b) Plagioclase embayes biotite (c) Andalusite and sillimanite are enclosed within pinitized cordierite.
(bt=biotite, cd=cordierite, and=andalusite, qtz=quartz, plag=plagioclase, sill=sillimanite)

red below. This reaction, however, is not considered to have produced sillimanite, as trace amounts of sillimanite is present in only a few of the cordierite coronas (as shown in Fig. 4.4c) and is therefore not the rule. In one instance fine sillimanite needles are developed along the grain boundary of andalusite, while elsewhere the sillimanite is some distance away from the andalusite, but within the cordierite corona. From this it is inferred that minor amounts of sillimanite inverted from andalusite

andalusite = sillimanite ........................................ (1)

while the cordierite producing reaction was proceeding.

The penecontemporaneous breakdown of andalusite could have proceeded as follows. Cordierite embayes andalusite, biotite and plagioclase while plagioclase embayes biotite (Fig. 4.4). From this microstructural evidence the following cordierite producing reaction is inferred with quartz added as a reactant to balance the equation.

9 quartz + 2 biotite + 6 andalusite + 18 albite = 3 cordierite
+ 20 albite + 2 $H_2O$ ........................................ (2)

As there is no K-bearing mineral to act as a sink for the potassium set free by the biotite, the reaction is balanced in such a way that the ratio Na:K is 9:1, and would allow the potassium to be absorbed by the andesine. The volume ratio between the cordierite and albite products, according to reaction 2, 1:2,8, is realistic, but some cordierite is required at the start of the reaction as the actual cordierite/andesine volume ratio in sample B-842 is 1,5:1.

2. Fibrolite development

Along the andalusite/sillimanite isograd in assemblages void of andalusite, sillimanite occurs as knots or bundles of fibrolite, a markedly different habit, as opposed to the discrete sillimanite needles, however fine, developing in andalusite assemblages. It seems that the development of fibrolite knots depends on the type of reaction involved.

Fibrolite is present in the following mineral assemblages :

sillimanite + biotite + quartz + ore + muscovite ± cordierite

In the assemblage sillimanite + biotite + quartz + ore + muscovite the following microstructural evidence have a bearing on the fibrolite-producing reaction. (i) The fibrolite is spatially associated with biotite which is either fringed by fibrolite, or the fibrolite is present within the biotite grains as intergrowths or inclusions. It seems as if biotite acted both as reactant and product. (ii) Apart from being included in biotite, fibrolite also appears in quartz and muscovite grains. A possible reaction includes biotite as reactant and biotite, muscovite, fibrolite and quartz as products.

Microstructures as described above, including the embayment of muscovite by quartz and sillimanite, are present well above the andalusite/sillimanite isograd. The suggestion is that the reaction, or reactions, producing sillimanite, are continuous and take place at least up to minimum melt temperatures. In view of this, isograds based on the first occurrence of sillimanite, without defining the reaction, or on some sliding reaction other than a polymorphic inversion, are not necessarily comparable in terms of P and T.

4.3.1.2 K-felspar + sillimanite isograd

A number of 88 thin sections of aluminous and semi-aluminous samples were investigated with the aim of establishing the K-felspar + sillimanite isograd.

| Number of samples | Muscovite | Quartz | Plagioclase | Biotite | Garnet | Cordierite | Sillimanite | K-felspar | |
|---|---|---|---|---|---|---|---|---|---|
| 9 | X | X | X | X | | | | | semi-aluminous |
| 4 | X | X | X | X | | | X | | semi-aluminous + aluminous |
| 1 | X | X | X | X | X | | | | semi-aluminous |
| 2 | X | X | X | X | X | | X | | semi-aluminous |
| 2 | X | X | X | X | | | | X | semi-aluminous |
| 1 | X | X | X | | | | | X | semi-aluminous |
| 1 | | X | X | X | X | | | | semi-aluminous |
| 1 | | X | X | X | X | | X | | semi-aluminous |
| 2 | | X | X | X | X | X | X | | semi-aluminous |
| 1 | | X | X | X | | X | | | semi-aluminous |
| 1 | X | X | | X | | | X | | aluminous |
| 2 | X | X | | X | | X | X | | aluminous |
| 1 | | X | | X | X | X | X | | aluminous; on isograd |

Table 4.1. Mineral assemblages/parageneses south of the K-felspar + sillimanite isograd, ore and accessory minerals are not shown.

Some 50 of these samples with suitable mineralogy, define the isograd (Fig. 4.5) by the preferred location of the following coexisting minerals.

South of the isograd : touching quartz + muscovite + plagioclase
North of the isograd : touching K-felspar + sillimanite/garnet/cordierite

In another five samples (Fig. 4.5) all five phases quartz + muscovite + plagioclase + K-felspar + sillimanite/garnet/cordierite coexist, but are not necessarily mutually in contact with each other; the muscovite in each case is present in trace quantities.

*Mineral assemblages/paragneses south of the isograd*

Semi-aluminous rocks, with a relative large quartz-felspar content, predominate south of the isograd. It can be seen from Table 4.1 that the most common parageneses are

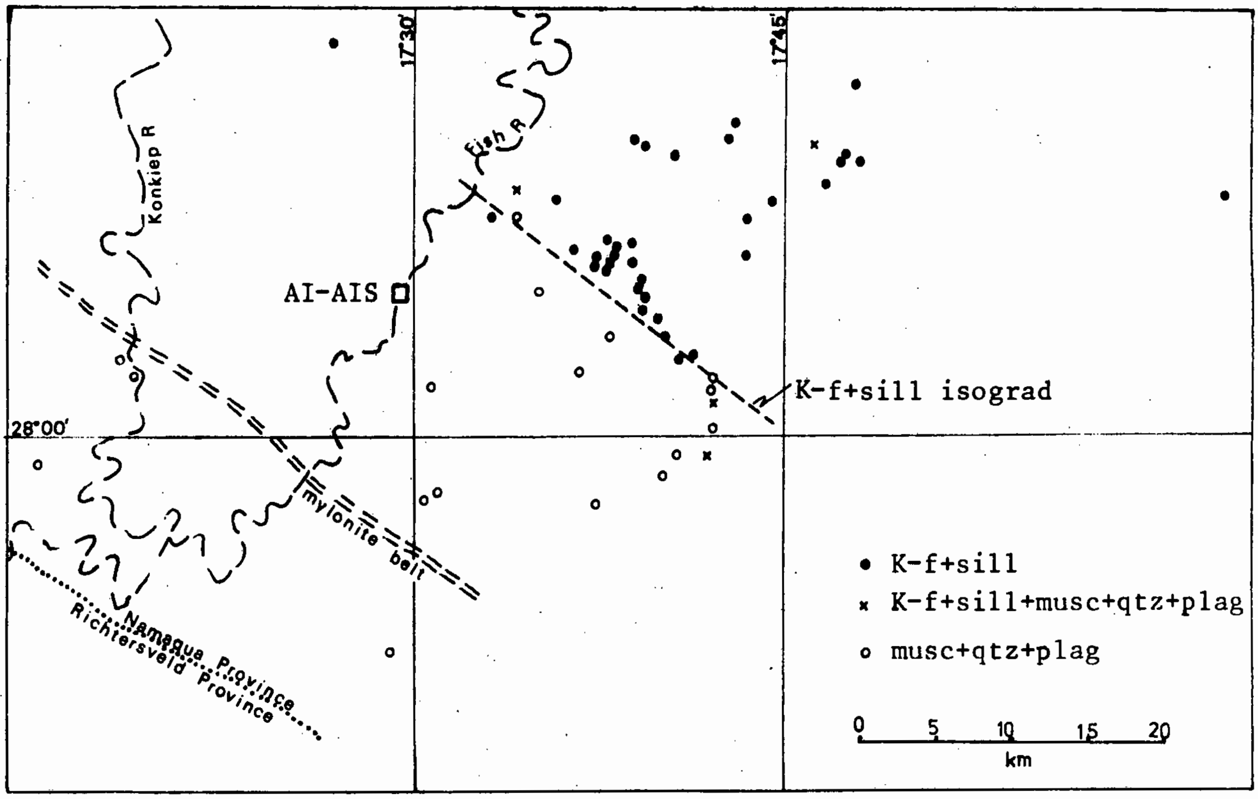


Fig.4.5. The K-felspar + sillimanite isograd defined by aluminous and semi-aluminous assemblages. (K-f=K-felspar, sill=sillimanite, musc=muscovite, qtz=quartz, plag=plagioclase)

muscovite + quartz + plagioclase + biotite ± sillimanite (Fig. 4.6a)

Garnet and cordierite coexist in three samples, while the K-felspar where present, do not occur together with sillimanite in the same sample.

*Mineral assemblages/parageneses north of the isograd*

The most common mineral assemblages (Table 4.2) are
K-felspar + sillimanite + cordierite + biotite + garnet + quartz ± plagioclase (Fig. 4.6b).
The K-felspar is perthitic orthoclase or microcline-microperthite, while the garnet is almandine-rich ($a^o$ = 11.53$A^o$; one determination by Dr G J Beukes, U.O.F.S.). Cordierite and the almandine-rich garnet commonly coexist. Quartz + muscovite with no microstructural evidence of secondary growth are rare; the muscovite is usually present in trace (<< 1%) quantities.

| Number of samples | Cordierite | Garnet | Biotite | Sillimanite | K-felspar | Plagioclase | Quartz | Muscovite | |
|---|---|---|---|---|---|---|---|---|---|
| 15 | X | X | X | X | X | X | X | | aluminous |
| 10 | X | X | X | X | X | | X | | aluminous; semi-aluminous |
| 4 | X | | X | X | X | | X | | aluminous |
| 2 | X | | X | X | X | X | X | | aluminous |
| 2 | X | X | X | X | | X | X | | aluminous |
| 2 | X | X | X | | | X | X | | aluminous |
| 2 | X | X | X | X | | | X | | aluminous |
| 1 | X | X | X | | | | X | | aluminous |
| 1 | X | | | | | | X | X | aluminous |
| 1 | X | | X | | | | X | X | aluminous |
| 2 | | X | X | X | X | X | X | | semi-aluminous |
| 1 | X | X | X | | X | X | X | | semi-aluminous |
| 3 | X | X | X | | | X | X | | semi-aluminous |
| 2 | X | | X | | X | X | X | | semi-aluminous |
| 1 | | X | X | | X | X | X | | semi-aluminous |
| 3 | | X | X | | | X | X | | semi-aluminous |
| 1 | X | X | X | X | | X | X | | semi-aluminous |
| 1 | | X | X | X | | X | X | | semi-aluminous |

Table 4.2. Mineral assemblages/parageneses north of the K-felspar + sillimanite isograd, ore and accessory minerals are not shown.

*Microstructures*

Microstructures which might relate to the reaction giving rise to the K-felspar + sillimanite isograd, were observed above the isograd.

1. A common relationship is the spatial association between cordierite and sillimanite; sillimanite needles together with round quartz grains are present within poikiloblastic cordierite. In some samples the sillimanite is preferentially located within cordierite to such an extent that no sillimanite is present outside cordierite. If this relation is interpreted as an intergrowth texture i.e. the contemporaneous growth of both minerals within a subdomain of suitable bulk chemistry (cf. Carmichael, 1969), possible reactions are

muscovite + quartz + plagioclase + biotite = K-felspar + more calcic plagioclase + sillimanite + cordierite + garnet + $H_2O$ ...................... (3)

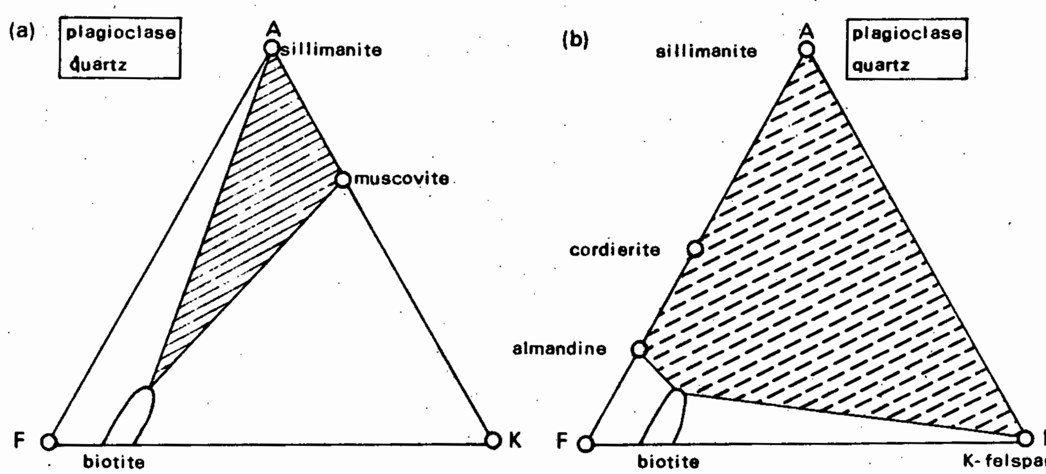


*Fig. 4.6 The compositional fields outlined by the most common mineral assemblages in aluminous and semi-aluminous rocks (a) south of the K-felspar+ sillimanite isograd and (b) north of the K-felspar+ sillimanite isograd.*

or

muscovite + quartz + biotite = K-felspar + sillimanite + cordierite + garnet + $H_2O$ ........................................................ (4)

Jacob (1974) interpreted the same feature as a replacement texture related to the formation of cordierite from sillimanite by the reaction

biotite + sillimanite + quartz = cordierite + garnet + K-felspar + $H_2O$ ... (5)

As the sillimanite within cordierite does not appear corroded in any way, an intergrowth origin by means of reactions (3) or (4) is preferred.

2. Garnet invariably occurs as a skeletal-like intergrowth with quartz; in some samples there is also a tendency towards a quartz rim around garnet. It is interpreted as an intergrowth microstructure resulting from the simultaneous crystallisation of quartz and garnet, and could be associated with a number of reactions.

3. Poikiloblastic K-felspar with sillimanite inclusions is interpreted as an intergrowth feature resulting from any of the K-felspar + sillimanite producing reactions.

*Reaction producing K-felspar + sillimanite*

By comparing the mineral assemblages both sides of the isograd it is obvious that all the muscovite reacted to produce K-felspar (cf. the AFK diagrams, Fig. 4.6). From the AFK diagrams it is also inferred that biotite must have reacted to form cordierite and garnet. The microstructures suggest K-felspar, sillimanite and cordierite as products. The discontinuous character of the reaction is born out by the isograd (Fig. 4.5) as defined by the majority of samples. Muscovite coexists with K-felspar, sillimanite, quartz and plagioclase in five samples scattered across the isograd over a distance of 20 km. In view of the distinct paucity of these assemblages, their random distribution (Fig. 4.5), the trace amounts in which the muscovite occurs and the sharp definition of the isograd otherwise, it is not considered likely that these assemblages relate to a 20 km zone of bivariant equilibrium; the formation of trace amounts of muscovite above the isograd by local retrogression is a more reasonable explanation.

On the premises outlined above the reactions

muscovite + quartz + biotite ($\pm$ plagioclase) = K-felspar + sillimanite + cordierite + garnet + $H_2O$ ($\pm$ more calcic plagioclase) .............. (6)

are suggested and considered in the light of (i) the minimum melt-producing reaction (Winkler, 1976)

$H_2O$ + muscovite + quartz + plagioclase + biotite = melt + sillimanite + garnet + cordierite .......................................... (7)

(ii) the 'muscovite + quartz out' reaction under pressures where almandine-rich garnet and cordierite coexist (Storre, 1972)

muscovite + quartz + water = melt + sillimanite .......................... (8)

muscovite + quartz = melt + K-felspar + sillimanite ..................... (9)

(iii) the solid/solid isograd reaction of Evans & Guidotti (1966)

muscovite + quartz + plagioclase (albite component) = K-felspar + sillimanite + $H_2O$ ...................................................... (10)

They admit the possibility of a melt instead of a vapour phase on the right-hand side of reaction (10).

The K-felspar + sillimanite isograd reaction is for the following reasons, not interpreted as the minimum melt reaction :

(i) Migmatites with leucosomes fringed by melanosomes (Mehnert, 1968) which indicate some segregation process and perhaps partial melting, are present well south of the isograd.

(ii) If the isograd represents minimum melting conditions, a zone with coexisting quartz + muscovite should be present on the high-grade side. It can be argued that the absence of such a zone is due to the consumption of all the available muscovite by melt-generating reactions; this is, however, considered unlikely because the samples, 54 in number, represent a wide range of bulk compositions (Fig. 4.6b) within the aluminous/semi-aluminous range.

The predominant solid/solid reaction (6) is thus preferred to have had produced the K-felspar + sillimanite isograd. Fyfe (1970, 1973) argues that a minimum melt acts as a water buffer with the result that subsequent reactions during progressive metamorphism take place under the conditions of $P_{H_2O} < P_{total}$. Under these conditions it is possible for plagioclase to take part in a solid/solid reaction (cf. Evans & Guidotti, 1966; Miyashiro, 1973, p. 226; Section 4.5.1).

It is not possible to detect the former presence of a pore melt (Mehnert et al., 1973) and therefore impossible to prove that a melt phase developed on the right hand side of reaction (6), although theoretically, a melt should develop instead of the water phase. It is reasonable to argue then that reaction (6) is predominantly a solid/solid reaction, with some melt developed due to the water made available by the breakdown of the micas.

4.3.1.3 K-felspar + sillimanite zone

The K-felspar + sillimanite zone is situated on the high-grade side of the K-felspar + sillimanite isograd. The various mineral assemblages are listed in Table 4.2. The following parageneses, *sensu stricto*, are common (Table 4.3); K-felspar, plagioclase and/or quartz are additional :

cordierite + garnet + biotite + sillimanite
cordierite + garnet + biotite
cordierite + biotite + sillimanite

The coexistence of the four phases cordierite + garnet + biotite + sillimanite (Fig. 4.7) is not considered stable (Reinhardt, 1968). To investigate the possibility that the paragenesis represents at least bivariant equilibrium, the parameters g and gc were used where

$$gc = \frac{\text{cordierite + garnet}}{\text{biotite + cordierite + garnet}} \quad \text{(volume \%)}$$

The parameter gc is based on the theoretical possibility that the discontinuous reaction (Schmid & Wood, 1976)

quartz + sillimanite + biotite = cordierite + garnet + K-felspar + $H_2O$..(5)

is in equilibrium in the K-felspar + sillimanite zone. Parameter g, where

$$g = \frac{\text{garnet}}{\text{garnet + cordierite}} \quad \text{(volume \%)}$$

illustrates a possible reaction relationship between cordierite and garnet, for example (Currie, 1971)

cordierite + biotite = garnet + K-felspar + water ..................... (11)

cordierite = garnet + sillimanite + quartz ............................ (12)

The distribution patterns of gc and g (Figs. 4.8 a & b) in the K-felspar + sillimanite zone are similar-like and illustrate :

(i) an increase in cordierite + garnet at the expense of biotite, towards the north, and

(ii) a corresponding increase of cordierite with respect to garnet, towards the north.

To decide which, if any, of reactions (5), (11) or (12) are taking place, the microstructures are discussed below.

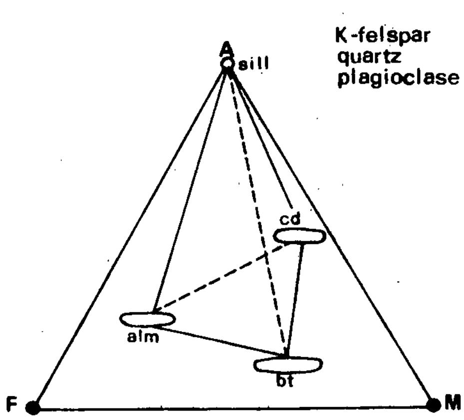


*Fig.4.7.The paragenesis cd + gnt + bt + sill in the K-felspar + sillimanite zone. (sill = sillimanite, cd = cordierite, bt = biotite)*

*Microstructures of the paragenesis cordierite + garnet + biotite + sillimanite*

The interpretation of the microstructures observed in aluminous rocks in the K-felspar + sillimanite metamorphic zone is ambiguous and becomes more so by the presence of relict microstructures which can be related to earlier reactions during the progressive metamorphic history.

1) In three samples a microstructure illustrating a frozen reaction, not completed, was observed which can possibly be related to continuous reactions above the K-felspar + sillimanite isograd. Skeletal garnet is enclosed or partly

| Number of sample | Partial parageneses | volume % | | | gc | g | |
|---|---|---|---|---|---|---|---|
| | | bt | gnt | cd | | | |
| B-867 | cd + gnt + bt | 7 | 1 | 33 | ,83 | ,03 | aluminous |
| B-822 | cd + gnt + bt + sill | 10 | 11 | 7 | ,64 | ,61 | " |
| B-805 | cd + gnt + bt + sill | 9 | 3 | 6 | ,50 | ,33 | " |
| B-801 | cd + gnt + bt + sill | 5 | 4 | 10 | ,74 | ,29 | " |
| B-777 | cd + gnt + bt + sill | 8 | 2 | 17 | ,70 | ,11 | " |
| B-699 | gnt + cd + bt<br>sill + cd + bt | 14 | tr | 18 | ,56 | 0 | " |
| B-697 | gnt + bt + cd<br>sill + cd + bt | 10 | 2 | 17 | ,66 | ,11 | " |
| B-200 | cd + bt + sill | 8 | 0 | 60 | ,88 | 0 | " |
| B-187 | cd + gnt + bt + sill | 6 | 14 | 9 | ,79 | ,61 | " |
| B-174 | cd + gnt + bt + sill | 7 | 12 | 11 | ,77 | ,52 | " |
| B- 95 | cd + gnt + bt + sill | 10 | 8 | 4 | ,55 | ,67 | " |
| B-820 | gnt + bt; bt + sill | 4 | 4 | 0 | ,50 | 1,0 | semi-aluminous |
| B-803 | cd + gnt + bt + sill | 8 | 1 | 3 | ,33 | ,25 | " |
| B-257 | cd + gnt + bt | 1 | 4 | 7 | ,92 | ,36 | " |
| B-798 | cd + gnt + bt + sill | 10 | 2 | 18 | ,67 | ,10 | aluminous |
| B-195 | cd + bt + sill | 8 | 0 | 10 | ,56 | 0 | " |
| B-179 | cd + gnt + bt + sill | 14 | 6 | 3 | ,39 | ,67 | semi-aluminous |
| B-763 | cd + bt + sill | 4 | 0 | 30 | ,88 | 0 | aluminous |
| B-190 | cd + bt + sill | 10 | 0 | 25 | ,71 | 0 | aluminous |
| B-258 | gnt + bt + cd<br>sill + bt + cd | 3 | 2 | 20 | ,88 | ,09 | aluminous |

Table 4.3. Partial modal mineralogy (visual estimations with the aid of comparison charts) and parageneses from the K-felspar + sillimanite zone (cd = cordierite, gnt = garnet, bt = biotite, sill = sillimanite).

enclosed within cordierite; the cordierite retains the quartz inclusions of the garnet and also carry biotite flakes. The formation of cordierite (+ biotite) coronas around garnet and penetration of the cordierite along fractures in garnet, clearly show that the reaction was still in progress before freezing. The features illustrating the corrosion of garnet and formation of cordierite and biotite are consistent with the distribution pattern of the parameter g indicating an increase of cordierite with respect to garnet towards the high-grade side. A possible continuous reaction which explains the observed features is

cordierite + biotite = garnet + K-felspar + $H_2O$ ...................... (11)

According to Winkler (1976) reaction (11) is coupled with reaction (12) and takes place at the same physical conditions.

2) Apart from the distribution pattern of the parameter gc, the microstructural evidence indicative of reaction (5), is the embayment of biotite by cordierite and cannot be considered conclusive.

### 4.3.2 Amphibolites

The amphibolites which here define a metamorphic zonation, are representative of the grey gneiss unit, the banded amphibolite unit, augen granodiorite and the paragneiss unit.

The mineralogical characteristics (Table 4.4) of the amphibolites define four metamorphic zones (Fig. 4.9). In all the samples hornblende and plagioclase constitute the major phases with hornblende predominating. Labradorite amphibolites define the higher grade zones while andesine amphibolites define the lower grade zone 1 :

*Zone 1*

The major part of zone 1 occupies the lower grade (medium-grade) portion of the marginal zone. The following parageneses are, on textural grounds, considered stable.

Blue-green ($\gamma$) hornblende + An42 $\pm$ quartz $\pm$ epidote $\pm$ biotite

The quartz, biotite and epidote are present in minor amounts. Epidote is characteristic of these andesine amphibolites and was not observed in the labradorite amphibolites.

*Zone 1/zone 2 boundary - 'epidote out' isograd*

The zone 1/zone 2 boundary is taken at the 'epidote out' isograd which is a

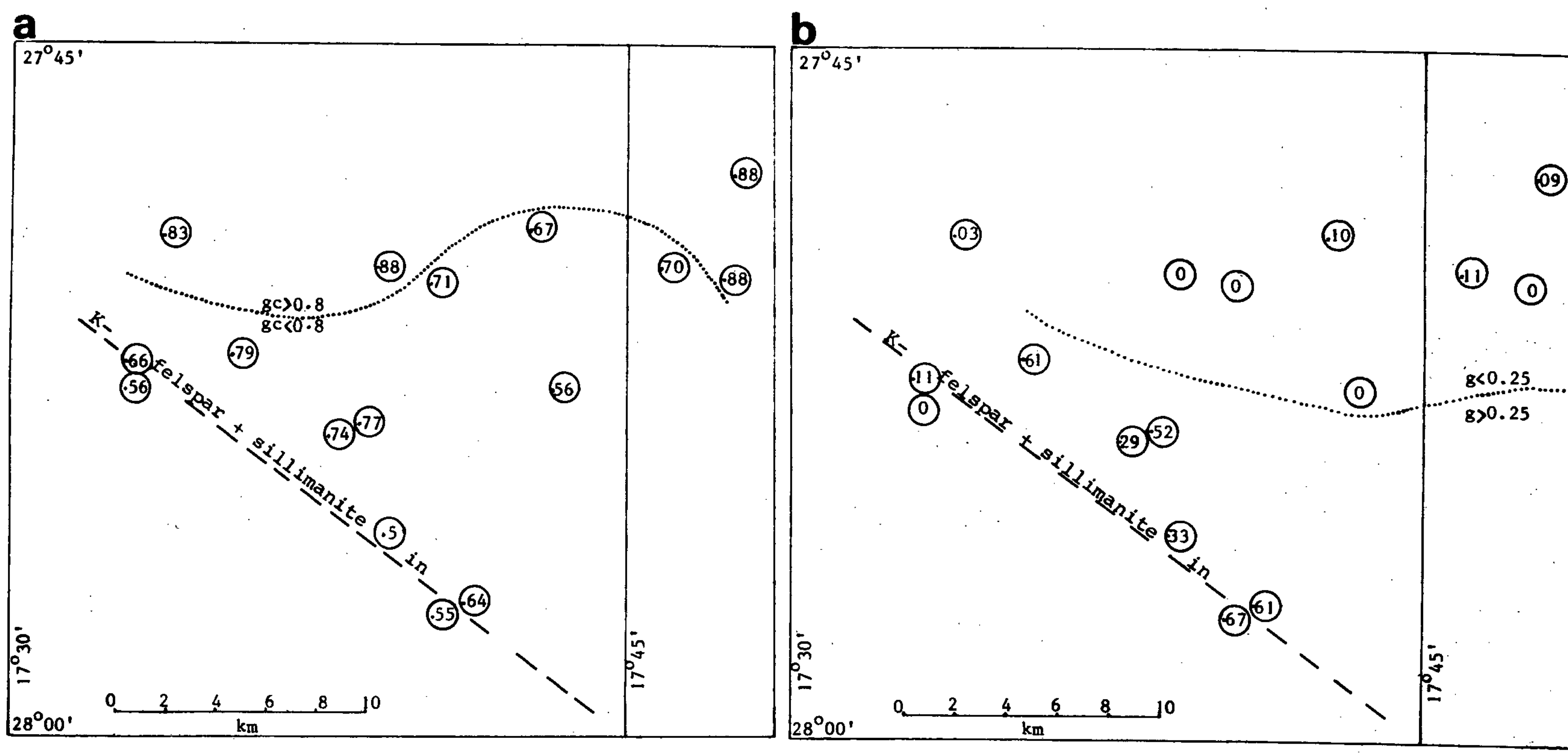


*Fig. 4.8 The distribution pattern of parameters g and gc in the K-felspar + sillimanite zone; the parameter values represent only samples which are highly aluminous; in volume% gc = (cd + gnt) / (cd + gnt + bt) and g = gnt / (gnt + cd) where cd = cordierite, gnt = garnet and bt = biotite.*

line demarcating the occurrence of epidote (Fig. 4.9) in amphibolites and in the grey biotite-hornblende gneisses. The line thus chosen also separates coexisting hornblende + An42 from coexisting hornblende + An60 (Table 4.4). The large jump in the anorthite content of the plagioclase substantiates the conclusion that the line approximately represents the 'epidote out' isograd along which the following reaction explains the observed mineralogical features.

hornblende(1) + epidote + An42 = hornblende(2) + An60 + $H_2O$ ........... (13)

*Zone 2*

With respect to the minimum melt isograd, zone 2 occupies the lower temperature part of the high-grade zone (Fig. 4.9). The metamorphic parageneses of the labradorite amphibolites are

blue-green ($\gamma$) hornblende + An60 $\pm$ quartz ($\pm$ biotite $\pm$ diopside $\pm$ cummingtonite)

The diopside, cummingtonite and biotite are not typical constituents and occur in minor amounts.

*Zone 3*

The zone 2/zone 3 boundary separates blue-green hornblende from green hornblende. This boundary is also defined by the K-felspar + sillimanite isograd as shown in Fig. 4.9. Zone 3, therefore, occupies the higher temperature part of the high-grade metamorphic zone.

The number of samples is not adequate for significant conslusions regarding the anorthite content of the plagioclase (Table 4.4), but a slight increase in the anorthite content from 60 - 64 per cent is, however, apparent from zone 2 to zone 4. The parageneses are

green ($\gamma$) hornblende + An61 $\pm$ quartz $\pm$ diopside $\pm$ biotite

*Zone 4*

Labradorite amphibolites with brown ($\gamma$) hornblende (Table 4.4) are found 24 km, north-east of the K-f + sillimanite isograd (Fig. 4.9) and characterise the highest grade amphibolites in the area. The parageneses are

brown ($\gamma$) hornblende + An64 $\pm$ biotite $\pm$ diopside $\pm$ quartz

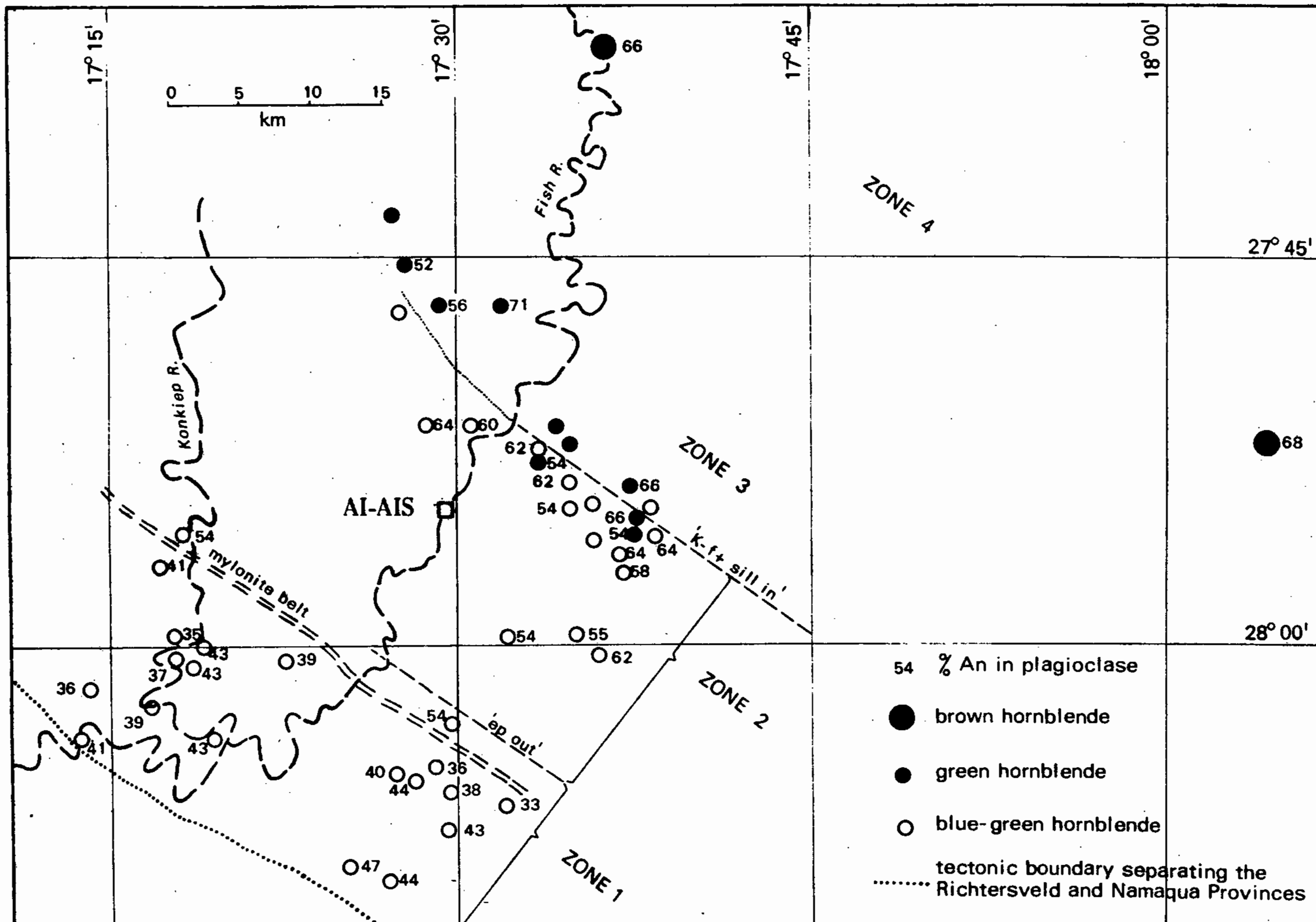


*Fig. 4.9. Metamorphic zonation defined by the mineralogy of the amphibolites. (K-f = K-felspar, sill = sillimanite, ep = epidote, An = anorthite)*

Brown hornblende in amphibolite is well known (Miyashiro, 1973) to occupy the higher temperature zones in metamorphic terrains. The change from green to brown hornblende does not occupy the same position with respect to other isograds in various metamorphic terrains. Binns (1969) associates this change in hornblende colour with the K-felspar + sillimanite isograd while, according to Wynne-Edwards (1971), olive-coloured hornblende becomes brown in the transition from amphibolite to granulite facies. Miyashiro (1968) reports brown hornblende in the higher temperature part of the amphibolite facies. In the Ai-ais area brown hornblende is located well above the K-felspar + sillimanite isograd.

## 4.4 Metamorphic zonation along the Grünau-Narubis section

A reconnaissance investigation revealed a metamorphic zonation which is symmetrical with respect to that in the Ai-ais area (Fig. 4.10) i.e. a lower grade zone is situated along the north-eastern extremity of basement outcrops. The distribution of amphibolitic and aluminous assemblages is shown in Fig. 4.10. The K-felspar + sillimanite zone is defined by the coexistence of K-felspar + cordierite in two samples while the lower-grade zone is characterised by one assemblage with touching muscovite + quartz + plagioclase and predominantly andesine amphibolites with blue-green ($\gamma$) hornblendes. In the zone on the north-eastern side of the Lord Hill shear zone

blue-green ($\gamma$) hornblende + An40 + epidote

coexist in the amphibolites and the grade is therefore on the low-temperature side of the 'epidote out' isograd.

| Zone | Mafic minerals | Hornblende colour ($\gamma$) | An content of plagioclase | | number of samples | Metamorphic grade |
|---|---|---|---|---|---|---|
| | | | mean | spread | | |
| 1 | hbl $\pm$ ep | blue-green | 42 | 33-54 | 20 | medium-grade |
| 2 | hbl $\pm$ diop | blue-green | 60 | 54-66 | 14 | high-grade |
| 3 | hbl $\pm$ diop | green | 61 | 52-71 | 4 | |
| 4 | hbl $\pm$ diop | brown | 64 | 58-68 | 3 | |

Table 4.4. The mineralogical subdivision of amphibolites into four metamorphic zones (cf. Fig. 4.9). The anorthite content of the plagioclase was determined by the Michel-Lévy's method on a fixed stage microscope. (An = anorthite, hbl = hornblende, ep = epidote, diop = diopside, cumm = cummingtonite).

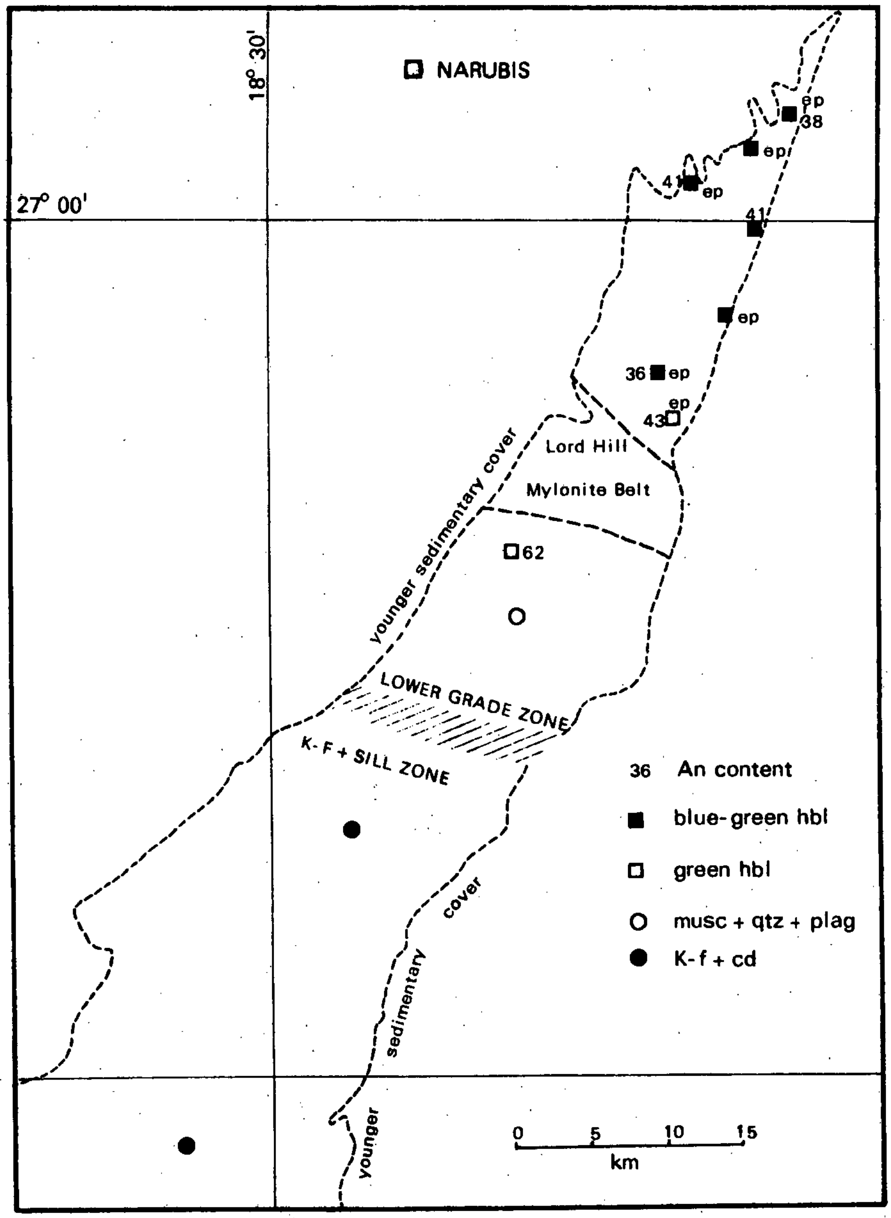


*Fig4.10.Diagnostic mineral assemblages in amphibolites and aluminous rocks defining a metamorphic zonation. (ep = epidote, An = anorthite, hbl = hornblende, musc = muscovite, qtz = quartz, plag = plagioclase, K-f = K-felspar, cd = cordierite, sill = sillimanite)*

## 4.5 Petrogenetic considerations

### 4.5.1 Metamorphic zonation in the Ai-ais area

The main metamorphism, $M_1$, as defined in the opening paragraphs of Section 4, defines a prograde metamorphic zonation from south-west to north-east (Fig. 4.11) across the general structural grain. A metamorphic discontinuity (cf. transcursive series of Chesworth, 1972) of large magnitude is not apparent. The metamorphic zonation as tabulated below characterises this particular metamorphic terrain.

| | |
|---|---|
| brown hornblende zone | high-grade |
| K-felspar + sillimanite zone | |
| 'epidote out' zone | |
| sillimanite zone | medium-grade |
| 'muscovite + chlorite out' zone | |
| muscovite + chlorite zone | low-grade |

*Muscovite + chlorite zone*

The low-grade metamorphism (terminology after Winkler, 1974) is imprinted on igneous rocks of the Richtersveld Province, which are only partly retrogressively reconstituted to crystalloblastic assemblages. There is a strong positive correlation between the recrystallisation/crystallisation defining $M_1$ and the intensity of $D_1$; $M_1$ acted contemporaneously and outlasted $D_1$ (Sections 4.1.1.2 & 4.1.2.1).

*Low-grade/medium-grade boundary*

The low-grade/medium-grade boundary is conjecturally shown (Fig. 4.11) to coincide with the front zone and based on the absence of coexisting muscovite + chlorite + quartz north-east of the front zone. Higher temperature conditions along the front zone and north-eastwards are inferred from the microstructures (Section 4.2), also relating $D_1$ with $M_1$.

*'Muscovite + chlorite out' zone*

The 'muscovite + chlorite out' zone is characterised by the absence of coexisting muscovite + chlorite + quartz and the presence of andalusite. The gneisses of the 'muscovite + chlorite out' zone and higher-grade zones consist wholely of crystalloblastic assemblages. The microstructural development from the muscovite + chlorite zone through the front zone to the fully reconstituted rocks of the higher grade zones is transitional (Section 4.1 & 4.2).

*Sillimanite zone and the minimum melt isograd*

The sillimanite zone is defined by the first development of sillimanite by inversion from andalusite (Section 4.3.1.1). Both the sillimanite and 'muscovite + chlorite out' zones are characterised by andesine amphibolites.

The minimum melt isograd, its approximate position is shown in Fig. 4.11, is located by the first occurrences of leucosomes fringed by melanosomes. These phenomena are generally interpreted as the products of anatexis (Mehnert, 1968) and are considered as such here, because stromatic migmatites (metatexites) give way to a preponderance of schlieren and nebulitic types (diatexites) in the brown hornblende zone. This crude zonation of migmatites imply a process which at first produced segregations, ultimately homogenised gneisses and is consistent with Mehnert's (1968) sequence of mobilization by anatexis. Metatexites can also form by segregation in the solid state across a chemical potential gradient (Vernon, 1976). Where metatexites, however, are succeeded by diatexites the metamorphic segregation process, if applicable, has to be reversed in order to produce progressively more homogeneous migmatite. A continuous process of increased partial melting is therefore preferred to explain the zonation of migmatites.

Assuming that the migmatites, as described above, indicate the advent of minimum melt conditions within the sillimanite zone, a serious discrepancy with respect to the analysis of Winkler (1976) is evident. Winkler states that for water-vapour pressures exceeding 3.5 kb the K-felspar + sillimanite (or in the negative sense, 'muscovite + quartz + plagioclase out') reaction curve coincides approximately in PT space with that of the minimum melt. In the Ai-ais area these isograds do not coincide (Fig. 4.11), but are 22 km apart; both Evans & Guidotti (1966) and Jacob (1974) have their K-felspar + sillimanite isograds within a migmatitic zone, showing that the zonation at Ai-ais is not an isolated occurrence. The statement of Winkler, above, is based on the experimental work of Storre & Karotke (1971) which was conducted under water-saturated conditions. Under relatively dry conditions the water liberated by the decomposition of hydrates is not sufficient to saturate all the potential melt (Brown & Fyfe, 1972), with the result that the reactants muscovite + quartz + plagioclase can be stable on the high temperature side of the minimum melt

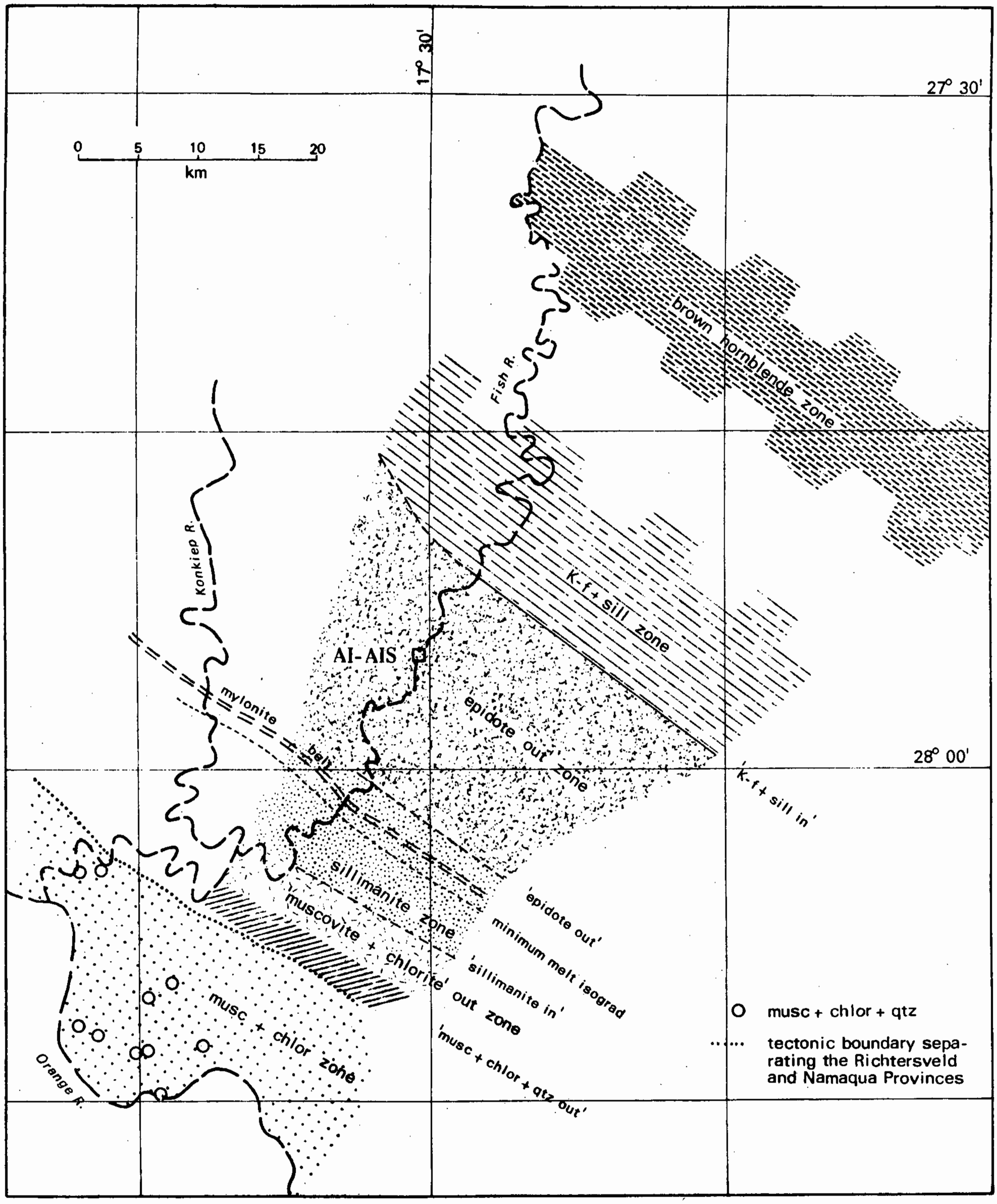


*Fig.4.11 Metamorphic zonation in the Ai-ais area. (K-f = K-felspar, sill = sillimanite, musc = muscovite, chlor = chlorite, qtz = quartz)*

curve. Fyfe (1970, 1973) points out why rocks should be relatively dry in regions where fusion is likely to take place and at higher grades.

*'Epidote out' zone*

The 'epidote out' zone coincides with zone 2 of the amphibolites (Section 4.3.2) and is characterised by labradorite amphibolites and absence of epidote both in amphiblite and mafic gneisses. Metatexites coexist with muscovite + quartz + plagioclase in the paleosome.

*K-felspar + sillimanite zone*

The K-felspar + sillimanite isograd coincides with the change from blue-green to green hornblende in amphibolites, but is situated on the high temperature side of the minimum melt isograd which is thought to indicate relatively dry conditions. The paragenesis cordierite + garnet + biotite + sillimanite is considered to be, at least, in bivariant equilibrium (reaction (11)) with cordierite forming at the expense of garnet.

*Brown hornblende zone*

The brown hornblende zone represents the highest grade metamorphic conditions recognised in the Ai-ais area and is located at a considerable distance from the K-felspar + sillimanite isograd. Diatexites, well exposed in the Fish River Canyons, are preferentially developed in the vicinity of the brown hornblende zone.

### 4.5.2 Pressure-temperature conditions

The progressive development of $M_1$ across the area investigated is traced out on the PT space by comparing reaction isograds and parageneses with experimentally and theoretically determined reaction curves. The resultant metamorphic path (Fig. 4.12) is derived at in the following way (discussed in order of increasing grade) and outline estimated PT conditions.

*Richtersveld Province.* The temperature interval is bracketed by the hornblende generating reaction and coexistence of muscovite + chlorite + quartz, while the occurrence of almandine-rich garnet give an indication of the pressure conditions (Fig. 4.13, Section 4.1.2.3). It is argued that the temperatures represent minimum values.

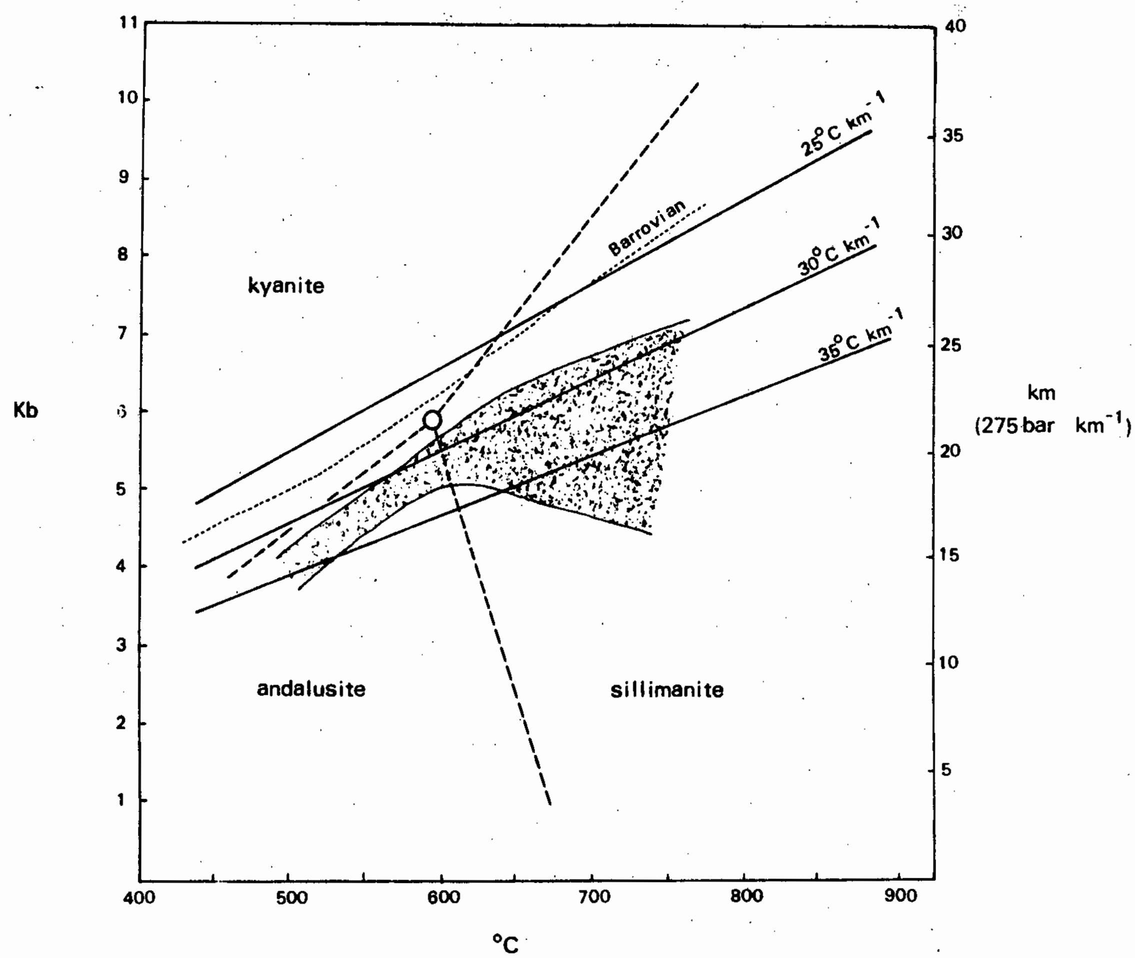


*Fig.4.12The low-pressure metamorphic path of the zonation in the Ai-ais area in relation to the Barrovian facies-series and geothermal gradients.*

*Andalusite/sillimanite inversion.* The coexistence of cordierite and garnet suggest a pressure interval (see K-felspar + sillimanite zone below), while the absence of kyanite denote maximum pressure. The andalusite/sillimanite reaction gives an indication of T. Following Winkler (1976) the andalusite/sillimanite boundary of Althaus (1967, 1969 a, b) is preferred, as sillimanite appears before the onset of anatexis in the Ai-ais area. The approximate temperature here assumed (Fig. 4.13) for the inversion might be a minimum, because of the possible metastable persistence of andalusite in the sillimanite field.

*Minimum melt isograd.* It is assumed that the first migmatites (leucosomes bordered by melanosomes) are minimum melt products. The reaction band of Winkler (1976) is used and allows for a variation in plagioclase composition of the paleosome and the different reactions leading to a melt.

*'Epidote out' zone.* Garnet, assumed to be almandine-rich, and cordierite which coexists in aluminous and semi-aluminous assemblages, allow for the classification within the (cordierite-almandine) high-grade pressure division of Winkler (1976).

*K-felspar + sillimanite isograd.* The isograd reaction is inferred (Section 4.3.1.2) to be muscovite + quartz + biotite = K-felspar + sillimanite + cordierite + garnet + $H_2O$ with plagioclase possibly taking part and a melt developed instead of the vapour phase. It is argued that the reaction took place under relatively dry conditions. The dry melting curve for the reaction

muscovite + quartz = K-felspar + sillimanite + melt

determined experimentally by Storre (1972) is a reasonable approximation of the isograd reaction and represents the isograd on the PT surface (Fig. 4.13).

*K-felspar + sillimanite zone.*

Almandine-rich garnet and cordierite, ubiquitously coexist in aluminous assemblages. The work of Currie (1971) and Henson & Green (1973) provides a pressure grid for cordierite-garnet-sillimanite-quartz-bearing assemblages. It is tentatively shown (Section 4.3.1.3) that the coupled sliding reactions (11) & (12) giving rise to these parageneses, are in equilibrium in the high-grade zone. The PT field which is dependent on the FeO/(MgO + FeO) ratio of the bulk composition, is outlined in Fig. 4.13 (after Winkler, 1976) for a ratio of 0,6. Chemical data are not available for the Ai-ais area, but two aluminous gneiss samples from the same unit in the Warmbad area (Beukes, 1973; samples GBW 302 & 98) have an average ratio of 0,60. On this assumption the PT field is outlined for the K-felspar + sillimanite zone close to the K-felspar + sillimanite isograd.

### 4.5.3 Metamorphic path

The metamorphic path (facies series) defined by the PT fields of the successive metamorphic zones, is compared with temperature gradients (Fig. 4.12). Geothermal gradients for stable shield areas are about 10°C/km while those

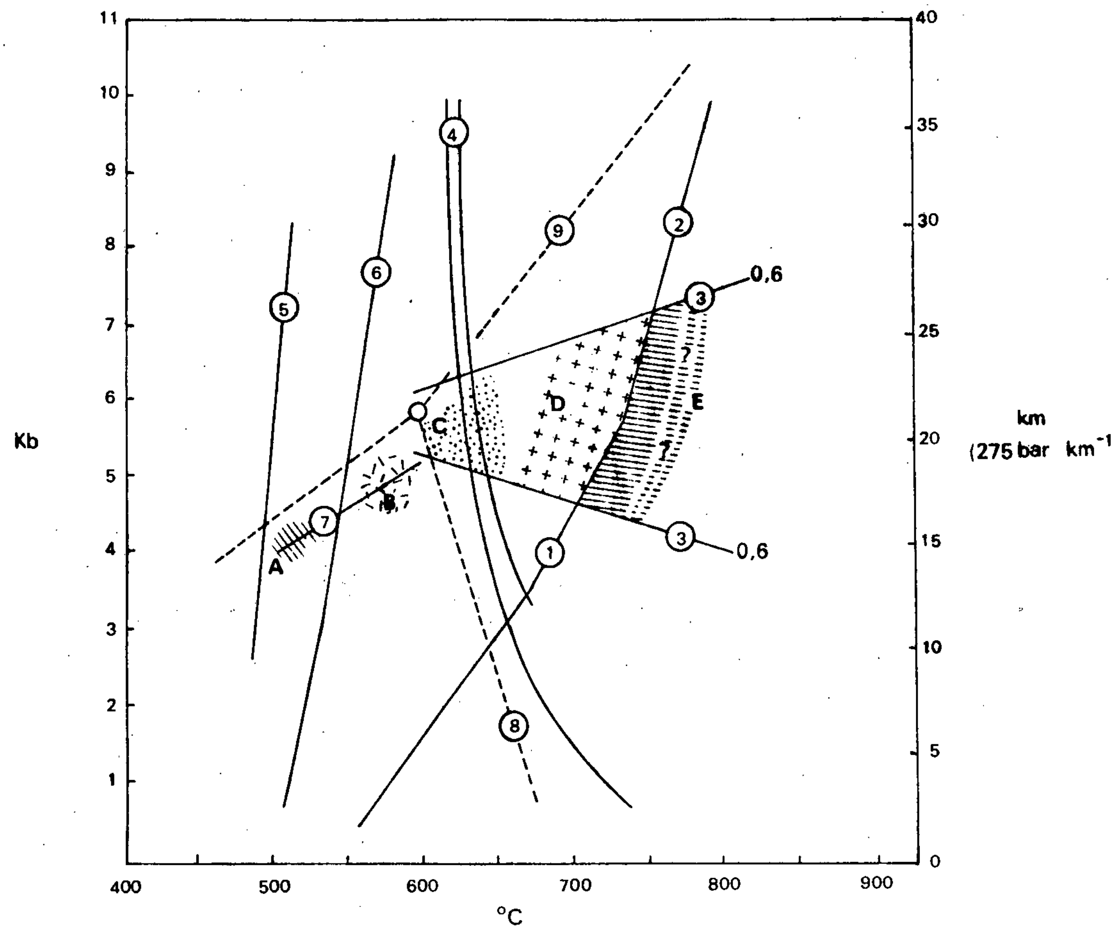


*Fig.4.13 The shaded areas represent the estimated PT conditions for the successive metamorphic zones and define the metamorphic path.*

A *Muscovite + chlorite zone*

B *'Muscovite + chlorite out' zone*

C *Sillimanite zone*

D *'Epidote out' zone*

E *K-felspar + sillimanite zone*

1 *Musc + qtz* $\rightleftharpoons$ *K-f +* $Al_2SiO_5$ + $H_2O$ *(Althaus et al, 1970)*

2 *Musc + qtz* $\rightleftharpoons$ *melt + sill + K-felspar (Storre, 1972)*

3 *Cord* $\rightleftharpoons$ *alm + sill + qtz (Winkler, 1976, after Currie, 1971, for FeO/(FeO + MgO) = 0,6)*

4 *Minimum melt curve (Winkler, 1976)*

5 *'Hbl in' curve as estimated by Winkler, 1976*

6 *'Musc + chlor + qtz out' (Winkler, 1976)*

7 *'Alm in' (extrapolated from Hirschberg and Winkler, 1968)*

8 *Andalusite/sillimanite boundary (Althaus, 1967, 1969 a,b)*

9 *Intermediate kyanite/sillimanite and kyanite/andalusite phase boundaries of those given by Althaus (1967, 1969) and Richardson et al. (1968, 1969) (After Winkler, 1976)*

*(musc = muscovite, qtz = quartz, K-f = K-felspar, sill = sillimanite, cord = cordierite, alm = almandine, hbl = hornblende, chlor = chlorite)*

for a young geosynclinal environment average about 15 to 25°C/km (Hyndman, 1972). These gradients refer to the variation in temperature with vertical depth. The fossil temperature gradient in the Ai-ais area is in the order of 30 to 35°C/km (Fig. 4.12) and does not necessarily refer to a temperature variation in the vertial direction (cf. Chesworth, 1972).

When compared to other fossil geothermal gradients, the geothermal gradient at Ai-ais falls within the low-pressure (andalusite-sillimanite) type of Miyashiro (1973, p. 86). In the classic sense this excludes burial and downthrusting of cold material by plate tectonic processes, as the cause of metamorphism at Ai-ais. According to Miyashiro (1973), low-pressure metamorphic belts are always accompanied by an abundance of granitic rocks, while rhyolitic and/or andesitic volcanic rocks may abound. Miyashiro further states that 'island arcs with andesitic volcanoes could be the surface manifestation of the formation of a low-pressure metamorphic complex in a crust'.

### 4.5.4 Geological body affected by $M_1$

It is important, for the ultimate tectonic model, to consider here which lithological units carry the imprint of $M_1$. It is shown in the foregoing sections that a continuous metamorphic zonation exists in the area under consideration (Fig. 4.11). The continuity suggests a single progressive development. The zonation is based on petrographic data from the Orange River volcanics, Vioolsdrif intrusives, mafic gneiss unit, banded amphibolite unit, grey gneiss and paragneiss units; the petrographic data from all these units are consistent with the regional zonation. Microstructural aspects are described in detail to show the transitional development of the fully reconstituted gneisses of the marginal zone from the semi-reconstituted rocks of the Richtersveld Province with increasing metamorphic grade.

It is concluded that $M_1$ is superimposed on both the igneous rocks of the Richtersveld Province and the pretectonic gneisses of the Namaqua Province, and produced a continuous metamorphic zonation.

### 4.5.5 Relation $M_1$/syntectonic granitoids

The spatial relation (Fig. 4.14) between the K-felspar + sillimanite zone and the early syntectonic granitoids and charnockites (Sections 2.3.3.3, 2.3.3.4 & 2.3.3.5) suggests a causal relationship. It is shown elsewhere that for a particular domain, $M_1$ at least outlasted the emplacement of the megacrystic granite. On the basis of these temporal and spatial associations it is consi-

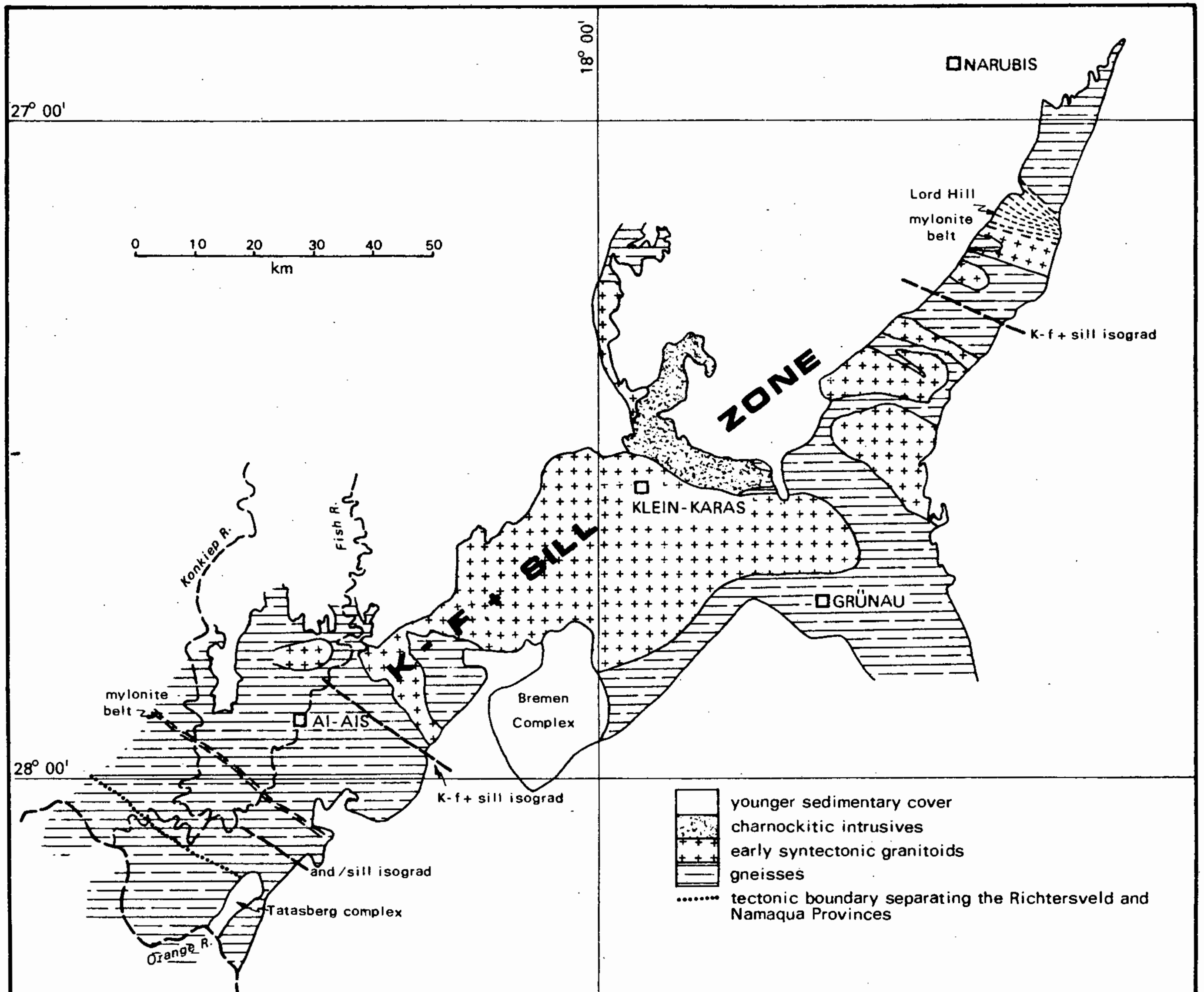


*Fig.4.14.The K-felspar + sillimanite zone which is flanked by lower grade zones, spatially coincides with early syntectonic granitoids and charnockitic intrusives. (and = andalusite, sill = sillimanite, K-f = K-felspar)*

dered that the early intrusives acted as a heat conveyor and is positioned at a locus of high heat flow which caused the main metamorphism shown to have a relative high fossil geothermal gradient (Fig. 4.12).

On the farm Goedemoed, in the vicinity of Klein-Karas, granulite enclaves were found in the megacrystic granite (Section 2.3.3.3). It is argued that the granite is allochthonous and therefore the granulite enclaves might have been transported from lower levels where conditions sufficed for the formation of granulite. Granulite enclaves in the megacrystic granite do not necessarily reflect metamorphic conditions at the present level of erosion.

# 5 INTERPRETATION

## 5.1 Stratigraphy

In the absence of stratigraphic facing directions the overall stratigraphic sequence is best viewed by means of a cross-section (Fig. 5.1).

It is argued in Section 2.3.2.4 that both the Richtersveld Province and marginal zone are underlain by an intrusive-extrusive complex which becomes gneissic towards the north-east. Available evidence is consistent with a similar interpretation, although tenuous, for the grey gneiss of the central zone. According to this interpretation, the Vioolsdrif igneous complex (sheeted Vioolsdrif intrusives in Orange River volcanics) has a distribution far outside the structural Richtersveld Province.

Towards the north-east the paragneiss unit structurally overlies the gneisses of the Vioolsdrif igneous complex (Fig. 5.1) and forms an important stratigraphic sequence underlying a vast area (Fig. 3.42). The interbanded nature of its contact with the underlying grey gneiss might be either tectonic or indicate that the metasediments and Orange River metavolcanics belong to the same volcano-sedimentary succession. The lithological composition of the paragneiss unit, alternating pelites and semi-pelites, suggests a mudstone/wacke sequence.

Granitoids postdating these metavolcanics and metasediments constitute at least 50 per cent of the areas investigated (cf. Fig. 5.1) and it is thought that the Namaqua Metamorphic Complex, here, in essence is an igneous complex.

## 5.2 Basement/cover problem

The only possibility of a pre-2000 Ma basement in the Ai-ais area (Annex. 1 & 2), is the grey gneiss of the central zone with the paragneiss unit hypothetically constituting the cover sequence. The geological data which have to be accounted for in considering the problem are enumerated below.

(i) The apparent lithologic likeness between the reconstituted rocks of

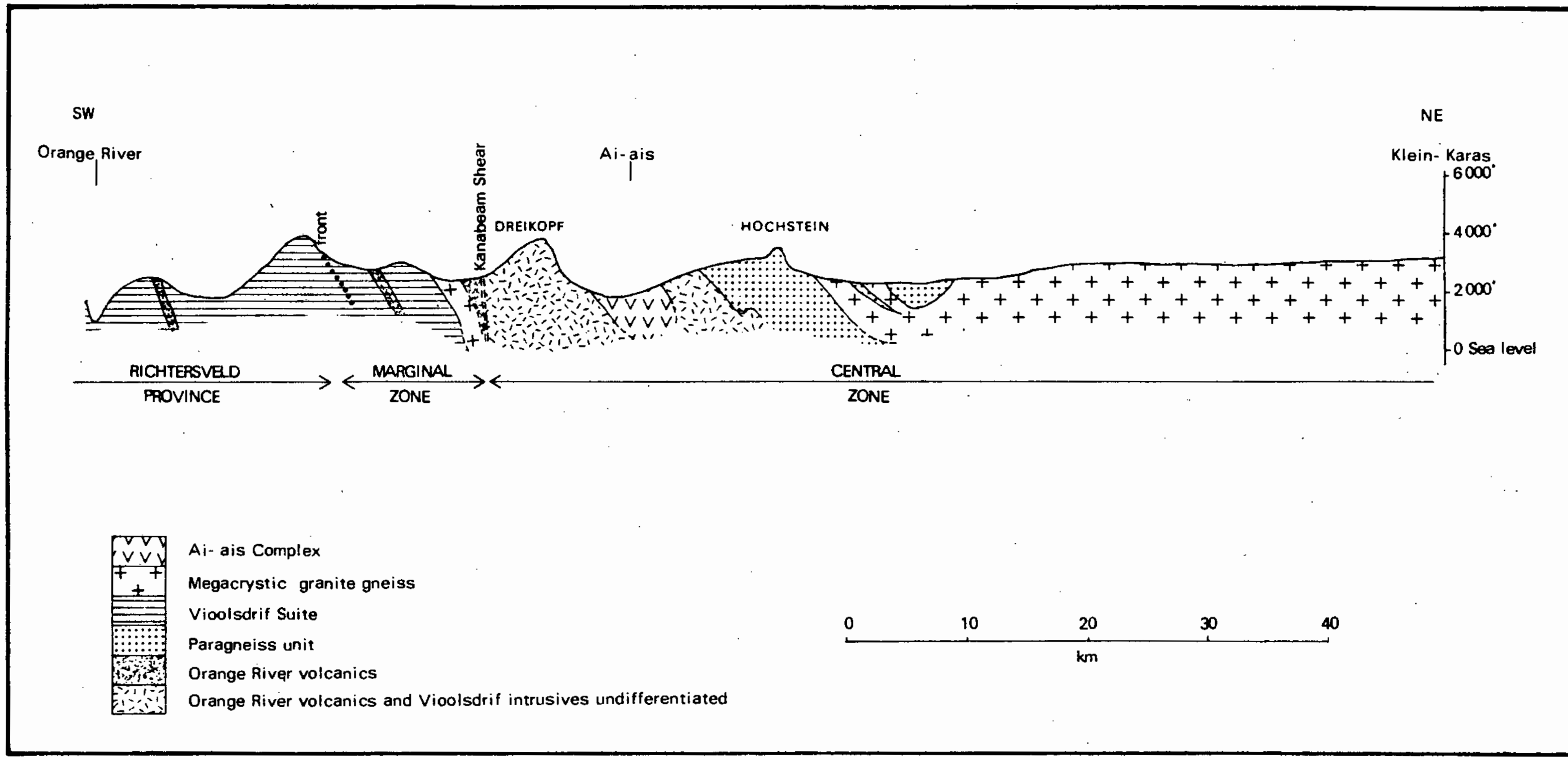


*Fig. 5.1. Interpretative stratigraphy in cross-section.*

the Vioolsdrif igneous complex and the grey gneiss of the central zone.

(ii) Interbanded gradational contacts between the structurally lower part of the paragneiss unit and the grey gneiss were observed at several localities. If the consistency of this relation could be established along strike, a tectonic origin for the interbanding would be considered unlikely.

(iii) It is indicated at one locality along the contact between the grey gneiss and paragneiss unit that the linear elements of $D_1$ and $D_2$ from both units are colinear (Section 3.5.2, Fig. 3.37); the foliation/banding of both units is always concordant. The similarity of planar and linear structures along the contact can be attributed either to relative movement between basement and cover or as structural similarity of the two units if the imprint remains the same in both rock units for considerable distances away from the contact.

(iv) Apart from the apparently more local development of $D_3$, the post-$D_1$ sequence of deformation phases in both rock units is the same everywhere in the central zone. If there was a difference in structural development prior to $D_1$, the evidence is largely obliterated by the penetrative early kinematic event ($D_1$ and $D_2$).

(v) A possible indication of a different pre-$D_2$ imprint is discussed in Section 3.5.1, but the evidence is inconclusive in view of a likely alternative explanation.

Because the sequence of deformation phases in the grey gneiss is similar throughout the central zone, irrespective of 'distance' from the paragneiss unit, it is thought unlikely that the grey gneiss constituted a crystalline basement to the paragneiss unit in pre-$D_1$ times.

## 5.3 Sequence of events

The interrelationship between time, intrusion, metamorphism and deformation is discussed below (cf. Table 5.1).

### 5.3.1 Richtersveld Province

The sequence of events as motivated in the text above is summarised in Table 5.1. It is well established that $D_1$ and $M_1$ were active after crystallisation of the Vioolsdrif intrusives. The possibility that the Vioolsdrif Suite was emplaced during the earlier stages of a progressive $D_1$ deformation cannot be excluded. $D_1$ is the only widely developed deformation in the Richtersveld Province associated with the Namaqua tectogenesis. The subsequent deformation of the Namaqua Province is not imprinted on the Richtersveld domain in any apparent and pervasive manner.

The emplacement of the front zone pegmatites along an *en enchelon* fracture array ($D_2$) contrasts, time and kinematic-wise largely with $D_1$ and a more brittle environment is indicated.

The character of the $D_1$ imprint, relatively low-grade of metamorphism and lack of post-Vioolsdrif intrusives associated with the Namaqua tectogenesis further characterise the Richtersveld Province as an upper-crustal domain.

### 5.3.2 Marginal zone

The relation $D_3/D_6$ is not rigorously established while the $D_4$ cross-structures are unimportant with respect to frequency of occurrence and scale of development. The consistently parallel and penetrative planar fabric ($s_1$) of the marginal zone is the main characteristic. The subsequent pervasive imprint of $F_2$-type folds and $D_3$ distinguishes this domain from the Richtersveld Province.

Intrusive relations between the Vioolsdrif granitoids and augen granodiorite were not seen, but the distinctly stronger planar fabric imprint on the Vioolsdrif intrusives substantiates the interpretation based on small structures (Section 3.4.6.2) that the augen gneiss is younger. The emplacement of the granodioritic augen gneiss is penecontemporaneous with the metamorphic peak ($M_1$).

### 5.3.3 Central zone

The central zone is structurally the most complex domain, includes the high-grade core of the mobile belt and is dominated by an early syntectonic suite of intrusives (the megacrystic granite, granodiorite and charnockite). It is shown that the intrusion of the early suite is penecontemporaneous with $D_2$ and $M_1$ and that the intrusives are spatially associated with the highest grade zone (Fig. 4.14). Sharp interbanded contacts between the megacrystic granite and nebulous migmatites and lack of segregation-type leucosomes in the megacrystic granite indicate that the intrusion of the early suite postdates the peak of anatectic development.

| Age | RICHTERSVELD PROVINCE | NAMAQUA PROVINCE: MARGINAL ZONE | NAMAQUA PROVINCE: CENTRAL ZONE | | EVENT | TECTOGENESIS |
|---|---|---|---|---|---|---|
| 2000 Ma | O.R. volcanics | ? | O.R. volcanics and paragneiss unit | 2000 Ma | | |
| | Vioolsdrif Suite; pre- $D_1$ | | | | | |
| 1800 Ma | $D_1$ $M_1$ | $D_1$ $M_1$; ? Augen gneiss; $D_2$ | $D_1$ $M_1$ Culmination of anatexis; $D_2$ Early intrusive suite | | Early (first) kinematic event | |
| | | $D_3$ | $D_3$; ? Ai-ais Complex | | | Namaqua |
| | | $(D_4)$ ? | $D_4/D_5$; Pegmatites | | Late (second) kinematic event | |
| 960 Ma | Front zone pegmatites; $D_2$ ? | $D_6$ | $D_6$ (Kanabeam shearing) | 1000 Ma? | | |
| | | | Older phase Bremen Complex | 920 Ma | | |
| 880 Ma | Gannakouriep dyke suite | | Gannakouriep dyke suite | 880 Ma | | Late Precambrian |
| | $D_3$ ? | $(D_4)$ | | | | |

*Table 5.1. Integrated calender of events. The time relation between the Kanabeam shearing and the emplacement of the older phases of the Bremen Complex is conjectural.*

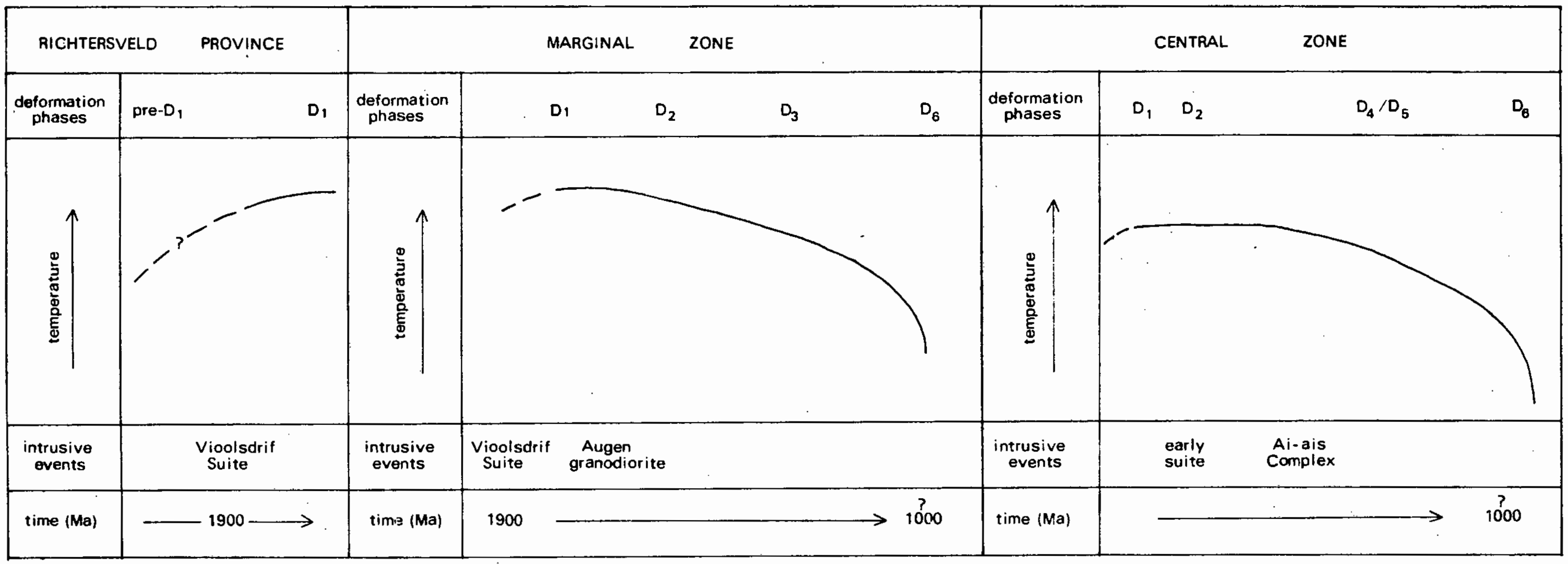


*Fig. 5.2. Time- temperature curve for each structural domain.*

A continuous retrogressive time-temperature curve (Fig. 5.2) is inferred with $M_1$ representing the peak of the metamorphic development. $D_6$ is interpreted to postdate $D_4/D_5$ because (i) retrogression advanced much further in the mylonite belt ($D_6$) than along zones of refoliation associated with $D_4$ and $D_5$ and (ii) the deflection of $F_4$ and $F_5$ towards the Kanabeam shear zone ($D_6$) is in part ascribed to the progressive rotational strain of the shear zone. The set of macroscopic cross-folds ($F_4$ and $F_5$) with basin and dome interference structures is diagnostic of the central zone.

5.3.4 Interrelations between domains (Table 5.1)

*Structure*

Structures correlated according to the principles outlined in Section 3.2, are likely to be diachronous (Price, 1972; Hobbs et al., 1976) in a geological body of sufficiently large dimensions. Neither do such correlated structures imply the same physical environment as movements are likely to transgress different metamorphic regimes or crustal levels. Structures correlated here, within and between domains, are considered to reflect a similar kinematic environment only.

On this basis and by comparing the sequence of deformation phases, the only plausible correlation between domains is that between the colinear and coplanar $D_1/D_2$ structural elements which constitute the early kinematic event. The main planar fabric, $s_1$, in each domain is associated with $M_1$ which defines a progressive metamorphic zonation from the south-west to the north-east spatially including all three structural domains. The prograde microstructural/ metamorphic development across the front is well established. It is concluded therefore, that as $s_1$ is associated with a single progressive metamorphic event, the correlation of the early kinematic event between the Richtersveld, marginal and central domains is further substantiated. The possibility of earlier (pre-$D_1$) structures 'hidden' by extreme flattening during the early kinematic event, must be borne in mind as erroneous stratigraphic correlations might result (cf. Robinson & Fyson, 1976). Apart from in the domain of $s_2$ refoliation (Fig. 3.38), the regional foliation, throughout, is $s_1$. The $D_2$ refoliation was affected in the more ductile paragneisses around the larger bodies of the early intrusives. $D_2$ is interpreted to have acted after the metamorphic peak ($M_1$) in the marginal zone while in the domain of $s_2$ refoliation lower pressure conditions are inferred but no apparent temperature drop is evident. Both the refoliation and sustained temperature can be ascribed to the contemporaneous emplacement of vast volumes of the early intrusive suite in close proximity.

The diachronous development of structures is a distinct theoretical possibility, both in the lateral (Hobbs et al., 1976) and vertical sense. Different parts of the crust react differently to imposed stresses, depending on the capacity of the different domains to transmit stress. The advance of a high-temperature front from point to point in the crust, permits structural types which are rheologically controlled, to develope in its wake. At the time of development of $F_1$ structures in an upper-crustal domain, $F_2$ structures might form in a more plastic lower-crustal domain. At a later stage after the upwards advance of the physical conditions, $F_2$ structures might develop in the upper-crustal domain which now react plastically. In view of this theoretical possibility it is tenuous to equate $F_n$ (Richtersveld Province) with $F_n$ (central zone) on a rigid time basis. If the structures are diachronous they would young towards the lower grade Richtersveld Province. One implication of this model of diachronism is that the early intrusives of the central zone (syn-$D_2$) might be time equivalents of the Vioolsdrif granitoids of the upper-crustal Richtersveld Province (pre- to early-$D_1$).

Structures of the late kinematic event are not developed on any significant scale within the Richtersveld and marginal domains.

*Metamorphism*

A continuous prograde metamorphic ($M_1$) development associated with the early kinematic event, is established across the area investigated. A reconnaissance survey indicates that the high-grade core is flanked towards the north-east (Narubis) by another lower grade zone (Fig. 4.14).

The time-temperature curves (Fig. 5.2) is based on a simplistic approach i.e. due to the lack of evidence indicating intermittent high-grade peaks, a continuous retrogressive curve, consistent with post-$D_1$ microstructural evidence, is suggested; $M_1$ represents the metamorphic peak.

Temperature and pressure cross-sections further illustrate the metamorphic character of each domain (Fig. 5.3). The temperature gradient (temperature increase/distance unit across zonation) differing from one domain to another, is markedly steep in the marginal zone and flattens off again in the central zone. The pressure gradient (increase in pressure/distance unit across zonation) is also steepest in the marginal zone. The central zone is therefore considered a lower-crustal domain with respect to the more upper-crustal Richtersveld Province. These two domains are separated by the relatively narrow marginal domain across which sharp temperature and pressure increases are apparent.

*Magmatism*

The area is underlain by three major intrusive suites, none of which was local-

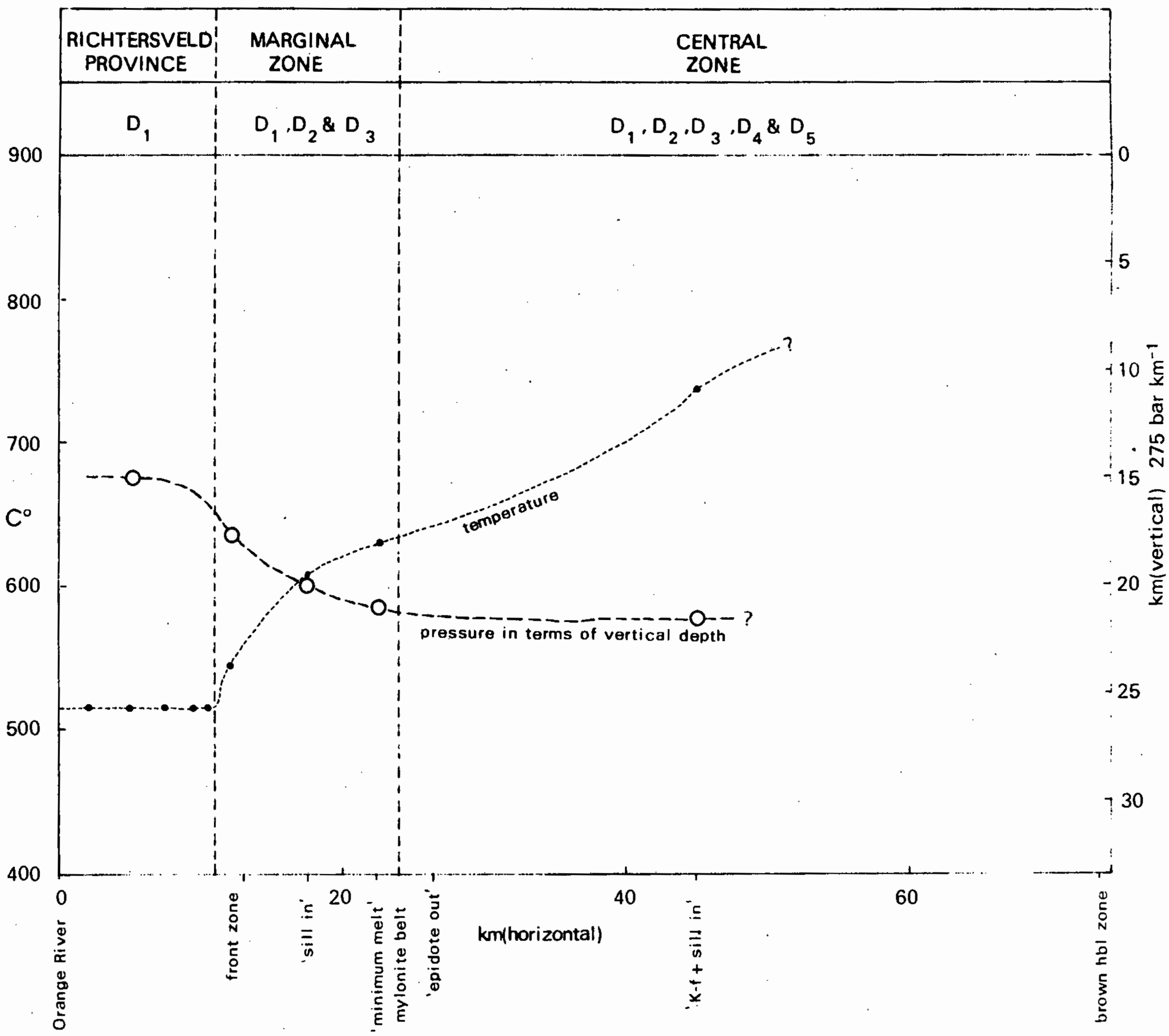


*Fig. 5.3. Structural and metamorphic ($M_1$) significance of the various domains. The abscissa represents a SW - NE cross-section. The points (•,O) represent middle values for T and P (Fig. 4.13). The uncertainty with respect to T (Fig. 4.13) does not affect the temperature curve significantly, but the possible P range for a spesific T might affect the P curve, especially the part in the central zone.*

ly derived by partial melting. (i) The Vioolsdrif Suite. (ii) The early intrusive suite of the central zone comprising the charnockite, granodiorite and megacrystic granite and by appearance and with respect to structural dating also the granodioritic augen gneiss of the marginal zone. (iii) The

Ais-ais Complex. On the basis of structural dating the Vioolsdrif Suite predates the early intrusive suite which is postdated by the Ai-ais Complex. In terms of the diachronous deformation model it is possible for the Vioolsdrif Suite and early intrusive suite to be time-equivalents. The augen gneiss, though, structurally postdates the Vioolsdrif granitoids of the marginal zone; on the strength of the correlation between the augen gneiss and the early intrusive suite then the Vioolsdrif intrusives constitute a discretely older magmatic event. The occurrence of granophyric textures in the Vioolsdrif granitoids, although sparse, indicates a more upper-level emplacement than the early intrusive suite which commonly contains cordierite and garnet.

The high-grade core of the central zone is spatially associated with large volumes of the early intrusive suite; the emplacement is penecontemporaneous but postdates the large-scale development of partial melts which mark the metamorphic peak.

The various phases of each of the three major intrusive suites vary in composition from basic to acid and young in the same sequence. The process yielding differentiated intrusives therefore repeated itself prior to the onset of the late kinematic event. The Vioolsdrif and early suite granitoids constitute at least 50 per cent of the areas investigated - a fact which underlines the significance of these magmatic events; their close association with the early kinematic event and metamorphic development suggests a causal relation.

## 5.4 Kinematic interpretation

### *Early kinematic event*

The structures of the early event ($D_1$ & $D_2$) are grouped together on the basis of their colinear and coplanar relation, a geometry which suggests a single progressive deformation. That these structures show a progressive development from the lower grade Richtersveld domain towards the higher grade central zone, is well established.

| | | | | |
|---|---|---|---|---|
| $F_1/s_1$ (non-penetrative) | → | $F_1/s_1$ | → | $F_1/s_1$ |
| (Richtersveld Province) | | $F_2$ | | $F_2/s_2$ |
| | | (Marginal zone) | | (Central zone) |

Prior to the onset of the late kinematic event, a consistently north-easterly dipping planar fabric with down-dip stretching lineations, as preserved in the marginal zone, is envisaged for the whole area. Both the $F_1$ and $F_2$ fold axes have a preferred orientation parallel to the stretching lineations which lie in the main planar fabric. The bulk finite strain ellipsoid is disposed with the XY-plane in the main planar fabric and is distinctly elongate with X in a down-dip direction. As judged qualitatively the largest amount of shortening across the Z direction was affected in the front zone where cataclastic textures are also more pronounced. That the increased flattening in the front zone is associated with increased displacement, is substantiated by the sharp increase of temperature and pressure along the front and marginal zones (Fig. 5.3). The bulk finite strain ellipsoid in the Richtersveld domain is more oblate-shaped.

There are structural aspects of the first event which cannot be explained by progressive pure shear and progressive simple shear is invoked for the deformation mechanism of the early kinematic event with the main planar fabric as the shear surface. If this is the case the parallelism between the finite elongation direction, X, and the main planar fabric is apparent only and implies large shear strain and considerable displacement. The following structural features suggest progressive simple shear.

(i) In the Richtersveld Province the main planar fabric is heterogeneously developed in bodies which were isotropic prior to the onset of $D_1$ and which are lithologically homogeneous.

(ii) The zones of dip reversal in the Richtersveld Province are explained as domains of lower shear strain where the foliation is at an angle to the shear direction; this foliation was intensified by subsequent parallel shearing.

(iii) The formation of $F_2$-type folds with their axial planes parallel to $s_1$, cannot be explained by progressive irrotational strain as the direction of shortening, across the axial plane, is normal to $s_1$, the folded surface. It is proposed that the $F_2$ folds formed in a simple shear system where material inhomogeneities, acting as obstructions to flow, caused folding with fold axes initially at right angles to the direction of shearing. One implication of such a model of progressive simple shear is that $F_2$-type folds are continuously formed and subsequently deformed into $F_1$-type folds; the $F_2$ folds encountered today therefore represent folds formed during the final stages of the progressive deformation. Their axes should be spread in the main planar fabric with a preferred orientation close to the stretching direction (cf. Figs. 3.22b & 3.27). This proposed mechanism of folding is real as numerous $F_2$-type folds are developed in the mylonite belt (Section 3.6) which constitute a shear system; the progressive formation of these folds is demonstrated by microstructural evidence. The models proposed by Wynne-Edwards (1963) and Hudleston (1977) for the formation of flow folds and subsimilar folds, respectively, are essentially the same.

The tectonic implication is that the early kinematic event represents a period of large scale *thrusting* with a vergence towards the south-west. The thrusting is associated with the main metamorphic and magmatic events and together constitute the essential part of the Namaqua tectogenesis which commenced at least at about 1900 Ma.

*Late kinematic event*

Two phases of macroscopic folding ($F_4$ & $F_5$) are developed at right angles to each other, the one subparallel and the other across the general trend of the mobile belt. Their axial surfaces are subvertical and therefore a component of shortening was active both across and along the central zone. As these structures are not developed on any significant scale in the marginal and Richtersveld domains, it is clear that to accommodate the shortening a structural discontinuity should be developed between the central zone and other domains. For this reason the Kanabeam shear zone is considered to have been caused by the late folding ($F_4$ & $F_5$) in the central zone. The time of development of the shear zone with respect to $D_4$ and $D_5$ can be considered initially late but should be ultimately synchronous. The sense of displacement across the shear zone is sympathetic with the horizontal movement related to the development of the front zone pegmatites. As the late kinematic event is thought to have developed from the central zone towards the upper-crustal Richtersveld domain, the 960 Ma radiometric age of the front zone pegmatites probably dates the waning stages of the late kinematic event and the Namaqua tectogenesis.

# 6 REFERENCES


Althaus, E. (1967). The triple point andalusite - sillimanite - kyanite. *Contr. Miner. Petrol.*, 16, 29-44.

_______ (1969a). Das System $Al_2O_3$ - $SiO_2$ - $H_2O$. Experimentelle Untersuchungen und Folgerungen für die Petrogenese der metamorphen Gesteine. *Neues Jb. Miner. Abh.*, 111, 111-161.

_______ (1969b). Experimental evidence that the reaction of kyanite to form sillimanite is at least bivariant. *Am. J. Sci.*, 267, 273-277.

_______, Nitsch, K.H., Karotke, E., and Winkler, H.G.F. (1970). An experimental re-examination of the upper stability limit of muscovite plus quartz. *Neues Jb. Mineral. Monatsh.*, 1970, 325-336.

Barker, D.S. (1970). Composition of granophyre, myrmekite, and graphic granite. *Bull. geol. Soc. Am.*, 81, 3339-3350.

Berger, A.R. and Pitcher, W.S. (1970). Structures in granitic rocks : a commentary and critique on granite tectonics. *Proc. Geol. Assoc.*, 81, 441-461.

Beukes, G.J. (1973). *'n Geologiese ondersoek van die gebied suid van Warmbad, Suidwes-Afrika, met spesiale verwysing na die metamorf-magmatiese assosiasies van die Voorkambriese gesteentes.* D.Sc. thesis, University of the Orange Free State (Unpublished), 333p.

Binns, R.A. (1969). Ferromagnesian minerals in high-grade metamorphic rocks. *Spec. Publs. geol. Soc. Aust.*, 2, 323-332.

Blignault, H.J. (1974a). The tectonic zonation of part of the Namaqua Province in the lower Fish River/Narubis cross-section. *Ann. Rept., Precambrian Res. Unit, Univ. Cape Town*, 10-11, 43-45.

_______ (1974b). Aspects of the Richtersveld Province. *In* Kröner, A. (Ed.), Contributions to the Precambrian geology of Southern Africa. *Bull. Precambrian Res. Unit, Univ. Cape Town*, 15, 49-56.

_______ (1975). Towards a stratigraphic nomenclature for the Namaqua Metamorphic Complex and associated rocks. *Ann. Rept., Precambrian Res. Unit, Univ. Cape Town*, 12, 41-42.

_______, Jackson, M.P.A., Beukes, G.J. and Toogood, D.J. (1974). The Namaqua tectonic province in South West Africa. *In* Kröner, A. (Ed.), Contributions to the Precambrian geology of Southern Africa. *Bull. Precambrian Res. Unit, Univ. Cape Town*, 15, 29-47.

Brown, G.C. and Fyfe W.S. (1972). The transition from metamorphism to melting : status of the granulite and eclogite facies. *24th IGC, section 2,* 27-34.

Buddington, A.F. (1959). Granite emplacement with special reference to north America. *Bull. geol. Soc. Am.,* 70, 671-747.

Burger, A.J. and Coertze F.J. (1973). Radiometric age measurements on rocks from Southern Africa to the end of 1971. *Bull. geol. Surv. Div. S. Afr.,* 58, 46p.

Burke, K. and Dewey, J.F. (1973). An outline of Precambrian plate development. *In* Tarling, D.H. and Runcorn, S.K. (Ed.), *Implications of continental drift to the earth sciences, V.2.* Academic Press, London, 1184p.

Carmichael, D.M. (1969). On the mechanism of prograde metamorphic reactions in quartz-bearing pelitic rocks. *Contr. Miner. Petrol.,* 20, 244-67.

Chesworth, W. (1972). Metamorphic facies series in the Grenville province of Ontario. *Tectonophysics,* 14, 71-78.

Coetzee, C.B. (1942). Petrology of the Goodhouse - Pella area, Namaqualand. *Trans. geol. Soc. S. Afr.,* 44, 167.

Corner, B. (1969). Honours project, University of the Witwatersrand (Unpublished).

Currie, K.L. (1971). The reaction 3 cordierite = 2 garnet + 4 sillimanite + 5 quartz as a geological thermometer in the Opinion Lake region, Ontario. *Contr. Miner. Petrol.,* 33, 215-226.

Dearnly, R. and Dunning, F.W. (1968). Metamorphosed and deformed pegmatites and basic dykes in the Lewisian complex of the Outer Hebrides and their geological significance. *Q. Jl. geol. Soc. Lond.,* 123, 335-378.

Deer, W.A., Howie, R.A. and Zussman, J. (1966). *An introduction to the rock-forming minerals.* Longmans, Green and Co. Ltd, London, 528p.

De Villiers, J. (1968). *Ann. Rept., Precambrian Res. Unit, Univ. Cape Town,* 6, 36.

_______, and Burger, A.J. (1967). Note on the minimum age of certain granites from the Richtersveld area. *Ann. geol. Surv. Dep. Min. S. Afr.,* 6, 83-84.

_______, and Söhnge, P.G. (1959). The Geology of the Richtersveld. *Mem. geol. Surv. Un. S. Afr.,* 48, 295p.

Dickinson, W.R. (1972). Evidence for platetectonic regimes in the rock record. *Am. J. Sc.*, 272, 551-576.

Didier, J. (1973). *Granites and their enclaves.* Elsevier scientific, Amsterdam, 393p.

Engel, A.E.J., Itson, S.P., Engel, C.G., Stickney, D.M. and Cray, E.J. (1974). Crustal evolution and global tectonics : a petrogenetic view. *Bull. geol. Soc. Am.*, 85, 843-858.

Evans, B.W. and Guidotti, C.V. (1966). The sillimanite-potash feldspar isograd in western Maine, U.S.A. *Contr. Miner. Petrol.*, 12, 25-62.

Fyfe, W.S. (1970). Some thoughts on granitic magmas. *In* Newall, G. and Rast, N. (Ed.), *Mechanism of igneous intrusion.* Gallery Press, Liverpool, 380p.

______ (1973). The generation of batholiths. *Tectonophysics*, 17, 273-283.

Gevers, T.W., Partridge, F.C. and Joubert, G.K. (1937). The pegmatite area south of the Orange River in Namaqualand. *Mem. geol. Surv. Un. S. Afr.*, 31, 180p.

Hensen, B.J. and Green, D.H. (1973). Experimental study of the stability of cordierite and garnet in pelitic compositions at high pressures and temperatures. III. Synthesis of experimental data and geological applications. *Contr. Miner. Petrol.*, 38, 151-166.

Higgins, M.W. (1971). Cataclastic rocks. *Prof. Pap. U.S. geol. Surv.*, 687, 97p.

Hirschberg, A. and Winkler, H.G.F. (1968). Stabilitätsbeziehungen zwischen Chlorit, Cordierit und Almandin bei der Metamorphose. *Contr. Miner. Petrol.*, 18, 17-42.

Hobbs, B.E., Means, W.D. and Williams, P.F. (1976). *An outline of structural geology.* John Wiley & Sons, Inc., New York, 571p.

Hudleston, P.J. (1977). Similar folds, recumbent folds, and gravity tectonics in ice and rocks. *J. Geol.*, 85, 113-122.

Hyndman, D.W. (1972). *Petrology of igneous and metamorphic rocks.* McGraw-Hill Book Company, New York, 533p.

IUGS Subcommission (1973). Classification and nomenclature of plutonic rocks. Recommendations. *Neues Jb. Miner. Mh.*, 1973, 149-164.

Jacob, R.E. (1974). Geology and metamorphic petrology of part of the Damara orogen along the lower Swakop River, South West Africa. *Bull. Precambrian Res. Unit, Univ. Cape Town*, 17, 185p.

Joubert, P. (1971). The regional tectonism of the gneisses of part of Namaqualand. *Bull. Precambrian Res. Unit, Univ. Cape Town*, 10, 220p.

______, and Kröner, A. (1972). The Stinkfontein Formation south of the Richtersveld. *Trans. geol. Soc. S. Afr.*, 75, 47-54.

Köstlin, E.C. and Köstlin, E.O. (1964). Honnours project, Univ. Cape Town (Unpublished).

Kröner, A. (1974). Late Precambrian formations in the western Richtersveld, northern Cape Province. *Bull. Precambrian Res. Unit, Univ. Cape Town*, 13, 115.

______, and Blignault, H.J. (1976). Towards a definition of some tectonic and igneous provinces in western South Africa and southern South West Africa. *Trans. geol. Soc. S. Afr.*, 79, 232-238.

Lamont, G.T. (1947). *The geology of part of the Vanrhynsdorp division, Cape Province.* Ph.D. thesis, Univ. Cape Town (Unpublished).

McMillan, M.D. (1968). The geology of the Witputs-Sendelingsdrif area. *Bull. Precambrian Res. Unit, Univ. Cape Town*, 4, 177.

Mehnert, K.R. (1968). *Migmatites and the origin of granitic rocks.* Elsevier Publishing Company, Amsterdam, 393p.

______, Büsch, W. and Schneider, G. (1973). Initial melting at grain boundaries of quartz and felspar in gneisses and granulites. *Neues Jb. Miner. Mh.*, 1973, 165-183.

Middlemost, E.A.K. (1963). *Geology of the south-eastern Richtersveld.* Ph.D. thesis, Univ. Cape Town (Unpublished).

______ (1964). Petrology of the plutonic and dyke-rocks of the south-eastern Richtersveld. *Trans. geol. Soc. S. Afr.*, 67, 227-261.

______ (1965). Ultramafic rocks of the south-eastern Richtersveld. *Trans. geol. Soc. S. Afr.*, 68, 53-60.

Miyashiro, A. (1968). Metamorphism of mafic rocks. *In* Hess, H.H. and Poldervaart, A. (Ed.). *Treatise on rocks of basaltic composition*, 2, 799-834, Interscience, New York.

______ (1973). *Metamorphism and metamorphic belts.* George Allen & Unwin Ltd., London, 492p.

______ (1974). Volcanic rock series in island arcs and active continental margins. *Am. J. Sc.*, 274, 321 - 355.

Park, R.G. (1969). Structural correlation in metamorphic belts. *Tectonophysics*, 7, 323-338.

Parsons, W.H. (1969). Criteria for the recognition of volcanic breccias : review. *Mem. geol. Soc. Am.*, 115.

Pettijohn, F.J., Potter, P.E. and Siever, R. (1972). *Sand and sandstone.* Springer, Berlin, 618p.

Pitcher, W.S. (1972). The coastal batholith of Peru : some structural aspects. *24th IGC, section 2,* 156-163.

Price, R.A. (1972). The distinction between displacement and distortion in flow, and the origin of diachronism in tectonic overprinting in orogenic belts. *24th IGC, section 3,* 545-551.

Ramsay, J.G. (1967). *Folding and fracturing of rocks.* McGraw-Hill Book Company, New York, 568p.

________, and Graham, R.H. (1970). Strain variation in shear belts. *Can. J. Earth Sc.*, 7, 786-813.

Reid, D.L. (1974). Preliminary report on petrologic studies of volcanic and intrusive rocks in the Vioolsdrif region, lower Orange River. *In* Kröner, A. (Ed), Contributions to the Precambrian geology of southern Africa. *Bull. Precambrian Res. Unit, Univ. Cape Town,* 15, 57-68.

________ (1975). Geochronology of the Haib-Vioolsdrif igneous province. *Ann. Rept., Precambrian Res. Unit, Univ. Cape Town,* 13, 49-60.

Reinhardt, E.W. (1968). Phase relations in cordierite-bearing gneisses from the Gananoque area, Ontario. *Can. J. Earth Sci.*, 5, 455-482.

Richardson, S.W., Bell, P.M. and Gilbert, M.C. (1968). Kyanite-sillimanite equilibrium between 700$^{o}$ and 1500$^{o}$C. *Am. J. Sc.*, 266, 513-541.

________, Gilbert, M.C. and Bell, P.M. (1969). Experimental determination of kyanite - andalusite and andalusite - sillimanite equilibria; the aluminium silicate triple point. *Am. J. Sc.*, 267, 259-272.

Robinson, S.D. and Fyson, W.K. (1976). Fold structures, southern Stoke Mountain area, eastern townships, Québec : Taconic or Acadian? *Can. J. Earth Sci.*, 13, 66-74.

Schmid, R. and Wood, B.J. (1976). Phase relationships in granulitic metapelites from the Ivrea - Verbano zone (northern Italy). *Contr. Miner. Petrol.*, 54, 255-279.

Sillitoe, R.H. (1973). The tops and bottoms of porphyry copper deposits. *Econ. Geol.*, 68, 799-815.

Smith, J.V. (1974). *Feldspar minerals. Volume 2.* Springer-Verlag, Berlin, 690p.

Spry, A. (1969). *Metamorphic textures.* Pergamon Press, London, 350p.

Stauffer, M.R. (1970). Deformation textures in tectonites. *Can. J. Earth Sci.*, 7, 498-511.

Storre, B. (1972). Dry melting of muscovite + quartz in the range $P_s = 7$ kb to $P_s = 20$ kb. *Contr. Miner. Petrol.*, 37, 87-89.

________, and Karotke, E. (1971). An experimental determination of the upper stability limit of muscovite + quartz in the range 7 - 20 kb water pressure. *Neues Jb. Miner. Mh.*, 1971, 237-240.

Taylor, S.R. (1969). Trace element chemistry of andesites and associated calc-alkaline rocks. *In* McBirney, A.R. (Ed), *Proceedings of the andesite conference. Dept. Geology and Mineral Industries, State of Oregon, Bull.* 65, 43-64.

Tobi, A.C. (1971). The nomenclature of the charnockitic rock suite. *Neues Jb. Miner. Mh.*, 1971, 193-205.

Tullis, J.A., Christie, J.M. and Griggs, D.T. (1973). Microstructures and preferred orientations of experimentally deformed quartzites. *Bull. geol. Soc. Am.*, 84, 297-314.

Vernon, R.H. (1976). *Metamorphic processes.* George Allen & Unwin Ltd, London, 247p.

Von Backström, J.W. (1964). The geology of an area around Keimoes, Cape Province, with special reference to phacoliths of charnockitic adamellite-porphyry. *Mem. geol. Surv. S. Afr.*, 53.

_______, and de Villiers, J. (1972). The geology along the Orange River valley between Onseepkans and the Richtersveld. *Explan. Sheet geol. Surv. Dep. Min. S. Afr.*, 101p.

Ward, J.H.W. (1972). The Vioolsdrif pegmatite belt. *Ann. Rept., Precambrian Res. Unit, Univ. Cape Town,* 7-9, 12-19.

________ (1973). The Vioolsdrif Episode. *Geol. Soc. S. Afr., 15th Congress* (abstract).

________ (1974). The Vioolsdrif pegmatite belt. *Ann. Rept., Precambrian Res. Unit, Univ. Cape Town,* 10-11, 38-42.

Waters, A.C. and Krauskopf, K. (1941). Protoclastic border of the Colville batholith. *Bull. geol. Soc. Am.*, 52, 1355-1418.

Welke, H.J., Burger, A.J., Corner, B., Kröner, A. and Blignault, H.J. (in press). U-Pb and Rb-Sr age determinations on middle Proterozoic rocks from the lower Orange River area, south-western Africa. *Trans. geol. Soc. S. Afr.*

White, S. (1973). Syntectonic recrystallization and texture development in quartz. *Nature*, 244, 276-278.

Williams, P.F. (1970). A critisism of the use of style in the study of deformed rocks. *Bull. geol. Soc. Am.*, 81, 3283-3296.

Winkler, H.G.F. (1974). *Petrogenesis of metamorphic rocks.* Third edition. Springer-Verlag, New York, 320p.

_______ (1976). *Petrogenesis of metamorphic rocks.* Fourth edition. Springer-Verlag, New York, 334p.

Wynne-Edwards, H.R. (1963). Flow folding. *Am. J. Sci.*, 261, 793-814.

_______ (1969). Tectonic overprinting in the Grenville Province, southwestern Quebec. *In* Wynne-Edwards, H.R. (Ed), Age relations in high-grade metamorphic terrains. *Geol. Ass. Can., Spec. Pap.*, 5, 163-182.

_______ (1971). Plutonites, gneisses and granulites of the granulite facies. *Freiberger Forschungshefte, Leipzig*, 268, 11-24.

_______ (1972). The Grenville Province. *In* Price, R.A. and Douglas R.J.W. (Ed.), Variations in tectonic styles in Canada. *Geol. Ass. Can. Spec. Pap.*, 11, 263-334.

_______, and Hasan Zia-ul (1972). Grey gneiss complexes and the evolution of the continental crust. *24th IGC, section 1* (abstract).

Plate 1. $F_1$ fold closure developed in a contact surface between two phases of the Vioolsdrif Suite.

Plate 2. Assimilation and flow in the Vioolsdrif granitoids.

Plate 3. Trains of felspar porphyroclasts in blastomylonite of the front zone, Witputs.

Plate 4. $F_1$ isoclines of the marginal zone developed in a primary banding of the banded amphibolite unit.

Plate 5. $F_1$ isoclines of the marginal zone developed in a metaquartzite(chert)/amphibolite sequence of the banded amphibolite unit.

Plate 6. $F_4$ in the grey gneiss unit of the central zone.

Plate 7. A macroscopic $F_5$ synform; grey gneiss underlies the ridge-forming pink gneiss and amphibolite which form the 'base' of the paragneiss unit.

Plate 8. Rhythmic banding in aluminous gneiss (paragneiss unit, Gaibes).

Plate 9. Crenulation foliation ($s_5$) in the megacrystic granite gneiss (Kochas).

Plate 10. Coaxial refolding of $F_1$ by $F_2$ in grey gneiss of the marginal zone.

Plate 11. Coaxial refolding of $F_1$ by $F_3$.

Plate 12. Mushroom interference between $F_2$ and $F_5$ at the 'base' of the paragneiss unit.

Plate 13. A refoliation ($s_2$) cross-cutting the main planar fabric ($s_1$) in paragneiss; domain of $s_2$ refoliation.

Plate 14. Domain of $s_2$ refoliation; the older planar fabric ($s_1$) is recognisable only in the competent band.

Plate 15. Convergent axial-plane foliation pattern in a $F_4$ hinge zone; paragneiss unit, Gaibes.

Plate 16. Asymmetric $F_5$ in interbanded megacrystic granite and paragneiss (Altdorn); a foliation ($s_5$) is commonly developed along the short limb.

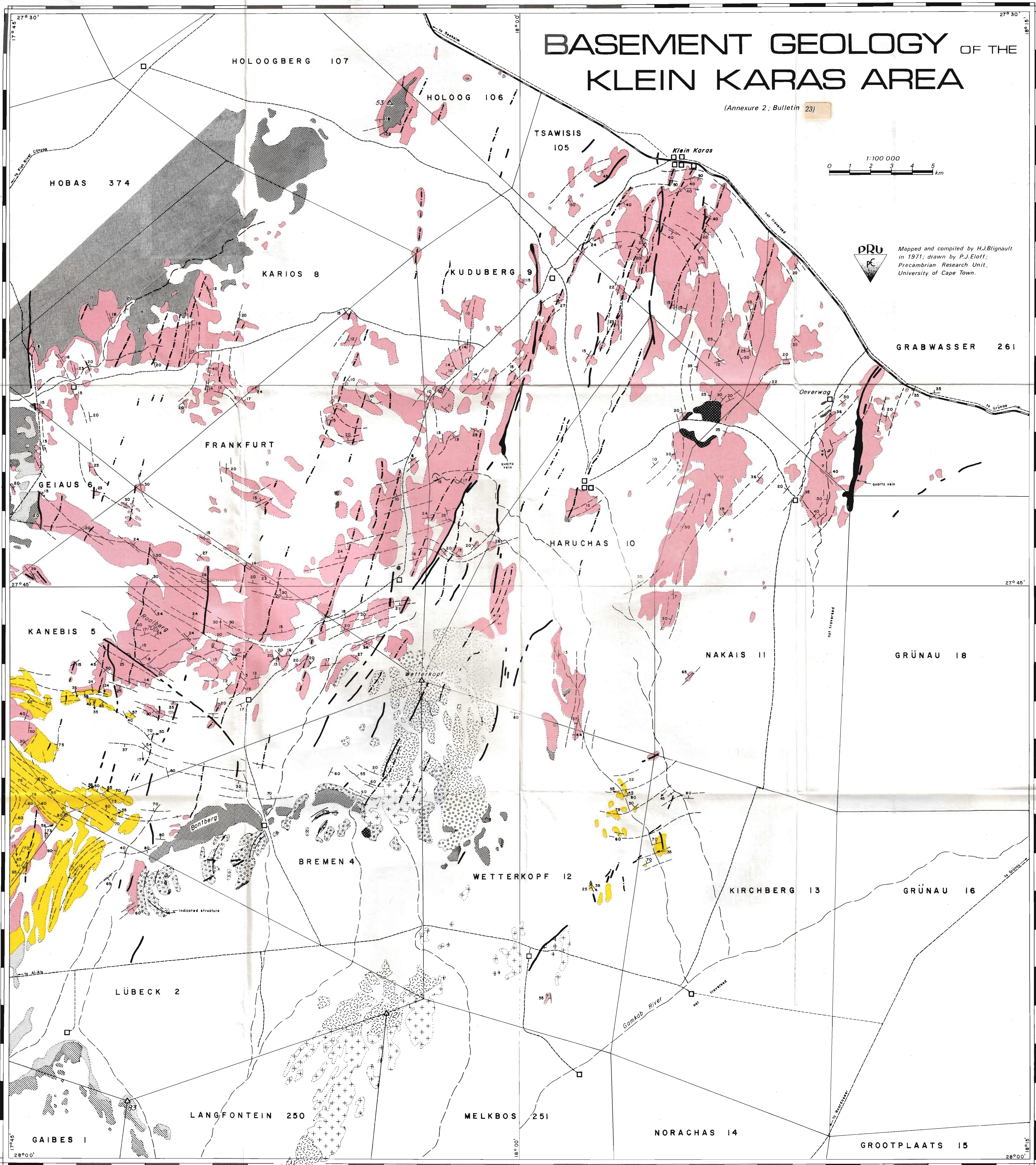
BASEMENT GEOLOGY OF THE KLEIN KARAS AREA
(Annexure 2 ; Bulletin 23)
1:100 000
0 1 2 3 4 5 km
Mapped and compiled by H.J.Blignault in 1971; drawn by P.J.Eloff; Precambrian Research Unit, University of Cape Town.
HOLOOGBERG 107
HOLOOG 106
TSAWISIS 105
Klein Karas
HOBAS 374
KARIOS 8
KUDUBERG 9
GRABWASSER 261
Onverwag
FRANKFURT
GEIAUS 6
HARUCHAS 10
KANEBIS 5
Rooiberg
NAKAIS 11
GRÜNAU 18
Wetterkopf
Bontberg
BREMEN 4
WETTERKOPF 12
KIRCHBERG 13
GRÜNAU 16
indicated structure
LÜBECK 2
Gamkab River
LANGFONTEIN 250
MELKBOS 251
NORACHAS 14
GROOTPLAATS 15
GAIBES 1
quartz vein
not traversed
to Seeheim
to Grünau
to Al-Ais
to Noordoewer
27°30'
27°45'
28°00'
17°45'
18°00'
18°15'

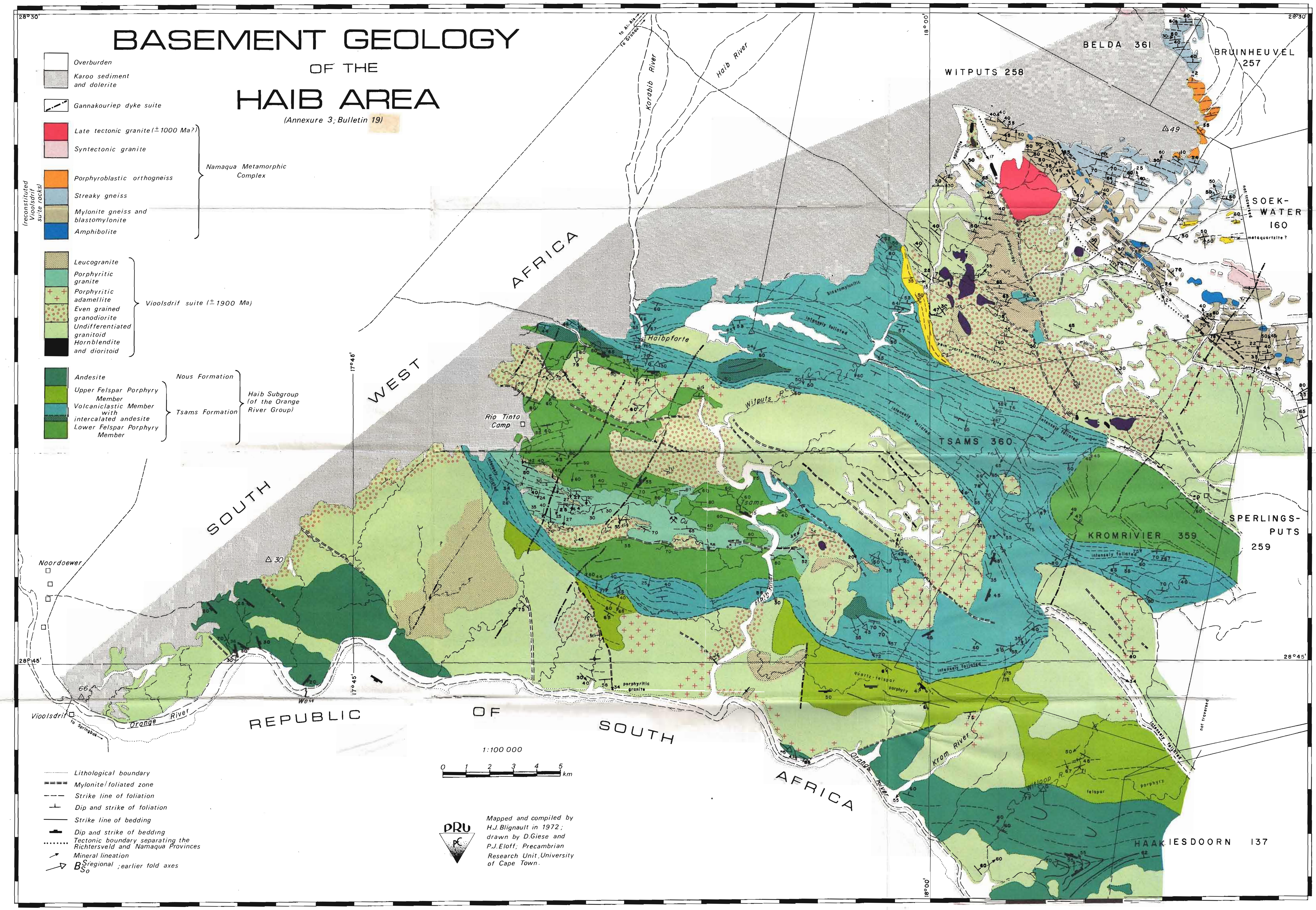

BASEMENT GEOLOGY OF THE HAIB AREA
(Annexure 3; Bulletin 19)
Overburden
Karoo sediment and dolerite
Gannakouriep dyke suite
Late tectonic granite (± 1000 Ma?)
Syntectonic granite
Porphyroblastic orthogneiss
Streaky gneiss
Mylonite gneiss and blastomylonite
Amphibolite
Namaqua Metamorphic Complex
(reconstituted Vioolsdrif suite rocks)
Leucogranite
Porphyritic granite
Porphyritic adamellite
Even grained granodiorite
Undifferentiated granitoid
Hornblendite and dioritoid
Vioolsdrif suite (± 1900 Ma)
Andesite
Nous Formation
Upper Felspar Porphyry Member
Volcaniclastic Member with intercalated andesite
Lower Felspar Porphyry Member
Tsams Formation
Haib Subgroup (of the Orange River Group)
Lithological boundary
Mylonite/foliated zone
Strike line of foliation
Dip and strike of foliation
Strike line of bedding
Dip and strike of bedding
Tectonic boundary separating the Richtersveld and Namaqua Provinces
Mineral lineation
B S regional So ; earlier fold axes
1:100 000
0 1 2 3 4 5 km
Mapped and compiled by H.J. Blignault in 1972; drawn by D.Giese and P.J. Eloff; Precambrian Research Unit, University of Cape Town.
PRU
SOUTH WEST AFRICA
REPUBLIC OF SOUTH AFRICA
BELDA 361
BRUINHEUVEL 257
WITPUTS 258
SOEK-WATER 160
TSAMS 360
KROMRIVIER 359
SPERLINGS-PUTS 259
HAAKIESDOORN 137
Haib River
Korabib River
Haibpforte
Rio Tinto Camp
Witputs R.
Tsams
Noordoewer
Vioolsdrif
Orange River
Krom River
Witloop R.
to Springbok
to Ai-Ais
to Grunau
28°30'
28°45'
17°45'
18°00'
intensely foliated
not traversed
quartz-felspar porphyry
porphyritic granite
metaquartzite ?

# BASEMENT GEOLOGY OF THE AI-AIS AREA

(Annexure 1; Bulletin 23)